

**Characterisation of arsenic hyper-resistance in  
bacteria isolated from a  
South African antimony mine**

by

**Elsabé Botes**

December 2007



**University of the Free State  
Universiteit van die Vrystaat**

**Characterisation of arsenic hyper-resistance in bacteria  
isolated from a South African antimony mine**

by

**Elsabé Botes**

Submitted in fulfillment of the requirements  
for the degree

**Philosophiae Doctor**

In the Faculty of Natural and Agricultural Sciences  
Department of Microbial, Biochemical and Food Biotechnology  
University of the Free State  
Bloemfontein  
South Africa

December 2007

Supervisor: Prof E van Heerden

Co-supervisor: Prof D Litthauer

## Acknowledgements

The completion of this degree has afforded me the rare opportunity to experience a tremendous amount of growth, both as a scientist and as a person.

In the former capacity, I would like to acknowledge the many researchers at UFS Biotechnology department who unselfishly devoted their time and expertise on me as well as many authorities in many other fields who assisted by promptly replying to many, many e-mails and requests for input, opinions, research articles and material.

I would also like to thank the National Research Foundation, the UFS BRIC project and the Metagenomics Platform based at the UFS for financial support.

Then, to my promoters, Prof. Esta van Heerden and Prof. Derek Litthauer, words cannot express the enormous contribution both of you have made in my life, both professional and personal. Much of who I am today is due to your patience, guidance, and (sometimes) pure indulgence.

I also have to acknowledge that due to the opportunities afforded to me during the Research Exchange for Undergraduate Students (REU) between the Extreme Biochemistry Research Group and University of Tennessee, I have been privileged to meet extraordinary scientists from various fields that have enriched and broadened my scientific scope enormously.

Personnel at the Instrumentation Division of UFS: their patience and willingness to build, rebuild and modify equipment and who probably could have built me a rocket if I had asked for it - I truly would not have been able to do this work without them.

Staff at the Institute for Ground Water Studies for their willingness to accommodate me in their lab, and especially to Lore-Marie who frequently worked long hours into the night to fix the ICP-MS and also for many encouraging conversations during my time spent there.

During the course of this degree, I have been shaped and molded by countless others. A few people should be mentioned by name:

Members of the Extreme Biochemistry Research Group, (both old and new), specifically my lab members since the beginning of time Dirk, Jacqui and Armand

Many friends for listening to countless hours of complaining and at times simply passing on dry tissues (Lizelle, Maralize, Marieta and many other unfortunate victims)

My immediate and extended family for their unwavering support regardless of my inability to explain my academic pursuits. Particularly, to the most wonderful brother in the world, for many words of encouragement, guidance and comfort as well as my parents for always believing in me, always being proud of me and many other loving gestures.

Olga, for encouragement and support, suggestions, and being able to stand my company during the last months of this study.

## Table of Contents

<b>List of Figures</b> .....	<b>i</b>
<b>List of Tables</b> .....	<b>v</b>
<b>List of Abbreviations</b> .....	<b>vi</b>
<b>Chapter 1: Isolation, Identification and Arsenic Resistance</b> .....	<b>1</b>
<b>1.1. Literature review: Biological transformations of arsenic</b> .....	<b>2</b>
<b>1.1.1 Background</b> .....	2
<b>1.1.2 The arsenic global geocycle</b> .....	4
<b>1.1.3 Entry of arsenic into cells</b> .....	5
<b>1.1.4 Methylation</b> .....	5
<b>1.1.5 Oxidation</b> .....	7
<b>1.1.6 Reduction</b> .....	9
1.1.6.1 Respiratory arsenate reductases .....	9
1.1.6.2 Cytoplasmic arsenate reductases .....	10
<b>1.1.7 Other mechanisms: Biosorption</b> .....	11
<b>1.2. Introduction to the present study</b> .....	<b>12</b>
<b>1.3 Aims</b> .....	<b>13</b>
<b>1.4 Materials and methods</b> .....	<b>14</b>
<b>1.4.1 General procedures and chemicals</b> .....	14
<b>1.4.2 Sampling and isolation</b> .....	14
<b>1.4.3 Cryopreservation</b> .....	15
<b>1.4.4 Identification</b> .....	15
1.4.4.1 16S rDNA sequencing.....	15
1.4.4.2 Biochemical testing.....	17
<b>1.4.5 Minimum inhibitory concentrations</b> .....	17
<b>1.4.6 Arsenate reduction</b> .....	18

1.4.6.1	Qualitative .....	18
1.4.6.2	Quantitative.....	18
<b>1.5</b>	<b>Results and discussion.....</b>	<b>19</b>
1.5.1	<u>Enrichments</u> .....	19
1.5.2	<u>Identification</u> .....	20
1.5.3	<u>Minimum inhibitory concentration</u> .....	23
1.5.4	<u>Arsenate reduction by resting cells</u> .....	27
<b>1.6</b>	<b>Literature cited.....</b>	<b>30</b>
<b>Chapter 2:</b>	<b>Molecular Aspects .....</b>	<b>37</b>
<b>2.1</b>	<b>Literature review: Dissimilatory arsenate reduction in bacteria .....</b>	<b>38</b>
2.1.1	<u>Regulation</u> .....	39
2.1.2	<u>Membrane pumps</u> .....	39
2.1.3	<u>Arsenate reductases</u> .....	40
2.1.3.1	The <i>E. coli</i> glutathione / glutaredoxin ArsC family.....	40
2.1.3.2	The <i>Staphylococcus</i> thioredoxin ArsC family .....	42
2.1.3.3	Exceptions to the rule .....	44
<b>2.2</b>	<b>Introduction .....</b>	<b>46</b>
<b>2.3</b>	<b>Aims .....</b>	<b>47</b>
<b>2.4</b>	<b>Materials and methods.....</b>	<b>48</b>
2.4.1	<u>General procedures and chemicals</u> .....	48
2.4.2	<u>Bacterial strains and primers</u> .....	48
2.4.3	<u>PCR approach</u> .....	49
2.4.3.1	DNA Extraction .....	49
2.4.3.1.1	Genomic DNA .....	49
2.4.3.1.2	Plasmid DNA.....	50
2.4.3.2	PCR.....	50

2.4.3.3	Gel band purification .....	50
2.4.3.4	PCR product ligation .....	50
2.4.3.5	Transformation .....	51
2.4.3.6	Plasmid extractions and restriction analysis.....	51
2.4.3.7	Sequencing.....	51
<b>2.4.4</b>	<b><u>Genomic library construction approach</u></b> .....	<b>51</b>
2.4.4.1	Minimum inhibitory concentration .....	51
2.4.4.2	Partial digestion of genomic DNA .....	52
2.4.4.3	Vector digest and dephosphorylation .....	52
2.4.4.4	Ligation and transformation .....	52
<b>2.5</b>	<b><u>Results and discussion</u></b> .....	<b>53</b>
2.5.1	<u>Polymerase Chain Reaction</u> .....	53
2.5.2	<u>Genomic libraries</u> .....	67
<b>2.6</b>	<b><u>Literature Cited</u></b> .....	<b>80</b>
<b>Chapter 3:</b>	<b><u>Cellular Characterisation for Adhesion</u></b> .....	<b>85</b>
<b>3.1</b>	<b><u>Literature review: Bacterial adhesion to inert surfaces</u></b> .....	<b>86</b>
3.1.1	<u>Primary adhesion</u> .....	86
3.1.1.1	Theory of adhesion .....	87
3.1.2	<u>Secondary adhesion</u> .....	88
3.1.3	<u>Factors influencing bacterial adhesion</u> .....	88
3.1.3.1	Surface of adhesion.....	88
3.1.3.2	Bacterial surface features .....	89
3.1.3.3	Cell size and shape .....	90
3.1.3.4	Bacterial hydrophobicity .....	90
3.1.3.5	Bacterial surface charge.....	91
3.1.4	<u>Conditioning</u> .....	91
3.1.5	<u>Concluding remarks</u> .....	92
<b>3.2</b>	<b><u>Aims</u></b> .....	<b>94</b>

<b><u>3.3 Materials and methods.....</u></b>	<b><u>95</u></b>
<b><u>3.3.1 Growth parameters (pH and temperature).....</u></b>	95
<b><u>3.3.2 Motility .....</u></b>	95
<b><u>3.3.3 Anaerobic growth .....</u></b>	95
<b><u>3.3.4 Cell size and morphology .....</u></b>	96
<b><u>3.3.5 Pigmentation .....</u></b>	96
<b><u>3.3.6 Cell surface properties .....</u></b>	96
3.3.6.1 Hydrophobicity .....	96
3.3.6.2 Electrostatic and acid / base properties.....	97
3.3.6.3 Lipopolysaccharides (LPS).....	97
3.3.6.4 Carbohydrate and protein content .....	98
<b><u>3.4 Results and discussion.....</u></b>	<b><u>99</u></b>
<b><u>3.4.1 Growth parameters (pH and temperature).....</u></b>	99
<b><u>3.4.2 Motility .....</u></b>	100
<b><u>3.4.3 Anaerobic growth .....</u></b>	100
<b><u>3.4.4 Morphological and surface properties.....</u></b>	104
3.4.4.1 Cell size and morphology .....	104
3.4.4.2 Pigmentation .....	105
3.4.4.3 Hydrophobicity .....	105
3.4.4.4 Electrostatic and acid / base properties.....	107
3.4.4.5 Lipopolysaccharides (LPS).....	109
3.4.4.6 Carbohydrate and protein content .....	110
<b><u>3.5 Conclusions .....</u></b>	<b><u>111</u></b>
<b><u>3.6 Literature cited.....</u></b>	<b><u>113</u></b>
<b><u>Chapter 4: <i>In situ</i> reduction of arsenate by <i>S. marcescens</i> SA Ant 16.....</u></b>	<b><u>118</u></b>

<b><u>4.1 Literature review: Arsenic remediation technologies .....</u></b>	<b><u>119</u></b>
<b><u>4.1.1 Chemical techniques for arsenic remediation .....</u></b>	119
4.1.1.1 Precipitative processes .....	119
4.1.1.2 Adsorptive processes .....	121
4.1.1.3 Ion exchange.....	121
4.1.1.4 Membrane processes .....	122
4.1.1.5 Alternative technologies .....	122
<b><u>4.1.2 Biological methods .....</u></b>	123
4.1.2.1 Passive biosorbents .....	123
4.1.2.2 Phytoremediation .....	125
4.1.2.3 Bioremediation with microorganisms.....	126
<b><u>4.2 Aims .....</u></b>	<b><u>129</u></b>
<b><u>4.3 Materials and methods.....</u></b>	<b><u>130</u></b>
<b><u>4.3.1 Optimisation of arsenate reducing conditions .....</u></b>	130
<b><u>4.3.2 Adhesion of cells to sand matrix.....</u></b>	131
<b><u>4.3.3 Real-Time PCR for quantification.....</u></b>	131
<b><u>4.3.4 Setup, conservative tracer and bacterial breakthrough .....</u></b>	132
<b><u>4.3.5 Column loading.....</u></b>	133
<b><u>4.3.6 In situ As(V) reduction.....</u></b>	134
<b><u>4.3.7 Scanning electron microscopy.....</u></b>	134
<b><u>4.4 Results and discussion.....</u></b>	<b><u>135</u></b>
<b><u>4.4.1 Factorial design for arsenate reduction optimisation .....</u></b>	135
<b><u>4.4.2 Real-Time enumeration and primer specificity.....</u></b>	143
<b><u>4.4.3 Adhesion .....</u></b>	144
<b><u>4.4.4 Tracer and breakthrough curves .....</u></b>	146
<b><u>4.4.5 Loading of column with cells .....</u></b>	147
<b><u>4.4.6 Arsenate reduction in column reactors .....</u></b>	147
<b><u>4.5 Conclusions .....</u></b>	<b><u>153</u></b>



<b>4.6 Literature cited .....</b>	<b>155</b>
<b>5 Summary .....</b>	<b>160</b>
<b>6 Opsomming .....</b>	<b>162</b>

## List of Abbreviations

16S	small ribosomal subunit
A	absorbance
AGW	artificial ground water
AIX	ampicillin/IPTG/X-Gal
As(III)	arsenite
As(V)	arsenate
ATP	adenosine triphosphate
BATH	bacterial adhesion to hydrocarbons
BCA	bicinchoninic acid
bp	basepair
BLAST	basic local alignment search tool
CM	carboxymethyl
C <sub>T</sub>	threshold cycle
Cys	cysteine
Da	Dalton
DEAE	diethylaminoethyl
DLVO	Derjaguin-Landau-Verwey-Overbeek
DMSO	dimethylsulfoxide
DNA	deoxyribonucleic acid
dNTP	dioxynucleotide
DO	dissolved oxygen
DTT	dithiothreitol
EDTA	ethylenediamine tetraacetic acid
EISC	electrostatic interaction chromatography
EMBL	European Molecular Biology Laboratory
FDH	formate dehydrogenase
g	acceleration due to gravity
Glc	glucose
Grx	glutaredoxin
GSH	glutathione
h	hour
HIC	hydrophobic interaction chromatography
HPLC	high performance liquid chromatography

ICP-MS	inductively coupled plasma mass spectrometry
IPTG	isopropyl- $\beta$ -D- thiogalactopyranoside
kb	kilobasepair
kcal/mol	kilocalories per mole
$K_{cat}$	catalytic rate
kDa	kilo Dalton
Kdo	2-keto-3-deoxyoctonoic acid
kg	kilogram
$K_i$	inhibitor dissociation constant
$K_m$	Michaelis constant
$K_{sp}$	solubility constant
L	litre
LB	Luria-Bertani
LPS	lipopolysaccharide
LMW	low molecular weight
M	molar
mA	milliampere
Mb	megabasepair
mg	milligram
mM	millimolar
nm	nanometer
OD	optical density
PAGE	polyacrylamide gel electrophoresis
PCR	polymerase chain reaction
PIPES	piperazine bisethanesulfonic acid
Pit	phosphate transport
$pK_a$	dissociation constant
ppb	parts per billion
ppm	parts per million
Pro	proline
Pst	phosphate specific transport
PTPase	phosphatase
PV	pore volume
rDNA	ribosomal DNA
RDP	ribosomal database project

rpm	revolutions per minute
RT	Real-Time
SDS	sodium dodecyl sulphate
TAE	Tris-acetic acid-EDTA
TE-buffer	Tris-EDTA buffer
TLC	thin layer chromatography
T <sub>m</sub>	melting temperature
Tris	Tris(hydroxymethyl)aminomethane
Trx	thioredoxin
TYG	tryptone, yeast extract, glucose
Tyr	tyrosine
U	units
UFS	University of the Free State
µg	microgram
µL	microlitre
µM	micromolar
µm	micrometer
µmax	maximum growth rate during exponential growth phase
US EPA	United States Environmental Protection Agency
UV	ultra violet
V	volt
v/v	volume per volume
w/v	weight per volume
XDLVO	extended DLVO
X-Gal	5-bromo-4-chloro-3-indolyl-β-D-galactoside

## List of Figures

Figure 1.1	The arsenic geocycle .....	4
Figure 1.2	Transport of arsenate into <i>E. coli</i> .....	5
Figure 1.3	Microbial formation of trimethylarsine from inorganic arsenate .....	6
Figure 1.4	ArsC families from Gram positive bacteria (I), Gram negative bacteria (II), and eukaryota (III).....	10
Figure 1.5	16S rDNA PCR products from arsenic resistant pure cultures .....	20
Figure 1.6	Phylogenetic tree generated with 16S rDNA PCR sequences.....	22
Figure 1.7	Growth of <i>Bacillus</i> sp. SA Ant 14 in absence and presence of arsenite and arsenate .....	25
Figure 1.8	Growth of <i>S. maltophilia</i> SA Ant 15 in absence and presence of arsenite and arsenate.....	26
Figure 1.9	Growth of <i>S. marcescens</i> SA Ant 16 in absence and presence of arsenite and arsenate.....	26
Figure 1.10	TLC plate demonstrating arsenate reduction to arsenite by resting cells of <i>Bacillus</i> sp. SA Ant 14, <i>S. maltophilia</i> SA Ant 15 and <i>S. marcescens</i> SA Ant 16 .....	27
Figure 1.11	Reduction of arsenate to arsenite by resting cells of <i>Bacillus</i> sp. SA Ant 14, <i>S. maltophilia</i> SA Ant 15 and <i>S. marcescens</i> SA Ant 16 .....	28
Figure 2.1	Catalytic reaction cycle of the Grx-coupled arsenate reductase of <i>E. coli</i> plasmid R773 .....	41
Figure 2.2	Ribbon diagram of the overall structure of reduced ArsC wild type.....	42
Figure 2.3	Catalytic reaction cycle of Trx-coupled arsenate reductase of <i>S. aureus</i> plasmid pI258 .....	43
Figure 2.4	Organisation of the four arsenic resistance operons in <i>Herminiimonas arsenicoxydans</i> .....	44
Figure 2.5	Alignments of <i>arsC</i> from Gram negative organisms with primer pair <i>arsC</i> -1-F / <i>arsC</i> -1-R indicated .....	53
Figure 2.6	1% TAE agarose gel with PCR products generated with primer pair <i>arsC</i> -1-F / <i>arsC</i> -1-R .....	54
Figure 2.7	PCR products from primer set <i>arsC</i> -1-F / <i>arsC</i> -1-R.....	54
Figure 2.8	Alignments of <i>arsC</i> from Gram negative organisms for design of degenerate primer pair <i>ArsCF</i> / <i>ArsCR</i> .....	55
Figure 2.9	PCR products generated with primer pair <i>ArsCF</i> / <i>ArsCR</i> .....	56
Figure 2.10	Alignment of DNA sequence of <i>ArsCF</i> / <i>ArsCR</i> PCR product with cytochrome oxidase subunit II ( <i>cyoXB</i> ) .....	57

Figure 2.11	PCR products from combinations of primer sets ArsCF / arsCR and arsC-1-F / arsC-1-R.....	58
Figure 2.12	Design of primer pair ArF / ArR based on the sequence of <i>S. marcescens</i> plasmid R478.....	59
Figure 2.13	Agarose gel with PCR fragments generated on serially diluted DNA of <i>S. marcescens</i> SA Ant 16.....	60
Figure 2.14	Alignment of arsR sequences and schematic of arsenate resistance operon spanning genes <i>arsR</i> to <i>arsC</i> .....	61
Figure 2.15	PCR products amplified with forward primer ArsRF and reverse primer arsC-1-R.....	61
Figure 2.16	Alignments of arsC from selected Gram negative bacteria for design of degenerate primer set ArsC7F / ArsC7R.....	62
Figure 2.17	PCR products amplified with primer set ArsC7F / ArsC7R on a 1.5% TAE agarose gel.....	62
Figure 2.18	1.5% TAE agarose gel with PCR products generated with primer set ArsC7F / ArsC7R using plasmid extracts as template.....	63
Figure 2.19	Alignment of <i>arsC</i> from Gram positive type arsenate reductases.....	65
Figure 2.20	Alignment of <i>arsC</i> from <i>P. aeruginosa</i> and <i>T. ferrooxidans</i> for design of degenerate primer set PsThF / PsThR.....	66
Figure 2.21	PCR amplification of <i>S. marcescens</i> SA Ant 16 genomic DNA with Gram positive primer set PsThF / PsThR.....	66
Figure 2.22	Minimum inhibitory As(V) concentration for <i>E. coli</i> <i>arsC</i> knockout strain AW3110 transformed with pUC18 and plated on increasing concentrations of arsenate.....	68
Figure 2.23	Partial digest of genomic DNA from <i>S. marcescens</i> SA Ant 16.....	68
Figure 2.24	Effect of interaction of ampicillin and chloramphenicol with <i>E. coli</i> strain AW3110.....	69
Figure 2.25	Minimum inhibitory arsenate concentration for untransformed <i>E. coli</i> JM109 and TOP10.....	70
Figure 2.26	Minimum inhibitory arsenite concentration for untransformed <i>E. coli</i> JM109 and TOP10.....	70
Figure 2.27	Minimum inhibitory arsenate concentration for <i>E. coli</i> JM109 cells transformed with pUC18.....	71
Figure 2.28	Control ligation of <i>Eco</i> RI and <i>Bam</i> HI digested $\lambda$ DNA.....	72
Figure 2.29	Control ligation of <i>Eco</i> RI digested $\lambda$ DNA into pUC18.....	72
Figure 2.30	<i>S. marcescens</i> SA Ant 16 genomic DNA partially digested with <i>Sau</i> 3AI.....	73
Figure 2.31	Minimum inhibitory arsenate and arsenite concentration for <i>E. coli</i> TOP10 cells transformed with pGem®-3Z.....	75

Figure 2.32	Partial digest of genomic DNA from <i>S. marcescens</i> SA Ant 16.....	76
Figure 2.33	Streaking out and replica plating of positive recombinants onto LB-plates containing 10mM and 15mM arsenate.....	76
Figure 2.34	Restriction analysis of plasmids containing inserts.....	77
Figure 2.35	1.5% TAE agarose gel of the <i>arsC</i> of <i>E. coli</i> W3110 amplified with primer pair <i>arsC</i> -1-F / <i>arsC</i> -1-R and sequence alignment with <i>arsC</i> <i>E. coli</i> X80057.....	78
Figure 2.36	Partial digest of genomic DNA from <i>E. coli</i> W3110 .....	78
Figure 3.1	Optimum growth temperature for <i>S. marcescens</i> SA Ant 16.....	99
Figure 3.2	Optimum growth pH for <i>S. marcescens</i> SA Ant 16 .....	100
Figure 3.3	Motility of <i>S. marcescens</i> SA Ant 16 and <i>E. coli</i> .....	100
Figure 3.4	Anaerobic growth of <i>S. marcescens</i> SA Ant 16 with nitrate as electron acceptor.....	103
Figure 3.5	Gram stained cells of <i>S. marcescens</i> SA Ant 16 grown under aerobic and anaerobic growth conditions.....	104
Figure 3.6	<i>S. marcescens</i> SA Ant 16 grown at 30°C and 37°C on peptone-glycerol agar to observe pigment production .....	105
Figure 3.7	Percentage hydrophobicity of aerobically and anaerobically grown cells of <i>S. marcescens</i> SA Ant 16 as determined with Bacterial Adhesion To Hydrocarbons.....	106
Figure 3.8	Percentage hydrophobicity of aerobically and anaerobically grown cells of <i>S. marcescens</i> SA Ant 16 as determined with Hydrophobic Interaction Chromatography.....	107
Figure 3.9	Acid / base properties of aerobically and anaerobically grown cells of <i>S. marcescens</i> SA Ant 16 .....	108
Figure 3.10	Percentage retention of aerobically and anaerobically grown cells of <i>S. marcescens</i> SA Ant 16 with various chromatographic resins.....	108
Figure 3.11	Lipopolysaccharides visualised with crystal violet and copper sulfate of aerobically grown cells and anaerobically grown cells of <i>S. marcescens</i> SA Ant 16 .....	109
Figure 3.12	Lipopolysaccharides from aerobically and anaerobically grown cells of <i>S. marcescens</i> SA Ant 16 separated on SDS-PAGE.....	110

Figure 4.1	Factorial design layout .....	130
Figure 4.2	Setup of column reactors .....	133
Figure 4.3	Negative controls (cells with no arsenate addition) for changes in pH, growth and glucose consumption under aerobic conditions.....	137
Figure 4.4	Growth and changes in pH during arsenate reduction under aerobic conditions .....	138
Figure 4.5	Arsenate reduction and glucose consumption under aerobic conditions.....	139
Figure 4.6	Growth and pH changes during arsenate reduction under anaerobic conditions .....	140
Figure 4.7	Arsenate reduction and glucose consumption under anaerobic conditions .....	140
Figure 4.8	3D representation of growth and changes in pH during arsenate reduction.....	141
Figure 4.9	Standard curve of cell concentration (cells/mL) vs. cycle number ( $C_T$ ) .....	143
Figure 4.10	Specificity of <i>S. marcescens</i> specific primers .....	144
Figure 4.11	Adhesion of concentration ranges of <i>S. marcescens</i> SA Ant 16 cells to sand grains .....	145
Figure 4.12	Adhesion of <i>S. marcescens</i> SA Ant 16 to sand in syringe columns over a period of 24 hours .....	145
Figure 4.13	Typical profile of NaCl tracer and bacterial breakthrough in a 500mm column .....	146
Figure 4.14	Cell numbers in small column reactor for maximum saturation .....	147
Figure 4.15	Arsenate reduction, glucose utilisation and changes in pH in column reactor containing 3mM glucose .....	149
Figure 4.16	SEM imaging of negative control sand grain, and sand grain covered with cells.....	149
Figure 4.17	Viable cells in the reactor (5mM As(V), 6mM glucose) during run .....	150
Figure 4.18	Changes in pH, dissolved oxygen percentage and glucose conversion in the reactor amended with 5mM arsenate and 6mM glucose .....	151
Figure 4.19	Percentage arsenate conversion over 10 pore volumes for bioreactor amended with 5mM arsenate and 6mM glucose .....	152



## List of Tables

Table 1.1	Sampling site description .....	15
Table 1.2	Primers used for 16S rDNA amplification and sequencing .....	17
Table 1.3	Growth for pure cultures inoculated into antimony supplemented TYG media .....	19
Table 1.4	Growth for pure cultures in arsenate and arsenite supplemented TYG media .....	20
Table 1.5	Closest sequence matches for 16S rDNA genes of pure cultures .....	21
Table 1.6	Effect of increasing concentrations arsenite or arsenate on biomass yield, maximum specific growth rate and lag phase for <i>Bacillus</i> sp. SA Ant 14, <i>S. maltophilia</i> SA Ant 15 and <i>S. marcescens</i> SA Ant 16 grown for 12 hours .....	24
Table 1.7	Arsenate removal by whole cells of <i>Bacillus</i> sp. SA Ant 14, <i>S. maltophilia</i> SA Ant 15 and <i>S. marcescens</i> SA Ant 16 during resting conditions .....	29
Table 2.1	<i>E. coli</i> strains used in the study .....	48
Table 2.2	Primers used for amplification and sequencing of arsenate reductase ( <i>arsC</i> ).....	49
Table 3.1	Summary of growth parameters during anaerobic growth of <i>S. marcescens</i> SA Ant 16 .....	102
Table 3.2	Total protein and carbohydrate content of cells of <i>S. marcescens</i> SA Ant 16 grown aerobically and anaerobically.....	111

# **Chapter 1**

## **Isolation, Identification and Arsenic Resistance**

## **1.1 Literature review: Biological transformations of arsenic**

### **1.1.1 Background**

Arsenic is widely spread in the upper crust of the earth, although mainly at very low concentrations. The main source of arsenic on the earth's surface is igneous activity, although anthropomorphic sources such as industrial effluents, various commercial processes and combustion of fossil fuels also contribute significantly<sup>i</sup>. Arsenic concentrations in soil range from 0.1 to more than 1000ppm (1 $\mu$ M - 10mM), while in atmospheric dust, the range is 50-400ppm (0.7mM - 5mM)<sup>ii</sup>.

While arsenic has a historically infamous reputation as a poison<sup>iii</sup>, its biological uses are less well known. Arsenic belongs to group VA of the periodic table of elements - these elements are metalloids that have both metallic and non-metallic properties. Arsenic exists in various forms, exhibiting different biological properties and degrees of toxicity. The common valence states of arsenic in nature include -3, +3, and +5, with decreasing toxicity. The specific toxicity of arsenate [As(V)] is generally attributed to its chemical similarity to phosphate where it is capable of mimicking the role of phosphate in cellular transport and enzymatic reactions. Thus, arsenate may replace an essential phosphate in various metabolic processes where a central target of As(V) is pyruvate dehydrogenase and inhibition of this enzyme blocks respiration. Arsenate uncouples oxidative phosphorylation by the formation of unstable arsenate esters, which substitute for phosphate esters in ATP formation<sup>iv</sup>. Arsenite [As(III)] reacts with -SH groups of cysteine residues, which often constitute an integral part of the active site of enzymes, thereby inhibiting their catalytic activity. Besides direct enzyme inhibition, arsenite induces oxidative damage *via* the accumulation of reactive oxygen species. This arsenite-stimulated generation of reactive oxygen, known to damage proteins, lipids and DNA, is probably the direct cause of the carcinogenic effects of arsenite<sup>v</sup>.

In aqueous systems arsenate oxyanions are ionized with three  $pK_a$  values of 2.2, 7.0, and 11.50 (comparable to 2.1, 7.2, and 12.7 for phosphate)<sup>vi</sup>, so that approximately equal amounts of  $\text{HAsO}_4^{2-}$  and  $\text{H}_2\text{AsO}_4^-$  occur at pH 7<sup>vii</sup> whereas  $\text{H}_3\text{AsO}_4$  and  $\text{H}_2\text{AsO}_4^-$  predominate in acidic environments<sup>viii</sup>. Arsenite appears mostly un-ionized as  $\text{As}(\text{OH})_3$  at neutral pH, with a  $pK_a$  of 9.2 for dissociation to  $\text{H}_2\text{AsO}_3^-$ <sup>vii</sup>. Therefore, the transport substrate in and out of the cells for arsenate will be the oxyanion comparable to phosphate at approximately the same pH, whereas arsenite may move across membrane bilayers passively un-ionized or be transported by a

carrier protein similar to un-ionized organic compounds<sup>ix</sup>. Arsenic toxicity is highly dependent on its oxidation state: trivalent arsenicals are at least 100 times more toxic than the pentavalent derivatives<sup>x</sup>. Arsenite and arsenate are interconverted by biological redox reactions and arsenite can also be methylated by bacteria, fungi and algae<sup>xi</sup>.

The effects of oxyanions of metalloids on both prokaryotic and eukaryotic cells have attracted substantial attention. In recent years, concern has increased about the release of arsenical compounds in the environment and their toxicity to a wide variety of organisms, including humans. There is a wealth of information on the biological effects of arsenic compounds on mammals: arsenic is able to induce cell transformations<sup>xii</sup>, gene amplification in marine cells<sup>xiii</sup>, gene damage in human alveolar type II cells<sup>xiv</sup>, and is a co-mutagen agent in exposed hamster cells<sup>xiii</sup>. Arsenic compounds elicit a cellular stress response similar to heatshock protein synthesis<sup>xv, xvi</sup> and causes lung and skin cancers in humans<sup>xvii, xviii, xix</sup>. There is also evidence to support the carcinogenic effect of ingested inorganic arsenic and the occurrence of bladder, kidney and liver cancers<sup>xx</sup>.

In the environment microorganisms are continuously exposed to metallic anions and cations. Some of these ions are taken up as essential nutrients (i.e. magnesium, potassium, copper, and zinc) whereas others exert toxic effects on microbial cells (i.e. mercury, lead, cadmium, arsenic, and silver)<sup>xxi</sup>. Although the presence of heavy metals is detrimental for microorganisms, toxic metals select variants possessing genetic resistance determinants which confer the ability to tolerate higher levels of the toxic compounds. Because metal ions cannot be degraded or modified like toxic organic compounds, there are six possible mechanisms for a metal resistance system:

- exclusion by permeability barrier;
- intra- and extra-cellular sequestration;
- active efflux pumps;
- enzymatic reduction; and
- reduction in the sensitivity of cellular targets to metal ions<sup>xxii, xxiii, xxiv, xxv, xxvi</sup>.

One or more of these resistance mechanisms allows microorganisms to function in metal contaminated environments. In bacteria, heavy metal resistance genes are usually located on plasmids or transposons. Several bacterial resistance mechanisms to toxic metals have been studied and described<sup>xxvii, xxviii</sup>.

### 1.1.2 The arsenic global geocycle

Just as there are well-studied geocycles for carbon, nitrogen, oxygen, sulfur and other elements that are components of all living cells, there are also geocycles for toxic elements including arsenic. Living cells (especially microbes) carry out redox and covalent bond chemistry and are important contributors in the arsenic geocycle. Higher plants and animals can bio-accumulate compounds to levels far above those of the environments in which they live. Arsenate (the main arsenic compound in seawater) is taken up by marine organisms, ranging from phytoplankton, algae, crustaceans, mollusks and fish<sup>xxix</sup>, and converted to organic compounds (such as methylarsonic acid or dimethylarsinic acid), or is converted to organic storage forms that are then secreted into the environment. However, some arsenic is retained by phytoplankton and metabolised into complex organic compounds<sup>xxix</sup>. More complex algal organoarsenical compounds include water-soluble arsenosugars (i.e. dimethylarsenosugars) and lipid-soluble compounds (arsenolipids). While phytoplankton and macroalgae are the primary producers of complex organoarsenic compounds in the sea, these organisms are themselves consumed and metabolized by marine animals. Fish and marine invertebrates retain 99% of accumulated arsenic in organic form, and crustacean and mollusk tissues contain higher concentrations of arsenic than fish. The major organoarsenic compound isolated from marine organisms is arsenobetaine. It occurs in algae, clams, lobsters, sharks, and shrimp, but it is not known how arsenosugars and arsenolipids are converted to arsenobetaine within the higher animals in the marine environment. Arsenobetaine is degraded by microbial metabolism in coastal seawater sediments to methylarsonic acid and to inorganic arsenic<sup>xxx</sup>.

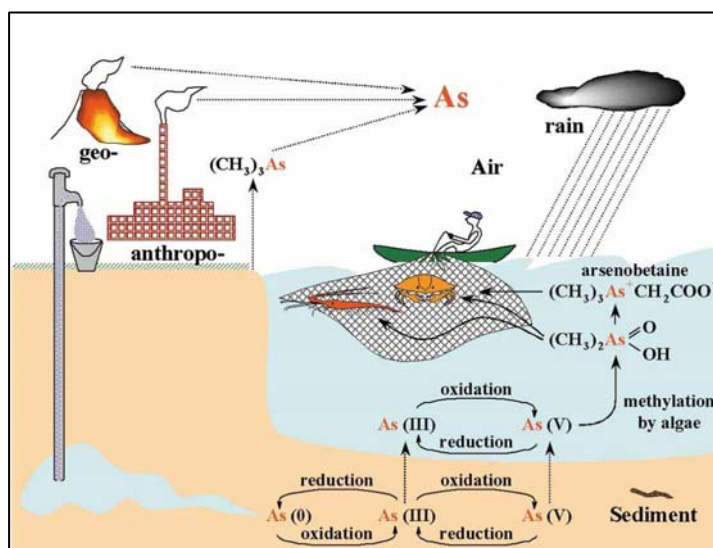
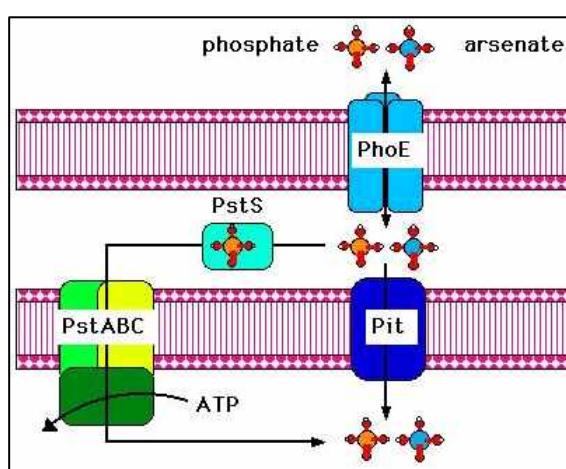


Figure 1.1 The arsenic geocycle (From Mukhopadhyay *et al.* 2002)<sup>xxx</sup>.

### **1.1.3 Entry of arsenic into cells**

To have a physiological or toxic effect, most metal ions have to enter the microbial cell. Pentavalent arsenate is analogous to inorganic phosphate and both anions utilize the same pathway to enter cells. In *Escherichia coli* arsenate enters the periplasmic space through the outer membrane porin, PhoE, and is transported into the cytoplasm by either of the phosphate transporters: The Pit system (phosphate transport) appears to be the predominant system<sup>xxxix</sup>, but arsenate also enters the cells via the phosphate translocating ABC-type ATP-ase complex, Pst (phosphate specific transport)<sup>xxxix</sup>, formed by the PstA, PstB, PstC and PhoS proteins<sup>xxxix</sup> (Figure 1.2).



**Figure 1.2** Transport of arsenate into *E. coli* (from Nies & Silver, 1995)<sup>xxxix</sup>.

Arsenite, on the other hand, might be considered an inorganic equivalent of glycerol and therefore the glycerol facilitator of *E. coli* GlpF is the main route of entry into cells<sup>xxxix</sup>. GlpF is an aquaglyceroporin, a member of the aquaporin superfamily consisting of multifunctional channels that transport neutral organic solutes such as glycerol and urea<sup>xxxix</sup>.

The frequent abundance of arsenic in the environment has guided the evolution of enzymes for a variety of ingenious resistance mechanisms for protection against the deleterious effects of arsenic as described below in section 1.1.4 – 1.1.7.

### **1.1.4 Methylation**

The conversion of arsenate to methylarsonic acid or to dimethylarsinic acid is a possible mechanism for detoxification and was first observed over 150 years ago. It has been

understood, at the level of products formed, from the work of Challenger and co-workers before World War II<sup>xxxvi, xxxvii</sup>. Fungi dominate the microbes that produce volatile, garlic-smelling trimethylarsine, although bacteria and animal tissues also have this potential<sup>xxxviii</sup>. Hall *et al.* (1997)<sup>xxxix</sup> showed that the microbial content of the mouse intestinal cecum (mostly anaerobic bacteria) methylates inorganic arsenic, where up to 40% of low levels of As(III) and As(V) were methylated *in vitro* by cecal contents in less than 24 hours. Both monomethyl- and dimethyl-arsenic compounds were formed and addition of potential methyl donors increased the yield of methylarsonic acid (Figure 1.3).

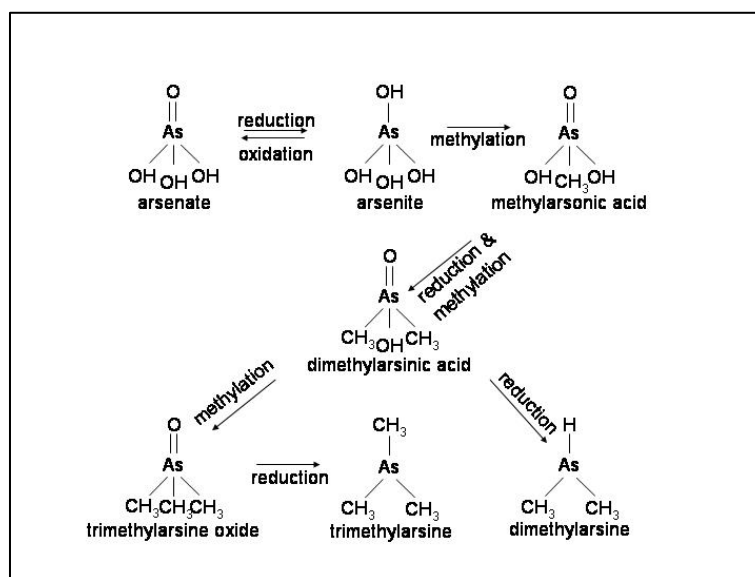


**Figure 1.3** Microbial formation of trimethylarsine from inorganic arsenate<sup>ix, xxxvi, xl</sup>.

Following the discovery of biomethylation of mercury by *Methanobacillus omelianski*<sup>xli</sup>, it was shown that *Methanobacterium bryantii* produced dimethylarsine from several arsenic compounds<sup>xlii</sup>. The facultative marine anaerobe *Serratia marinorubra* can also convert arsenate to arsenite and methylarsonic acid when grown aerobically, but volatile arsines are not produced under either aerobic or anaerobic conditions<sup>xliii</sup>. Five bacterial species, (*Corynebacterium* sp., *E. coli*, *Flavobacterium* sp., *Proteus* sp., and *Pseudomonas* sp.) isolated from the environment were able to produce dimethylarsine after acclimatisation with sodium arsenate. The *Pseudomonas* sp. was able to form all three of the methylated arsines. Six bacterial species (*Achromobacter* sp., *Aeromonas* sp., *Alcaligenes* sp., *Flavobacterium* sp., *Nocardia* sp., and *Pseudomonas* sp.) produced both mono- and dimethylarsine from methylarsonate; only two of them produced trimethylarsine. The *Nocardia* sp. was the only organism that produced all of the methylarsines from this substrate<sup>xliv</sup>.

Qin *et al.*<sup>xlv</sup> reported the isolation of the protein product of the newly named *arsM* gene from *Rhodospseudomonas palustris*. Whole cell and cell-free enzyme assays showed the formation of mono-, di- and trimethylarsenic compounds. *S*-adenosylmethionine and glutathione were required for enzyme activity *in vitro* and when this gene was cloned into *E. coli* cells, the ability to produce volatile trimethylAs(III) and resistance to inorganic arsenite was transferred.

### **1.1.5 Oxidation**

Oxidation of As(III) represents a potential detoxification process that allows microorganisms to tolerate higher levels of arsenite. Several examples of bacterial oxidation of arsenite to arsenate were being reported as early as 1918<sup>xlvi</sup> and aerobic isolates from arsenic-impacted environments have since been isolated and described<sup>xlvi, xlviii, xlix</sup>. Similar isolates have also been found in soils and sewage not known to be exposed to elevated levels of arsenic<sup>l, li</sup>. More than 30 strains representing at least nine genera of the *Bacteria* and *Archaea*, including members of the *Alphaproteobacteria*, *Betaproteobacteria*, *Gammaproteobacteria*, *Deinococcus–Thermus* and *Crenarchaeota*, have been reported to be involved in arsenite oxidation<sup>lii, liii</sup>.

To date, all known aerobic arsenite oxidases exhibit a heterodimeric structure with molybdopterin and Rieske-like subunits<sup>liv, lv</sup>. The large subunit (AroA ~90kDa) of the arsenite oxidase is the first example of a new subgroup of the dimethylsulfoxide (DMSO) reductase family of molybdoenzymes<sup>lvi</sup>. All enzymes in this family are involved in electron transport whereby the Mo-centre serves to cycle electrons via the Mo(IV) and Mo(VI) valence states, and appear to have a common ancestor present prior to the divergence of the *Bacteria* and *Archaea*<sup>lvii, lviii</sup>. Unfortunately, much confusion surrounds the naming of arsenite oxidases, and currently three different nomenclatures exist to describe what are essentially homologous proteins encoded by *asoA* & *asoB*<sup>lv</sup>, *aoxB* & *aoxA*<sup>lix</sup>, *aroA* & *aroB*<sup>xlvi</sup>.

The arsenite-oxidizing bacteria isolated can be divided into two groups:

- (i) heterotrophs (growth in the presence of organic matter) or
- (ii) chemolithoautotrophs (aerobes or anaerobes, using arsenite as the electron donor and CO<sub>2</sub>/ HCO<sub>3</sub><sup>-</sup> as the sole carbon source).



The oxidation of As(III) by heterotrophic microorganisms is generally considered to be a detoxification mechanism as the microbes do not gain energy from the reaction<sup>lv</sup>. Arsenite oxidase genes have been described from the heterotrophic strains *Alcaligenes faecalis*<sup>lv</sup>, *Cenibacterium arsenoxidans*<sup>lix</sup>, *Thermus* sp. str. HR13<sup>lx</sup>, *Thermus thermophilus* str. HB8<sup>lxi</sup>, *Agrobacterium tumefaciens*<sup>lxii</sup> and *Chloroflexus aurantiacus*<sup>lviii</sup>. The arsenite oxidase from *Alcaligenes faecalis* is located on the outer surface of the inner membrane and the arsenite oxidase transfers electrons to the periplasmic electron carriers amicyanin or cytochrome c. The crystal structure shows the enzyme is heterodimeric with two subunits ( $\alpha_1\beta_1$ ). The large subunit, AsoA is an 88kDa polypeptide that contains a molybdopterin and a 3Fe-4S center. The small subunit AsoB is a 14kDa polypeptide which contains a Rieske 2Fe-2S center<sup>liv</sup>. AsoA is structurally related to members of the dimethyl sulfoxide (DMSO) reductase family of molybdoenzymes. Based on amino acid sequence identity, AsoA shows the closest relatedness to the dissimilatory nitrate reductase (NAP) (23%) and formate dehydrogenase (FDH) (20%)<sup>lvi</sup>. The structure of the large subunit allows As(OH)<sub>3</sub> to enter and allows HAsO<sub>4</sub><sup>2-</sup> to exit following oxidation<sup>liv, lvi</sup>. Characterization of the arsenite oxidase genes (*aox*) in *C. arsenoxidans* shows that the sequence of the small subunit AoxA is 65% identical to the AsoB found in *A. faecalis*, while AoxB, the large subunit in *C. arsenoxidans*, is 72% identical to AsoA. The enzyme is also located on the outer surface of the inner membrane<sup>lix</sup>. These results indicate that the arsenite oxidase genes found in heterotrophic As(III)-oxidizers are homologous even though they are named differently<sup>lv</sup>.

In contrast, autotrophic As(III) oxidizers can utilize As(III) as an electron donor coupled to CO<sub>2</sub> fixation for cell growth under

- (i) aerobic conditions<sup>lxiii, lxiv</sup>,
- (ii) denitrifying conditions<sup>lii, lxv</sup>.

There are currently two chemolithoautotrophic arsenite-oxidizing bacteria that have been studied in detail: the aerobe NT-26<sup>lxiv</sup> and the facultative anaerobe MLHE1<sup>lii</sup>. The NT-26 arsenite oxidase (Aro) belongs to the dimethyl sulfoxide (DMSO) reductase family of molybdoenzymes. The enzyme is induced by arsenite and located within the periplasm. AroA (98kDa) is a molybdenum containing  $\alpha$ -subunit and AroB (14kDa) is the small subunit containing a Rieske-type [2Fe-2S] cluster. The amino acid sequence of AroA is 49.2% identical to AsoA from *A. faecalis* and 48.4% identical to AoxB of *C. arsenoxidans*<sup>xlvi</sup>. Additionally, six novel bacterial strains have been described in 2007, which can couple CO<sub>2</sub> fixation to As(III) oxidation under either aerobic or denitrifying conditions<sup>lxvi</sup>, but none have

been studied in depth. Four of these autotrophic arsenite oxidizers are aerobes (*Ancylobacter* sp. strain OL1, *Thiobacillus* sp. strain S1, *Hydrogenophaga* sp. strain CL3, and *Bosea* sp. strain WAO), and two are denitrifiers (*Azoarcus* sp. strain DAO1 and *Sinorhizobium* sp. strain DAO10) which are able to use  $\text{NO}_3^-$  as the respiratory electron acceptor with complete reduction to  $\text{N}_2$  gas<sup>lxv</sup>.

## **1.1.6 Reduction**

### **1.1.6.1 Respiratory arsenate reductases**

There are several microbes that use As(V) as an electron acceptor in dissimilatory anaerobic respiration. These prokaryotes oxidize a variety of organic (e.g. lactate, acetate, formate and aromatics), or inorganic (hydrogen and sulfide) electron donors, resulting in the production of As(III). Anaerobic arsenate respiration was discovered in 1994 with a bacterial isolate that coupled anaerobic heterotrophic growth to arsenate reduction<sup>lxvii</sup> and since then, diverse bacterial types with anaerobic respiratory arsenate reductase have been described<sup>lxviii</sup>,  
lxix.

The anaerobic respiratory arsenate reductase from *Crysiogenis arsenatis* is a heterodimeric, periplasmic or membrane associated protein with a native molecular mass of 123kDa with a  $K_m$  of 300 $\mu\text{M}$ . It consists of a large molybdopterin subunit (ArrA) (87kDa) which contains an iron-sulfur center, possibly a high potential [4Fe-4S] cluster (but is not related to the aerobic arsenite oxidases), and a smaller [Fe-S] center protein (ArrB) (29kDa)<sup>lxx</sup>. Both ArrA and ArrB subunits have a conserved N-proximal cysteine-rich iron-sulphur cluster-binding motif (ArrA, CX<sub>2</sub>CX<sub>3</sub>C; and ArrB, CX<sub>2</sub>CX<sub>2</sub>CX<sub>3</sub>C) and phylogenetic analysis of ArrA and related sequences indicates that ArrA is distantly related to AsoA in the dimethyl sulfoxide (DMSO) oxydoreductase family<sup>lxxi</sup>. ArrB appears to be an iron-sulfur protein related to DmsB of DMSO reductase and NrfC of nitrite reductase<sup>lxxii</sup>.

The arsenate reductase from *Sulfurospirillum barnesii* is a trimeric membrane bound complex with a molecular weight of 120kDa<sup>lxxiii</sup>. This protein has an  $\alpha$  subunit of 65kDa, a  $\beta$  subunit of 31kDa, and a  $\gamma$  subunit of 22kDa. A b-type cytochrome appears to complement membrane fractions. *Desulfomicrobium* strain Ben-RB reduces arsenate by a membrane-bound enzyme, probably associated with a c-type cytochrome of which c55 is the major cytochrome in this organism<sup>lxxiii</sup>.

### 1.1.6.2 Cytoplasmic arsenate reductases

The arsenate reductases (ArsC) from different sources have unrelated sequences and structural folds, and can be divided into different classes on the basis of their structures, reduction mechanisms and the locations of catalytic cysteine residues. ArsC cytoplasmic arsenate reductases are found widely in microbes, and the *arsC* gene occurs in *ars* operons in most bacteria with total genomes measuring 2Mb or larger, as well as in some *Archaeal* genomes<sup>lv</sup>. In bacteria, the resistance determinants are often found on plasmids<sup>lxxiv, lxxv, lxxvi</sup> which has facilitated their study at the molecular level. As more and more bacterial genomes are sequenced, it has become evident that arsenic resistance operons are ubiquitous. Homologous chromosomal systems have also been found and are functional and provide arsenic tolerance<sup>lxxvii, lxxviii</sup>. Three unrelated groups of ArsC sequences are currently recognized (Figure 1.4), and these share a common biochemical function<sup>xxx</sup>.

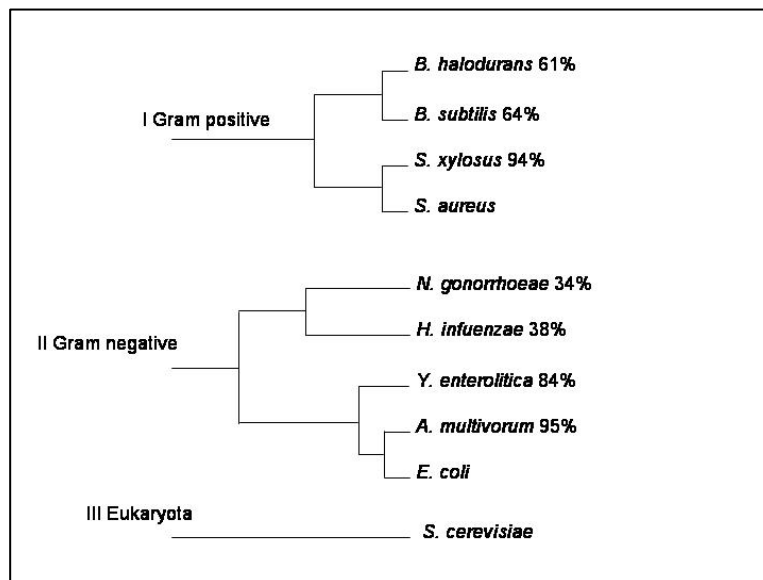


**Figure 1.4** ArsC families from Gram positive bacteria (I), Gram negative bacteria (II), and eukaryota (III). (*Bacillus halodurans*, *B. subtilis*, *Staphylococcus xylosus*, *Neisseria gonorrhoeae*, *Haemophilus influenzae*, *Yersinia enterocolitica*, *Acidiphilium multivorum*. Percentage sequence identity with the model enzyme for each family is indicated. (Interfamilial sequence identity is lower than 20%.)<sup>lxxix</sup>.

The first family, represented by ArsC from *Escherichia coli* plasmid R773 is present on many plasmids and chromosomes of Gram negative bacteria. This is a glutaredoxin-glutathione-coupled enzyme, and has a distinct HX3CX3R catalytic sequence motif that partially resembles crambin and partially glutaredoxin<sup>lxxx</sup>. The thioredoxin-coupled arsenate

reductases form the second family of arsenate reductases and was found initially in Gram positive bacteria, but more recently also in Gram negative proteobacteria. ArsC from *Staphylococcus aureus* plasmid pI258 as model enzyme for this family has a tyrosine phosphatase (PTPase) I fold typical for low molecular weight (LMW) PTPases. It includes a P-loop with the characteristic CX5R sequence motif flanked by a  $\beta$ -strand and an  $\alpha$ -helix<sup>lxxxii</sup>. There is no relationship between the tertiary structures of the glutaredoxin and thioredoxin coupled arsenate reductases, supporting the conclusion that these two classes of enzyme are not related. Both classes of arsenate reductases have a core of four  $\beta$ -strands forming a  $\beta$ -sheet region. The strands are all parallel for the thioredoxin coupled family but with one anti-parallel  $\beta$ -sheet strand for the glutaredoxin coupled ArsC from plasmid R773<sup>lxxxiii</sup>. The third and less-well-defined glutaredoxin-dependent arsenate reductase family is found in yeast (*Saccharomyces cerevisiae*) and also contains the abovementioned motif but is homologous to the human cell cycle control phosphatase Cdc25a<sup>lxxxiii</sup>.

### **1.1.7 Other mechanisms: Biosorption**

The accumulation of toxic metals by bacterial biomass presents an effective means of removing these metals from solution and has been applied in the remediation of several metals such as cadmium<sup>lxxxiv</sup>, copper<sup>lxxxv</sup>, lead, chromium<sup>lxxxvi</sup>, copper, zinc, nickel, cobalt<sup>lxxxvii</sup>, vanadium<sup>lxxxviii</sup> and arsenic<sup>lxxxix</sup>. The complexity of the microorganism's structure implies that there are many ways for the metal to be captured by the cell. Heavy-metal ions can be entrapped in the cellular structure and subsequently biosorbed onto the binding sites present in the cellular structure. Cell walls of microbial biomass, mainly composed of polysaccharides, proteins and lipids, offer particularly abundant metal-binding functional groups, such as carboxylate, hydroxyl, sulfate, phosphate and amino groups<sup>xc</sup>.

According to the dependence on the cells' metabolism, biosorption mechanisms can be divided into (a) non-metabolism dependent / passive uptake and (b) metabolism dependent / active uptake. Furthermore, according to the location where the metal removed from the solution is found, biosorption may be classified as (a) extracellular accumulation, (b) cell surface sorption and (c) intracellular accumulation<sup>xcii</sup>.

## **1.2 Introduction to the present study**

Since the late 19<sup>th</sup> century, South Africa's economy has been based on the production and export of minerals, which, in turn, have contributed significantly to the country's industrial development. The Consolidated Murchinson mine, situated in the Murchison greenstone belt, is located in the Limpopo Province at Gravelotte, some 40 km due west of Phalaborwa. The orebody is contained in a shear zone, being a hydrothermally emplaced occurrence<sup>xcii</sup>. A fold in the earth's crust caused a cleavage, along which there has been a large shear extending deep into the earth's crust and into this, carbon dioxide, silica, antimony and gold were introduced<sup>xciii</sup>. The mine can be classified as a medium-scale mine and has been in operation since 1937, making it the oldest known antimony deposit in the world. It is also the only producer of antimony concentrate in South Africa and accounts for some 8% of the world's antimony production - the largest producer outside China<sup>xciv</sup>. Gold was discovered in the Murchison range towards the end of the nineteenth century, and was mined on a small scale for many years, with antimony as a by-product. The primary antimony ore is stibnite which is crushed and milled and an antimony concentrate is then produced by flotation. Gold is recovered in a gravity circuit and a number of leach and carbon absorption stages<sup>xcv</sup>.

Impurities in the concentrate are a key concern to end-users and in the case of Consolidated Murchison, these are lead and arsenic<sup>xcvi</sup>. Lead, introduced artificially, as lead nitrate is used as an activator for the stibnite in the flotation process. Arsenic, on the other hand, is contained in the ore and cyanide is used to depress the arsenic during flotation<sup>xcvii</sup>. Arsenic removal from the antimony product causes considerable concentration of arsenic in the tailings and currently slag from middlings dumps (with arsenic concentrations of approximately 8g/ton ~1mM) is being reprocessed.

Arsenic and antimony are both transition metal elements of subgroup VA of the periodic table and share both chemical and structural properties with nitrogen, phosphorus and bismuth. The electronic configuration of transition metal elements are characterised as having full outer orbitals and as having the second outermost orbitals incompletely filled. There are five electrons in the valence shells of these elements and thus, the principal oxidation states of these elements are +3 and +5.

### **1.3    Aims**

1.    Site description of an arsenic impacted mining environment for sampling
  - enrichment for and isolation of arsenic resistant bacteria
  - preservation methods of isolated bacteria
  
2.    Identification of bacterial isolates
  - 16S rDNA PCR and sequencing
  - substrate utilisation identification
  
3.    Determining minimum inhibitory growth concentrations of arsenic
  - arsenate - As(V)
  - arsenite - As(III)
  
4.    Growth of arsenic resistant bacteria in arsenate and arsenite
  - effect on biomass production,
  - growth rates,
  - induction of extended lag-phases
  
5.    Demonstrating and quantifying arsenate reduction as a resistance mechanism of arsenic resistant bacteria

## **1.4 Materials and methods**

### **1.4.1 General procedures and chemicals**

Chemicals used were of molecular, analytical or lab reagent grade, were obtained from various commercial suppliers and was used without further purification.

### **1.4.2 Sampling and isolation**

Soil, water and sludge samples were collected aseptically at the Consolidated Murchison antimony mining and refining site in sterile Falcon Tubes or Whirl Packs. In total, 16 sites were sampled and varied from very dry, compacted soil to sludge samples. The average pH of all samples collected was 5.8 (determined by wetting approximately 5g of soil with ddH<sub>2</sub>O and measured with pH indicators) and ambient temperature on the day of collection was approximately 35°C (specific site descriptions are given in Table 1.1). One gram of sample was mixed with 2mL basal medium (0.9g/L NaCl, 0.2g/L MgCl<sub>2</sub>, 0.1g/L CaCl<sub>2</sub>.2H<sub>2</sub>O, pH 7.5) and 400µL of this supernatant inoculated into 5mL TYG medium (5g/L tryptone, 3g/L yeast extract, 1g/L glucose) pH 5.8. TYG medium (5mL) was supplemented with 5mM, 10mM, 50mM and 100mM<sup>xcviii</sup> potassium antimony tartrate and inocula were incubated for two days at 37°C with shaking at 200rpm to enrich for resistant aerobic mesophiles. From this, 500µL supernatant was transferred successively into fresh TYG medium similarly supplemented with potassium antimony tartrate to identify possible positive enrichments by comparing with uninoculated medium. Positive enrichments were streaked on antimony supplemented TYG plates (100mM) and passaged on plates to obtain uniform colonies. Pure cultures were Gram stained<sup>xcix</sup> to confirm purity and were then inoculated into TYG medium containing increasing concentrations of arsenate (Na<sub>2</sub>HAsO<sub>4</sub>) and arsenite (NaAsO<sub>2</sub>) (5mM, 10mM, 50mM and 100mM) to perform a preliminary arsenic resistance screen. Isolates capable of growth in arsenic were used for further experiments.

Table 1.1 Sampling site description.

Sample #	Site description	pH
<b>1-4</b>	<b>Dumping site (very dry)</b>	
1	Red, arsenic rich, ± 1m from surface	5-6
2	Mixed soil, ± 2m from surface	5-6
3	Black, antimony rich, ± 1m from surface	5-6
4	Yellow, gold rich, ± 1m from surface	5-6
<b>5-7</b>	<b>Silt dam # 2</b>	
5	Surface sample with strong sulfur smell	4-5
6	Same as 5 but ± 15cm deep	5
7	Red, arsenic and cyanide rich, ± 15cm deep	6-7
8	Surface sample at penstock	7-8
<b>9-14</b>	<b>Northern wall of silt dam # 2</b>	
9	Logwater from dam # 2	6-7
10	Silt	6
11	Water	6
12	Silt	6
13	Soil ± 3cm deep	6
14	Biofilm	7
<b>15-17</b>	<b>Silt dam # 3</b>	
15	Water	6
16	Water and sludge from hole #5, 30°C	6-7
17	Water and sludge	6

### **1.4.3 Cryopreservation**

Cryopreservation was performed according to the method of Perry (1995)<sup>c</sup>. A single colony was inoculated into TYG medium and grown with shaking at 37°C overnight. The cells were diluted in a 1:1 (v/v) ratio with 40% sterile glycerol and stored at -80°C. All subsequent experiments were inoculated from these cryopreserved cultures.

### **1.4.4 Identification**

#### **1.4.4.1 16S rDNA sequencing**

Genomic DNA from each isolate was extracted with DNA<sub>ZOL</sub><sup>TM</sup> Reagent (Gibco BRL): cells were harvested by centrifugation, frozen and thawed once, resuspended in TE-buffer, pH



8.0 and an equal volume of DNA<sub>ZOL</sub> added. Lysozyme was added to a final concentration of 5mg/mL and incubated at 37°C with vigorous shaking for 30 minutes and thereafter at 55°C for 30 minutes with shaking. Proteinase K, to final concentration of 0.35mg/mL, was added and incubated at 37°C with vigorous shaking for 30 minutes. An equal volume of chloroform : isoamyl alcohol (24:1) was added and mixed by vortexing. Phase separation was performed by centrifugation at 10 000rpm for 15 minutes and genomic DNA in the supernatant precipitated with 0.5 volumes of ice cold 100% ethanol and centrifugation. Recovered DNA was washed with 70% cold ethanol and resuspended in 5mM Tris-HCl, pH 8.0.

16S rDNA fragments were amplified using universal bacterial primers 27F and 1492R<sup>ci</sup> (Table 1.2). PCR reactions consisted of 1X Reaction Buffer, 2.5U DNA Polymerase (SuperTherm), 2mM MgCl<sub>2</sub>, 200nM of each primer, 200µM of each dNTP and approximately 50ng template DNA. Amplification was performed after an initial denaturation step at 94°C for 5 minutes and thereafter 35 cycles of denaturing at 94°C for 30 seconds, primer annealing at 52°C for 45 seconds and product extension at 72°C for 1 minute. A final polishing extension was performed at 72°C for 7 minutes. PCR products were ligated into the pGem<sup>®</sup>T-Easy vector (Promega) followed by transformation into chemically competent *E. coli* JM109 cells<sup>cii</sup>. Selection was performed on LB-AIX-plates (10g/L tryptone, 5g/L yeast extract, 10g/L NaCl amended with 60µg/mL ampicillin, 9.6µg/mL IPTG (isopropyl-β-D-thiogalactopyranoside) and 40µg/mL X-gal (5-bromo-4-chloro-3-indolyl-β-D-galactoside)). Plasmids were extracted using the Wizard<sup>®</sup> Plus Miniprep DNA Purification System (Promega) and inserts of the correct size were identified by restriction analysis. The plasmid DNA (200µg) was digested at 37°C for 2 hours in a reaction mixture containing 10U *Eco*RI by combining with 1X Reaction Buffer (50mM NaCl, 100mM Tris-HCl pH 7.5, 10mM MgCl<sub>2</sub>, 0.025% Triton X-100, 100µg/mL BSA). Sequencing was performed using primers T7, Sp6 as well as internal primers U514F, Bac341F, EUB338, 915R (Table 1.2) with a BigDye<sup>®</sup> Terminator v3.1 Cycle Sequencing Kit (Applied Biosystems) on an ABI377 DNA Sequencer (PE Biosystems). The sequences obtained were aligned with that of bacteria previously found in the subsurface of mining environments as well as the closest matches revealed with BLAST searches<sup>ciii</sup>, and at RDP<sup>civ</sup> with ClustalX (1.83)<sup>cv</sup>. A heuristic search was performed with PAUP 4.0b5<sup>cvi</sup> and yielded 10 000 parsimonious trees. A strict consensus tree was constructed and rooted with the outgroup *Aquifex pyrophilus*. Bootstrap analysis of 100 replicates was done to determine the robustness of the clades / groups. The bootstrap cut-off was 50%<sup>cvi</sup>. A bootstrap value greater than 75% was considered good support. Values of 65% - 75% were considered moderate support and less than 65% as weak.

**Table 1.2 Nucleotide sequence and positioning information of the primers used to amplify and sequence 16S rDNA amplicons.**

Name	Sequence (5'-3')	Position <i>E. coli</i> 16S rDNA	Reference
27F	AGAGTTTGATCMTGGCTCAG	27	
1492R	GGTTACCTTGTTACGACTT	1492	Lane <i>et al.</i> (1991) <sup>ci</sup>
U514F	GTGCCAGCMGCCGCGG	514	
Bac341F	CCTACGGGAGGCAGCAG	341	Muyzer <i>et al.</i> (1993) <sup>cviii</sup>
EUB338	GCTGCCTCCCGTAGGAGT	338	Davis <i>et al.</i> (2005) <sup>cix</sup>
915R	GTGCTCCCCCGCCAATTCCT	915	Casamayor <i>et al.</i> <sup>cx</sup>
T7 Promoter	TAATACGACTCACTATAGGG		
Sp6 Promoter	TATTTAGGTGACACTATAG		

#### 1.4.4.2 Biochemical testing

Isolates were streaked on TYG-plates (pH 5.8) amended with 10mM arsenate. Nutritional requirements and the use of specific carbon sources for growth were tested with GN2 and GP2 MicroPlates™ (Biolog, Hayward). Following incubation at 37°C, positive test results were recorded at 16h and 24h, respectively where a similarity index greater than 0.5 was considered positive identification. API 20E panels (bioMerieux, Inc.) were also used to confirm the identification.

#### 1.4.5 Minimum inhibitory concentrations

Bacteria were inoculated into 50mL of TYG medium, pH 5.8 and grown at 37°C as a pre-inoculum. From this, TYG medium (pH 5.8), amended with increasing concentrations of arsenite (ranging from 2.5mM to 15mM) and arsenate (0.5mM to 500mM) were inoculated in duplicate with exponential growth phase cells, to an optical density of approximately 0.1 at 560nm. Flasks containing TYG medium with arsenic omitted were used as negative controls. Inocula were grown at 37°C with shaking, samples withdrawn hourly and optical density monitored at 560nm over a 12h period.

## **1.4.6 Arsenate reduction**

### **1.4.6.1 Qualitative**

Bacteria were grown overnight at 37°C in 100mL TYG medium containing 1mM Na<sub>2</sub>HAsO<sub>4</sub>. Cells were harvested by centrifugation in a Beckman J2-MC centrifuge at 11000 x g for 10 minutes at 4°C. The cells were washed in 10mM PIPES buffer, pH 6.5 and resuspended in the same buffer in a 1:1 cell wet weight to volume ratio. This was then supplemented with 0.2% glucose (w/v) (approximately 10mM) and 10mM arsenate and incubated at 37°C<sup>cxii</sup>. Aliquots were withdrawn periodically over a two day period, centrifuged, the supernatant removed and stored at -20°C until further analysis. Supernatant was spotted onto Silica gel 60 F<sub>254</sub> TLC sheets (Merck), overlaid with 5µL of 100mM DTT to enhance separation<sup>cxii</sup>, and developed in 1:1 (v/v) EtOH : NH<sub>4</sub>OH. After drying, the plates were sprayed with 2% (w/v) AgNO<sub>3</sub><sup>cxiii</sup>. Separation profiles were compared to As(III) and As(V) controls for identification. A negative control, without any cells, was employed to monitor chemical reduction.

### **1.4.6.2 Quantitative**

The same procedure as described in the preceding section (1.4.6.1) was followed, but the separated As(III) was recovered from the silica matrix and assayed using a modified molybdate assay for phosphate<sup>cxiv</sup>.

To quantify arsenate reduction, aliquots of 50µL (SIL-20A auto sampler, Shimadzu) of the supernatant were analyzed by HPLC (LC-20AT liquid chromatograph, Shimadzu) injected onto a Hamilton PRP X-100 column. The mobile phase consisted of 12mM H<sub>3</sub>PO<sub>4</sub>, pH 3.2, and the products were eluted isocratically at a constant temperature of 30°C (CTO-10AS column oven, Shimadzu). Both substrate depletion (arsenate) and product formation (arsenite) were determined at 195nm (SPD-20AV UV/vis detector, Shimadzu). A negative control, without any cells, was employed to monitor chemical reduction.

## **1.5 Results and discussion**

### **1.5.1 Enrichments**

Soil, water and sludge samples from 16 sites were inoculated to enrich for resistant bacteria. Samples from six sites (10, 12, 14 -17) showed growth in medium amended with 100mM potassium antimony tartrate (Table 1.3) and were successively streaked out to obtain pure cultures. These cultures were named according to site collection numbers.

**Table 1.3 Growth for pure cultures inoculated into antimony supplemented TYG medium.**

<b>Sample #</b>	<b>0mM</b>	<b>5mM</b>	<b>10mM</b>	<b>50mM</b>	<b>100mM</b>
1	-	-	-	-	-
2	-	-	-	-	-
3	-	-	-	-	-
4	√	√	-	-	-
5	√	√	-	-	-
6	√	√	-	-	-
7	√	√	-	-	-
8	√	-	-	-	-
9	√	√	-	-	-
10	√	√	√	√	√
11	√	√	-	-	-
12	√	√	√	√	√
13	√	√	-	-	-
14	√	√	√	√	√
15	√	√	√	√	√
16	√	√	√	√	√
17	√	√	√	√	√

Site 10 yielded 2 isolates, while the bacteria from sample 12 lost resistance during the purification, possibly due to syntrophy within the bacterial consortium. All six pure cultures were screened for arsenic resistance in liquid medium amended with arsenate and arsenite. The bacteria were more resistant to arsenate than arsenite and three of the isolates (10(2), 16, 17) were resistant to up to 100mM arsenate while isolates 15, 16 and 17 were resistant to 10mM arsenite (Table 1.4).

**Table 1.4 Growth for pure cultures in arsenate and arsenite supplemented TYG medium.**

Sample #	Arsenate				Arsenite			
	5mM	10mM	50mM	100mM	5mM	10mM	50mM	100mM
10(1)	√	-	-	-	√	-	-	-
10(2)	√	√	√	√	√	-	-	-
14	√	-	-	-	√	-	-	-
15	√	√	√	-	√	√	-	-
16	√	√	√	√	√	√	-	-
17	√	√	√	√	√	√	-	-

### **1.5.2 Identification**

Amplification of the 16S rDNA sequence from these isolates yielded PCR products of the expected size of approximately 1500bp (Figure 1.5). Near full length sequences were deposited in the NCBI database and compared with BLAST (software version 2.2.13, National Center for Biotechnology Institute, <http://www.ncbi.nlm.nih.gov/BLAST/>) analysis to entries available at the EMBL, GenBank, and Ribosomal Data Project (release 9.35, <http://rdp.cme.msu.edu/>). Table 1.5 shows the closest sequence matches, % identity and RDP scores of the 16S rDNA gene from each of the pure cultures.

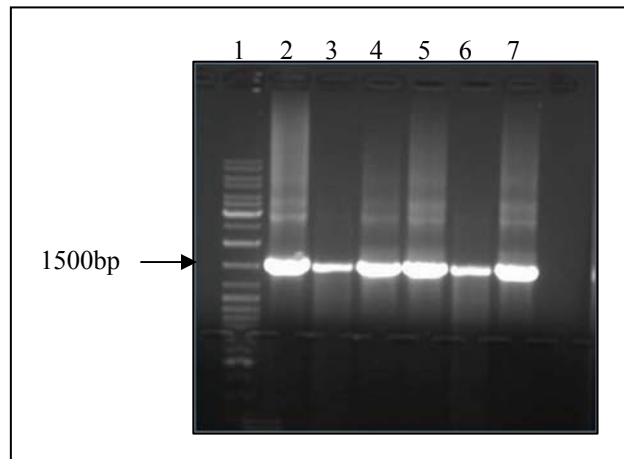


**Figure 1.5 16S rDNA PCR products from arsenic resistant pure cultures. Lane 1: GeneRuler™ molecular weight marker, Lane 2: isolate 10(1), Lane 3: isolate 10(2), Lane 4: isolate 14, Lane 5: isolate 15, Lane 6: isolate 16, Lane 7: isolate 17.**

**Table 1.5** Closest sequence matches for 16S rDNA genes of pure cultures.

Isolate #	Accession #	Length (bp)	BLAST % Identity	RDP Score %	Closest match
10(1)	DQ079060	1401	99	0.993	<i>Bacillus cereus</i> EU169167 / <i>Bacillus thuringiensis</i> AB363741
10(2)	AY566180	1504	99	0.992	<i>Serratia marcescens</i> AB061685
14	DQ079058	1409	99	0.981	<i>Bacillus cereus</i> EU169167 / <i>Bacillus thuringiensis</i> AB363741
15	DQ079059	1439	99	0.951	<i>Stenotrophomonas maltophilia</i> EF580914
16	AY551938	1506	98	0.951	<i>Serratia marcescens</i> AB061685
17	DQ079057	1386	99	0.971	<i>Serratia marcescens</i> AY043386

Three isolates (*Bacillus* sp. SA Ant 14, *S. maltophilia* SA Ant 15 and *S. marcescens* SA Ant 16) were used for further investigations. Sequencing results are illustrated by the phylogenetic tree (Figure 1.6) generated with 16S rDNA sequences as described in section 1.4.4.1. Biochemical identification was repeated with API panels and Biolog MicroPlate™ testing and confirmed isolate SA Ant 16 as *Serratia marcescens* with a similarity index of 0.58. It was not possible to definitively identify isolates SA Ant 14 and SA Ant 15 using biochemical testing with the Microlog™ software and database.

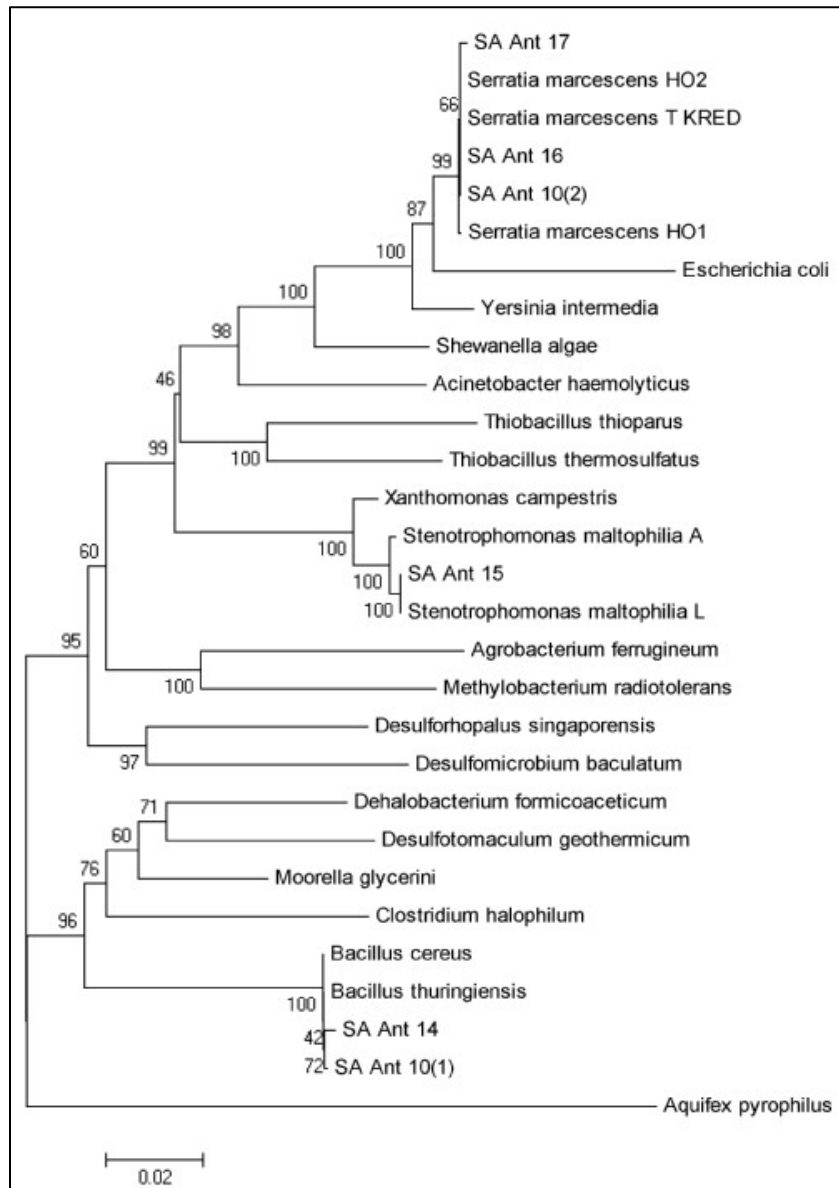


**Figure 1.6** Phylogenetic tree generated with 16S rDNA PCR sequences. (*Bacillus cereus* AF290547; *Bacillus thuringiensis* Z84588; *Moorella glycerini* U82327; *Dehalobacterium formicoaceticum* X86690; *Desulfotomaculum geothermicum* X80789; *Clostridium halophilum* X77837; *Desulforhopalus singaporensis* AF118453; *Desulfomicrobium baculatum* AF030438; *Serratia marcescens* HO2-A AJ297950; *Serratia marcescens* (T) KRED AB061685; *Serratia marcescens* HO1-A AJ 297946; *Escherichia coli* AY776275; *Yersinia intermedia* (ER-3854) X75279; *Shewanella alga* X81622; *Acinetobacter haemolyticus* X81662; *Stenotrophomonas maltophilia* ATCC 19861T AB021406; *Stenotrophomonas maltophilia* LMG 10989 AJ131907; *Xanthomonas campestris* AJ811695; *Thiobacillus thioparus* M79426; *Thiobacillus therosulfatus*, U27839; *Agrobacterium ferrugineum* D88522; *Methylobacterium radiotolerans* D32227; *Aquifex pyrophilus* M83548.)

### **1.5.3 Minimum inhibitory concentration**

The bacteria exhibited different tolerance levels for both arsenite and arsenate, and with the exception of *Bacillus* sp. SA Ant 14, it was found that these bacteria were hyper-tolerant and could grow in exceptionally high concentrations of arsenate, (up to 500mM ~ 38000ppm) and also high concentrations of arsenite (up to 10mM ~ 770ppm). *Bacillus* sp. SA Ant 14 was able to grow in concentrations of arsenic below 5mM, *S. maltophilia* SA Ant 15 grew in 'moderate' arsenic concentrations (up to 10mM arsenite and 20mM arsenate respectively), while *S. marcescens* SA Ant 16 was able to grow in 'moderate' concentrations of arsenite, but was able to grow in up to 500mM arsenate. (Results are summarised in Table 1.6.) A model bacterium such as *E. coli* has been shown to grow in up to 50mM arsenate<sup>cxv</sup>, while bacteria isolated from arsenic contaminated sites in New Zealand were not able to grow in arsenite concentrations exceeding 45mM and arsenate above 50mM<sup>cxvi</sup>. Reports of resistance to arsenic in eukaryotes are in the range of 1.2mM arsenite and 6mM arsenate for *Saccharomyces cerevisiae*<sup>cxvii</sup>, 1500ppm chromated copper arsenate (approximately 20mM) for *Pteris vittata* (brake fern)<sup>cxviii</sup> and 200mM arsenate for an *Aspergillus* strain isolated from a heavily contaminated river in Spain<sup>cxix</sup>. *Corynebacterium glutamicum* is able to grow in medium containing up to 12mM arsenite and 500mM arsenate<sup>cxx</sup>. It is therefore clear that *S. marcescens* SA Ant 16 isolated during this study represents one of the most arsenate tolerant prokaryote described to date.



**Table 1.6** Effect of increasing concentrations arsenite or arsenate on biomass yield, maximum specific growth rate and lag phase for *Bacillus* sp. SA Ant 14, *S. maltophilia* SA Ant 15 and *S. marcescens* SA Ant 16 grown for 12 hours.

		Concentration (mM)	Biomass (12 h) (mg/mL dry weight)	Max. Specific Growth Rate (/h)	Lag Phase (h)
<i>Bacillus</i> sp. SA Ant 14	TYG		0.48	0.19	4
	As (III)	2.5	0.55	0.25	4
		5	0.64	0.24	5
		6.5	0.07	0.03	6
	As(V)	0.5	0.49	0.20	5
		1	0.53	0.23	4
		2.25	0.53	0.20	6
		4	0.10	0.31	8
<i>S. maltophilia</i> SA Ant 15	TYG		1.41	0.30	-
	As(III)	2.5	1.14	0.27	-
		5	0.23	0.15	-
		7.5	0.33	0.10	-
		10	0.21	0.06	-
	As(V)	5	1.06	0.30	-
		10	0.98	0.22	5
		20	0.87	0.20	6
100		0.04	0.04	10	
<i>S. marcescens</i> SA Ant 16	TYG		1.50	0.42	-
	As(III)	2.5	1.42	0.44	-
		5	1.36	0.37	-
		10	1.23	0.23	-
		15	0.09	0.08	-
	As(V)	20	1.32	0.21	1
		100	0.97	0.18	1
		150	0.87	0.19	1
300		0.47	0.12	2	
500		0.08	0.04	6	

Both biomass and specific growth rate of *Bacillus* sp. SA Ant 14 showed an increasing trend in the presence of arsenite, below 6.5mM (Figure 1.7). During growth in increasing concentrations of arsenate, *Bacillus* sp. SA Ant 14 had comparable biomass yields after 12h of growth in both arsenite and arsenate. Considerably higher maximum specific growth rates were also observed. Possible explanations such as contamination was ruled out by microscopic

investigation; the arsenic amendments were in too high concentrations to be able to act as micronutrients to stimulate growth; and since the cells were grown aerobically, it is not possible that the arsenic ions could function as either electron donor or -acceptor. In terms of conventional bioenergetic systems this stimulation of growth is difficult to rationalize. Anderson and Cook<sup>cxxi</sup> observed a similar trend when growing arsenate reducing bacteria (*Aeromonas* and *Exiguobacterium*) in rich medium, but not when grown in chemically defined medium. The mechanism and rationale for this phenomenon remains unexplained.

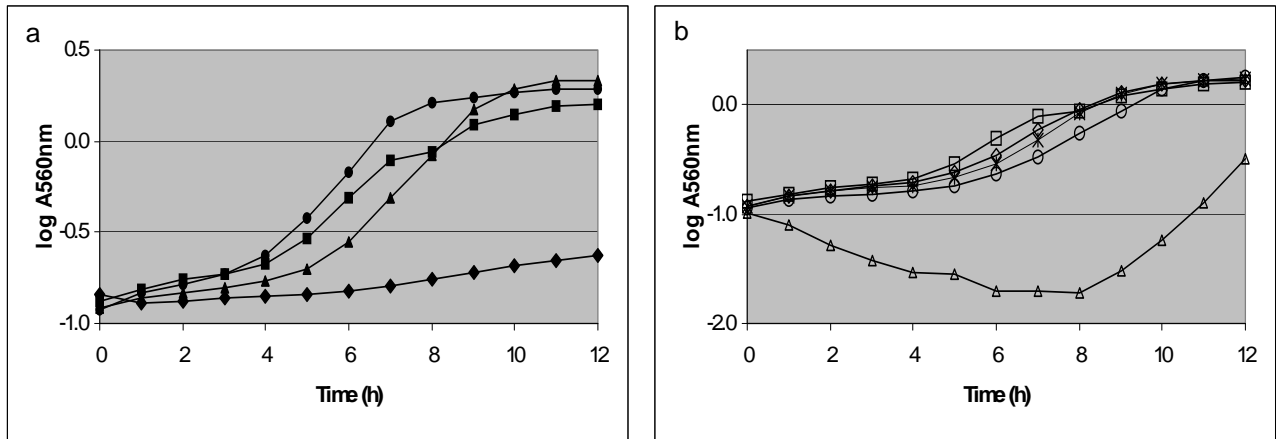


**Figure 1.7** Growth of *Bacillus* sp. SA Ant 14 in absence and presence of arsenite (a) (■ TYG; ● 2.5mM; ▲ 5mM; ◆ 6.5mM) and arsenate (b) (□ TYG; ◇ 0.5mM; \* 1mM; ○ 2.25mM; △ 4mM). Error bars are too small to be indicated.

Both the specific growth rate and biomass yield was severely inhibited for *S. maltophilia* SA Ant 15 in the presence of arsenite. Arsenate inhibited growth to a much lesser extent, as indicated by specific growth rate and biomass yield, but an increasing lag phase was observed with increasing concentrations of arsenate (Figure 1.8).

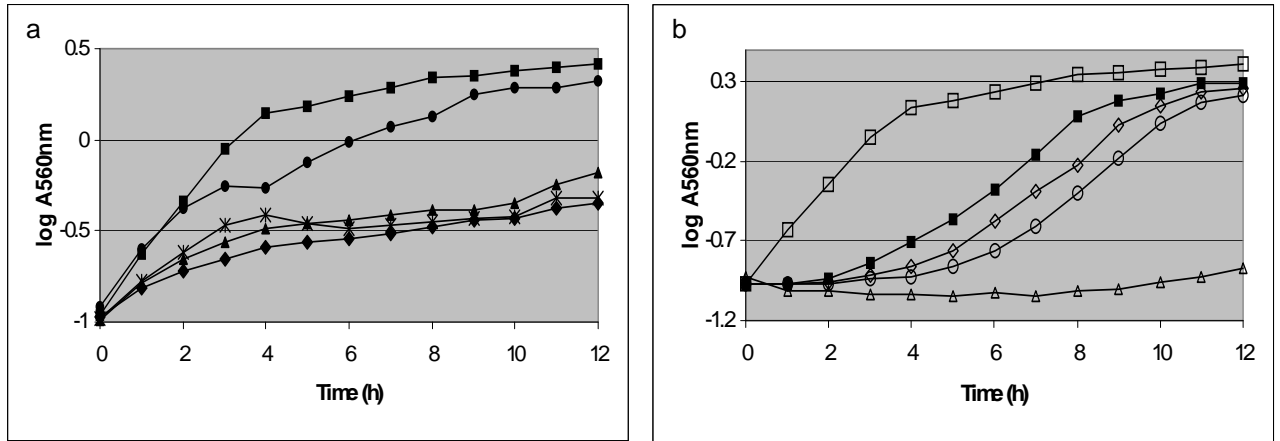


**Figure 1.8** Growth of *S. maltophilia* SA Ant 15 in absence and presence of arsenite (a) (■ TYG; ● 2.5mM; \* 5mM; ▲ 7.5mM; ◆ 10mM) and arsenate (b) (□ TYG; ■ 5mM; ◇ 10mM; ○ 20mM; △ 100mM). Error bars are too small to be indicated.

For *S. marcescens* SA Ant 16, addition of arsenite resulted in a decrease in both specific growth rate and biomass up to a threshold concentration above 10mM, whereafter a sharp decline in both these parameters were observed. Addition of arsenate resulted in a lag phase that lengthened with increasing concentrations. A linear decrease in biomass yield was seen after 12h of growth as well as a decline in specific growth rate up to 500mM arsenate (Figure 1.9).

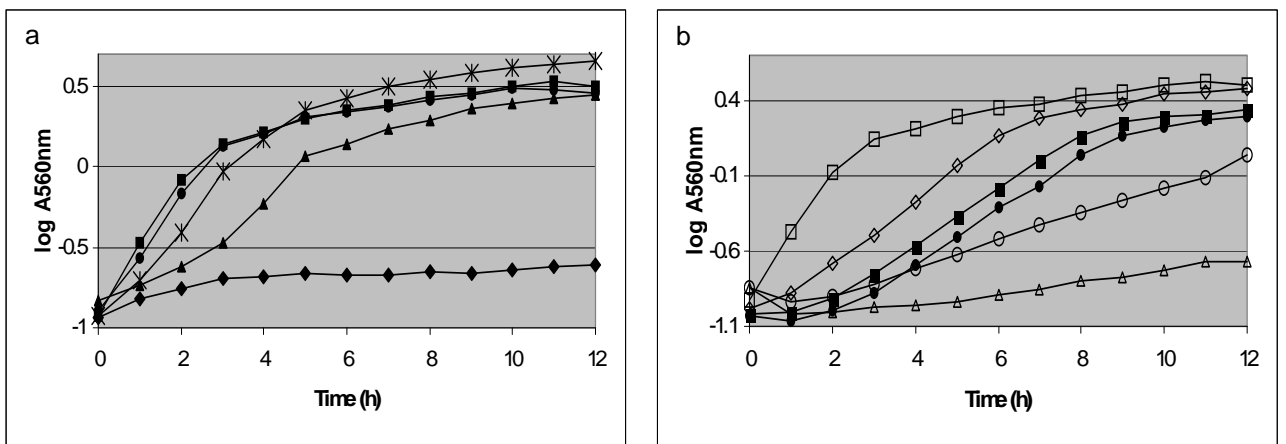


**Figure 1.9** Growth of *S. marcescens* SA Ant 16 in absence and presence of arsenite (a) (■ TYG; ● 5mM; \* 7.5mM; ▲ 10 mM; ◆ 15mM) and arsenate (b) (□ TYG; ◇ 20mM; ■ 100mM; ● 150mM; ○ 300mM; △ 500mM). Error bars are too small to be indicated.

Longer lag phases could be indicative of an initial adaptation phase where, for example, arsenate could be adsorbed or reduced to arsenite. Lower growth rates and biomass are likely results of the toxicity of arsenate or the inhibitory effects of arsenite formed by reduction. External factors might also play an auxiliary role in the exceptionally high resistance to arsenate. Acidification of the culture medium by arsenate resistant bacteria during growth has been demonstrated with an increase in the external pH as a result of arsenate reduction<sup>cxvi</sup>. This ‘neutralization’ of the medium might prevent the pH from decreasing to a point where the bacteria are no longer able to grow and therefore indirectly enable the bacteria to survive at higher concentrations.

#### **1.5.4 Arsenate reduction by resting cells**

The ability of cells to reduce arsenate to arsenite under resting conditions was determined by TLC (Figure 1.10). Quantitative arsenate reduction was initially monitored by recovering As(III) from the TLC plates and performing a modified phosphate assay. However, this progression of testing showed poor reproducibility and HPLC-analysis was performed as an alternative.

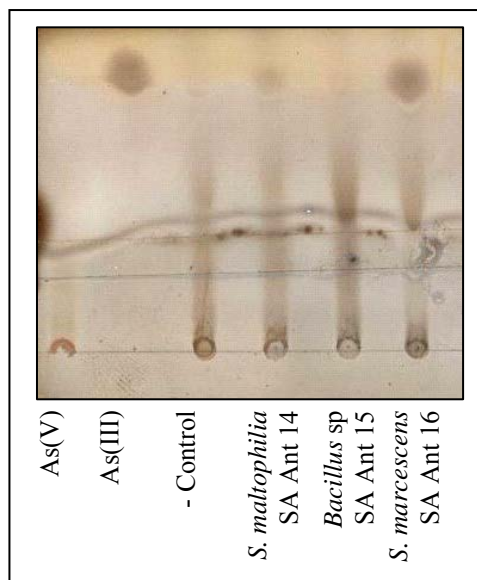


**Figure 1.10** TLC plate demonstrating arsenate reduction to arsenite by resting cells of *Bacillus* sp. SA Ant 14, *S. maltophilia* SA Ant 15 and *S. marcescens* SA Ant 16.

No chemical reduction was observed under this set of experimental conditions (results not shown). All three the bacterial isolates were able to reduce arsenate and extrude the resulting arsenite, but it is clear that this is not the only resistance strategy employed to cope

with arsenate, as a significant portion of arsenate removed (69 – 77%) was not recovered as arsenite, especially in the case of the *Bacillus* sp. (Figure 1.11 a, b and c).

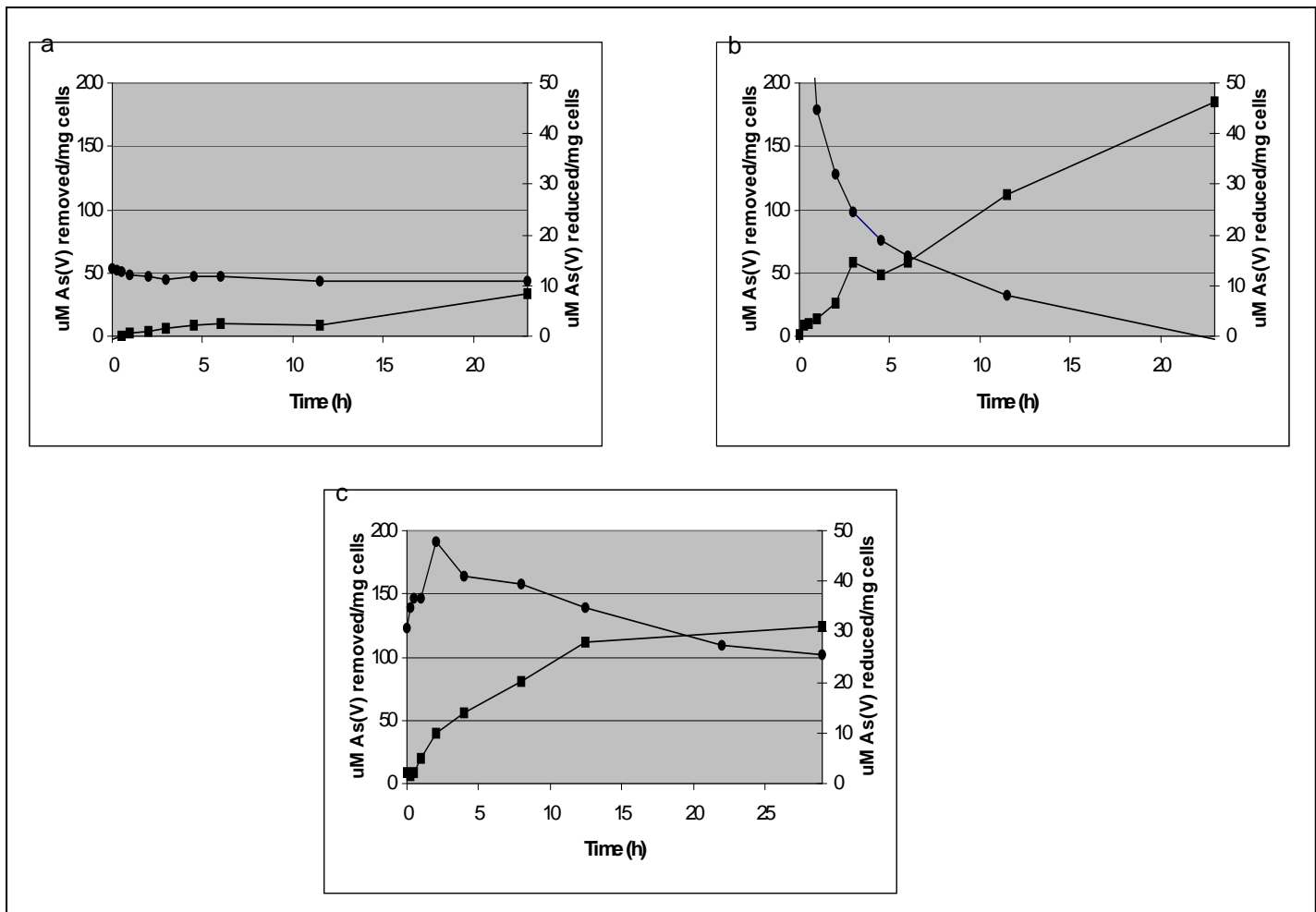


**Figure 1.11** Reduction of arsenate (●) to arsenite (■) by resting cells of (a) *Bacillus* sp. SA Ant 14 (b) *S. maltophilia* SA Ant 15 (c) and *S. marcescens* SA Ant 16.

A summary of the results are presented in Table 1.7. Removal of arsenate from the solution did not correlate with arsenite appearing and therefore it has to be deduced that an alternative resistance mechanism to arsenate, additional to reduction, is being employed. *Bacillus* sp. SA Ant 14 was able to remove approximately 80% of the arsenate supplied in a very short period of time, but only 4% was converted to arsenite at a reduction rate of 0.3 $\mu$ M/h/mg cells. *S. maltophilia* SA Ant 15 was able to remove all of the arsenate at a rate of 92.4 $\mu$ M/h/mg cells over the first 2h and thereafter by reducing approximately 25% to arsenite at 4 $\mu$ M/h/mg cells. *S. marcescens* SA Ant 16 removed 50% of the arsenate by reducing 15% to arsenite at approximately 2 $\mu$ M/h/mg cells.

**Table 1.7** Arsenate removal by whole cells of *Bacillus* sp. SA Ant 14, *S. maltophilia* SA Ant 15 and *S. marcescens* SA Ant 16 during resting conditions. (Arsenate removed and arsenite formed are expressed as percentages of the total of 10mM initially added. Removal and reduction rates are defined as arsenate (substrate) utilised and arsenite (product) formed.)

	<i>Bacillus</i> sp. SA Ant 14	<i>S. maltophilia</i> SA Ant 15	<i>S. marcescens</i> SA Ant 16
<b>% As(V) Removed</b>	78.3	100	49.3
<b>% As(III) Formed</b>	4.2	23.2	15.5
<b>Removal Rate (<math>\mu\text{M}/\text{h}/\text{mg}</math> cells)</b>	0.4	92.4 (0 – 2h) 4.1	3.7
<b>Reduction Rate (<math>\mu\text{M}/\text{h}/\text{mg}</math> cells)</b>	0.3	2	2.1

In addition to reduction, alternative resistance possibilities exist, such as adsorption of the negatively charged arsenic ions (both arsenate and arsenite) to oppositely charged amino groups in the bacterial cell walls<sup>cxxii, cxxiii</sup>. For the Gram positive *Bacillus* sp. the ability of the cell walls to sequester a large range of dilute metal ions from the environment has been well documented<sup>cxxiv</sup>, and in a separate study, biosorption by isolates from the same sampling site has been demonstrated<sup>cxxv</sup>. It is also possible that after reduction, the resulting arsenite can be sequestered by a range of cysteine-rich peptides such as  $\gamma$ -glutamylcysteine and glutathione<sup>cxxvi</sup> or methylated<sup>cxxvii</sup>.

It is important to interpret the resistance to arsenate in the context of a dynamic system where both the influence of the initial oxyanion amendment and the effect of products resulting from biological transformations should be taken into account.

## **1.6 Literature cited**

- 
- i Smedley PL & Kinniburgh DG (2002). A review of the source, behavior and distribution of arsenic in natural waters. *Appl Geochem* 17: 517-568
- ii Cullen WR & Reimer KJ (1989). Arsenic speciation in the environment. *Chem Rev* 89: 713-764
- iii Azcue JM & Nriagu JO (1994) Arsenic, historical perspectives. In: *Arsenic In the Environment*. Vol 26 (Nriagu JO Ed.). Wiley & Sons, New York, N.Y. pp 1-16
- iv Szinicz L & Forth W (1988). Effect of As<sub>2</sub>O<sub>3</sub> on gluconeogenesis. *Arch Toxicol* 61: 444-476
- v Liu SX, Athar M, Lippai I, Waldern C & Hei TK (2001). Induction of oxyradicals by arsenic: implication for mechanism of genotoxicity. *Proc Natl Acad Sci USA* 98: 1643-1648
- vi Barrett J, Hughes MN, Karavaiko GI & Spencer PA (1993). *Metal Extraction by Bacterial Oxidation of Minerals*. Ellis Horwood Ltd., England
- vii Dean JA (1985). Proton-transfer reactions of inorganic materials in water at 25°C. In: *Lange's Handbook of Chemistry*. 13th edn. (Dean JA, Ed). McGraw Hill, New York N.Y. pp. 5-14
- viii Loehr TM & Plane RA (1968). Raman spectra and structures of arsenious acid and arsenites in aqueous solution *Inorg Chem* 7: 1708-1714
- ix Cervantes C, Ji G, Ramirez JL & Silver S (1994). Resistance to arsenic compounds in microorganisms. *FEMS Microbol Rev* 15: 355-367
- x Nakamuro K & Sayato Y (1981). Comparative studies of chromosomal aberrations induced by trivalent and pentavalent arsenic. *Mutat Res* 88: 73-80
- xi Turpein R, Pantsar-Kallio M, Haggblom M & Kairesalo T (1999). Influence of microbes on the mobilization, toxicity and biomethylation of arsenic in soil. *Sci Total Environ* 236: 173-180
- xii Lee TC, Oshimara M & Barrett JC (1985). Comparison of arsenic induced cell transformation, cytotoxicity, mutation and cytogenetic effects in syrian hamster embryo cells in culture. *Carcinogenesis* 6: 1421-1426
- xiii Lee TC, Tanaka N, Lamb PW, Gilmer TM & Barrett JC (1988). Induction of gene amplification by arsenic. *Science* 241: 79-81
- xiv Tezuka M, Hanioka K, Yamanaka K & Okada, S (1993). Gene damage induced in human alveolar type II (L-132) cells by exposure to dimethylarsinic acid. *Biochem Biophys Res Commun* 191: 1178-1183
- xv Caltabiano MM, Koestler TP, Poste G & Greig RG (1986). Induction of 32- and 34kDa stress proteins by sodium arsenite, heavy metals and thiol reactive agents. *J Biol Chem* 261: 13382-13386
- xvi Deaton MA, Bowman PD, Jones GP & Powanda MC (1990). Stress protein synthesis in human keratinocytes treated with sodimn arsenite, phenyldichloroarsine, and nitrogen mustard. *Fund Appl Toxicol* 14: 471-476
- xvii Leonard A & Lauwerys RR (1980). Carcinogenicity, teratogenicity and mutagenicity of arsenic. *Mutat Res* 75: 49-62
- xviii Pershagen G (1985). Lung cancer mortality among men living near arsenic-emitting smelters. *Am J Epidemiol* 122: 684-694
- xix Shneidman D & Belizaire R (1986). Arsenic exposure followed by the development of dermatofibrosarcoma protuberans. *Cancer* 58: 1585-1587

- 
- xx Bates MN, Smith AH & Hopenhayn-Rich C (1992). Arsenic ingestion and internal cancers: a review. *Am J Epidemiol* 135: 462-476
- xxi Silver S (1983). Bacterial interaction with mineral cations and anions: Good ions and bad. In: *Biomineralization and Biological Metal Accumulation* (Westbroek P & de Jong EW, Eds.), D Reidel, Dordrecht pp. 439-457
- xxii Ji G & Silver S (1995). Bacterial resistance mechanisms for heavy metals of environmental concern. *J Ind Microbiol* 14: 61-75
- xxiii Nies DH & Silver S (1995). Ion efflux systems involved in bacterial metal resistances. *J Ind Microbiol* 14: 186-199
- xxiv Nies DH (1999). Microbial heavy-metal resistance. *Appl Microbiol Biotechnol* 51: 730-750
- xxv Rensing C, Ghosh M & Rosen BP (1999). Families of soft-metal-ion-transporting ATPases. *J Bacteriol* 181: 5891-5897
- xxvi Bruins MR, Kapil S & Oehme FW (2000). Microbial resistance to metals in the environment. *Ecotoxicol and Environ Safety* 45: 198-207
- xxvii Silver S, Ji G, Broer S, Dey S, Dou D & Rosen BP (1993). Orphan enzyme or patriarch of a new tribe: the arsenic resistance ATPase of bacterial plasmids. *Mol Microbiol* 8: 637-642
- xxviii Silver S & Walderhaug M (1992). Regulation of chromosomal and plasmid cation and anion transport systems. *Microbiol Rev* 56: 1-33
- xxix Knowles FC & Benson AA (1983). The biochemistry of arsenic. *Trends Biochem Sci* 8: 178-180
- xxx Mukhopadhyay R, Rosen BP, Phung LT & Silver S (2002). Microbial arsenic: from geocycles to genes. *FEMS Microbiol Rev* 26: 311-325
- xxxi Willsky GR & Malamy MH (1980). Characterization of two genetically separable inorganic phosphate transport systems in *Escherichia coli*. *J Bacteriol* 144: 356-365
- xxxii Rosenberg H, Gerdes RG & Chegwidden K (1977). Two systems for the uptake of phosphate in *Escherichia coli*. *J Bacteriol* 131: 505-511
- xxxiii Gatti D, Mitra B & Rosen BP (2000). *Escherichia coli* soft metal ion translocating ATPases. *J Biol Chem* 275: 34009-34012
- xxxiv Sanders OI, Rensing C, Kuroda M, Mitra B. & Rosen BP (1997). Antimonite is accumulated by the glycerol facilitator GlpF in *Escherichia coli*. *J Bacteriol* 179: 3365-3367
- xxxv Borgnia M, Nielsen S, Engel A & Agre P (1999). Cellular and molecular biology of the aquaporin water channels. *Annu Rev Biochem* 68: 425-458
- xxxvi Challenger F (1951). Biological methylation. *Adv Enzymol* 12: 429-491
- xxxvii NiDhubghaill OM & Sadler PJ (1991). The structure and reactivity of arsenic compounds: biological activity and drug design. *Struct Bond* 78: 129-190
- xxxviii Aposhian HV (1997). Enzymatic methylation of arsenic species and other new approaches to arsenic toxicity. *Annu Rev Pharmacol Toxicol* 37: 397-419
- xxxix Hall LL, George SE, Kohan MJ, Styblo M & Thomas DJ (1997). *In vitro* methylation of inorganic arsenic in mouse intestinal cecum. *Toxicol Appl Pharmacol* 147: 101-109
- xl Bentley R & Chasteen TG (2002). Microbial methylation of metalloids: arsenic, antimony and bismuth. *Microbiol Mol Biol Rev* 66: 250-271
- xli Bryant MP, Wolin EA, Wolin MJ & Wolfe RS (1967). *Methanobacillus omelianskii*, a symbiotic



- 
- association of two species of bacteria. Arch Mikrobiol 59: 20-31
- xlii McBride BC & Wolfe RS (1971). Biosynthesis of dimethylarsine by a methanobacterium. Biochem 10: 4312-4317
- xliii Vidal FV & Vidal VMV (1980). Arsenic metabolism in marine bacteria. Mar Biol 60: 1-7
- xliv Shariatpanahi M, Anderson AC, Abdelghani AA, Englande AJ, Hughes J & Wilkinson RF (1981). Biotransformation of the pesticide, sodium arsenate. J Environ Sci Health 16: 35-47
- xlv Qin J, Rosen BP, Zhang Y, Wang G, Franke S & Rensing C (2006). Arsenic detoxification and evolution of trimethylarsine gas by a microbial arsenite S-adenyosylmethionine methyltransferase. Proc Natl Acad Sci USA 103: 2075-2080
- xlvi Green HH (1918). Description of a bacterium which oxidizes arsenite to arsenate, and of one which reduces arsenate to arsenite, isolated from a cattle-dipping tank. S Afr J Sci 14: 465-467
- xlvii Santini JM, Sly LI, Schnagl RD & Macy JM (2000). A new chemolithoautotrophic arsenite-oxidizing bacterium isolated from a gold mine: phylogenetic, physiological, and preliminary biochemical studies. Appl Environ Microbiol 66: 92-97
- xlviii Santini JM & vanden Hoven RN (2004). Molybdenum-containing arsenite oxidase of the chemolithoautotrophic arsenite oxidizer NT-26. J Bacteriol 186: 1614-1619
- xliv Vanden Hoven RN & Santini JM (2004). Arsenite oxidation by the heterotroph *Hydrogenophaga* sp. str. NT-14: the arsenite oxidase and its physiological electron acceptor. Biochim Biophys Acta 1656: 148-155
- l Osborne FH & Ehrlich HL (1976). Oxidation of arsenite by a soil isolate of *Alcaligenes*. J Appl Bacteriol 41: 295-305
- li Phillips SE & Taylor ML (1976). Oxidation of arsenite to arsenate by *Alcaligenes faecalis*. Appl Environ Microbiol 32: 392-399
- lii Oremland RS, Hoelt SE, Santini JM, Bano N, Hollibaugh RA & Hollibaugh JT (2002). Anaerobic oxidation of arsenite in Mono Lake water and by a facultative, arsenite-oxidizing chemoautotroph, strain MLHE-1. Appl Environ Microbiol 68: 4795-4802
- liii Weeger W, Lievrement D, Perret M, Lagarde F, Hubert JC, Leroy M & Lett M-C (1999). Oxidation of arsenite to arsenate by a bacterium isolated from an aquatic environment. Biometals 12: 141-149
- liv Anderson GL, Williams J & Hille R (1992). The purification and characterization of arsenite oxidase from *Alcaligenes faecalis*, a molybdenum-containing hydroxylase. J Biol Chem 267: 23674-23682
- lv Silver S & Phung LT (2005). Genes and enzymes involved in bacterial oxidation and reduction of inorganic arsenic. Appl Environ Microbiol 71: 599-608
- lvi Ellis PJ, Conrads T, Hille R & Kuhn P (2001). Crystal structure of the 100kDa arsenite oxidase from *Alcaligenes faecalis* in two crystal forms at 1.64 Å and 2.03 Å. Structure 9: 125-132
- lvii McEwan AG, Ridge JP, McDevitt CA & Hugenholtz P (2002). The DMSO reductase family of microbial molybdenum enzymes; molecular properties and role in the dissimilatory reduction of toxic elements. Geomicrobiol J 19: 3-21
- lviii Lebrun E, Brugna M, Baymann F, Muller D, Lievrement D, Lett M-C & Nitschke W (2003). Arsenite oxidase, an ancient bioenergetic enzyme. Mol Biol Evol 20: 686-693
- lix Muller D, Lievrement D, Simeonova DD, Hubert JC & Lett M-C (2003). Arsenite oxidase *aox* genes from a metal-resistant beta-proteobacterium. J Bacteriol 185: 135-141

- 
- lx Gihring TM & Banfield JF (2001). Arsenite oxidation and arsenate respiration by a new *Thermus* isolate. *FEMS Microbiol Lett* 204: 335-340
- lxi Gihring TM, Druschel GK, McCleskey RB, Hamers RJ & Banfield JF (2001). Rapid arsenite oxidation by *Thermus aquaticus* and *Thermus thermophilus*: field and laboratory investigations. *Environ Sci Technol* 35: 3857-3862
- lxii Kashyap DR, Botero LM, Franck WL, Hassett DJ & McDermott TR (2006). Complex regulation of arsenite oxidation in *Agrobacterium tumefaciens*. *J Bacteriol* 188: 1081-1088
- lxiii Ilyaletdinov AN & Abdrashitova SA (1981). Autotrophic oxidation of arsenic by a culture of *Pseudomonas arsenitoxidans*. *Mikrobiologiya* 50: 198-204
- lxiv Santini M, Sly LI, Wen A, Comrie D, De Wulf-Durand P & Macy JM (2002). New arsenite-oxidizing bacteria isolated from Australian gold mining environments-phylogenetic relationships. *Geomicrobiol J* 19: 67-76
- lxv Rhine ED, Phelps CD & Young LY (2006). Anaerobic arsenite oxidation by novel denitrifying isolates. *Environ Microbiol* 8: 899-908
- lxvi Rhine ED, Ni Chadhain SM, Zylstra GJ & Young LY (2007). The arsenite oxidase genes (*aroAB*) in novel chemoautotrophic arsenite oxidizers. *Biochem Biophys Res Comm* 354: 662-667
- lxvii Ahmann D, Roberts AL, Krumholz LR, & Morel FM (1994). Microbe grows by reducing arsenic. *Nature* 371: 750
- lxviii Oremland RS & Stolz JF (2003). The ecology of arsenic. *Science* 300: 939-944
- lxix Saltikov CW & Newman DK (2003). Genetic identification of a respiratory arsenate reductase. *Proc Natl Acad Sci USA* 100: 10983-10988
- lxx Krafft T & Macy JM (1998). Purification and characterization of the respiratory arsenate reductase of *Chrysiogenes arsenatis*. *Eur J Biochem* 255: 647-653
- lxxi Afkar E, Lisak J, Saltikov C, Basu P, Oremland RS & Stolz JF (2003). The respiratory arsenate reductase from *Bacillus selenitireducens* strain MLS10. *FEMS Microbiol Lett* 226: 107-112
- lxxii Malasarn D, Saltikov CW, Campbell KM, Santini JM, Hering JG & Newman DK 2004. *arrA* is a reliable marker for As(V) respiration. *Science* 306: 455
- lxxiii Macy JM, Santini JM, Pauling BV, O'Neill AH & Sly LI (2000). Two new arsenate/sulfate-reducing bacteria: mechanisms of arsenate reduction. *Arch Microbiol* 173: 49-57
- lxxiv Broer S, Ji G, Broer A & Silver S (1993). Arsenic efflux governed by the arsenic resistance determinant of *Staphylococcus aureus* plasmid pI258. *J Bacteriol* 175: 3840-3845
- lxxv Cervantes C & Chavez J (1992). Plasmid-determined resistance to arsenic and antimony in *Pseudomonas aeruginosa*. *Antonie van Leeuwenhoek* 61: 333-337
- lxxvi Gladysheva TB, Oden KL & Rosen BP (1994). Properties of the arsenate reductase of plasmid R773. *Biochem* 33: 7288-7293
- lxxvii Carlin A, Shi W, Dey S & Rosen BP (1995). The *ars* operon of *Escherichia coli* confers arsenical and antimonical resistance. *J Bacteriol* 177: 981-986
- lxxviii Cai J, Salmon K & DuBow MS (1998). A chromosomal *ars* operon homologue of *Pseudomonas aeruginosa* confers increased resistance to arsenic and antimony in *Escherichia coli*. *Microbiol* 144: 2705-2713
- lxxix Messens J, Martins JC, Van Belle K, Brosens E, Desmyter A, De Gieter M, Wieruszkeski JM, Willem R,

- 
- Wyns L & Zegers I (2002). All intermediates of the arsenate reductase mechanism, including an intramolecular dynamic disulfide cascade. *Proc Natl Acad Sci USA* 99: 8506-8511
- lxxx Martin P, DeMel S, Shi J, Rosen BP & Edwards BFP (2001). Insights into the structure, solvation, and mechanism of ArsC arsenate reductase, a novel arsenic detoxification enzyme. *Structure* 9: 1071-1081
- lxxxI Zegers I, Martins JC, Willem R, Wyns L & Messens J (2001). Arsenate reductase from *S. aureus* pI258 is a phosphatase drafted for redox duty. *Nature Struct Biol* 8: 843-847
- lxxxII Messens J & Silver S (2006). Arsenate reduction: Thiol cascade chemistry with convergent evolution. *J Mol Biol* 362: 1-17
- lxxxIII Mukhopadhyay R, Shi J & Rosen BP (2000). Purification and characterization of Acr2p, the *Saccharomyces cerevisiae* arsenate reductase. *J Biol Chem* 275: 21149-21157
- lxxxIV Baillet F, Magnin JP, Cheruy A & Ozil P (1997). Cadmium tolerance and uptake by a *Thiobacillus ferrooxidans* biomass. *Environ Technol* 18: 631-8
- lxxxV Boyer A, Magnin J-P & Ozil P (1998). Copper ion removal by *Thiobacillus ferrooxidans* biomass. *Biotechnol Lett* 20: 187-90
- lxxxVI Hassen A, Saidi N, Cherif M & Boudabous A (1998). Effects of heavy metals on *Pseudomonas aeruginosa* and *Bacillus thuringiensis*. *Bioresour Technol* 65: 73-82
- lxxxVII Gomez Y, Coto O, Hernandez C, Marrero J & Abin L (2001). Biosorption of nickel, cobalt and zinc by *Serratia marcescens* strain 7 and *Enterobacter agglomerans* strain 16. *Process Metall* 11: 247-55
- lxxxVIII Hernandez A, Mellado RP & Martinez JL (1998). Metal accumulation and vanadium-induced multidrug resistance by environmental isolates of *Escherichia hermannii* and *Enterobacter cloacae*. *Appl Environ Microbiol* 64: 4317-20
- lxxxIX Say R, Yilmaz N, & Denizli A (2003). Biosorption of cadmium, lead, mercury, and arsenic ions by the fungus *Penicillium purpurogenum*. *Sep Sci Technol* 38: 2039-2053
- xc Kuyucak N & Volesky B (1988) Biosorbents for recovery of metals from industrial solutions. *Biotechnol Lett* 10: 137-142
- xcI Veglio F & Beolchini F (1997). Removal of metals by biosorption: a review. *Hydrometallurgy* 44: 301-316
- xcII Pearton TN & Viljoen MJ (1986). Antimony mineralization in the Murchison greenstone belt - an overview. In: *Mineral Deposits of Southern Africa* (Anhaeusser CR & Maske S Eds). *Geol Soc S Afr* 2329: 293-320
- xcIII Abbot JE, Van Vuuren CJJ & Viljoen MJ (1986). The Alpha-Gravelotte antimony ore body, Murchison greenstone belt. In: *Mineral Deposits of Southern Africa* (Anhaeusser CR & Maske S Eds.). *Geol Soc S Africa* 2335: 321-332
- xcIV Wu J (1993). Antimony vein deposits of China. *Ore Geology Reviews* 8: 213-232
- xcV Willson C & Viljoen MJ (1986). The Athens antimony ore body, Murchison greenstone belt. In: *Mineral Deposits of Southern Africa* (Anhaeusser CR & Maske S Eds.). *Geol Soc S Afr* 2329: 333-338
- xcVI Davis DR, Paterson DB & Griffiths DHC (1986). Antimony in South Africa. *J S Afr Inst Min Metall* 86: 173-193
- xcVII Boocock CN, Cheshire PE, Killick AM, Maiden KJ & Vearncombe JR (1988). Antimony-gold mineralization at Monarch mine, Murchison schist belt, Kaapvaal craton. In: *Advances in Understanding Precambrian Gold Deposits, Volume II* (Ho SE & Groves DI Eds), Geology Department and University

- 
- Extension, University of Western Australia, Publ. No.12, 360: 81-97
- xcviii Chen C-M, Mobley HLT & Rosen BP (1985). Separate resistances to arsenate and arsenite (antimonate) encoded by the arsenical resistance operon of R factor R773. *J Bacteriol* 161: 758-763
- xcix Bartholomew JW & Mittwer T (1952). The Gram stain. *Bacteriol Rev* 16: 1-29
- <sup>c</sup> Perry SF (1995). Freeze-drying and cryopreservation of bacteria. *Methods Mol Biol* 38: 21-30
- ci Lane DJ, Weisberg WG, Barns SM & Pelletier DA (1991). 16S ribosomal DNA amplification for phylogenetic study. *J Bacteriol* 173: 697-703
- cii Hanahan D (1982). Studies on transformation of *E. coli* with plasmid. *J Mol Biol* 166: 557-580
- ciii Altschul SF, Gish W, Miller W, Myers EW & Lipman DJ (1990). Basic local alignment search tool. *J Mol Biol* 215: 403-410
- civ Cole JR, Chai B, Farris RJ, Wang Q, Kulam SA, McGarrell DM, Garrity GM & Tiedje JM (2005). The Ribosomal Database Project (RDP-II): sequences and tools for high-throughput rRNA analysis. *Nucleic Acids Res* 33 (Database Issue): D294-D296
- cv Thompson JD, Gibson TJ Plewniak F, Jeanmougin F & Higgins DG (1997). The ClustalX windows interface: flexible strategies for multiple sequence alignment aided by quality analysis tools. *Nucl Acids Res* 24: 4876-4882
- cvi Swofford DL (2002) *PAUP\**. *Phylogenetic Analysis Using Parsimony (\*and other Methods)* Version 4. Sinauer Associates, Sunderland, Massachusetts, USA
- cvii Meerow AW, Lehmilller DJ & Clayton JR (2003). Phylogeny and biogeography of *Crinum* L. (Amaryllidaceae) inferred from nuclear and limited plastid non-coding DNA sequences. *Bot J Linn Soc* 141: 349-363
- cviii Muyzer G, De Waal E & Uittierlinden A (1993). Profiling of complex microbial populations by denaturing gradient gel electrophoresis analysis of polymerase chain reaction-amplified genes coding for 16S rRNA. *Appl Environ Microbiol* 59: 695-700
- cix Davis KER, Joseph SJ & Janssen PH (2005). Effects of growth medium, inoculum size, and incubation time on the culturability and isolation of soil bacteria. *Appl Environ Microbiol* 71: 826-834
- cx Casamayor EO, Massana R, Benlloch S, Overas L, Diez B, Goddard VJ, Gasol MS, Joint I, Rodriguez-Valera F & Pedros-Alio C (2002). Changes in archaeal, bacterial and eukaryal assemblages along a salinity gradient by comparison of genetic fingerprinting methods in a multipond solar saltern. *Environ Microbiol* 4: 338-348
- cxii Ji G & Silver S (1992). Reduction of arsenate to arsenite by the ArsC protein of the arsenic resistance operon of *Staphylococcus aureus* plasmid pI258. *Proc Natl Acad Sci USA* 89: 9474-9478
- cxiii Zahler WL & Cleland WW (1968). A specific and sensitive assay for disulfides. *J Biol Chem* 243: 716-719
- cxiiii Simeonova DD, Lievreumont D, Lagarde F, Muller DAE, Groudeva VI & Lett M-C (2004). Microplate screening assay for the detection of arsenite-oxidizing and arsenate-reducing bacteria. *FEMS Microbiol Lett* 237: 249-253
- cxv Johnson DL & Pilson MEQ (1972). Spectrophotometric determination of arsenite, arsenate, and phosphate in natural waters. *Anal Chim Acta* 58: 289-299
- cxvi Silver S, Budd K, Leahy KM, Shaw WV, Hammond D, Novick RP, Willsky GR, Malamy MH & Rosenberg H (1981). Inducible plasmid-determined resistance to arsenate, arsenite, and antimony (III) in

---

*Escherichia coli* and *Staphylococcus aureus*. J Bact 146: 983-996

- cxvi Anderson, CR. Personal communication
- cxvii Wysocki R, Chery CC, Wawrzycka D, Van Hulle M, Cornelis R, Thevelein JM & Tamas M (2001). The glycerol channel Fps1p mediates the uptake of arsenite and antimonite in *Saccharomyces cerevisiae*. Mol Microbiol 40: 1391-1401
- cxviii Ma LQ, Komar KM, Tu C, Zhang W, Cai Y & Kennelley ED (2001). A fern that hyperaccumulates arsenic. Nature 409: 579
- cxix Canovas D, Duran C, Rodriguez N, Amils R & De Lorenzo V (2003). Testing the limits of biological tolerance to arsenic in a fungus isolated from the River Tinto. Environ Microbiol 5: 133-138
- cxx Ordonez E, Letek M, Valbuena N, Gil JA & Mateos LM (2005). Analysis of genes involved in arsenic resistance in *Corynebacterium glutamicum* ATCC 13032. Appl Environ Microbiol 71: 6206-6215
- cxxi Anderson CR & Cook GM (2004). Isolation and characterization of arsenate-reducing bacteria from arsenic-contaminated sites in New Zealand. Curr Microbiol 48: 341-347
- cxvii Urrutia MM & Beveridge TM (1994). Formation of fine-grained metal and silicate precipitates on a bacterial surface (*Bacillus subtilis*). Chem Geol 116: 261-280
- cxviii Bai RS & Abraham TE (2003). Studies on Chromium (VI) adsorption-desorption using immobilized fungal biomass. Bioresour Technol 87: 17-26
- cxviiii Schultze-Lam S, Thompson JB & Beveridge TJ (1993). Metal ion immobilization by bacterial surfaces in freshwater environments. Water Pollut Res J Can 28: 51-81
- cxvix Sekhula KS, Abotsi EK & Becker RW (2005). M.Sc. thesis: Heavy metal ion resistance and bioremediation capacities of bacterial strains isolated from an antimony mine
- cxvii Dhankeher OM, Li Y, Rosen BP, Shi J, Salt D, Senecoff JF, Sashti NA & Meagher RB (2002). Engineering tolerance and hyperaccumulation of arsenic in plants by combining arsenate reductase and  $\gamma$ -glutamylcysteine synthetase expression. Nature Biotechnol 20: 1140-1145
- cxvii Brunken HS, Nehrhorn A & Breunig HJ (1996). Isolation and characterization of a new arsenic methylating bacterium from soil. Microbiol Res 151: 37-41

## **DECLARATION**

I, Elsabé Botes, hereby declare that the dissertation hereby submitted by me for the degree Philosophiae Doctor at the University of the Free State is my own independent work and has not previously been submitted by me at another university/faculty. I furthermore cede copyright of the dissertation in favor of the University of the Free State. Appropriate acknowledgements in the text have been made where use of work, conducted by others, has been included.

The experimental work conducted and discussed in this thesis was carried out in the Department of Microbial, Biochemical and Food Biotechnologies, University of the Free State, Bloemfontein. The study was conducted during the period October 2001 to November 2007 under the supervision of Prof. E. Van Heerden, and co-supervision of Prof. D. Litthauer, of the Department of Microbial, Biochemical and Food Biotechnology, University of the Free State, Bloemfontein.

Signature: \_\_\_\_\_

Elsabé Botes

Date: \_\_\_\_\_

## Acknowledgements

The completion of this degree has afforded me the rare opportunity to experience a tremendous amount of growth, both as a scientist and as a person.

In the former capacity, I would like to acknowledge the many researchers at UFS Biotechnology department who unselfishly devoted their time and expertise on me as well as many authorities in many other fields who assisted by promptly replying to many, many e-mails and requests for input, opinions, research articles and material.

I would also like to thank the National Research Foundation, the UFS BRIC project and the Metagenomics Platform based at the UFS for financial support.

Then, to my promoters, Prof. Esta van Heerden and Prof. Derek Litthauer, words cannot express the enormous contribution both of you have made in my life, both professional and personal. Much of who I am today is due to your patience, guidance, and (sometimes) pure indulgence.

I also have to acknowledge that due to the opportunities afforded to me during the Research Exchange for Undergraduate Students (REU) between the Extreme Biochemistry Research Group and University of Tennessee, I have been privileged to meet extraordinary scientists from various fields that have enriched and broadened my scientific scope enormously.

Personnel at the Instrumentation Division of UFS: their patience and willingness to build, rebuild and modify equipment and who probably could have built me a rocket if I had asked for it - I truly would not have been able to do this work without them.

Staff at the Institute for Ground Water Studies for their willingness to accommodate me in their lab, and especially to Lore-Marie who frequently worked long hours into the night to fix the ICP-MS and also for many encouraging conversations during my time spent there.

During the course of this degree, I have been shaped and molded by countless others. A few people should be mentioned by name:

Members of the Extreme Biochemistry Research Group, (both old and new), specifically my lab members since the beginning of time Dirk, Jacqui and Armand

Many friends for listening to countless hours of complaining and at times simply passing on dry tissues (Lizelle, Maralize, Marieta and many other unfortunate victims)

My immediate and extended family for their unwavering support regardless of my inability to explain my academic pursuits. Particularly, to the most wonderful brother in the world, for many words of encouragement, guidance and comfort as well as my parents for always believing in me, always being proud of me and many other loving gestures.

Olga, for encouragement and support, suggestions, and being able to stand my company during the last months of this study.

## Table of Contents

<b>List of Figures .....</b>	<b>i</b>
<b>List of Tables.....</b>	<b>v</b>
<b>List of Abbreviations.....</b>	<b>vi</b>

### **Chapter 1: Isolation, Identification and Arsenic Resistance ..... 1**

#### **1.1. Literature review: Biological transformations of arsenic ..... 2**

<b><u>1.1.1 Background</u> .....</b>	<b>2</b>
<b><u>1.1.2 The arsenic global geocycle</u>.....</b>	<b>4</b>
<b><u>1.1.3 Entry of arsenic into cells</u>.....</b>	<b>5</b>
<b><u>1.1.4 Methylation</u> .....</b>	<b>5</b>
<b><u>1.1.5 Oxidation</u>.....</b>	<b>7</b>
<b><u>1.1.6 Reduction</u>.....</b>	<b>9</b>
<b>1.1.6.1 Respiratory arsenate reductases</b> .....	<b>9</b>
<b>1.1.6.2 Cytoplasmic arsenate reductases</b> .....	<b>10</b>
<b><u>1.1.7 Other mechanisms: Biosorption</u>.....</b>	<b>11</b>

#### **1.2. Introduction to the present study ..... 12**

#### **1.3 Aims ..... 13**

#### **1.4 Materials and methods..... 14**

<b><u>1.4.1 General procedures and chemicals</u> .....</b>	<b>14</b>
<b><u>1.4.2 Sampling and isolation</u>.....</b>	<b>14</b>
<b><u>1.4.3 Cryopreservation</u>.....</b>	<b>15</b>
<b><u>1.4.4 Identification</u>.....</b>	<b>15</b>
<b>1.4.4.1 16S rDNA sequencing</b> .....	<b>15</b>
<b>1.4.4.2 Biochemical testing</b> .....	<b>17</b>
<b><u>1.4.5 Minimum inhibitory concentrations</u>.....</b>	<b>17</b>



<b><u>1.4.6</u></b> <b><u>Arsenate reduction</u></b> .....	18
1.4.6.1  Qualitative .....	18
1.4.6.2  Quantitative.....	18
<b><u>1.5 Results and discussion.....</u></b>	<b>19</b>
<b><u>1.5.1</u></b> <b><u>Enrichments</u></b> .....	19
<b><u>1.5.2</u></b> <b><u>Identification</u></b> .....	20
<b><u>1.5.3</u></b> <b><u>Minimum inhibitory concentration</u></b> .....	23
<b><u>1.5.4</u></b> <b><u>Arsenate reduction by resting cells</u></b> .....	27
<b><u>1.6 Literature cited .....</u></b>	<b>30</b>
<b><u>Chapter 2: Molecular Aspects .....</u></b>	<b>37</b>
<b><u>2.1 Literature review: Dissimilatory arsenate reduction in bacteria .....</u></b>	<b>38</b>
<b><u>2.1.1</u></b> <b><u>Regulation</u></b> .....	39
<b><u>2.1.2</u></b> <b><u>Membrane pumps</u></b> .....	39
<b><u>2.1.3</u></b> <b><u>Arsenate reductases</u></b> .....	40
2.1.3.1  The <i>E. coli</i> glutathione / glutaredoxin ArsC family.....	40
2.1.3.2  The <i>Staphylococcus</i> thioredoxin ArsC family .....	42
2.1.3.3  Exceptions to the rule .....	44
<b><u>2.2 Introduction .....</u></b>	<b>46</b>
<b><u>2.3 Aims .....</u></b>	<b>47</b>
<b><u>2.4 Materials and methods.....</u></b>	<b>48</b>
<b><u>2.4.1</u></b> <b><u>General procedures and chemicals</u></b> .....	48
<b><u>2.4.2</u></b> <b><u>Bacterial strains and primers</u></b> .....	48
<b><u>2.4.3</u></b> <b><u>PCR approach</u></b> .....	49
2.4.3.1  DNA Extraction .....	49
2.4.3.1.1  Genomic DNA .....	49
2.4.3.1.2  Plasmid DNA.....	50

2.4.3.2	PCR.....	50
2.4.3.3	Gel band purification .....	50
2.4.3.4	PCR product ligation .....	50
2.4.3.5	Transformation.....	51
2.4.3.6	Plasmid extractions and restriction analysis.....	51
2.4.3.7	Sequencing.....	51
<b>2.4.4</b>	<b><u>Genomic library construction approach</u></b> .....	<b>51</b>
2.4.4.1	Minimum inhibitory concentration .....	51
2.4.4.2	Partial digestion of genomic DNA .....	52
2.4.4.3	Vector digest and dephosphorylation .....	52
2.4.4.4	Ligation and transformation .....	52
<b>2.5</b>	<b><u>Results and discussion</u></b> .....	<b>53</b>
2.5.1	<u>Polymerase Chain Reaction</u> .....	53
2.5.2	<u>Genomic libraries</u> .....	67
<b>2.6</b>	<b><u>Literature Cited</u></b> .....	<b>80</b>
<b>Chapter 3:</b>	<b><u>Cellular Characterisation for Adhesion</u></b> .....	<b>85</b>
<b>3.1</b>	<b><u>Literature review: Bacterial adhesion to inert surfaces</u></b> .....	<b>86</b>
3.1.1	<u>Primary adhesion</u> .....	86
3.1.1.1	Theory of adhesion .....	87
3.1.2	<u>Secondary adhesion</u> .....	88
3.1.3	<u>Factors influencing bacterial adhesion</u> .....	88
3.1.3.1	Surface of adhesion.....	88
3.1.3.2	Bacterial surface features .....	89
3.1.3.3	Cell size and shape.....	90
3.1.3.4	Bacterial hydrophobicity .....	90
3.1.3.5	Bacterial surface charge.....	91
3.1.4	<u>Conditioning</u> .....	91
3.1.5	<u>Concluding remarks</u> .....	92

<b>3.2 Aims .....</b>	<b>94</b>
<b>3.3 Materials and methods.....</b>	<b>95</b>
<b>3.3.1 Growth parameters (pH and temperature).....</b>	95
<b>3.3.2 Motility .....</b>	95
<b>3.3.3 Anaerobic growth .....</b>	95
<b>3.3.4 Cell size and morphology.....</b>	96
<b>3.3.5 Pigmentation .....</b>	96
<b>3.3.6 Cell surface properties .....</b>	96
3.3.6.1 Hydrophobicity .....	96
3.3.6.2 Electrostatic and acid / base properties.....	97
3.3.6.3 Lipopolysaccharides (LPS) .....	97
3.3.6.4 Carbohydrate and protein content .....	98
<b>3.4 Results and discussion.....</b>	<b>99</b>
<b>3.4.1 Growth parameters (pH and temperature).....</b>	99
<b>3.4.2 Motility .....</b>	100
<b>3.4.3 Anaerobic growth .....</b>	100
<b>3.4.4 Morphological and surface properties.....</b>	104
3.4.4.1 Cell size and morphology .....	104
3.4.4.2 Pigmentation .....	105
3.4.4.3 Hydrophobicity .....	105
3.4.4.4 Electrostatic and acid / base properties.....	107
3.4.4.5 Lipopolysaccharides (LPS) .....	109
3.4.4.6 Carbohydrate and protein content .....	110
<b>3.5 Conclusions .....</b>	<b>111</b>
<b>3.6 Literature cited.....</b>	<b>113</b>

## **Chapter 4: *In situ* reduction of arsenate by *S. marcescens* SA Ant 16..... 118**

### **4.1 Literature review: Arsenic remediation technologies ..... 119**

<b><u>4.1.1</u></b>	<b><u>Chemical techniques for arsenic remediation</u></b> .....	119
4.1.1.1	Precipitative processes .....	119
4.1.1.2	Adsorptive processes .....	121
4.1.1.3	Ion exchange.....	121
4.1.1.4	Membrane processes .....	122
4.1.1.5	Alternative technologies .....	122
<b><u>4.1.2</u></b>	<b><u>Biological methods</u></b> .....	123
4.1.2.1	Passive biosorbents .....	123
4.1.2.2	Phytoremediation .....	125
4.1.2.3	Bioremediation with microorganisms.....	126

### **4.2 Aims ..... 129**

### **4.3 Materials and methods..... 130**

<b><u>4.3.1</u></b>	<b><u>Optimisation of arsenate reducing conditions</u></b> .....	130
<b><u>4.3.2</u></b>	<b><u>Adhesion of cells to sand matrix</u></b> .....	131
<b><u>4.3.3</u></b>	<b><u>Real-Time PCR for quantification</u></b> .....	131
<b><u>4.3.4</u></b>	<b><u>Setup, conservative tracer and bacterial breakthrough</u></b> .....	132
<b><u>4.3.5</u></b>	<b><u>Column loading</u></b> .....	133
<b><u>4.3.6</u></b>	<b><u><i>In situ</i> As(V) reduction</u></b> .....	134
<b><u>4.3.7</u></b>	<b><u>Scanning electron microscopy</u></b> .....	134

### **4.4 Results and discussion..... 135**

<b><u>4.4.1</u></b>	<b><u>Factorial design for arsenate reduction optimisation</u></b> .....	135
<b><u>4.4.2</u></b>	<b><u>Real-Time enumeration and primer specificity</u></b> .....	143
<b><u>4.4.3</u></b>	<b><u>Adhesion</u></b> .....	144
<b><u>4.4.4</u></b>	<b><u>Tracer and breakthrough curves</u></b> .....	146
<b><u>4.4.5</u></b>	<b><u>Loading of column with cells</u></b> .....	147
<b><u>4.4.6</u></b>	<b><u>Arsenate reduction in column reactors</u></b> .....	147

<b><u>4.5 Conclusions .....</u></b>	<b><u>153</u></b>
<b><u>4.6 Literature cited .....</u></b>	<b><u>155</u></b>
<b><u>5 Summary .....</u></b>	<b><u>160</u></b>
<b><u>6 Opsomming .....</u></b>	<b><u>162</u></b>

## List of Abbreviations

16S	small ribosomal subunit
A	absorbance
AGW	artificial ground water
AIX	ampicillin/IPTG/X-Gal
As(III)	arsenite
As(V)	arsenate
ATP	adenosine triphosphate
BATH	bacterial adhesion to hydrocarbons
BCA	bicinchoninic acid
bp	basepair
BLAST	basic local alignment search tool
CM	carboxymethyl
C <sub>T</sub>	threshold cycle
Cys	cysteine
Da	Dalton
DEAE	diethylaminoethyl
DLVO	Derjaguin-Landau-Verwey-Overbeek
DMSO	dimethylsulfoxide
DNA	deoxyribonucleic acid
dNTP	dioxynucleotide
DO	dissolved oxygen
DTT	dithiothreitol
EDTA	ethylenediamine tetraacetic acid
EISC	electrostatic interaction chromatography
EMBL	European Molecular Biology Laboratory
FDH	formate dehydrogenase
g	acceleration due to gravity
Glc	glucose
Grx	glutaredoxin
GSH	glutathione
h	hour
HIC	hydrophobic interaction chromatography
HPLC	high performance liquid chromatography

ICP-MS	inductively coupled plasma mass spectrometry
IPTG	isopropyl- $\beta$ -D- thiogalactopyranoside
kb	kilobasepair
kcal/mol	kilocalories per mole
$K_{cat}$	catalytic rate
kDa	kilo Dalton
Kdo	2-keto-3-deoxyoctonoic acid
kg	kilogram
$K_i$	inhibitor dissociation constant
$K_m$	Michaelis constant
$K_{sp}$	solubility constant
L	litre
LB	Luria-Bertani
LPS	lipopolysaccharide
LMW	low molecular weight
M	molar
mA	milliampere
Mb	megabasepair
mg	milligram
mM	millimolar
nm	nanometer
OD	optical density
PAGE	polyacrylamide gel electrophoresis
PCR	polymerase chain reaction
PIPES	piperazine bisethanesulfonic acid
Pit	phosphate transport
$pK_a$	dissociation constant
ppb	parts per billion
ppm	parts per million
Pro	proline
Pst	phosphate specific transport
PTPase	phosphatase
PV	pore volume
rDNA	ribosomal DNA
RDP	ribosomal database project

rpm	revolutions per minute
RT	Real-Time
SDS	sodium dodecyl sulphate
TAE	Tris-acetic acid-EDTA
TE-buffer	Tris-EDTA buffer
TLC	thin layer chromatography
T <sub>m</sub>	melting temperature
Tris	Tris(hydroxymethyl)aminomethane
Trx	thioredoxin
TYG	tryptone, yeast extract, glucose
Tyr	tyrosine
U	units
UFS	University of the Free State
µg	microgram
µL	microlitre
µM	micromolar
µm	micrometer
µmax	maximum growth rate during exponential growth phase
US EPA	United States Environmental Protection Agency
UV	ultra violet
V	volt
v/v	volume per volume
w/v	weight per volume
XDLVO	extended DLVO
X-Gal	5-bromo-4-chloro-3-indolyl-β-D-galactoside



## List of Figures

Figure 1.1	The arsenic geocycle .....	4
Figure 1.2	Transport of arsenate into <i>E. coli</i> .....	5
Figure 1.3	Microbial formation of trimethylarsine from inorganic arsenate .....	6
Figure 1.4	ArsC families from Gram positive bacteria (I), Gram negative bacteria (II), and eukaryota (III).....	10
Figure 1.5	16S rDNA PCR products from arsenic resistant pure cultures .....	20
Figure 1.6	Phylogenetic tree generated with 16S rDNA PCR sequences.....	22
Figure 1.7	Growth of <i>Bacillus</i> sp. SA Ant 14 in absence and presence of arsenite and arsenate .....	25
Figure 1.8	Growth of <i>S. maltophilia</i> SA Ant 15 in absence and presence of arsenite and arsenate.....	26
Figure 1.9	Growth of <i>S. marcescens</i> SA Ant 16 in absence and presence of arsenite and arsenate.....	26
Figure 1.10	TLC plate demonstrating arsenate reduction to arsenite by resting cells of <i>Bacillus</i> sp. SA Ant 14, <i>S. maltophilia</i> SA Ant 15 and <i>S. marcescens</i> SA Ant 16 .....	27
Figure 1.11	Reduction of arsenate to arsenite by resting cells of <i>Bacillus</i> sp. SA Ant 14, <i>S. maltophilia</i> SA Ant 15 and <i>S. marcescens</i> SA Ant 16 .....	28
Figure 2.1	Catalytic reaction cycle of the Grx-coupled arsenate reductase of <i>E. coli</i> plasmid R773 .....	41
Figure 2.2	Ribbon diagram of the overall structure of reduced ArsC wild type.....	42
Figure 2.3	Catalytic reaction cycle of Trx-coupled arsenate reductase of <i>S. aureus</i> plasmid pI258 .....	43
Figure 2.4	Organisation of the four arsenic resistance operons in <i>Herminiimonas arsenicoxydans</i> .....	44
Figure 2.5	Alignments of arsC from Gram negative organisms with primer pair arsC-1-F / arsC-1-R indicated .....	53
Figure 2.6	1% TAE agarose gel with PCR products generated with primer pair arsC-1-F / arsC-1-R .....	54
Figure 2.7	PCR products from primer set arsC-1-F / arsC-1-R.....	54
Figure 2.8	Alignments of arsC from Gram negative organisms for design of degenerate primer pair ArsCF / ArsCR .....	55
Figure 2.9	PCR products generated with primer pair ArsCF / ArsCR .....	56
Figure 2.10	Alignment of DNA sequence of ArsCF / ArsCR PCR product with cytochrome oxidase subunit II ( <i>cyoXB</i> ) .....	57

Figure 2.11	PCR products from combinations of primer sets ArsCF / arsCR and arsC-1-F / arsC-1-R.....	58
Figure 2.12	Design of primer pair ArF / ArR based on the sequence of <i>S. marcescens</i> plasmid R478.....	59
Figure 2.13	Agarose gel with PCR fragments generated on serially diluted DNA of <i>S. marcescens</i> SA Ant 16.....	60
Figure 2.14	Alignment of arsR sequences and schematic of arsenate resistance operon spanning genes <i>arsR</i> to <i>arsC</i> .....	61
Figure 2.15	PCR products amplified with forward primer ArsRF and reverse primer arsC-1-R.....	61
Figure 2.16	Alignments of arsC from selected Gram negative bacteria for design of degenerate primer set ArsC7F / ArsC7R.....	62
Figure 2.17	PCR products amplified with primer set ArsC7F / ArsC7R on a 1.5% TAE agarose gel.....	62
Figure 2.18	1.5% TAE agarose gel with PCR products generated with primer set ArsC7F / ArsC7R using plasmid extracts as template.....	63
Figure 2.19	Alignment of <i>arsC</i> from Gram positive type arsenate reductases.....	65
Figure 2.20	Alignment of <i>arsC</i> from <i>P. aeruginosa</i> and <i>T. ferrooxidans</i> for design of degenerate primer set PsThF / PsThR.....	66
Figure 2.21	PCR amplification of <i>S. marcescens</i> SA Ant 16 genomic DNA with Gram positive primer set PsThF / PsThR.....	66
Figure 2.22	Minimum inhibitory As(V) concentration for <i>E. coli</i> <i>arsC</i> knockout strain AW3110 transformed with pUC18 and plated on increasing concentrations of arsenate.....	68
Figure 2.23	Partial digest of genomic DNA from <i>S. marcescens</i> SA Ant 16.....	68
Figure 2.24	Effect of interaction of ampicillin and chloramphenicol with <i>E. coli</i> strain AW3110.....	69
Figure 2.25	Minimum inhibitory arsenate concentration for untransformed <i>E. coli</i> JM109 and TOP10.....	70
Figure 2.26	Minimum inhibitory arsenite concentration for untransformed <i>E. coli</i> JM109 and TOP10.....	70
Figure 2.27	Minimum inhibitory arsenate concentration for <i>E. coli</i> JM109 cells transformed with pUC18.....	71
Figure 2.28	Control ligation of <i>Eco</i> RI and <i>Bam</i> HI digested $\lambda$ DNA.....	72
Figure 2.29	Control ligation of <i>Eco</i> RI digested $\lambda$ DNA into pUC18.....	72
Figure 2.30	<i>S. marcescens</i> SA Ant 16 genomic DNA partially digested with <i>Sau</i> 3AI.....	73
Figure 2.31	Minimum inhibitory arsenate and arsenite concentration for <i>E. coli</i> TOP10 cells transformed with pGem®-3Z.....	75

Figure 2.32	Partial digest of genomic DNA from <i>S. marcescens</i> SA Ant 16.....	76
Figure 2.33	Streaking out and replica plating of positive recombinants onto LB-plates containing 10mM and 15mM arsenate.....	76
Figure 2.34	Restriction analysis of plasmids containing inserts.....	77
Figure 2.35	1.5% TAE agarose gel of the <i>arsC</i> of <i>E. coli</i> W3110 amplified with primer pair <i>arsC</i> -1-F / <i>arsC</i> -1-R and sequence alignment with <i>arsC</i> <i>E. coli</i> X80057.....	78
Figure 2.36	Partial digest of genomic DNA from <i>E. coli</i> W3110 .....	78
Figure 3.1	Optimum growth temperature for <i>S. marcescens</i> SA Ant 16.....	99
Figure 3.2	Optimum growth pH for <i>S. marcescens</i> SA Ant 16 .....	100
Figure 3.3	Motility of <i>S. marcescens</i> SA Ant 16 and <i>E. coli</i> .....	100
Figure 3.4	Anaerobic growth of <i>S. marcescens</i> SA Ant 16 with nitrate as electron acceptor.....	103
Figure 3.5	Gram stained cells of <i>S. marcescens</i> SA Ant 16 grown under aerobic and anaerobic growth conditions.....	104
Figure 3.6	<i>S. marcescens</i> SA Ant 16 grown at 30°C and 37°C on peptone-glycerol agar to observe pigment production .....	105
Figure 3.7	Percentage hydrophobicity of aerobically and anaerobically grown cells of <i>S. marcescens</i> SA Ant 16 as determined with Bacterial Adhesion To Hydrocarbons.....	106
Figure 3.8	Percentage hydrophobicity of aerobically and anaerobically grown cells of <i>S. marcescens</i> SA Ant 16 as determined with Hydrophobic Interaction Chromatography.....	107
Figure 3.9	Acid / base properties of aerobically and anaerobically grown cells of <i>S. marcescens</i> SA Ant 16 .....	108
Figure 3.10	Percentage retention of aerobically and anaerobically grown cells of <i>S. marcescens</i> SA Ant 16 with various chromatographic resins.....	108
Figure 3.11	Lipopolysaccharides visualised with crystal violet and copper sulfate of aerobically grown cells and anaerobically grown cells of <i>S. marcescens</i> SA Ant 16 .....	109
Figure 3.12	Lipopolysaccharides from aerobically and anaerobically grown cells of <i>S. marcescens</i> SA Ant 16 separated on SDS-PAGE .....	110

Figure 4.1	Factorial design layout .....	130
Figure 4.2	Setup of column reactors .....	133
Figure 4.3	Negative controls (cells with no arsenate addition) for changes in pH, growth and glucose consumption under aerobic conditions.....	137
Figure 4.4	Growth and changes in pH during arsenate reduction under aerobic conditions .....	138
Figure 4.5	Arsenate reduction and glucose consumption under aerobic conditions.....	139
Figure 4.6	Growth and pH changes during arsenate reduction under anaerobic conditions .....	140
Figure 4.7	Arsenate reduction and glucose consumption under anaerobic conditions .....	140
Figure 4.8	3D representation of growth and changes in pH during arsenate reduction.....	141
Figure 4.9	Standard curve of cell concentration (cells/mL) vs. cycle number ( $C_T$ ) .....	143
Figure 4.10	Specificity of <i>S. marcescens</i> specific primers .....	144
Figure 4.11	Adhesion of concentration ranges of <i>S. marcescens</i> SA Ant 16 cells to sand grains .....	145
Figure 4.12	Adhesion of <i>S. marcescens</i> SA Ant 16 to sand in syringe columns over a period of 24 hours .....	145
Figure 4.13	Typical profile of NaCl tracer and bacterial breakthrough in a 500mm column .....	146
Figure 4.14	Cell numbers in small column reactor for maximum saturation .....	147
Figure 4.15	Arsenate reduction, glucose utilisation and changes in pH in column reactor containing 3mM glucose .....	149
Figure 4.16	SEM imaging of negative control sand grain, and sand grain covered with cells.....	149
Figure 4.17	Viable cells in the reactor (5mM As(V), 6mM glucose) during run .....	150
Figure 4.18	Changes in pH, dissolved oxygen percentage and glucose conversion in the reactor amended with 5mM arsenate and 6mM glucose .....	151
Figure 4.19	Percentage arsenate conversion over 10 pore volumes for bioreactor amended with 5mM arsenate and 6mM glucose .....	152

## List of Tables

Table 1.1	Sampling site description .....	15
Table 1.2	Primers used for 16S rDNA amplification and sequencing .....	17
Table 1.3	Growth for pure cultures inoculated into antimony supplemented TYG media .....	19
Table 1.4	Growth for pure cultures in arsenate and arsenite supplemented TYG media .....	20
Table 1.5	Closest sequence matches for 16S rDNA genes of pure cultures .....	21
Table 1.6	Effect of increasing concentrations arsenite or arsenate on biomass yield, maximum specific growth rate and lag phase for <i>Bacillus</i> sp. SA Ant 14, <i>S. maltophilia</i> SA Ant 15 and <i>S. marcescens</i> SA Ant 16 grown for 12 hours .....	24
Table 1.7	Arsenate removal by whole cells of <i>Bacillus</i> sp. SA Ant 14, <i>S. maltophilia</i> SA Ant 15 and <i>S. marcescens</i> SA Ant 16 during resting conditions .....	29
Table 2.1	<i>E. coli</i> strains used in the study .....	48
Table 2.2	Primers used for amplification and sequencing of arsenate reductase ( <i>arsC</i> ).....	49
Table 3.1	Summary of growth parameters during anaerobic growth of <i>S. marcescens</i> SA Ant 16 .....	102
Table 3.2	Total protein and carbohydrate content of cells of <i>S. marcescens</i> SA Ant 16 grown aerobically and anaerobically.....	111

# **Chapter 1**

## **Isolation, Identification and Arsenic Resistance**

## **1.1 Literature review: Biological transformations of arsenic**

### **1.1.1 Background**

Arsenic is widely spread in the upper crust of the earth, although mainly at very low concentrations. The main source of arsenic on the earth's surface is igneous activity, although anthropomorphic sources such as industrial effluents, various commercial processes and combustion of fossil fuels also contribute significantly<sup>1</sup>. Arsenic concentrations in soil range from 0.1 to more than 1000ppm (1 $\mu$ M - 10mM), while in atmospheric dust, the range is 50-400ppm (0.7mM - 5mM)<sup>2</sup>.

While arsenic has a historically infamous reputation as a poison<sup>3</sup>, its biological uses are less well known. Arsenic belongs to group VA of the periodic table of elements - these elements are metalloids that have both metallic and non-metallic properties. Arsenic exists in various forms, exhibiting different biological properties and degrees of toxicity. The common valence states of arsenic in nature include -3, +3, and +5, with decreasing toxicity. The specific toxicity of arsenate [As(V)] is generally attributed to its chemical similarity to phosphate where it is capable of mimicking the role of phosphate in cellular transport and enzymatic reactions. Thus, arsenate may replace an essential phosphate in various metabolic processes where a central target of As(V) is pyruvate dehydrogenase and inhibition of this enzyme blocks respiration. Arsenate uncouples oxidative phosphorylation by the formation of unstable arsenate esters, which substitute for phosphate esters in ATP formation<sup>4</sup>. Arsenite [As(III)] reacts with -SH groups of cysteine residues, which often constitute an integral part of the active site of enzymes, thereby inhibiting their catalytic activity. Besides direct enzyme inhibition, arsenite induces oxidative damage *via* the accumulation of reactive oxygen species. This arsenite-stimulated generation of reactive oxygen, known to damage proteins, lipids and DNA, is probably the direct cause of the carcinogenic effects of arsenite<sup>5</sup>.

In aqueous systems arsenate oxyanions are ionized with three pK<sub>a</sub> values of 2.2, 7.0, and 11.50 (comparable to 2.1, 7.2, and 12.7 for phosphate)<sup>6</sup>, so that approximately equal amounts of HAsO<sub>4</sub><sup>2-</sup> and H<sub>2</sub>AsO<sub>4</sub><sup>-</sup> occur at pH 7<sup>7</sup> whereas H<sub>3</sub>AsO<sub>4</sub> and H<sub>2</sub>AsO<sub>4</sub><sup>-</sup> predominate in acidic environments<sup>8</sup>. Arsenite appears mostly un-ionized as As(OH)<sub>3</sub> at neutral pH, with a pK<sub>a</sub> of 9.2 for dissociation to H<sub>2</sub>AsO<sub>3</sub><sup>-</sup><sup>7</sup>. Therefore, the transport substrate in and out of the cells for arsenate will be the oxyanion comparable to phosphate at approximately the same pH, whereas arsenite may move across membrane bilayers passively un-ionized or be transported by a

carrier protein similar to un-ionized organic compounds<sup>9</sup>. Arsenic toxicity is highly dependent on its oxidation state: trivalent arsenicals are at least 100 times more toxic than the pentavalent derivatives<sup>10</sup>. Arsenite and arsenate are interconverted by biological redox reactions and arsenite can also be methylated by bacteria, fungi and algae<sup>11</sup>.

The effects of oxyanions of metalloids on both prokaryotic and eukaryotic cells have attracted substantial attention. In recent years, concern has increased about the release of arsenical compounds in the environment and their toxicity to a wide variety of organisms, including humans. There is a wealth of information on the biological effects of arsenic compounds on mammals: arsenic is able to induce cell transformations<sup>12</sup>, gene amplification in marine cells<sup>13</sup>, gene damage in human alveolar type II cells<sup>14</sup>, and is a co-mutagen agent in exposed hamster cells<sup>13</sup>. Arsenic compounds elicit a cellular stress response similar to heatshock protein synthesis<sup>15, 16</sup> and causes lung and skin cancers in humans<sup>17, 18, 19</sup>. There is also evidence to support the carcinogenic effect of ingested inorganic arsenic and the occurrence of bladder, kidney and liver cancers<sup>20</sup>.

In the environment microorganisms are continuously exposed to metallic anions and cations. Some of these ions are taken up as essential nutrients (i.e. magnesium, potassium, copper, and zinc) whereas others exert toxic effects on microbial cells (i.e. mercury, lead, cadmium, arsenic, and silver)<sup>21</sup>. Although the presence of heavy metals is detrimental for microorganisms, toxic metals select variants possessing genetic resistance determinants which confer the ability to tolerate higher levels of the toxic compounds. Because metal ions cannot be degraded or modified like toxic organic compounds, there are six possible mechanisms for a metal resistance system:

- exclusion by permeability barrier;
- intra- and extra-cellular sequestration;
- active efflux pumps;
- enzymatic reduction; and
- reduction in the sensitivity of cellular targets to metal ions<sup>22, 23, 24, 25, 26</sup>.

One or more of these resistance mechanisms allows microorganisms to function in metal contaminated environments. In bacteria, heavy metal resistance genes are usually located on plasmids or transposons. Several bacterial resistance mechanisms to toxic metals have been studied and described<sup>27, 28</sup>.



### 1.1.2 The arsenic global geocycle

Just as there are well-studied geocycles for carbon, nitrogen, oxygen, sulfur and other elements that are components of all living cells, there are also geocycles for toxic elements including arsenic. Living cells (especially microbes) carry out redox and covalent bond chemistry and are important contributors in the arsenic geocycle. Higher plants and animals can bio-accumulate compounds to levels far above those of the environments in which they live. Arsenate (the main arsenic compound in seawater) is taken up by marine organisms, ranging from phytoplankton, algae, crustaceans, mollusks and fish<sup>29</sup>, and converted to organic compounds (such as methylarsonic acid or dimethylarsinic acid), or is converted to organic storage forms that are then secreted into the environment. However, some arsenic is retained by phytoplankton and metabolised into complex organic compounds<sup>29</sup>. More complex algal organoarsenical compounds include water-soluble arsenosugars (i.e. dimethylarsenosugars) and lipid-soluble compounds (arsenolipids). While phytoplankton and macroalgae are the primary producers of complex organoarsenic compounds in the sea, these organisms are themselves consumed and metabolized by marine animals. Fish and marine invertebrates retain 99% of accumulated arsenic in organic form, and crustacean and mollusk tissues contain higher concentrations of arsenic than fish. The major organoarsenic compound isolated from marine organisms is arsenobetaine. It occurs in algae, clams, lobsters, sharks, and shrimp, but it is not known how arsenosugars and arsenolipids are converted to arsenobetaine within the higher animals in the marine environment. Arsenobetaine is degraded by microbial metabolism in coastal seawater sediments to methylarsonic acid and to inorganic arsenic<sup>30</sup>.

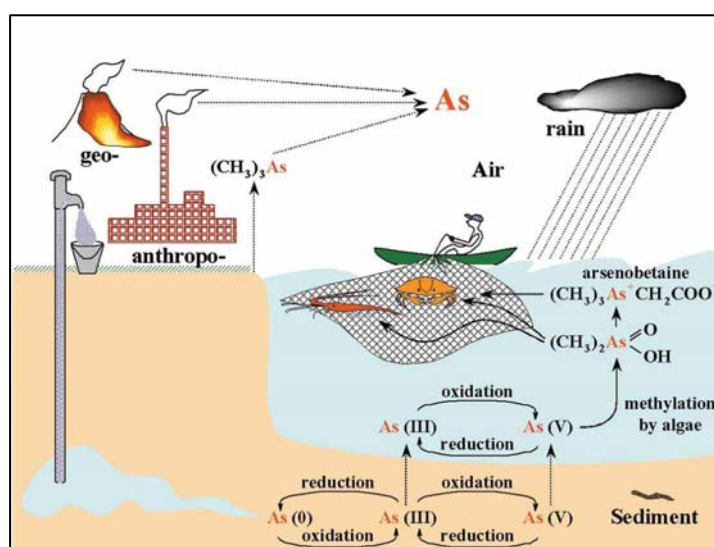
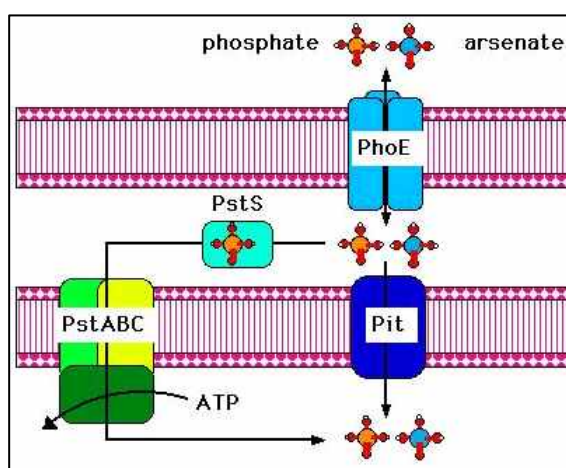


Figure 1.1 The arsenic geocycle (From Mukhopadhyay *et al.* 2002)<sup>30</sup>.

### **1.1.3 Entry of arsenic into cells**

To have a physiological or toxic effect, most metal ions have to enter the microbial cell. Pentavalent arsenate is analogous to inorganic phosphate and both anions utilize the same pathway to enter cells. In *Escherichia coli* arsenate enters the periplasmic space through the outer membrane porin, PhoE, and is transported into the cytoplasm by either of the phosphate transporters: The Pit system (phosphate transport) appears to be the predominant system<sup>31</sup>, but arsenate also enters the cells via the phosphate translocating ABC-type ATP-ase complex, Pst (phosphate specific transport)<sup>32</sup>, formed by the PstA, PstB, PstC and PhoS proteins<sup>33</sup> (Figure 1.2).



**Figure 1.2** Transport of arsenate into *E. coli* (from Nies & Silver, 1995)<sup>23</sup>.

Arsenite, on the other hand, might be considered an inorganic equivalent of glycerol and therefore the glycerol facilitator of *E. coli* GlpF is the main route of entry into cells<sup>34</sup>. GlpF is an aquaglyceroporin, a member of the aquaporin superfamily consisting of multifunctional channels that transport neutral organic solutes such as glycerol and urea<sup>35</sup>.

The frequent abundance of arsenic in the environment has guided the evolution of enzymes for a variety of ingenious resistance mechanisms for protection against the deleterious effects of arsenic as described below in section 1.1.4 – 1.1.7.

### **1.1.4 Methylation**

The conversion of arsenate to methylarsonic acid or to dimethylarsinic acid is a possible mechanism for detoxification and was first observed over 150 years ago. It has been

understood, at the level of products formed, from the work of Challenger and co-workers before World War II<sup>36, 37</sup>. Fungi dominate the microbes that produce volatile, garlic-smelling trimethylarsine, although bacteria and animal tissues also have this potential<sup>38</sup>. Hall *et al.* (1997)<sup>39</sup> showed that the microbial content of the mouse intestinal cecum (mostly anaerobic bacteria) methylates inorganic arsenic, where up to 40% of low levels of As(III) and As(V) were methylated *in vitro* by cecal contents in less than 24 hours. Both monomethyl- and dimethyl-arsenic compounds were formed and addition of potential methyl donors increased the yield of methylarsonic acid (Figure 1.3).

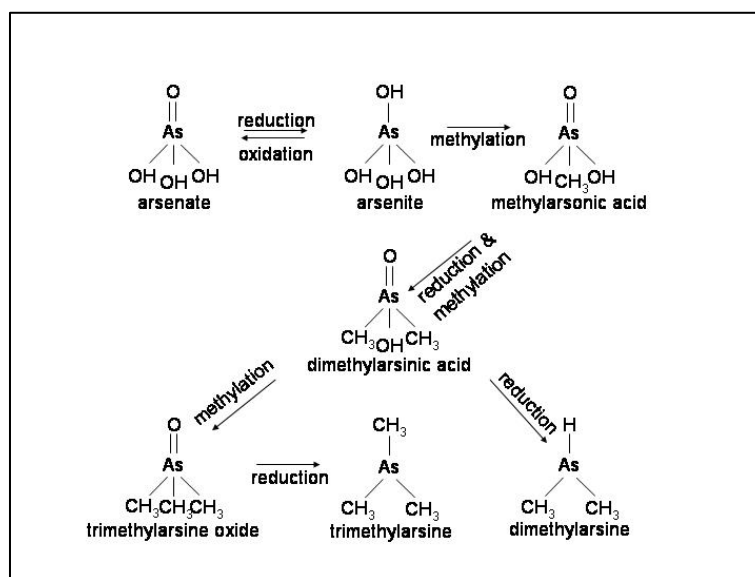


**Figure 1.3** Microbial formation of trimethylarsine from inorganic arsenate<sup>9, 36, 40</sup>.

Following the discovery of biomethylation of mercury by *Methanobacillus omelianski*<sup>41</sup>, it was shown that *Methanobacterium bryantii* produced dimethylarsine from several arsenic compounds<sup>42</sup>. The facultative marine anaerobe *Serratia marnorubra* can also convert arsenate to arsenite and methylarsonic acid when grown aerobically, but volatile arsines are not produced under either aerobic or anaerobic conditions<sup>43</sup>. Five bacterial species, (*Corynebacterium* sp., *E. coli*, *Flavobacterium* sp., *Proteus* sp., and *Pseudomonas* sp.) isolated from the environment were able to produce dimethylarsine after acclimatisation with sodium arsenate. The *Pseudomonas* sp. was able to form all three of the methylated arsines. Six bacterial species (*Achromobacter* sp., *Aeromonas* sp., *Alcaligenes* sp., *Flavobacterium* sp., *Nocardia* sp., and *Pseudomonas* sp.) produced both mono- and dimethylarsine from methylarsonate; only two of them produced trimethylarsine. The *Nocardia* sp. was the only organism that produced all of the methylarsines from this substrate<sup>44</sup>.

Qin *et al.*<sup>45</sup> reported the isolation of the protein product of the newly named *arsM* gene from *Rhodospseudomonas palustris*. Whole cell and cell-free enzyme assays showed the formation of mono-, di- and trimethylarsenic compounds. *S*-adenoylmethionine and glutathione were required for enzyme activity *in vitro* and when this gene was cloned into *E. coli* cells, the ability to produce volatile trimethylAs(III) and resistance to inorganic arsenite was transferred.

### **1.1.5 Oxidation**

Oxidation of As(III) represents a potential detoxification process that allows microorganisms to tolerate higher levels of arsenite. Several examples of bacterial oxidation of arsenite to arsenate were being reported as early as 1918<sup>46</sup> and aerobic isolates from arsenic-impacted environments have since been isolated and described<sup>47, 48, 49</sup>. Similar isolates have also been found in soils and sewage not known to be exposed to elevated levels of arsenic<sup>50, 51</sup>. More than 30 strains representing at least nine genera of the *Bacteria* and *Archaea*, including members of the *Alphaproteobacteria*, *Betaproteobacteria*, *Gammaproteobacteria*, *Deinococcus–Thermus* and *Crenarchaeota*, have been reported to be involved in arsenite oxidation<sup>52, 53</sup>.

To date, all known aerobic arsenite oxidases exhibit a heterodimeric structure with molybdopterin and Rieske-like subunits<sup>54, 55</sup>. The large subunit (AroA ~90kDa) of the arsenite oxidase is the first example of a new subgroup of the dimethylsulfoxide (DMSO) reductase family of molybdoenzymes<sup>56</sup>. All enzymes in this family are involved in electron transport whereby the Mo-centre serves to cycle electrons via the Mo(IV) and Mo(VI) valence states, and appear to have a common ancestor present prior to the divergence of the *Bacteria* and *Archaea*<sup>57, 58</sup>. Unfortunately, much confusion surrounds the naming of arsenite oxidases, and currently three different nomenclatures exist to describe what are essentially homologous proteins encoded by *asoA* & *asoB*<sup>55</sup>, *aoxB* & *aoxA*<sup>59</sup>, *aroA* & *aroB*<sup>48</sup>.

The arsenite-oxidizing bacteria isolated can be divided into two groups:

- (i) heterotrophs (growth in the presence of organic matter) or
- (ii) chemolithoautotrophs (aerobes or anaerobes, using arsenite as the electron donor and CO<sub>2</sub>/ HCO<sub>3</sub><sup>-</sup> as the sole carbon source).

The oxidation of As(III) by heterotrophic microorganisms is generally considered to be a detoxification mechanism as the microbes do not gain energy from the reaction<sup>55</sup>. Arsenite oxidase genes have been described from the heterotrophic strains *Alcaligenes faecalis*<sup>55</sup>, *Cenibacterium arsenoxidans*<sup>59</sup>, *Thermus* sp. str. HR13<sup>60</sup>, *Thermus thermophilus* str. HB8<sup>61</sup>, *Agrobacterium tumefaciens*<sup>62</sup> and *Chloroflexus aurantiacus*<sup>58</sup>. The arsenite oxidase from *Alcaligenes faecalis* is located on the outer surface of the inner membrane and the arsenite oxidase transfers electrons to the periplasmic electron carriers amicyanin or cytochrome c. The crystal structure shows the enzyme is heterodimeric with two subunits ( $\alpha_1\beta_1$ ). The large subunit, AsoA is an 88kDa polypeptide that contains a molybdopterin and a 3Fe-4S center. The small subunit AsoB is a 14kDa polypeptide which contains a Rieske 2Fe-2S center<sup>54</sup>. AsoA is structurally related to members of the dimethyl sulfoxide (DMSO) reductase family of molybdoenzymes. Based on amino acid sequence identity, AsoA shows the closest relatedness to the dissimilatory nitrate reductase (NAP) (23%) and formate dehydrogenase (FDH) (20%)<sup>56</sup>. The structure of the large subunit allows As(OH)<sub>3</sub> to enter and allows HAsO<sub>4</sub><sup>2-</sup> to exit following oxidation<sup>54, 56</sup>. Characterization of the arsenite oxidase genes (*aox*) in *C. arsenoxidans* shows that the sequence of the small subunit AoxA is 65% identical to the AsoB found in *A. faecalis*, while AoxB, the large subunit in *C. arsenoxidans*, is 72% identical to AsoA. The enzyme is also located on the outer surface of the inner membrane<sup>59</sup>. These results indicate that the arsenite oxidase genes found in heterotrophic As(III)-oxidizers are homologous even though they are named differently<sup>55</sup>.

In contrast, autotrophic As(III) oxidizers can utilize As(III) as an electron donor coupled to CO<sub>2</sub> fixation for cell growth under

- (i) aerobic conditions<sup>63, 64</sup>,
- (ii) denitrifying conditions<sup>52, 65</sup>.

There are currently two chemolithoautotrophic arsenite-oxidizing bacteria that have been studied in detail: the aerobe NT-26<sup>64</sup> and the facultative anaerobe MLHE1<sup>52</sup>. The NT-26 arsenite oxidase (Aro) belongs to the dimethyl sulfoxide (DMSO) reductase family of molybdoenzymes. The enzyme is induced by arsenite and located within the periplasm. AroA (98kDa) is a molybdenum containing  $\alpha$ -subunit and AroB (14kDa) is the small subunit containing a Rieske-type [2Fe-2S] cluster. The amino acid sequence of AroA is 49.2% identical to AsoA from *A. faecalis* and 48.4% identical to AoxB of *C. arsenoxidans*<sup>48</sup>. Additionally, six novel bacterial strains have been described in 2007, which can couple CO<sub>2</sub> fixation to As(III) oxidation under either aerobic or denitrifying conditions<sup>66</sup>, but none have

been studied in depth. Four of these autotrophic arsenite oxidizers are aerobes (*Ancylobacter* sp. strain OL1, *Thiobacillus* sp. strain S1, *Hydrogenophaga* sp. strain CL3, and *Bosea* sp. strain WAO), and two are denitrifiers (*Azoarcus* sp. strain DAO1 and *Sinorhizobium* sp. strain DAO10) which are able to use  $\text{NO}_3^-$  as the respiratory electron acceptor with complete reduction to  $\text{N}_2$  gas<sup>65</sup>.

## **1.1.6 Reduction**

### **1.1.6.1 Respiratory arsenate reductases**

There are several microbes that use As(V) as an electron acceptor in dissimilatory anaerobic respiration. These prokaryotes oxidize a variety of organic (e.g. lactate, acetate, formate and aromatics), or inorganic (hydrogen and sulfide) electron donors, resulting in the production of As(III). Anaerobic arsenate respiration was discovered in 1994 with a bacterial isolate that coupled anaerobic heterotrophic growth to arsenate reduction<sup>67</sup> and since then, diverse bacterial types with anaerobic respiratory arsenate reductase have been described<sup>68, 69</sup>.

The anaerobic respiratory arsenate reductase from *Crysiogenis arsenatis* is a heterodimeric, periplasmic or membrane associated protein with a native molecular mass of 123kDa with a  $K_m$  of 300 $\mu\text{M}$ . It consists of a large molybdopterin subunit (ArrA) (87kDa) which contains an iron-sulfur center, possibly a high potential [4Fe-4S] cluster (but is not related to the aerobic arsenite oxidases), and a smaller [Fe-S] center protein (ArrB) (29kDa)<sup>70</sup>. Both ArrA and ArrB subunits have a conserved N-proximal cysteine-rich iron-sulphur cluster-binding motif (ArrA, CX<sub>2</sub>CX<sub>3</sub>C; and ArrB, CX<sub>2</sub>CX<sub>2</sub>CX<sub>3</sub>C) and phylogenetic analysis of ArrA and related sequences indicates that ArrA is distantly related to AsoA in the dimethyl sulfoxide (DMSO) oxydoreductase family<sup>71</sup>. ArrB appears to be an iron-sulfur protein related to DmsB of DMSO reductase and NrfC of nitrite reductase<sup>72</sup>.

The arsenate reductase from *Sulfurospirillum barnesii* is a trimeric membrane bound complex with a molecular weight of 120kDa<sup>68</sup>. This protein has an  $\alpha$  subunit of 65kDa, a  $\beta$  subunit of 31kDa, and a  $\gamma$  subunit of 22kDa. A b-type cytochrome appears to complement membrane fractions. *Desulfomicrobium* strain Ben-RB reduces arsenate by a membrane-bound enzyme, probably associated with a c-type cytochrome of which c55 is the major cytochrome in this organism<sup>73</sup>.

### 1.1.6.2 Cytoplasmic arsenate reductases

The arsenate reductases (ArsC) from different sources have unrelated sequences and structural folds, and can be divided into different classes on the basis of their structures, reduction mechanisms and the locations of catalytic cysteine residues. ArsC cytoplasmic arsenate reductases are found widely in microbes, and the *arsC* gene occurs in *ars* operons in most bacteria with total genomes measuring 2Mb or larger, as well as in some *Archaeal* genomes<sup>55</sup>. In bacteria, the resistance determinants are often found on plasmids<sup>74, 75, 76</sup> which has facilitated their study at the molecular level. As more and more bacterial genomes are sequenced, it has become evident that arsenic resistance operons are ubiquitous. Homologous chromosomal systems have also been found and are functional and provide arsenic tolerance<sup>77, 78</sup>. Three unrelated groups of ArsC sequences are currently recognized (Figure 1.4), and these share a common biochemical function<sup>30</sup>.

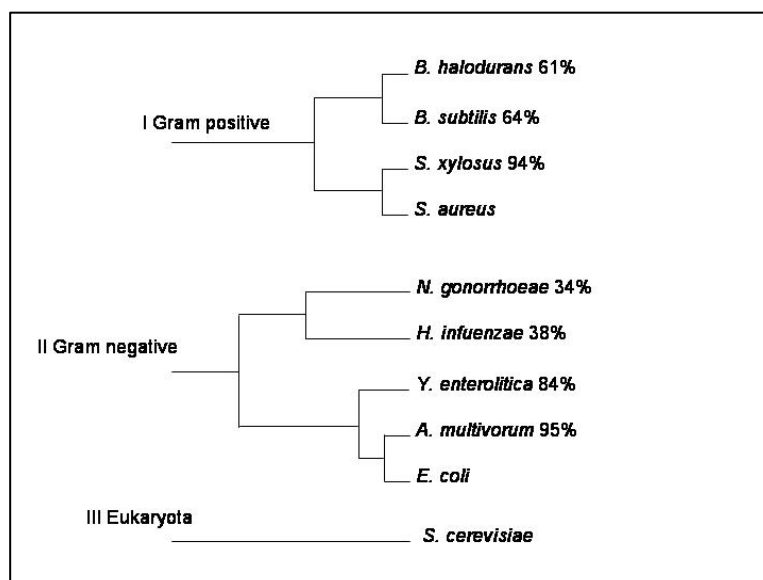


**Figure 1.4** ArsC families from Gram positive bacteria (I), Gram negative bacteria (II), and eukaryota (III). (*Bacillus halodurans*, *B. subtilis*, *Staphylococcus xylosus*, *Neisseria gonorrhoeae*, *Haemophilus influenzae*, *Yersinia enterocolitica*, *Acidiphilium multivorum*. Percentage sequence identity with the model enzyme for each family is indicated. (Interfamilial sequence identity is lower than 20%.)<sup>79</sup>.

The first family, represented by ArsC from *Escherichia coli* plasmid R773 is present on many plasmids and chromosomes of Gram negative bacteria. This is a glutaredoxin-glutathione-coupled enzyme, and has a distinct HX3CX3R catalytic sequence motif that partially resembles crambin and partially glutaredoxin<sup>80</sup>. The thioredoxin-coupled arsenate

reductases form the second family of arsenate reductases and was found initially in Gram positive bacteria, but more recently also in Gram negative proteobacteria. ArsC from *Staphylococcus aureus* plasmid pI258 as model enzyme for this family has a tyrosine phosphatase (PTPase) I fold typical for low molecular weight (LMW) PTPases. It includes a P-loop with the characteristic CX5R sequence motif flanked by a  $\beta$ -strand and an  $\alpha$ -helix<sup>81</sup>. There is no relationship between the tertiary structures of the glutaredoxin and thioredoxin coupled arsenate reductases, supporting the conclusion that these two classes of enzyme are not related. Both classes of arsenate reductases have a core of four  $\beta$ -strands forming a  $\beta$ -sheet region. The strands are all parallel for the thioredoxin coupled family but with one anti-parallel  $\beta$ -sheet strand for the glutaredoxin coupled ArsC from plasmid R773<sup>82</sup>. The third and less-well-defined glutaredoxin-dependent arsenate reductase family is found in yeast (*Saccharomyces cerevisiae*) and also contains the abovementioned motif but is homologous to the human cell cycle control phosphatase Cdc25a<sup>83</sup>.

### **1.1.7 Other mechanisms: Biosorption**

The accumulation of toxic metals by bacterial biomass presents an effective means of removing these metals from solution and has been applied in the remediation of several metals such as cadmium<sup>84</sup>, copper<sup>85</sup>, lead, chromium<sup>86</sup>, copper, zinc, nickel, cobalt<sup>87</sup>, vanadium<sup>88</sup> and arsenic<sup>89</sup>. The complexity of the microorganism's structure implies that there are many ways for the metal to be captured by the cell. Heavy-metal ions can be entrapped in the cellular structure and subsequently biosorbed onto the binding sites present in the cellular structure. Cell walls of microbial biomass, mainly composed of polysaccharides, proteins and lipids, offer particularly abundant metal-binding functional groups, such as carboxylate, hydroxyl, sulfate, phosphate and amino groups<sup>90</sup>.

According to the dependence on the cells' metabolism, biosorption mechanisms can be divided into (a) non-metabolism dependent / passive uptake and (b) metabolism dependent / active uptake. Furthermore, according to the location where the metal removed from the solution is found, biosorption may be classified as (a) extracellular accumulation, (b) cell surface sorption and (c) intracellular accumulation<sup>91</sup>.



## **1.2 Introduction to the present study**

Since the late 19<sup>th</sup> century, South Africa's economy has been based on the production and export of minerals, which, in turn, have contributed significantly to the country's industrial development. The Consolidated Murchinson mine, situated in the Murchison greenstone belt, is located in the Limpopo Province at Gravelotte, some 40 km due west of Phalaborwa. The orebody is contained in a shear zone, being a hydrothermally emplaced occurrence<sup>92</sup>. A fold in the earth's crust caused a cleavage, along which there has been a large shear extending deep into the earth's crust and into this, carbon dioxide, silica, antimony and gold were introduced<sup>93</sup>. The mine can be classified as a medium-scale mine and has been in operation since 1937, making it the oldest known antimony deposit in the world. It is also the only producer of antimony concentrate in South Africa and accounts for some 8% of the world's antimony production - the largest producer outside China<sup>94</sup>. Gold was discovered in the Murchison range towards the end of the nineteenth century, and was mined on a small scale for many years, with antimony as a by-product. The primary antimony ore is stibnite which is crushed and milled and an antimony concentrate is then produced by flotation. Gold is recovered in a gravity circuit and a number of leach and carbon absorption stages<sup>95</sup>.

Impurities in the concentrate are a key concern to end-users and in the case of Consolidated Murchison, these are lead and arsenic<sup>96</sup>. Lead, introduced artificially, as lead nitrate is used as an activator for the stibnite in the flotation process. Arsenic, on the other hand, is contained in the ore and cyanide is used to depress the arsenic during flotation<sup>97</sup>. Arsenic removal from the antimony product causes considerable concentration of arsenic in the tailings and currently slag from middlings dumps (with arsenic concentrations of approximately 8g/ton ~1mM) is being reprocessed.

Arsenic and antimony are both transition metal elements of subgroup VA of the periodic table and share both chemical and structural properties with nitrogen, phosphorus and bismuth. The electronic configuration of transition metal elements are characterised as having full outer orbitals and as having the second outermost orbitals incompletely filled. There are five electrons in the valence shells of these elements and thus, the principal oxidation states of these elements are +3 and +5.

### **1.3    Aims**

1.    Site description of an arsenic impacted mining environment for sampling
  - enrichment for and isolation of arsenic resistant bacteria
  - preservation methods of isolated bacteria
  
2.    Identification of bacterial isolates
  - 16S rDNA PCR and sequencing
  - substrate utilisation identification
  
3.    Determining minimum inhibitory growth concentrations of arsenic
  - arsenate - As(V)
  - arsenite - As(III)
  
4.    Growth of arsenic resistant bacteria in arsenate and arsenite
  - effect on biomass production,
  - growth rates,
  - induction of extended lag-phases
  
5.    Demonstrating and quantifying arsenate reduction as a resistance mechanism of arsenic resistant bacteria

## **1.4 Materials and methods**

### **1.4.1 General procedures and chemicals**

Chemicals used were of molecular, analytical or lab reagent grade, were obtained from various commercial suppliers and was used without further purification.

### **1.4.2 Sampling and isolation**

Soil, water and sludge samples were collected aseptically at the Consolidated Murchison antimony mining and refining site in sterile Falcon Tubes or Whirl Packs. In total, 16 sites were sampled and varied from very dry, compacted soil to sludge samples. The average pH of all samples collected was 5.8 (determined by wetting approximately 5g of soil with ddH<sub>2</sub>O and measured with pH indicators) and ambient temperature on the day of collection was approximately 35°C (specific site descriptions are given in Table 1.1). One gram of sample was mixed with 2mL basal medium (0.9g/L NaCl, 0.2g/L MgCl<sub>2</sub>, 0.1g/L CaCl<sub>2</sub>·2H<sub>2</sub>O, pH 7.5) and 400µL of this supernatant inoculated into 5mL TYG medium (5g/L tryptone, 3g/L yeast extract, 1g/L glucose) pH 5.8. TYG medium (5mL) was supplemented with 5mM, 10mM, 50mM and 100mM<sup>98</sup> potassium antimony tartrate and inocula were incubated for two days at 37°C with shaking at 200rpm to enrich for resistant aerobic mesophiles. From this, 500µL supernatant was transferred successively into fresh TYG medium similarly supplemented with potassium antimony tartrate to identify possible positive enrichments by comparing with uninoculated medium. Positive enrichments were streaked on antimony supplemented TYG plates (100mM) and passaged on plates to obtain uniform colonies. Pure cultures were Gram stained<sup>99</sup> to confirm purity and were then inoculated into TYG medium containing increasing concentrations of arsenate (Na<sub>2</sub>HAsO<sub>4</sub>) and arsenite (NaAsO<sub>2</sub>) (5mM, 10mM, 50mM and 100mM) to perform a preliminary arsenic resistance screen. Isolates capable of growth in arsenic were used for further experiments.

Table 1.1 Sampling site description.

Sample #	Site description	pH
<b>1-4</b>	<b>Dumping site (very dry)</b>	
1	Red, arsenic rich, ± 1m from surface	5-6
2	Mixed soil, ± 2m from surface	5-6
3	Black, antimony rich, ± 1m from surface	5-6
4	Yellow, gold rich, ± 1m from surface	5-6
<b>5-7</b>	<b>Silt dam # 2</b>	
5	Surface sample with strong sulfur smell	4-5
6	Same as 5 but ± 15cm deep	5
7	Red, arsenic and cyanide rich, ± 15cm deep	6-7
8	Surface sample at penstock	7-8
<b>9-14</b>	<b>Northern wall of silt dam # 2</b>	
9	Logwater from dam # 2	6-7
10	Silt	6
11	Water	6
12	Silt	6
13	Soil ± 3cm deep	6
14	Biofilm	7
<b>15-17</b>	<b>Silt dam # 3</b>	
15	Water	6
16	Water and sludge from hole #5, 30°C	6-7
17	Water and sludge	6

### **1.4.3 Cryopreservation**

Cryopreservation was performed according to the method of Perry (1995)<sup>100</sup>. A single colony was inoculated into TYG medium and grown with shaking at 37°C overnight. The cells were diluted in a 1:1 (v/v) ratio with 40% sterile glycerol and stored at -80°C. All subsequent experiments were inoculated from these cryopreserved cultures.

### **1.4.4 Identification**

#### **1.4.4.1 16S rDNA sequencing**

Genomic DNA from each isolate was extracted with DNA<sub>ZOL</sub><sup>TM</sup> Reagent (Gibco BRL): cells were harvested by centrifugation, frozen and thawed once, resuspended in TE-buffer, pH

8.0 and an equal volume of DNA<sub>ZOL</sub> added. Lysozyme was added to a final concentration of 5mg/mL and incubated at 37°C with vigorous shaking for 30 minutes and thereafter at 55°C for 30 minutes with shaking. Proteinase K, to final concentration of 0.35mg/mL, was added and incubated at 37°C with vigorous shaking for 30 minutes. An equal volume of chloroform : isoamyl alcohol (24:1) was added and mixed by vortexing. Phase separation was performed by centrifugation at 10 000rpm for 15 minutes and genomic DNA in the supernatant precipitated with 0.5 volumes of ice cold 100% ethanol and centrifugation. Recovered DNA was washed with 70% cold ethanol and resuspended in 5mM Tris-HCl, pH 8.0.

16S rDNA fragments were amplified using universal bacterial primers 27F and 1492R<sup>101</sup> (Table 1.2). PCR reactions consisted of 1X Reaction Buffer, 2.5U DNA Polymerase (SuperTherm), 2mM MgCl<sub>2</sub>, 200nM of each primer, 200µM of each dNTP and approximately 50ng template DNA. Amplification was performed after an initial denaturation step at 94°C for 5 minutes and thereafter 35 cycles of denaturing at 94°C for 30 seconds, primer annealing at 52°C for 45 seconds and product extension at 72°C for 1 minute. A final polishing extension was performed at 72°C for 7 minutes. PCR products were ligated into the pGem<sup>®</sup>T-Easy vector (Promega) followed by transformation into chemically competent *E. coli* JM109 cells<sup>102</sup>. Selection was performed on LB-AIX-plates (10g/L tryptone, 5g/L yeast extract, 10g/L NaCl amended with 60µg/mL ampicillin, 9.6µg/mL IPTG (isopropyl-β-D-thiogalactopyranoside) and 40µg/mL X-gal (5-bromo-4-chloro-3-indolyl-β-D-galactoside)). Plasmids were extracted using the Wizard<sup>®</sup> Plus Miniprep DNA Purification System (Promega) and inserts of the correct size were identified by restriction analysis. The plasmid DNA (200µg) was digested at 37°C for 2 hours in a reaction mixture containing 10U *Eco*RI by combining with 1X Reaction Buffer (50mM NaCl, 100mM Tris-HCl pH 7.5, 10mM MgCl<sub>2</sub>, 0.025% Triton X-100, 100µg/mL BSA). Sequencing was performed using primers T7, Sp6 as well as internal primers U514F, Bac341F, EUB338, 915R (Table 1.2) with a BigDye<sup>®</sup> Terminator v3.1 Cycle Sequencing Kit (Applied Biosystems) on an ABI377 DNA Sequencer (PE Biosystems). The sequences obtained were aligned with that of bacteria previously found in the subsurface of mining environments as well as the closest matches revealed with BLAST searches<sup>103</sup>, and at RDP<sup>104</sup> with ClustalX (1.83)<sup>105</sup>. A heuristic search was performed with PAUP 4.0b5<sup>106</sup> and yielded 10 000 parsimonious trees. A strict consensus tree was constructed and rooted with the outgroup *Aquifex pyrophilus*. Bootstrap analysis of 100 replicates was done to determine the robustness of the clades / groups. The bootstrap cut-off was 50%<sup>107</sup>. A bootstrap value greater than 75% was considered good support. Values of 65% - 75% were considered moderate support and less than 65% as weak.

**Table 1.2 Nucleotide sequence and positioning information of the primers used to amplify and sequence 16S rDNA amplicons.**

Name	Sequence (5'-3')	Position <i>E. coli</i> 16S rDNA	Reference
27F	AGAGTTTGATCMTGGCTCAG	27	Lane <i>et al.</i> (1991) <sup>101</sup>
1492R	GGTTACCTTGTTACGACTT	1492	
U514F	GTGCCAGCMGCCGCGG	514	
Bac341F	CCTACGGGAGGCAGCAG	341	Muyzer <i>et al.</i> (1993) <sup>108</sup>
EUB338	GCTGCCTCCCGTAGGAGT	338	Davis <i>et al.</i> (2005) <sup>109</sup>
915R	GTGCTCCCCCGCCAATTCCT	915	Casamayor <i>et al.</i> <sup>110</sup>
T7 Promoter	TAATACGACTCACTATAGGG		
Sp6 Promoter	TATTTAGGTGACACTATAG		

#### **1.4.4.2 Biochemical testing**

Isolates were streaked on TYG-plates (pH 5.8) amended with 10mM arsenate. Nutritional requirements and the use of specific carbon sources for growth were tested with GN2 and GP2 MicroPlates™ (Biolog, Hayward). Following incubation at 37°C, positive test results were recorded at 16h and 24h, respectively where a similarity index greater than 0.5 was considered positive identification. API 20E panels (bioMerieux, Inc.) were also used to confirm the identification.

#### **1.4.5 Minimum inhibitory concentrations**

Bacteria were inoculated into 50mL of TYG medium, pH 5.8 and grown at 37°C as a pre-inoculum. From this, TYG medium (pH 5.8), amended with increasing concentrations of arsenite (ranging from 2.5mM to 15mM) and arsenate (0.5mM to 500mM) were inoculated in duplicate with exponential growth phase cells, to an optical density of approximately 0.1 at 560nm. Flasks containing TYG medium with arsenic omitted were used as negative controls. Inocula were grown at 37°C with shaking, samples withdrawn hourly and optical density monitored at 560nm over a 12h period.

## **1.4.6 Arsenate reduction**

### **1.4.6.1 Qualitative**

Bacteria were grown overnight at 37°C in 100mL TYG medium containing 1mM Na<sub>2</sub>HAsO<sub>4</sub>. Cells were harvested by centrifugation in a Beckman J2-MC centrifuge at 11000 x g for 10 minutes at 4°C. The cells were washed in 10mM PIPES buffer, pH 6.5 and resuspended in the same buffer in a 1:1 cell wet weight to volume ratio. This was then supplemented with 0.2% glucose (w/v) (approximately 10mM) and 10mM arsenate and incubated at 37°C<sup>111</sup>. Aliquots were withdrawn periodically over a two day period, centrifuged, the supernatant removed and stored at -20°C until further analysis. Supernatant was spotted onto Silica gel 60 F<sub>254</sub> TLC sheets (Merck), overlaid with 5µL of 100mM DTT to enhance separation<sup>112</sup>, and developed in 1:1 (v/v) EtOH : NH<sub>4</sub>OH. After drying, the plates were sprayed with 2% (w/v) AgNO<sub>3</sub><sup>113</sup>. Separation profiles were compared to As(III) and As(V) controls for identification. A negative control, without any cells, was employed to monitor chemical reduction.

### **1.4.6.2 Quantitative**

The same procedure as described in the preceding section (1.4.6.1) was followed, but the separated As(III) was recovered from the silica matrix and assayed using a modified molybdate assay for phosphate<sup>114</sup>.

To quantify arsenate reduction, aliquots of 50µL (SIL-20A auto sampler, Shimadzu) of the supernatant were analyzed by HPLC (LC-20AT liquid chromatograph, Shimadzu) injected onto a Hamilton PRP X-100 column. The mobile phase consisted of 12mM H<sub>3</sub>PO<sub>4</sub>, pH 3.2, and the products were eluted isocratically at a constant temperature of 30°C (CTO-10AS column oven, Shimadzu). Both substrate depletion (arsenate) and product formation (arsenite) were determined at 195nm (SPD-20AV UV/vis detector, Shimadzu). A negative control, without any cells, was employed to monitor chemical reduction.

## **1.5 Results and discussion**

### **1.5.1 Enrichments**

Soil, water and sludge samples from 16 sites were inoculated to enrich for resistant bacteria. Samples from six sites (10, 12, 14 -17) showed growth in medium amended with 100mM potassium antimony tartrate (Table 1.3) and were successively streaked out to obtain pure cultures. These cultures were named according to site collection numbers.

**Table 1.3 Growth for pure cultures inoculated into antimony supplemented TYG medium.**

<b>Sample #</b>	<b>0mM</b>	<b>5mM</b>	<b>10mM</b>	<b>50mM</b>	<b>100mM</b>
1	-	-	-	-	-
2	-	-	-	-	-
3	-	-	-	-	-
4	√	√	-	-	-
5	√	√	-	-	-
6	√	√	-	-	-
7	√	√	-	-	-
8	√	-	-	-	-
9	√	√	-	-	-
10	√	√	√	√	√
11	√	√	-	-	-
12	√	√	√	√	√
13	√	√	-	-	-
14	√	√	√	√	√
15	√	√	√	√	√
16	√	√	√	√	√
17	√	√	√	√	√

Site 10 yielded 2 isolates, while the bacteria from sample 12 lost resistance during the purification, possibly due to syntrophy within the bacterial consortium. All six pure cultures were screened for arsenic resistance in liquid medium amended with arsenate and arsenite. The bacteria were more resistant to arsenate than arsenite and three of the isolates (10(2), 16, 17) were resistant to up to 100mM arsenate while isolates 15, 16 and 17 were resistant to 10mM arsenite (Table 1.4).



**Table 1.4 Growth for pure cultures in arsenate and arsenite supplemented TYG medium.**

Sample #	Arsenate				Arsenite			
	5mM	10mM	50mM	100mM	5mM	10mM	50mM	100mM
10(1)	√	-	-	-	√	-	-	-
10(2)	√	√	√	√	√	-	-	-
14	√	-	-	-	√	-	-	-
15	√	√	√	-	√	√	-	-
16	√	√	√	√	√	√	-	-
17	√	√	√	√	√	√	-	-

### **1.5.2 Identification**

Amplification of the 16S rDNA sequence from these isolates yielded PCR products of the expected size of approximately 1500bp (Figure 1.5). Near full length sequences were deposited in the NCBI database and compared with BLAST (software version 2.2.13, National Center for Biotechnology Institute, <http://www.ncbi.nlm.nih.gov/BLAST/>) analysis to entries available at the EMBL, GenBank, and Ribosomal Data Project (release 9.35, <http://rdp.cme.msu.edu/>). Table 1.5 shows the closest sequence matches, % identity and RDP scores of the 16S rDNA gene from each of the pure cultures.

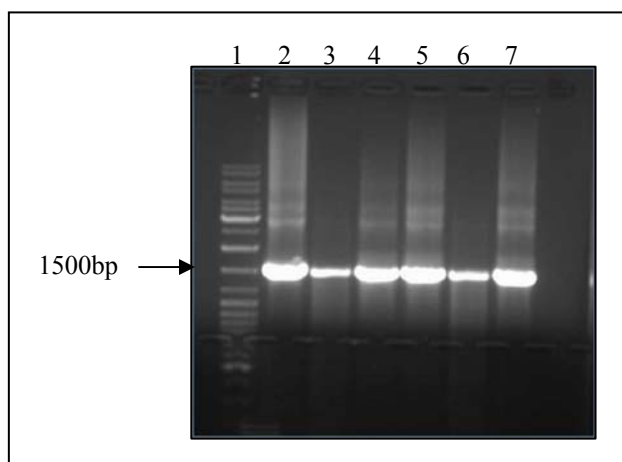


**Figure 1.5 16S rDNA PCR products from arsenic resistant pure cultures. Lane 1: GeneRuler™ molecular weight marker, Lane 2: isolate 10(1), Lane 3: isolate 10(2), Lane 4: isolate 14, Lane 5: isolate 15, Lane 6: isolate 16, Lane 7: isolate 17.**

**Table 1.5** Closest sequence matches for 16S rDNA genes of pure cultures.

Isolate #	Accession #	Length (bp)	BLAST % Identity	RDP Score %	Closest match
10(1)	DQ079060	1401	99	0.993	<i>Bacillus cereus</i> EU169167 /
			99	0.993	<i>Bacillus thuringiensis</i> AB363741
10(2)	AY566180	1504	99	0.992	<i>Serratia marcescens</i> AB061685
14	DQ079058	1409	99	0.981	<i>Bacillus cereus</i> EU169167 /
			99	0.981	<i>Bacillus thuringiensis</i> AB363741
15	DQ079059	1439	99	0.951	<i>Stenotrophomonas maltophilia</i> EF580914
16	AY551938	1506	98	0.951	<i>Serratia marcescens</i> AB061685
17	DQ079057	1386	99	0.971	<i>Serratia marcescens</i> AY043386

Three isolates (*Bacillus* sp. SA Ant 14, *S. maltophilia* SA Ant 15 and *S. marcescens* SA Ant 16) were used for further investigations. Sequencing results are illustrated by the phylogenetic tree (Figure 1.6) generated with 16S rDNA sequences as described in section 1.4.4.1. Biochemical identification was repeated with API panels and Biolog MicroPlate™ testing and confirmed isolate SA Ant 16 as *Serratia marcescens* with a similarity index of 0.58. It was not possible to definitively identify isolates SA Ant 14 and SA Ant 15 using biochemical testing with the Microlog™ software and database.

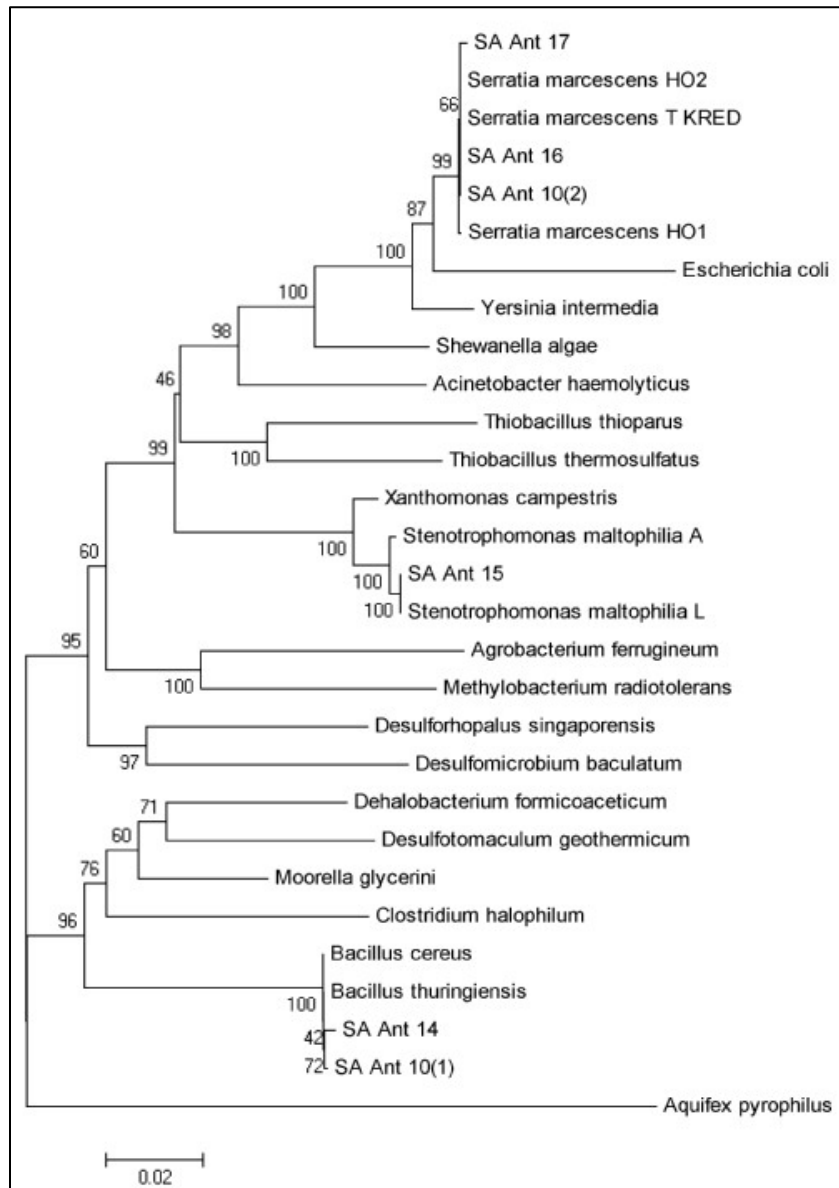


**Figure 1.6** Phylogenetic tree generated with 16S rDNA PCR sequences. (*Bacillus cereus* AF290547; *Bacillus thuringiensis* Z84588; *Moorella glycerini* U82327; *Dehalobacterium formicoaceticum* X86690; *Desulfotomaculum geothermicum* X80789; *Clostridium halophilum* X77837; *Desulforhopalus singaporensis* AF118453; *Desulfomicrobium baculatum* AF030438; *Serratia marcescens* HO2-A AJ297950; *Serratia marcescens* (T) KRED AB061685; *Serratia marcescens* HO1-A AJ 297946; *Escherichia coli* AY776275; *Yersinia intermedia* (ER-3854) X75279; *Shewanella alga* X81622; *Acinetobacter haemolyticus* X81662; *Stenotrophomonas maltophilia* ATCC 19861T AB021406; *Stenotrophomonas maltophilia* LMG 10989 AJ131907; *Xanthomonas campestris* AJ811695; *Thiobacillus thioparus* M79426; *Thiobacillus therosulfatus*, U27839; *Agrobacterium ferrugineum* D88522; *Methylobacterium radiotolerans* D32227; *Aquifex pyrophilus* M83548.)

### **1.5.3 Minimum inhibitory concentration**

The bacteria exhibited different tolerance levels for both arsenite and arsenate, and with the exception of *Bacillus* sp. SA Ant 14, it was found that these bacteria were hyper-tolerant and could grow in exceptionally high concentrations of arsenate, (up to 500mM ~ 38000ppm) and also high concentrations of arsenite (up to 10mM ~ 770ppm). *Bacillus* sp. SA Ant 14 was able to grow in concentrations of arsenic below 5mM, *S. maltophilia* SA Ant 15 grew in ‘moderate’ arsenic concentrations (up to 10mM arsenite and 20mM arsenate respectively), while *S. marcescens* SA Ant 16 was able to grow in ‘moderate’ concentrations of arsenite, but was able to grow in up to 500mM arsenate. (Results are summarised in Table 1.6.) A model bacterium such as *E. coli* has been shown to grow in up to 50mM arsenate<sup>115</sup>, while bacteria isolated from arsenic contaminated sites in New Zealand were not able to grow in arsenite concentrations exceeding 45mM and arsenate above 50mM<sup>116</sup>. Reports of resistance to arsenic in eukaryotes are in the range of 1.2mM arsenite and 6mM arsenate for *Saccharomyces cerevisiae*<sup>117</sup>, 1500ppm chromated copper arsenate (approximately 20mM) for *Pteris vittata* (brake fern)<sup>118</sup> and 200mM arsenate for an *Aspergillus* strain isolated from a heavily contaminated river in Spain<sup>119</sup>. *Corynebacterium glutamicum* is able to grow in medium containing up to 12mM arsenite and 500mM arsenate<sup>120</sup>. It is therefore clear that *S. marcescens* SA Ant 16 isolated during this study represents one of the most arsenate tolerant prokaryote described to date.

**Table 1.6** Effect of increasing concentrations arsenite or arsenate on biomass yield, maximum specific growth rate and lag phase for *Bacillus* sp. SA Ant 14, *S. maltophilia* SA Ant 15 and *S. marcescens* SA Ant 16 grown for 12 hours.

		Concentration (mM)	Biomass (12 h) (mg/mL dry weight)	Max. Specific Growth Rate (/h)	Lag Phase (h)
<i>Bacillus</i> sp. SA Ant 14	TYG		0.48	0.19	4
	As (III)	2.5	0.55	0.25	4
		5	0.64	0.24	5
		6.5	0.07	0.03	6
	As(V)	0.5	0.49	0.20	5
		1	0.53	0.23	4
		2.25	0.53	0.20	6
		4	0.10	0.31	8
<i>S. maltophilia</i> SA Ant 15	TYG		1.41	0.30	-
	As(III)	2.5	1.14	0.27	-
		5	0.23	0.15	-
		7.5	0.33	0.10	-
		10	0.21	0.06	-
	As(V)	5	1.06	0.30	-
		10	0.98	0.22	5
		20	0.87	0.20	6
100		0.04	0.04	10	
<i>S. marcescens</i> SA Ant 16	TYG		1.50	0.42	-
	As(III)	2.5	1.42	0.44	-
		5	1.36	0.37	-
		10	1.23	0.23	-
		15	0.09	0.08	-
	As(V)	20	1.32	0.21	1
		100	0.97	0.18	1
		150	0.87	0.19	1
300		0.47	0.12	2	
	500	0.08	0.04	6	

Both biomass and specific growth rate of *Bacillus* sp. SA Ant 14 showed an increasing trend in the presence of arsenite, below 6.5mM (Figure 1.7). During growth in increasing concentrations of arsenate, *Bacillus* sp. SA Ant 14 had comparable biomass yields after 12h of growth in both arsenite and arsenate. Considerably higher maximum specific growth rates were also observed. Possible explanations such as contamination was ruled out by microscopic

investigation; the arsenic amendments were in too high concentrations to be able to act as micronutrients to stimulate growth; and since the cells were grown aerobically, it is not possible that the arsenic ions could function as either electron donor or -acceptor. In terms of conventional bioenergetic systems this stimulation of growth is difficult to rationalize. Anderson and Cook<sup>121</sup> observed a similar trend when growing arsenate reducing bacteria (*Aeromonas* and *Exiguobacterium*) in rich medium, but not when grown in chemically defined medium. The mechanism and rationale for this phenomenon remains unexplained.

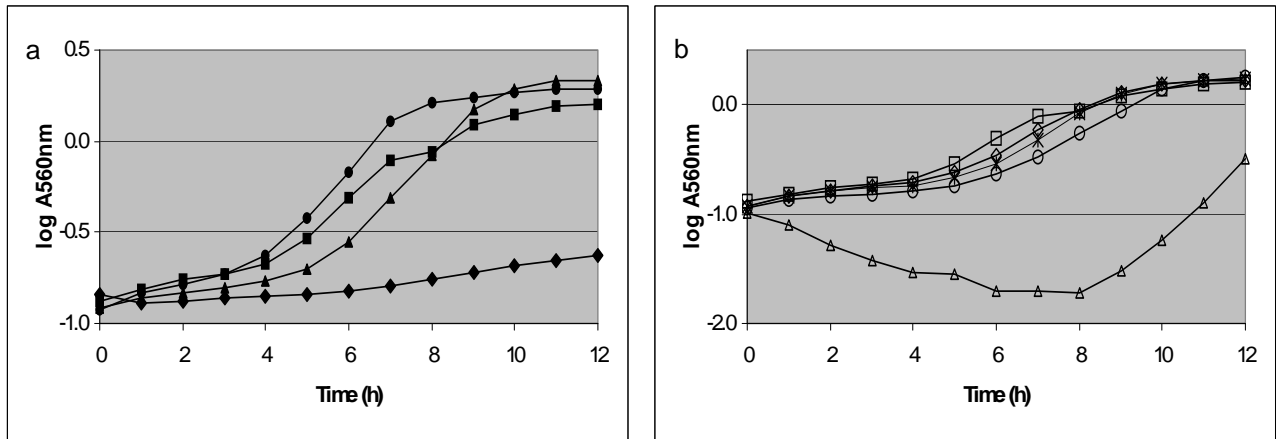


**Figure 1.7** Growth of *Bacillus* sp. SA Ant 14 in absence and presence of arsenite (a) (■ TYG; ● 2.5mM; ▲ 5mM; ◆ 6.5mM) and arsenate (b) (□ TYG; ◇ 0.5mM; \* 1mM; ○ 2.25mM; △ 4mM). Error bars are too small to be indicated.

Both the specific growth rate and biomass yield was severely inhibited for *S. maltophilia* SA Ant 15 in the presence of arsenite. Arsenate inhibited growth to a much lesser extent, as indicated by specific growth rate and biomass yield, but an increasing lag phase was observed with increasing concentrations of arsenate (Figure 1.8).

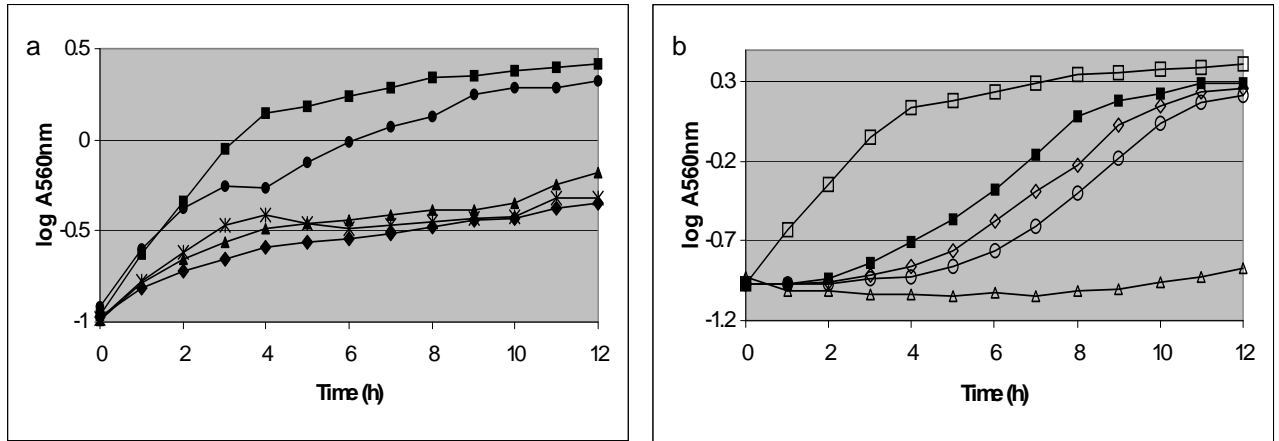


**Figure 1.8** Growth of *S. maltophilia* SA Ant 15 in absence and presence of arsenite (a) (■ TYG; ● 2.5mM; \* 5mM; ▲ 7.5mM; ◆ 10mM) and arsenate (b) (□ TYG; ■ 5mM; ◇ 10mM; ○ 20mM; △ 100mM). Error bars are too small to be indicated.

For *S. marcescens* SA Ant 16, addition of arsenite resulted in a decrease in both specific growth rate and biomass up to a threshold concentration above 10mM, whereafter a sharp decline in both these parameters were observed. Addition of arsenate resulted in a lag phase that lengthened with increasing concentrations. A linear decrease in biomass yield was seen after 12h of growth as well as a decline in specific growth rate up to 500mM arsenate (Figure 1.9).

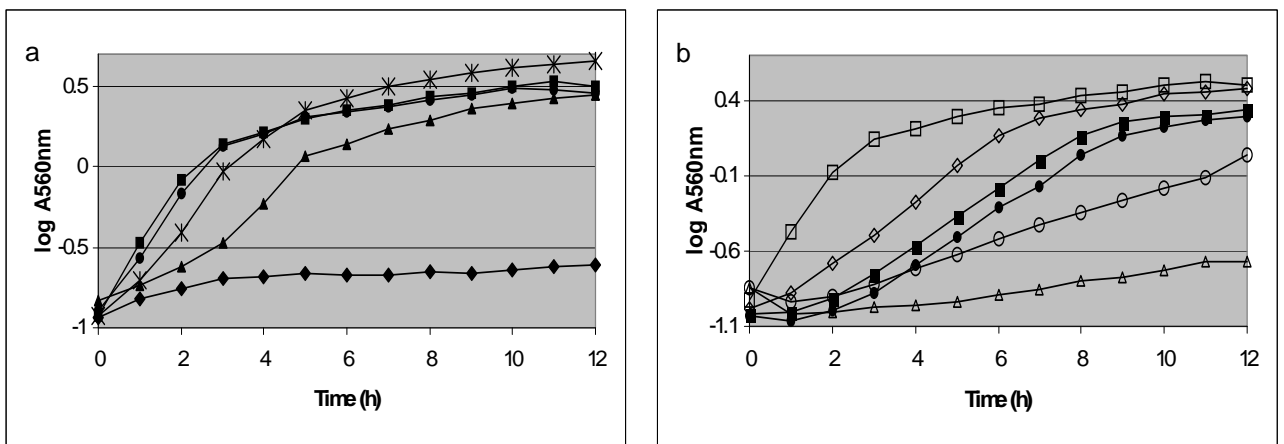


**Figure 1.9** Growth of *S. marcescens* SA Ant 16 in absence and presence of arsenite (a) (■ TYG; ● 5mM; \* 7.5mM; ▲ 10 mM; ◆ 15mM) and arsenate (b) (□ TYG; ◇ 20mM; ■ 100mM; ● 150mM; ○ 300mM; △ 500mM). Error bars are too small to be indicated.

Longer lag phases could be indicative of an initial adaptation phase where, for example, arsenate could be adsorbed or reduced to arsenite. Lower growth rates and biomass are likely results of the toxicity of arsenate or the inhibitory effects of arsenite formed by reduction. External factors might also play an auxiliary role in the exceptionally high resistance to arsenate. Acidification of the culture medium by arsenate resistant bacteria during growth has been demonstrated with an increase in the external pH as a result of arsenate reduction<sup>121</sup>. This ‘neutralization’ of the medium might prevent the pH from decreasing to a point where the bacteria are no longer able to grow and therefore indirectly enable the bacteria to survive at higher concentrations.

#### **1.5.4 Arsenate reduction by resting cells**

The ability of cells to reduce arsenate to arsenite under resting conditions was determined by TLC (Figure 1.10). Quantitative arsenate reduction was initially monitored by recovering As(III) from the TLC plates and performing a modified phosphate assay. However, this progression of testing showed poor reproducibility and HPLC-analysis was performed as an alternative.

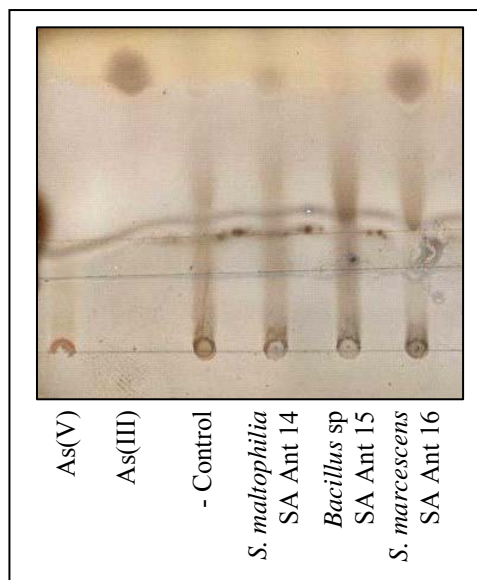


**Figure 1.10** TLC plate demonstrating arsenate reduction to arsenite by resting cells of *Bacillus* sp. SA Ant 14, *S. maltophilia* SA Ant 15 and *S. marcescens* SA Ant 16.

No chemical reduction was observed under this set of experimental conditions (results not shown). All three the bacterial isolates were able to reduce arsenate and extrude the resulting arsenite, but it is clear that this is not the only resistance strategy employed to cope



with arsenate, as a significant portion of arsenate removed (69 – 77%) was not recovered as arsenite, especially in the case of the *Bacillus* sp. (Figure 1.11 a, b and c).

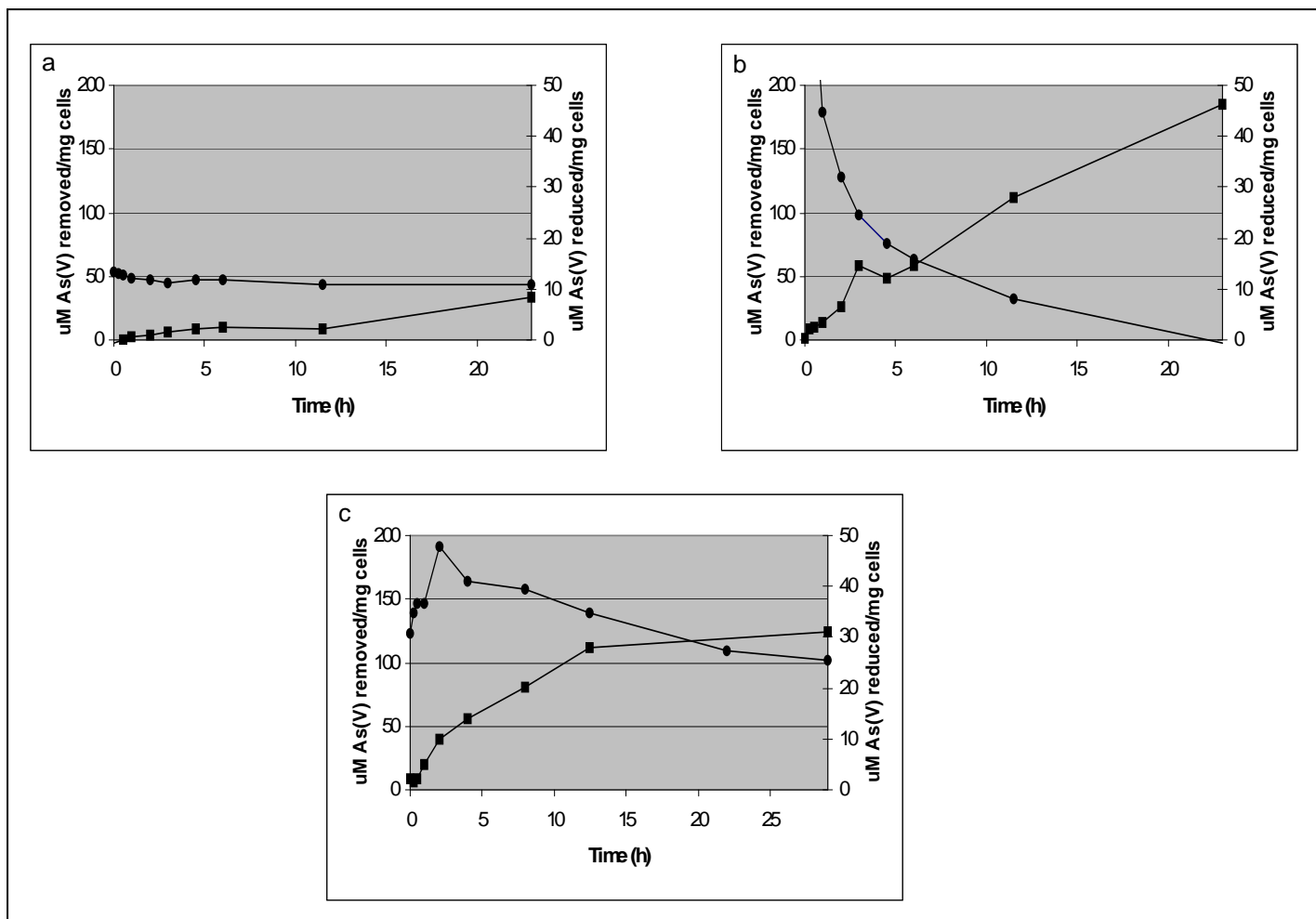


**Figure 1.11** Reduction of arsenate (●) to arsenite (■) by resting cells of (a) *Bacillus* sp. SA Ant 14 (b) *S. maltophilia* SA Ant 15 (c) and *S. marcescens* SA Ant 16.

A summary of the results are presented in Table 1.7. Removal of arsenate from the solution did not correlate with arsenite appearing and therefore it has to be deduced that an alternative resistance mechanism to arsenate, additional to reduction, is being employed. *Bacillus* sp. SA Ant 14 was able to remove approximately 80% of the arsenate supplied in a very short period of time, but only 4% was converted to arsenite at a reduction rate of 0.3 $\mu$ M/h/mg cells. *S. maltophilia* SA Ant 15 was able to remove all of the arsenate at a rate of 92.4 $\mu$ M/h/mg cells over the first 2h and thereafter by reducing approximately 25% to arsenite at 4 $\mu$ M/h/mg cells. *S. marcescens* SA Ant 16 removed 50% of the arsenate by reducing 15% to arsenite at approximately 2 $\mu$ M/h/mg cells.

**Table 1.7** Arsenate removal by whole cells of *Bacillus* sp. SA Ant 14, *S. maltophilia* SA Ant 15 and *S. marcescens* SA Ant 16 during resting conditions. (Arsenate removed and arsenite formed are expressed as percentages of the total of 10mM initially added. Removal and reduction rates are defined as arsenate (substrate) utilised and arsenite (product) formed.)

	<i>Bacillus</i> sp. SA Ant 14	<i>S. maltophilia</i> SA Ant 15	<i>S. marcescens</i> SA Ant 16
<b>% As(V) Removed</b>	78.3	100	49.3
<b>% As(III) Formed</b>	4.2	23.2	15.5
<b>Removal Rate (<math>\mu\text{M}/\text{h}/\text{mg}</math> cells)</b>	0.4	92.4 (0 – 2h) 4.1	3.7
<b>Reduction Rate (<math>\mu\text{M}/\text{h}/\text{mg}</math> cells)</b>	0.3	2	2.1

In addition to reduction, alternative resistance possibilities exist, such as adsorption of the negatively charged arsenic ions (both arsenate and arsenite) to oppositely charged amino groups in the bacterial cell walls<sup>122, 123</sup>. For the Gram positive *Bacillus* sp. the ability of the cell walls to sequester a large range of dilute metal ions from the environment has been well documented<sup>124</sup>, and in a separate study, biosorption by isolates from the same sampling site has been demonstrated<sup>125</sup>. It is also possible that after reduction<sup>125</sup>, the resulting arsenite can be sequestered by a range of cysteine-rich peptides such as  $\gamma$ -glutamylcysteine and glutathione<sup>126</sup> or methylated<sup>127</sup>.

It is important to interpret the resistance to arsenate in the context of a dynamic system where both the influence of the initial oxyanion amendment and the effect of products resulting from biological transformations should be taken into account.

## **1.6 Literature cited**

- 
- <sup>1</sup> Smedley PL & Kinniburgh DG (2002). A review of the source, behavior and distribution of arsenic in natural waters. *Appl Geochem* 17: 517-568
- <sup>2</sup> Cullen WR & Reimer KJ (1989). Arsenic speciation in the environment. *Chem Rev* 89: 713-764
- <sup>3</sup> Azcue JM & Nriagu JO (1994) Arsenic, historical perspectives. In: *Arsenic In the Environment*. Vol 26 (Nriagu JO Ed.). Wiley & Sons, New York, N.Y. pp 1-16
- <sup>4</sup> Szinicz L & Forth W (1988). Effect of As<sub>2</sub>O<sub>3</sub> on gluconeogenesis. *Arch Toxicol* 61: 444-476
- <sup>5</sup> Liu SX, Athar M, Lippai I, Waldern C & Hei TK (2001). Induction of oxyradicals by arsenic: implication for mechanism of genotoxicity. *Proc Natl Acad Sci USA* 98: 1643-1648
- <sup>6</sup> Barrett J, Hughes MN, Karavaiko GI & Spencer PA (1993). *Metal Extraction by Bacterial Oxidation of Minerals*. Ellis Horwood Ltd., England
- <sup>7</sup> Dean JA (1985). Proton-transfer reactions of inorganic materials in water at 25°C. In: *Lange's Handbook of Chemistry*. 13th edn. (Dean JA, Ed). McGraw Hill, New York N.Y. pp. 5-14
- <sup>8</sup> Loehr TM & Plane RA (1968). Raman spectra and structures of arsenious acid and arsenites in aqueous solution *Inorg Chem* 7: 1708-1714
- <sup>9</sup> Cervantes C, Ji G, Ramirez JL & Silver S (1994). Resistance to arsenic compounds in microorganisms. *FEMS Microbol Rev* 15: 355-367
- <sup>10</sup> Nakamuro K & Sayato Y (1981). Comparative studies of chromosomal aberrations induced by trivalent and pentavalent arsenic. *Mutat Res* 88: 73-80
- <sup>11</sup> Turpein R, Pansar-Kallio M, Haggblom M & Kairesalo T (1999). Influence of microbes on the mobilization, toxicity and biomethylation of arsenic in soil. *Sci Total Environ* 236: 173-180
- <sup>12</sup> Lee TC, Oshimara M & Barrett JC (1985). Comparison of arsenic induced cell transformation, cytotoxicity, mutation and cytogenetic effects in syrian hamster embryo cells in culture. *Carcinogenesis* 6: 1421-1426
- <sup>13</sup> Lee TC, Tanaka N, Lamb PW, Gilmer TM & Barrett JC (1988). Induction of gene amplification by arsenic. *Science* 241: 79-81
- <sup>14</sup> Tezuka M, Hanioka K, Yamanaka K & Okada, S (1993). Gene damage induced in human alveolar type II (L-132) cells by exposure to dimethylarsinic acid. *Biochem Biophys Res Commun* 191: 1178-1183
- <sup>15</sup> Caltabiano MM, Koestler TP, Poste G & Greig RG (1986). Induction of 32- and 34kDa stress proteins by sodium arsenite, heavy metals and thiol reactive agents. *J Biol Chem* 261: 13382-13386
- <sup>16</sup> Deaton MA, Bowman PD, Jones GP & Powanda MC (1990). Stress protein synthesis in human keratinocytes treated with sodimn arsenite, phenyldichloroarsine, and nitrogen mustard. *Fund Appl Toxicol* 14: 471-476
- <sup>17</sup> Leonard A & Lauwerys RR (1980). Carcinogenicity, teratogenicity and mutagenicity of arsenic. *Mutat Res* 75: 49-62
- <sup>18</sup> Pershagen G (1985). Lung cancer mortality among men living near arsenic-emitting smelters. *Am J Epidemiol* 122: 684-694
- <sup>19</sup> Shneidman D & Belizaire R (1986). Arsenic exposure followed by the development of dermatofibrosarcoma protuberans. *Cancer* 58: 1585-1587

- 
- 20 Bates MN, Smith AH & Hopenhayn-Rich C (1992). Arsenic ingestion and internal cancers: a review. *Am J Epidemiol* 135: 462-476
- 21 Silver S (1983). Bacterial interaction with mineral cations and anions: Good ions and bad. In: *Biom mineralization and Biological Metal Accumulation* (Westbroek P & de Jong EW, Eds.), D Reidel, Dordrecht pp. 439-457
- 22 Ji G & Silver S (1995). Bacterial resistance mechanisms for heavy metals of environmental concern. *J Ind Microbiol* 14: 61-75
- 23 Nies DH & Silver S (1995). Ion efflux systems involved in bacterial metal resistances. *J Ind Microbiol* 14: 186-199
- 24 Nies DH (1999). Microbial heavy-metal resistance. *Appl Microbiol Biotechnol* 51: 730-750
- 25 Rensing C, Ghosh M & Rosen BP (1999). Families of soft-metal-ion-transporting ATPases. *J Bacteriol* 181: 5891-5897
- 26 Bruins MR, Kapil S & Oehme FW (2000). Microbial resistance to metals in the environment. *Ecotoxicol and Environ Safety* 45: 198-207
- 27 Silver S, Ji G, Broer S, Dey S, Dou D & Rosen BP (1993). Orphan enzyme or patriarch of a new tribe: the arsenic resistance ATPase of bacterial plasmids. *Mol Microbiol* 8: 637-642
- 28 Silver S & Walderhaug M (1992). Regulation of chromosomal and plasmid cation and anion transport systems. *Microbiol Rev* 56: 1-33
- 29 Knowles FC & Benson AA (1983). The biochemistry of arsenic. *Trends Biochem Sci* 8: 178-180
- 30 Mukhopadhyay R, Rosen BP, Phung LT & Silver S (2002). Microbial arsenic: from geocycles to genes. *FEMS Microbiol Rev* 26: 311-325
- 31 Willsky GR & Malamy MH (1980). Characterization of two genetically separable inorganic phosphate transport systems in *Escherichia coli*. *J Bacteriol* 144: 356-365
- 32 Rosenberg H, Gerdes RG & Chegwidden K (1977). Two systems for the uptake of phosphate in *Escherichia coli*. *J Bacteriol* 131: 505-511
- 33 Gatti D, Mitra B & Rosen BP (2000). *Escherichia coli* soft metal ion translocating ATPases. *J Biol Chem* 275: 34009-34012
- 34 Sanders OI, Rensing C, Kuroda M, Mitra B. & Rosen BP (1997). Antimonite is accumulated by the glycerol facilitator GlpF in *Escherichia coli*. *J Bacteriol* 179: 3365-3367
- 35 Borgnia M, Nielsen S, Engel A & Agre P (1999). Cellular and molecular biology of the aquaporin water channels. *Annu Rev Biochem* 68: 425-458
- 36 Challenger F (1951). Biological methylation. *Adv Enzymol* 12: 429-491
- 37 NiDhubhghaill OM & Sadler PJ (1991). The structure and reactivity of arsenic compounds: biological activity and drug design. *Struct Bond* 78: 129-190
- 38 Aposhian HV (1997). Enzymatic methylation of arsenic species and other new approaches to arsenic toxicity. *Annu Rev Pharmacol Toxicol* 37: 397-419
- 39 Hall LL, George SE, Kohan MJ, Styblo M & Thomas DJ (1997). *In vitro* methylation of inorganic arsenic in mouse intestinal cecum. *Toxicol Appl Pharmacol* 147: 101-109
- 40 Bentley R & Chasteen TG (2002). Microbial methylation of metalloids: arsenic, antimony and bismuth. *Microbiol Mol Biol Rev* 66: 250-271
- 41 Bryant MP, Wolin EA, Wolin MJ & Wolfe RS (1967). *Methanobacillus omelianskii*, a symbiotic

- 
- association of two species of bacteria. Arch Mikrobiol 59: 20-31
- 42 McBride BC & Wolfe RS (1971). Biosynthesis of dimethylarsine by a methanobacterium. Biochem 10: 4312-4317
- 43 Vidal FV & Vidal VMV (1980). Arsenic metabolism in marine bacteria. Mar Biol 60: 1-7
- 44 Shariatpanahi M, Anderson AC, Abdelghani AA, Englande AJ, Hughes J & Wilkinson RF (1981). Biotransformation of the pesticide, sodium arsenate. J Environ Sci Health 16: 35-47
- 45 Qin J, Rosen BP, Zhang Y, Wang G, Franke S & Rensing C (2006). Arsenic detoxification and evolution of trimethylarsine gas by a microbial arsenite S-adenosylmethionine methyltransferase. Proc Natl Acad Sci USA 103: 2075-2080
- 46 Green HH (1918). Description of a bacterium which oxidizes arsenite to arsenate, and of one which reduces arsenate to arsenite, isolated from a cattle-dipping tank. S Afr J Sci 14: 465-467
- 47 Santini JM, Sly LI, Schnagl RD & Macy JM (2000). A new chemolithoautotrophic arsenite-oxidizing bacterium isolated from a gold mine: phylogenetic, physiological, and preliminary biochemical studies. Appl Environ Microbiol 66: 92-97
- 48 Santini JM & vanden Hoven RN (2004). Molybdenum-containing arsenite oxidase of the chemolithoautotrophic arsenite oxidizer NT-26. J Bacteriol 186: 1614-1619
- 49 Vanden Hoven RN & Santini JM (2004). Arsenite oxidation by the heterotroph *Hydrogenophaga* sp. str. NT-14: the arsenite oxidase and its physiological electron acceptor. Biochim Biophys Acta 1656: 148-155
- 50 Osborne FH & Ehrlich HL (1976). Oxidation of arsenite by a soil isolate of *Alcaligenes*. J Appl Bacteriol 41: 295-305
- 51 Phillips SE & Taylor ML (1976). Oxidation of arsenite to arsenate by *Alcaligenes faecalis*. Appl Environ Microbiol 32: 392-399
- 52 Oremland RS, Hoefl SE, Santini JM, Bano N, Hollibaugh RA & Hollibaugh JT (2002). Anaerobic oxidation of arsenite in Mono Lake water and by a facultative, arsenite-oxidizing chemoautotroph, strain MLHE-1. Appl Environ Microbiol 68: 4795-4802
- 53 Weeger W, Lievreumont D, Perret M, Lagarde F, Hubert JC, Leroy M & Lett M-C (1999). Oxidation of arsenite to arsenate by a bacterium isolated from an aquatic environment. Biometals 12: 141-149
- 54 Anderson GL, Williams J & Hille R (1992). The purification and characterization of arsenite oxidase from *Alcaligenes faecalis*, a molybdenum-containing hydroxylase. J Biol Chem 267: 23674-23682
- 55 Silver S & Phung LT (2005). Genes and enzymes involved in bacterial oxidation and reduction of inorganic arsenic. Appl Environ Microbiol 71: 599-608
- 56 Ellis PJ, Conrads T, Hille R & Kuhn P (2001). Crystal structure of the 100kDa arsenite oxidase from *Alcaligenes faecalis* in two crystal forms at 1.64 Å and 2.03 Å. Structure 9: 125-132
- 57 McEwan AG, Ridge JP, McDevitt CA & Hugenholtz P (2002). The DMSO reductase family of microbial molybdenum enzymes; molecular properties and role in the dissimilatory reduction of toxic elements. Geomicrobiol J 19: 3-21
- 58 Lebrun E, Brugna M, Baymann F, Muller D, Lievreumont D, Lett M-C & Nitschke W (2003). Arsenite oxidase, an ancient bioenergetic enzyme. Mol Biol Evol 20: 686-693
- 59 Muller D, Lievreumont D, Simeonova DD, Hubert JC & Lett M-C (2003). Arsenite oxidase *aox* genes from a metal-resistant beta-proteobacterium. J Bacteriol 185: 135-141

- 60 Gihring TM & Banfield JF (2001). Arsenite oxidation and arsenate respiration by a new *Thermus*  
isolate. FEMS Microbiol Lett 204: 335-340
- 61 Gihring TM, Druschel GK, McCleskey RB, Hamers RJ & Banfield JF (2001). Rapid arsenite oxidation  
by *Thermus aquaticus* and *Thermus thermophilus*: field and laboratory investigations. Environ Sci  
Technol 35: 3857-3862
- 62 Kashyap DR, Botero LM, Franck WL, Hassett DJ & McDermott TR (2006). Complex regulation of  
arsenite oxidation in *Agrobacterium tumefaciens*. J Bacteriol 188: 1081-1088
- 63 Ilyaletdinov AN & Abdrashitova SA (1981). Autotrophic oxidation of arsenic by a culture of  
*Pseudomonas arsenitoxidans*. Mikrobiologiya 50: 198-204
- 64 Santini M, Sly LI, Wen A, Comrie D, De Wulf-Durand P & Macy JM (2002). New arsenite-oxidizing  
bacteria isolated from Australian gold mining environments-phylogenetic relationships. Geomicrobiol J  
19: 67-76
- 65 Rhine ED, Phelps CD & Young LY (2006). Anaerobic arsenite oxidation by novel denitrifying isolates.  
Environ Microbiol 8: 899-908
- 66 Rhine ED, Ni Chadhain SM, Zylstra GJ & Young LY (2007). The arsenite oxidase genes (*aroAB*) in  
novel chemoautotrophic arsenite oxidizers. Biochem Biophys Res Comm 354: 662-667
- 67 Ahmann D, Roberts AL, Krumholz LR, & Morel FM (1994). Microbe grows by reducing arsenic.  
Nature 371: 750
- 68 Oremland RS & Stolz JF (2003). The ecology of arsenic. Science 300: 939-944
- 69 Saltikov CW & Newman DK (2003). Genetic identification of a respiratory arsenate reductase. Proc  
Natl Acad Sci USA 100: 10983-10988
- 70 Krafft T & Macy JM (1998). Purification and characterization of the respiratory arsenate reductase of  
*Chrysiogenes arsenatis*. Eur J Biochem 255: 647-653
- 71 Afkar E, Lisak J, Saltikov C, Basu P, Oremland RS & Stolz JF (2003). The respiratory arsenate  
reductase from *Bacillus selenitireducens* strain MLS10. FEMS Microbiol Lett 226: 107-112
- 72 Malasarn D, Saltikov CW, Campbell KM, Santini JM, Hering JG & Newman DK 2004. *arrA* is a  
reliable marker for As(V) respiration. Science 306: 455
- 73 Macy JM, Santini JM, Pauling BV, O'Neill AH & Sly LI (2000). Two new arsenate/sulfate-reducing  
bacteria: mechanisms of arsenate reduction. Arch Microbiol 173: 49-57
- 74 Broer S, Ji G, Broer A & Silver S (1993). Arsenic efflux governed by the arsenic resistance determinant  
of *Staphylococcus aureus* plasmid pI258. J Bacteriol 175: 3840-3845
- 75 Cervantes C & Chavez J (1992). Plasmid-determined resistance to arsenic and antimony in  
*Pseudomonas aeruginosa*. Antonie van Leeuwenhoek 61: 333-337
- 76 Gladysheva TB, Oden KL & Rosen BP (1994). Properties of the arsenate reductase of plasmid R773.  
Biochem 33: 7288-7293
- 77 Carlin A, Shi W, Dey S & Rosen BP (1995). The *ars* operon of *Escherichia coli* confers arsenical and  
antimonial resistance. J Bacteriol 177: 981-986
- 78 Cai J, Salmon K & DuBow MS (1998). A chromosomal *ars* operon homologue of *Pseudomonas*  
*aeruginosa* confers increased resistance to arsenic and antimony in *Escherichia coli*. Microbiol 144:  
2705-2713
- 79 Messens J, Martins JC, Van Belle K, Brosens E, Desmyter A, De Gieter M, Wieruszkeski JM, Willem R,

- 
- Wyns L & Zegers I (2002). All intermediates of the arsenate reductase mechanism, including an intramolecular dynamic disulfide cascade. *Proc Natl Acad Sci USA* 99: 8506-8511
- 80 Martin P, DeMel S, Shi J, Rosen BP & Edwards BFP (2001). Insights into the structure, solvation, and mechanism of ArsC arsenate reductase, a novel arsenic detoxification enzyme. *Structure* 9: 1071-1081
- 81 Zegers I, Martins JC, Willem R, Wyns L & Messens J (2001). Arsenate reductase from *S. aureus* pI258 is a phosphatase drafted for redox duty. *Nature Struct Biol* 8: 843-847
- 82 Messens J & Silver S (2006). Arsenate reduction: Thiol cascade chemistry with convergent evolution. *J Mol Biol* 362: 1-17
- 83 Mukhopadhyay R, Shi J & Rosen BP (2000). Purification and characterization of Acr2p, the *Saccharomyces cerevisiae* arsenate reductase. *J Biol Chem* 275: 21149-21157
- 84 Baillet F, Magnin JP, Cheruy A & Ozil P (1997). Cadmium tolerance and uptake by a *Thiobacillus ferrooxidans* biomass. *Environ Technol* 18: 631-8
- 85 Boyer A, Magnin J-P & Ozil P (1998). Copper ion removal by *Thiobacillus ferrooxidans* biomass. *Biotechnol Lett* 20: 187-90
- 86 Hassen A, Saidi N, Cherif M & Boudabous A (1998). Effects of heavy metals on *Pseudomonas aeruginosa* and *Bacillus thuringiensis*. *Bioresour Technol* 65: 73-82
- 87 Gomez Y, Coto O, Hernandez C, Marrero J & Abin L (2001). Biosorption of nickel, cobalt and zinc by *Serratia marcescens* strain 7 and *Enterobacter agglomerans* strain 16. *Process Metall* 11: 247-55
- 88 Hernandez A, Mellado RP & Martinez JL (1998). Metal accumulation and vanadium-induced multidrug resistance by environmental isolates of *Escherichia hermannii* and *Enterobacter cloacae*. *Appl Environ Microbiol* 64: 4317-20
- 89 Say R, Yilmaz N, & Denizli A (2003). Biosorption of cadmium, lead, mercury, and arsenic ions by the fungus *Penicillium purpurogenum*. *Sep Sci Technol* 38: 2039-2053
- 90 Kuyucak N & Volesky B (1988) Biosorbents for recovery of metals from industrial solutions. *Biotechnol Lett* 10: 137-142
- 91 Veglio F & Beolchini F (1997). Removal of metals by biosorption: a review. *Hydrometallurgy* 44: 301-316
- 92 Pearton TN & Viljoen MJ (1986). Antimony mineralization in the Murchison greenstone belt - an overview. In: *Mineral Deposits of Southern Africa* (Anhaeusser CR & Maske S Eds). *Geol Soc S Afr* 2329: 293-320
- 93 Abbot JE, Van Vuuren CJJ & Viljoen MJ (1986). The Alpha-Gravelotte antimony ore body, Murchison greenstone belt. In: *Mineral Deposits of Southern Africa* (Anhaeusser CR & Maske S Eds.). *Geol Soc S Africa* 2335: 321-332
- 94 Wu J (1993). Antimony vein deposits of China. *Ore Geology Reviews* 8: 213-232
- 95 Willson C & Viljoen MJ (1986). The Athens antimony ore body, Murchison greenstone belt. In: *Mineral Deposits of Southern Africa* (Anhaeusser CR & Maske S Eds.). *Geol Soc S Afr* 2329: 333-338
- 96 Davis DR, Paterson DB & Griffiths DHC (1986). Antimony in South Africa. *J S Afr Inst Min Metall* 86: 173-193
- 97 Boocock CN, Cheshire PE, Killick AM, Maiden KJ & Vearncombe JR (1988). Antimony-gold mineralization at Monarch mine, Murchison schist belt, Kaapvaal craton. In: *Advances in Understanding Precambrian Gold Deposits, Volume II* (Ho SE & Groves DI Eds), Geology Department and University

- 
- Extension, University of Western Australia, Publ. No.12, 360: 81-97
- 98 Chen C-M, Mobley HLT & Rosen BP (1985). Separate resistances to arsenate and arsenite (antimonate) encoded by the arsenical resistance operon of R factor R773. *J Bacteriol* 161: 758-763
- 99 Bartholomew JW & Mittwer T (1952). The Gram stain. *Bacteriol Rev* 16: 1-29
- 100 Perry SF (1995). Freeze-drying and cryopreservation of bacteria. *Methods Mol Biol* 38: 21-30
- 101 Lane DJ, Weisberg WG, Barns SM & Pelletier DA (1991). 16S ribosomal DNA amplification for phylogenetic study. *J Bacteriol* 173: 697-703
- 102 Hanahan D (1982). Studies on transformation of *E. coli* with plasmid. *J Mol Biol* 166: 557-580
- 103 Altschul SF, Gish W, Miller W, Myers EW & Lipman DJ (1990). Basic local alignment search tool. *J Mol Biol* 215: 403-410
- 104 Cole JR, Chai B, Farris RJ, Wang Q, Kulam SA, McGarrell DM, Garrity GM & Tiedje JM (2005). The Ribosomal Database Project (RDP-II): sequences and tools for high-throughput rRNA analysis. *Nucleic Acids Res* 33 (Database Issue): D294-D296
- 105 Thompson JD, Gibson TJ Plewniak F, Jeanmougin F & Higgins DG (1997). The ClustalX windows interface: flexible strategies for multiple sequence alignment aided by quality analysis tools. *Nucl Acids Res* 24: 4876-4882
- 106 Swofford DL (2002) *PAUP\*. Phylogenetic Analysis Using Parsimony (\*and other Methods)* Version 4. Sinauer Associates, Sunderland, Massachusetts, USA
- 107 Meerow AW, Lehmilller DJ & Clayton JR (2003). Phylogeny and biogeography of *Crinum* L. (Amaryllidaceae) inferred from nuclear and limited plastid non-coding DNA sequences. *Bot J Linn Soc* 141: 349-363
- 108 Muyzer G, De Waal E & Uiterlinden A (1993). Profiling of complex microbial populations by denaturing gradient gel electrophoresis analysis of polymerase chain reaction-amplified genes coding for 16S rRNA. *Appl Environ Microbiol* 59: 695-700
- 109 Davis KER, Joseph SJ & Janssen PH (2005). Effects of growth medium, inoculum size, and incubation time on the culturability and isolation of soil bacteria. *Appl Environ Microbiol* 71: 826-834
- 110 Casamayor EO, Massana R, Benlloch S, Overas L, Diez B, Goddard VJ, Gasol MS, Joint I, Rodriguez-Valera F & Pedros-Alio C (2002). Changes in archaeal, bacterial and eukaryal assemblages along a salinity gradient by comparison of genetic fingerprinting methods in a multipond solar saltern. *Environ Microbiol* 4: 338-348
- 111 Ji G & Silver S (1992). Reduction of arsenate to arsenite by the ArsC protein of the arsenic resistance operon of *Staphylococcus aureus* plasmid pI258. *Proc Natl Acad Sci USA* 89: 9474-9478
- 112 Zahler WL & Cleland WW (1968). A specific and sensitive assay for disulfides. *J Biol Chem* 243: 716-719
- 113 Simeonova DD, Lievreumont D, Lagarde F, Muller DAE, Groudeva VI & Lett M-C (2004). Microplate screening assay for the detection of arsenite-oxidizing and arsenate-reducing bacteria. *FEMS Microbiol Lett* 237: 249-253
- 114 Johnson DL & Pilson MEQ (1972). Spectrophotometric determination of arsenite, arsenate, and phosphate in natural waters. *Anal Chim Acta* 58: 289-299
- 115 Silver S, Budd K, Leahy KM, Shaw WV, Hammond D, Novick RP, Willisky GR, Malamy MH & Rosenberg H (1981). Inducible plasmid-determined resistance to arsenate, arsenite, and antimony (III) in



- 
- Escherichia coli* and *Staphylococcus aureus*. J Bact 146: 983-996
- 116 Anderson, CR. Personal communication
- 117 Wysocki R, Chery CC, Wawrzycka D, Van Hulle M, Cornelis R, Thevelein JM & Tamas M (2001). The glycerol channel Fps1p mediates the uptake of arsenite and antimonite in *Saccharomyces cerevisiae*. Mol Microbiol 40: 1391-1401
- 118 Ma LQ, Komar KM, Tu C, Zhang W, Cai Y & Kennelley ED (2001). A fern that hyperaccumulates arsenic. Nature 409: 579
- 119 Canovas D, Duran C, Rodriguez N, Amils R & De Lorenzo V (2003). Testing the limits of biological tolerance to arsenic in a fungus isolated from the River Tinto. Environ Microbiol 5: 133-138
- 120 Ordonez E, Letek M, Valbuena N, Gil JA & Mateos LM (2005). Analysis of genes involved in arsenic resistance in *Corynebacterium glutamicum* ATCC 13032. Appl Environ Microbiol 71: 6206–6215
- 121 Anderson CR & Cook GM (2004). Isolation and characterization of arsenate-reducing bacteria from arsenic-contaminated sites in New Zealand. Curr Microbiol 48: 341-347
- 122 Urrutia MM & Beveridge TM (1994). Formation of fine-grained metal and silicate precipitates on a bacterial surface (*Bacillus subtilis*). Chem Geol 116: 261-280
- 123 Bai RS & Abraham TE (2003). Studies on Chromium (VI) adsorption-desorption using immobilized fungal biomass. Bioresour Technol 87: 17-26
- 124 Schultze-Lam S, Thompson JB & Beveridge TJ (1993). Metal ion immobilization by bacterial surfaces in freshwater environments. Water Pollut Res J Can 28: 51-81
- 125 Sekhula KS, Abotsi EK & Becker RW (2005). M.Sc. thesis: Heavy metal ion resistance and bioremediation capacities of bacterial strains isolated from an antimony mine
- 126 Dhankher OM, Li Y, Rosen BP, Shi J, Salt D, Senecoff JF, Sashti NA & Meagher RB (2002). Engineering tolerance and hyperaccumulation of arsenic in plants by combining arsenate reductase and  $\gamma$ -glutamylcysteine synthetase expression. Nature Biotechnol 20: 1140-1145
- 127 Brunken HS, Nehrhorn A & Breunig HJ (1996). Isolation and characterization of a new arsenic methylating bacterium from soil. Microbiol Res 151: 37-41

## **Chapter 2**

### **Molecular Aspects**

## **2.1 Literature review: Dissimilatory arsenate reduction in bacteria**

Bacterial resistance to arsenic ions was first discovered by Novick and Roth (1968)<sup>1</sup> in a group of *Staphylococcus aureus*  $\beta$ -lactamase plasmids which also determine resistance to heavy metals. The *ars* operon was subsequently recognized in plasmids of *S. aureus*<sup>2</sup>, *S. xylosus*<sup>3</sup> and *Escherichia coli*. These plasmid borne arsenic resistance determinants were investigated in depth in the early 1980's and it was shown that resistance to arsenate in both these organisms was due to reduced uptake of arsenate by resistant cells and also that high phosphate concentrations protected cells from arsenate toxicity<sup>4</sup>. In this regard, studies of arsenic resistant *E. coli* and *S. aureus* showed that the apparent attenuated arsenate uptake is due to an accelerated efflux of the toxic ions in an energy-dependent manner<sup>5, 6</sup>. It was found that arsenic resistance plasmids confer tolerance to both arsenate and arsenite as well as to antimony(III)<sup>7</sup>. Arsenic resistance operons have subsequently been found in other microorganisms, *Acidiphilum multivorum*<sup>8</sup>, *Bacillus subtilis*<sup>9</sup> and *Pseudomonas aeruginosa*<sup>10</sup> and have been shown to be very common in both Gram positive<sup>11, 12</sup> and Gram negative bacteria<sup>13, 14, 15</sup>.

Arsenic resistance determinants from *E. coli* and *Staphylococcus* plasmids were the first to be cloned and sequenced and have been extensively characterised<sup>16</sup>. The structural organisation, function and overall mechanism of each of the operon constituents are highly conserved throughout the bacterial domain. The arsenic resistance (*ars*) operon from *E. coli* plasmid R773 contains five genes, named *arsR*, *arsD*, *arsA*, *arsB* and *arsC*, each with very different, but ultimately synergistic functions and is the model for arsenic resistance in Gram negative bacteria<sup>17</sup>. In contrast, *ars* operons of Gram positive bacteria are exemplified by *S. aureus* plasmid pI258 that consist of only three genes, *arsR*, *arsB* and *arsC*<sup>2</sup>.

In 1995 Carlin *et al.*<sup>18</sup> described the first account of a chromosomally located arsenic resistance operon in *E. coli* (GenBank accession U00039). Upon further investigation, it was found that it was very closely homologous to that of the *E. coli* plasmid R773. The only exception is that this particular chromosomal *ars* operon only contains the *arsR*, *arsB* and *arsC* genes<sup>18</sup>. Phylogenetic analysis of the plasmid-borne genes has shown no monophyleticity, suggesting multiple cases of chromosomal-plasmid exchange and subsequent horizontal gene transfer events<sup>19</sup>. With the advent of genome sequencing projects, the number of putative *ars* genes (lacking empirical characterisation specifically in terms of arsenic resistance) have

grown considerably and is expected to keep doing so.

### **2.1.1 Regulation**

In both the abovementioned bacteria, *ars* operons are regulated by the *arsR* gene which encodes a dimeric trans-acting repressor. The arsenic resistance operon can be induced by arsenate, arsenite and antimonite *in vivo*<sup>2, 3, 20</sup>, but *in vitro* protein-operator interaction analysis revealed that only arsenite and antimonite were inducers<sup>21</sup>. In addition to *arsR*, the *E. coli ars* operon has a second regulatory gene *arsD*, that appears to be an inducer-independent trans-acting regulatory protein which controls the upper level of *ars* gene expression<sup>22</sup>.

### **2.1.2 Membrane pumps**

The *E. coli arsA* gene encodes an ATPase subunit as inferred initially from significant homology with other ATP-binding proteins. This homology is only within the ATP-binding regions and not in the entire protein sequence<sup>23</sup>. The ArsA homodimer actively extrudes arsenite (and antimonite) ions in an energy dependent manner<sup>24</sup> and contains two ATP binding sites which appear to have evolved by duplication<sup>25</sup>. The protein has been purified and shown to be an arsenite- or antimonite-stimulated ATPase tightly bound to the ArsB membrane protein<sup>26, 27</sup>.

The *E. coli* ArsB is an integral inner membrane protein, that anchors the ArsA ATPase subunits<sup>28, 29</sup>. There are only a few proteins which show sequence homology with ArsB and none appear to be closely related<sup>30</sup>. The ArsA-ArsB complex is the first example of an anion-transporting ATPase and functions as a primary arsenite (and presumably antimonite) pump<sup>31</sup>. In *S. aureus*, ArsB alone is sufficient for arsenite efflux and resistance without the presence of an ArsA ATPase and with the membrane potential as the energy source<sup>32</sup>. Co-expression of the *E. coli* ArsA with the *S. aureus* ArsB dramatically increases the level of arsenite resistance, suggesting an interaction between these two proteins<sup>33</sup>. On the other hand, the *E. coli* ArsB functions as an obligatory ATP-coupled primary pump in the presence of ArsA protein, but also works as a membrane potential driven secondary pump in the absence of ArsA like the *S. aureus* ArsB<sup>32</sup>.

### **2.1.3 Arsenate reductases**

The last gene in the arsenic resistance operon, *arsC*, in bacteria encodes a soluble protein (131 amino acid residues, for *S. aureus* and 141 amino acids for *E. coli*), that reduces less toxic arsenate [As(V)] to more toxic arsenite [As(III)]<sup>2, 34</sup>. It seems peculiar to convert a less toxic compound to a more toxic form, but ArsC activity is closely coupled with efflux from the cells *via* the (ArsA)-ArsB protein complex<sup>33, 35</sup> so that intracellular arsenite never accumulates. Presumably, since arsenate is structurally similar to phosphate, ‘arsenate extrusion pumps’ would inadvertently also expel phosphate from the cytosol, leading to phosphate starvation. Arsenate reductases from plasmids pI258<sup>35, 36</sup> and R773<sup>34</sup> have been purified and studied: Both enzymes reduce arsenate *via* mechanisms based on cysteine thiol oxidation / reduction cycling<sup>34, 35, 36</sup>, but share less than 20% amino acid identity. Thus, arsenate reductases can be subdivided into families whose sequences are unrelated and whose mechanisms differ in detail. Furthermore, purified enzymes exhibit no endogenous activity, but need other proteins to carry out reduction reactions. The most striking difference between the two enzymes is the energy coupling systems: Here, the *S. aureus* enzyme couples with thioredoxin both *in vivo* and *in vitro*<sup>2</sup>, and in contrast, the *E. coli* enzyme couples with glutaredoxin<sup>37</sup>.

#### **2.1.3.1 The *E. coli* glutathione / glutaredoxin ArsC family**

The arsenate reductase from the large *E. coli* resistance plasmid R773 has been well characterised both enzymatically and structurally: It is a small (16kDa) monomeric, soluble protein that has a  $K_m$  of 8mM. Competitive inhibitors are phosphate, sulfate and arsenite<sup>34</sup> and ArsC also confers low level resistance to tellurite<sup>38</sup>. The overall protein fold for R773 ArsC has been shown to contain large regions of extensive mobility, especially at the active site<sup>39</sup>, possibly explaining the broad range of inhibitors. The primary structure of Gram negative arsenate reductases are remarkably similar and share very high homology with each other. The secondary structure and organisation has a small measure of structural homology to glutaredoxin, thiol transferases, and glutathione S-transferases, but this protein shows no significant global similarity to other known proteins<sup>40</sup>.

For enzymatic activity, three essential cysteine residues are involved in a cascade sequence and there are no inorganic or other bound co-factors in the ArsC enzyme. The first cysteine residue is located at position 12 from the N terminus of ArsC, but the other two

catalytic cysteines are provided by glutathione and glutaredoxin rather than the ArsC polypeptide<sup>41</sup>.

- The reaction mechanism for arsenate reduction in *E. coli* R773 (Figure 2.1) is as follows:
- (1) the catalytic Cys12 residue associates with arsenate, forming an As-S covalent bond
  - (2) glutathione (GSH) displaces a hydroxyl group to produce a tertiary glutathionylated As(V)<sup>42</sup>
  - (3) subsequent reduction by a cysteine on glutaredoxin (Grx) producing a dihydroxy arsenite intermediate and releasing oxidized GrxS-SG
  - (4) a monohydroxy positively charged arsenite intermediate is formed
  - (5) following hydroxylation and release of arsenite and regeneration of reduced ArsC<sup>43</sup>

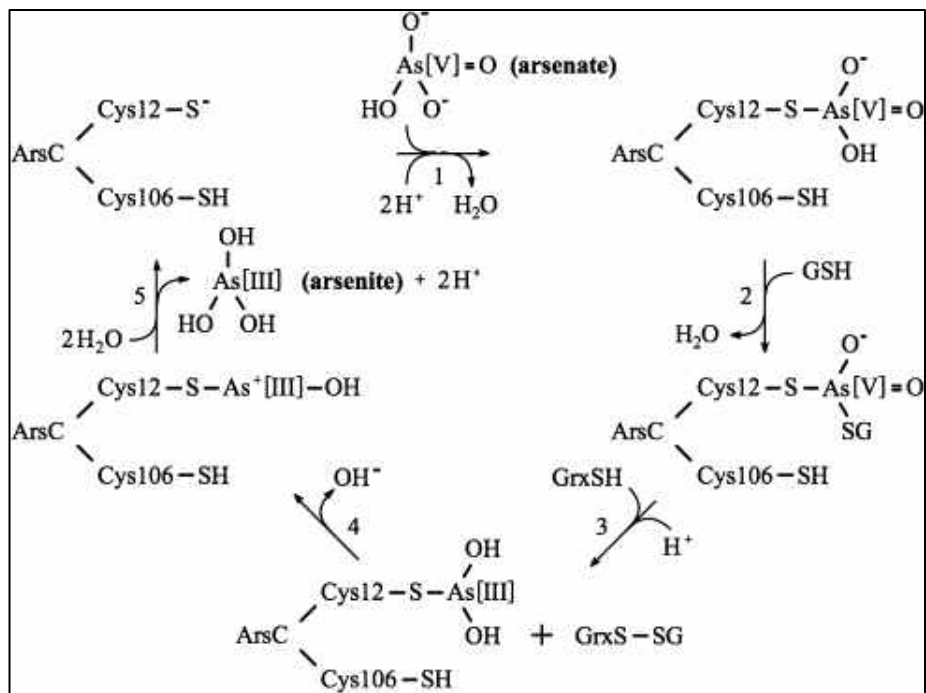


Figure 2.1 Catalytic reaction cycle of the Grx-coupled arsenate reductase of *E. coli* plasmid R773<sup>44</sup>.

*E. coli* has three glutaredoxins, Grx1, Grx2 and Grx3, each of which has a Cys-Pro-Tyr-Cys dithiol consensus sequence<sup>45</sup>. Glutaredoxin can catalyze either intraprotein disulfide bond reduction or reduction of mixed disulfides between a protein cysteine thiol and glutathione<sup>46</sup>. Although all three glutaredoxins can serve as electron donor for the reduction of arsenate by the *E. coli* R773 reductase, Shi *et al* (1999). demonstrated relative efficiencies of Grx2 → Grx3 → Grx1<sup>47</sup>.

### 2.1.3.2 The *Staphylococcus* thioredoxin ArsC family

The first recognized arsenate reductase was found on a Gram positive *Staphylococcus* plasmid (pI258)<sup>35</sup> and has since been found widely among plasmids and genomes of Gram positive bacteria as well as in some Gram negative bacteria<sup>48</sup>. The *Staphylococcus aureus* ArsC enzyme is a cytosolic monomer of approximately 14.5kDa and has a high affinity for arsenate with a  $K_m$  of  $1\mu\text{M}$ <sup>36</sup>. Phosphate (the analog of arsenate) and nitrate (but not sulfate) are stimulators, whereas arsenite, antimonite and tellurite are inhibitors<sup>49</sup>.

From protein crystallography, enzymology, and mutational studies<sup>50, 51</sup> it is known that this arsenate reductase, like that from *E. coli* R773, utilizes three cysteines for a cascade of reducing reactions. However, unlike the glutaredoxin linked *E. coli* R773 reaction scheme, all three these cysteines are encoded within the ArsC polypeptide primary sequence (Figure 2.2).

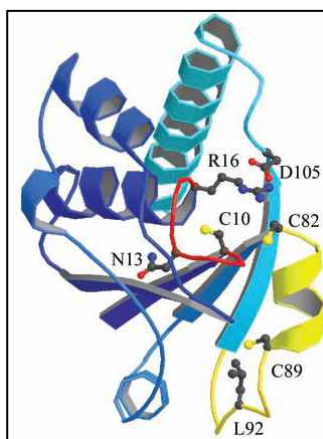


**Figure 2.2** Ribbon diagram of the overall structure of reduced ArsC wild type visualized from two different positions. The P-loop CXsR motif (red), the catalytic key residues in ball-and-stick representation, and the flexible short  $\alpha$ -helix region (yellow) are shown<sup>50</sup>.

As shown in Figure 2.3, the *S. aureus* pI258 enzyme reduces arsenate by:

- (1) covalently binding arsenate to the N-terminal Cys10 residue (corresponds to *E. coli* R773 Cys12), forming a covalent Cys10-S-AsHO<sub>3</sub>-intermediate
- (2) Cys82 attacks Cys10 (analogous with glutathione in *E. coli* R773) with formation of a Cys10-Cys82 disulfide intermediate
- (3) the electrons from the S-As bond shuttle to arsenic and arsenite is released
- (4) Cys89 (glutaredoxin in *E. coli* R773) then attacks Cys82 producing a Cys82-Cys89 disulfide and the Cys10 thiolate is regenerated (this comprises the major conformational change in the enzyme)

- (5) thioredoxin (Trx) reduces the final Cys82-S-S-Cys89 oxidized bond regenerating reduced arsC

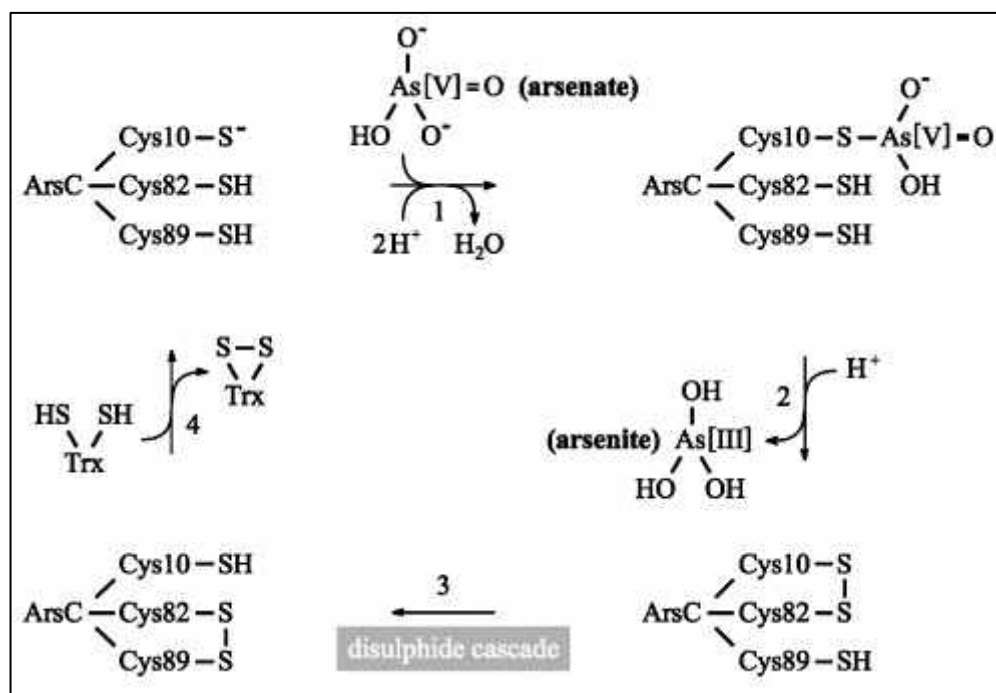


Figure 2.3 Catalytic reaction cycle of Trx-coupled arsenate reductase of *S. aureus* plasmid pI258<sup>50</sup>.

The secondary and tertiary structures of *S. aureus* pI258 arsenate reductase are remarkably similar to those of low molecular weight protein tyrosine phosphatases (LMW-PTPases) from mammals, a relationship predicted based on overall sequence homology (26% amino acid identities) as well as conservation of key residues in the ‘P-loop’ active site<sup>52, 53</sup>. Interestingly, the stability of the P-loop structure requires the presence of an oxyanion such as arsenate or phosphate<sup>54, 55</sup>. The *S. aureus* pI258 arsenate reductase shows phosphatase activity with the model substrate *p*-nitrophenyl phosphate and has a  $K_{cat}$  of 0.5/min, a very high  $K_m$  of 146mM, and an overall activity far below the range found with enzymatically characterised LMW-PTPases. Arsenate is a competitive inhibitor of phosphatase activity, with a  $K_i$  very similar to the  $K_m$  for arsenate reductase activity<sup>56</sup>. It would thus seem that the *S. aureus* pI258 arsenate reductase is a dual-function enzyme and it has been suggested that climate changes over geological timescales have forced the evolution from one substrate (phosphate) to the other (arsenate)<sup>57</sup>. Arsenate reductases from Gram positive organisms show much less sequence homology to each other than their Gram negative counterparts, but without exception, the reaction pathways still follow the same thiol-cascade mechanisms. Interestingly, it has been demonstrated that Gram positive arsenate reductases can be successfully expressed in Gram negative bacteria, and that this expression results in higher arsenic resistance<sup>2</sup>.



### 2.1.3.3 Exceptions to the rule

Some variation within the organisation and structure of certain components in the arsenate reduction scheme has been found:

The recently deposited genome sequence of *Herminiimonas arsenicoxydans* contains four putative arsenic resistance operons, each containing an arsenate reductase from either the glutaredoxin or thioredoxin family, with two of the four operons incorporating arsenate reductases from both families<sup>58</sup> (Figure 2.4).

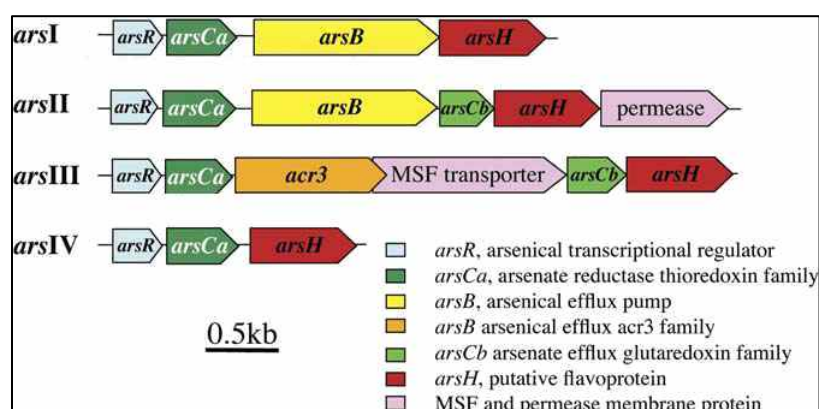


Figure 2.4 Organisation of the four arsenic resistance operons in *Herminiimonas arsenicoxydans*<sup>58</sup>.

The arsenate reductase from the cyanobacterium *Synechocystis* sp. belongs partially to the glutaredoxin coupled arsenate reductase family and partially to the thioredoxin coupled family<sup>56</sup>. It contains the P-loop conserved sequence features of the thioredoxin coupled arsenate reductase family but, for its catalytic mechanism, employs glutathione and glutaredoxin as the source of reducing equivalents<sup>59</sup>. Like R773 ArsC, this arsenate reductase forms a covalent complex with glutathione in an arsenate-dependent manner but contains three essential cysteine residues, like pI258 ArsC, whereas the *E. coli* enzymes require only one cysteine for catalysis. As in the thioredoxin coupled arsenate reductases, these additional cysteine residues apparently shuttle a disulfide bond to the enzyme's surface to render it accessible for reduction.

A different family of Grx-coupled cytoplasmic arsenate reductase is represented by ACR2p arsenate reductase of *Saccharomyces cerevisiae*<sup>60</sup>. This enzyme is independent in terms of structure from the two bacterial ArsC classes, and is related to a different class of protein tyrosine phosphatases, which includes eukaryotic cell division cycle proteins<sup>57</sup> and

thiolsulfate transferases<sup>61</sup>. Unlike the bacterial arsenate reductases, purified ACR2p appears to be a homodimer of two 130 residue monomers<sup>40</sup>, but has the requirements for glutathione and glutaredoxin as a source of reducing equivalents in a catalytic pathway similar to that of R773 ArsC. On the other hand, ACR2p has the consensus sequence CX5R, which corresponds to the phosphatase active site and to the active site of the thioredoxin-coupled family of arsenate reductases<sup>62</sup>.

There is no relationship between the tertiary structures of the *E. coli* R773, *S. aureus* pI258 and *S. cerevisiae* arsenate reductases (Figure 1.4), supporting the conclusion that these three classes of enzyme are not related. Mukhopadhyay and Rosen (2002) suggested simultaneous convergent evolution to solve the same problem of arsenate toxicity<sup>63</sup>, but phylogenetic analysis suggests a common, ancient origin and subsequent horizontal gene transfer events<sup>19</sup>.

## **2.2 Introduction**

*Serratia marcescens* SA Ant 16 was chosen for further investigation based on its hyper-resistance to arsenate demonstrated in Chapter 1. *Serratia marcescens*, a member of the *Enterobacteriaceae*, has been confirmed to possess glutaredoxin-glutathione family *arsC* homologs<sup>64, 65</sup> and it would therefore not be unreasonable to expect that the arsenate reductase of *S. marcescens* SA Ant 16 would share similarities with other Gram negative arsenate reductases. With this in mind, it was decided to target the arsenate reductase of *S. marcescens* SA Ant 16 using a PCR-based approach.

When attempting to isolate a gene of interest in this manner, knowledge of the basepair composition (sequence) of the gene is clearly required. Typically, Polymerase Chain Reactions consist of target DNA, short nucleotide primers, free nucleotides, a buffer mixture with MgCl<sub>2</sub> being the most important component, and DNA Polymerase<sup>66</sup>. These components may be varied singly or in combinations to alter the specificity of the amplicons<sup>67</sup>. For amplification of *arsC* of *S. marcescens* SA Ant 16, oligonucleotide primers were designed based on regions showing high homology within various *arsC* sequences from Gram negative bacteria.

An alternative approach based on similar protein function, instead of sequence similarities, is presented in the form of constructing and screening genomic libraries. The most pertinent issue regarding this approach, is the ability of the screening host to express (transcribe, translate and process) the targeted gene using endogenous cellular machinery. If the host organism possesses proteins with the same function as the gene of interest, this basal level of expression needs to be complemented in excess of endogenous activity, or alternately, the native protein has to be inactivated. Both these options imply their individual set of challenges: proteins rarely function in isolation, and generally the product of one protein constitutes the substrate for a second reaction. If over-complementation is attempted, additional strain will be put on 'downstream' reactions. In the case of 'knockout strains', experience has taught us that when genes are removed from an organism's genome, it often results in a weakened host that is frequently difficult to maintain and manipulate.

## **2.3 Aims**

1. Isolation of *arsC* from *S. marcescens* SA Ant 16 using:
  - PCR-based approach using specific and degenerate primers with varying reaction conditions
  - genomic library construction approach with arsenate reductase deletion mutants of *E. coli* and laboratory strains

## **2.4 Materials and methods**

### **2.4.1 General procedures and chemicals**

Chemicals used were of molecular reagent grade or lab grade (in the case of general reagents), obtained from various suppliers and used without further purification. Specific alterations to methods described in this section are included in Results and Discussion for clarity.

### **2.4.2 Bacterial strains and primers**

*E. coli* strains used for general cloning and screening procedures are described in Table 2.1, while primers for the amplification and sequencing of *arsC* are described in Table 2.2.

**Table 2.1** *E. coli* strains used in the study.

<b>Name</b>	<b>Genotype</b>	<b>Reference or source</b>
W3110	<i>dam dcm supE44hsdR17 thi leu rpsL lacY galK galT ara TonA thr tsx Δ(lac-proAB) F' [traD36 proAB+ lacI<sup>q</sup> lacZΔM15]</i>	68 (Gift from Prof. B. Rosen)
AW3110	W3110 $\Delta$ <i>ars::cam</i>	18 (Gift from Prof. B. Rosen)
ACSH50 I <sup>q</sup>	<i>rpsL Δ(lac-pro) [F', traD36 proAB lacI<sup>q</sup> ΔM15 Δars::cam</i>	69 (Gift from Prof. D. Rawlings)
JM109	<i>recA1 supE44 endA1 hsdR17 gyrA96 relA1 thi Δ(lac-proAB) F' [traD36 proA<sup>+</sup>B<sup>+</sup>lac<sup>q</sup> ΔlacZ M15]</i>	70
TOP10	<i>F-mcrA Δ(mrr-hsdRMS-mcrBC) Φ80lacZΔM15 ΔlacX74 depR recA1 araD139 Δ(araA-leu)7697 galU galK rpsL endA1 nupG</i>	Invitrogen

*E. coli* strains were cultured in Luria-Bertani medium (LB) (10g/L peptone, 5g/L yeast extract, 10g/L NaCl) at 37°C on a rotary shaker at 200rpm, or on LB-plates containing 60μg/mL ampicillin, 9.6μg/mL IPTG (isopropyl-β-D-thiogalactopyranoside) and 40μg/mL X-gal (5-bromo-4-chloro-3-indolyl-β-D-galactoside) (AIX) at 37°C.

**Table 2.2 Primers used for amplification and sequencing of arsenate reductase (*arsC*).**

Name	Sequence (5'-3')	Position <i>E. coli</i> X80057 <i>arsC</i>	Mean Tm (°C)	Product (bp)
ArsCF	ATGAGCAACATHACCATC	1-18	54.9	430
ArsCR	TTAKTTCAGSCGNTTAC	409-426	46.2	
ArF	TGAGATACTCATAGTAGCAACATTACC	-12-15	54.5	700
ArR	CTCCATTTTCATAAGCTTTGC	666-686*	49.6	
arsC-1-F	GTAATACGCTGGAGATGATCCG <sup>65</sup>	46-68	54.9	370 2060 / 4170
arsC-1-R	TTTTCTGCTTCATCAACGAC65	393-414	53.5	
ArsRF	GGGTTCAYTAYCGCTTATCMCCG	256-276 <sup>#</sup>	58.5	
ArsC7F	GGTCAAACACTATTGCVGATATGGGG	132-157	59.2	150
ArsC7R	GGRCGRTTAATCAGAATSGGRTG	262-285	56.7	
PsThF	AACWSYTGCCGYWSCATTCT	37-56 <sup>†</sup>	57.4	200
PsThR	ACATCGTCATCACCGTTTGCG	221-241 <sup>†</sup>	58.2	
M13F	CGCCAGGGTTTTCCAGTCACGAC	-106-130 <sup>‡</sup>		-
M13R	TCACACAGGAAACAGCTATGAC	+115-137 <sup>‡</sup>		-
T7 Promoter	TAATACGACTCACTATAGGG	-58-78 <sup>‡</sup>		-
Sp6 Promoter	TATTTAGGTGACACTATAG	+80-99 <sup>‡</sup>		-

\* *Serratia marcescens* plasmid R478 AJ288983

<sup>#</sup> *E. coli arsR* X80057

<sup>†</sup> *Thiobacillus ferrooxidans* AF173880

<sup>‡</sup> pGem®T-Easy Vector (Promega) relative to T-overhang ligation site

### **2.4.3 PCR approach**

#### **2.4.3.1 DNA Extraction**

##### **2.4.3.1.1 Genomic DNA**

DNA was extracted using DNA<sub>ZOL</sub> (Gibco BRL): Cells were grown overnight at 37°C with shaking in TYG medium and harvested by centrifugation in a Beckman J2-MC centrifuge at 11000 x g for 10 minutes at 4°C. The cell pellet was frozen and thawed once, resuspended in 5mL Tris-EDTA buffer (10mM Tris-HCl, 5mM EDTA, pH 7.5) and 5mL DNA<sub>ZOL</sub> reagent added. Lysozyme was added to a final concentration of 5mg/mL and incubated at 37°C for 30 minutes and thereafter at 55°C for 30 minutes with shaking. Proteinase K was added to a final concentration of 350µg/mL and incubated at 37°C with shaking. An equal volume chloroform : isoamylalcohol (24:1) was added, vortexed to mix and centrifuged at 10000 x g for 15

minutes. The supernatant was transferred to a clean tube and the organic extraction repeated if necessary. Genomic DNA was precipitated by the addition of 0.5 volumes 100% cold ethanol and centrifugation at 14000 x g for 10 minutes. The pellet was washed with 70% cold ethanol, air dried and resuspended in 5mM Tris, pH 8.0.

#### **2.4.3.1.2 Plasmid DNA**

Plasmids were extracted from *S. marcescens* SA Ant 16 and *Bacillus* sp. SA Ant 10(1) using the low copy number protocol of the GeneJET™ Plasmid Miniprep Kit (Fermentas).

#### **2.4.3.2 PCR**

PCR reactions consisted of 1X PCR Buffer, 200µM of each dNTP, 200nM of each forward and reverse primer, approximately 50ng template DNA, MgCl<sub>2</sub> to a final concentration of 2mM and 2.5U Taq DNA Polymerase in a final volume of 50µL (unless otherwise stated). Cycling was performed after an initial denaturing step at 94°C for 10 minutes: dsDNA was denatured at 94°C for 1 minute, primer annealing at the appropriate temperature for 30 seconds and elongation at 72°C for 1 minute. Amplification was repeated for 30 - 35 cycles with a final extension cycle at 72°C for 7 minutes. PCR products were separated on 1% agarose gels (unless otherwise stated) with 1X TAE buffer (40mM Tris-HCl, 20mM sodium acetate, 2mM EDTA) pH 8.0 at 100V, stained with ethidium bromide and visualised under UV illumination.

#### **2.4.3.3 Gel band purification**

PCR amplified bands were purified using High Pure PCR Purification Kit (Roche Applied Science) or GFX PCR Product Purification Kit spin columns (Amersham) according to the manufacturer's instructions.

#### **2.2.3.4 PCR product ligation**

Ligation reactions were performed in a final volume of 10µL and consisted of 5 or 6 Weiss Units T4 DNA Ligase (Fermentas, New England Biolabs or Promega), 1X Ligation Buffer (Fermentas, New England Biolabs or Promega), pGem®T-Easy vector (Promega) and insert DNA in an approximately 1 : 3 molar ratio. Reactions were incubated for at least 3

hours at room temperature or in the case of Promega reagents, at 4°C over night.

#### **2.4.3.5 Transformation**

Ligation reactions were transformed into  $\text{RuCl}_2$  competent<sup>71</sup> *E. coli* JM109 or TOP10 cells, and plated onto LB medium (10g/L tryptone, 5g/L yeast extract, 7g/L NaCl, pH 7.0) containing 50 $\mu\text{g}/\text{mL}$  ampicillin, 9.6 $\mu\text{g}/\text{mL}$  IPTG and 40 $\mu\text{g}/\text{mL}$  X-gal. Single, white colonies were inoculated into LB medium containing ampicillin to a final concentration of 50 $\mu\text{g}/\text{mL}$  and grown overnight with shaking at 200rpm.

#### **2.4.3.6 Plasmid extractions and restriction analysis**

Plasmids containing PCR amplified inserts were extracted with NucleoSpin® Plasmid Extraction Kit (Macherey-Nagel) or Fast Plasmid Mini Kit (Eppendorf) according to the manufacturer's instructions and verified by restriction analysis by combining 1X *EcoRI* Buffer (Fermentas), 5U *EcoRI* restriction enzyme (Fermentas) and plasmid DNA in a final volume of 10 $\mu\text{L}$  and incubating at 37°C for at least 2 hours.

#### **2.4.3.7 Sequencing**

Sequencing was performed by using the ABI BigDye Terminator v3.1 Ready Reaction Cycle Sequencing Kit (Applied Biosystems). Reactions were made up to a final volume of 10 $\mu\text{L}$  and consisted of 2 $\mu\text{L}$  Premix, 1X Dilution Buffer, 3.2pmol of the appropriate primer and approximately 500ng dsDNA template. Cycling consisted of 25 cycles of denaturing at 96°C for 10 seconds, primer annealing at 50°C for 5 seconds and elongation at 60°C for 4 minutes. Products were purified using SigmaSpin Purification Columns (Sigma) and separated on an ABI377 Sequencer (PE Biosystems).

### **2.4.4 Genomic library construction approach**

#### **2.4.4.1 Minimum inhibitory concentration**

To determine the minimum inhibitory concentration of arsenic for the various *E. coli* strains, LB-plates containing increasing concentrations of arsenic (and the appropriate



antibiotic where applicable) were prepared. Strains were streaked out as well as transformed with empty plasmid and plated out. Inhibition of growth was visually ascertained after approximately 16h of growth at 37°C.

#### **2.4.4.2 Partial digestion of genomic DNA**

DNA was partially digested by serially diluting 20U restriction enzyme (*EcoRI*, *BamHI* or *Sau3AI* (Fermentas)) in a total volume of 100µL and incubating at 37°C for 15 minutes. Each tube contained approximately 10ng genomic DNA and 1X of the appropriate restriction buffer (Fermentas). Fragments ranging from 1kb - >10kb were either excised from 1% agarose gels and cleaned with the QIAEX II Gel Extraction Kit (Qiagen) or were directly purified using the GFX PCR Product Purification Kit spin columns (Amersham) or High Pure PCR Purification Kit (Roche Applied Science).

#### **2.4.4.3 Vector digest and dephosphorylation**

Vectors were digested with 10U restriction enzyme *EcoRI*, *BamHI* or *Sau3AI* (Fermentas) in a 10X dilution of the appropriate buffer at 37°C for at least 3 h. Restriction products were separated on 1% TAE agarose gels and linearised vector recovered and cleaned with the High Pure PCR Purification Kit (Roche Applied Science) or GFX PCR Product Purification Kit spin columns (Amersham). Vector 5'-overhangs were dephosphorylated to prevent self-ligation with the use of 5U Antarctic Alkaline Phosphatase (New England Biolabs) in 1X Antarctic Phosphatase Buffer (New England Biolabs). The mixture was incubated at 37°C for 15 minutes and the phosphatase heat inactivated at 65°C for 20 minutes. Dephosphorylation was confirmed by performing a self-circularisation reaction and transformation into competent *E. coli* cells.

#### **2.4.4.4 Ligation and transformation**

Partially digested genomic DNA was ligated into dephosphorylated vector in a 1 : 3 molar ratio, but not exceeding a total concentration of 10ng/µL<sup>72</sup>. Reactions consisted of 5 or 6 Weiss Units T4 DNA Ligase (Fermentas or New England Biolabs) and 1X Ligation Buffer (Fermentas or New England Biolabs) which was then incubated at room temperature overnight and transformation of ligated products performed as described in section 2.4.3.5).

## 2.5 Results and discussion

### 2.5.1 Polymerase Chain Reaction

Saltikov and Olson (2002)<sup>65</sup> designed primer set *arsC*-1-F / *arsC*-1-R and demonstrated that these primers were highly successful to detect Gram negative R773-like *arsC* genes in raw sewage and arsenic rich waters. This primer set amplifies an approximately 370bp product from the *arsC* gene (Figure 2.5). Since the success of this primer pair had been well documented in literature, and with the relatedness of *S. marcescens* and *E. coli* as well as the high degree of homology between Gram negative arsenate reductases kept in mind, these primers were employed to amplify the *arsC* from *S. marcescens* SA Ant 16.

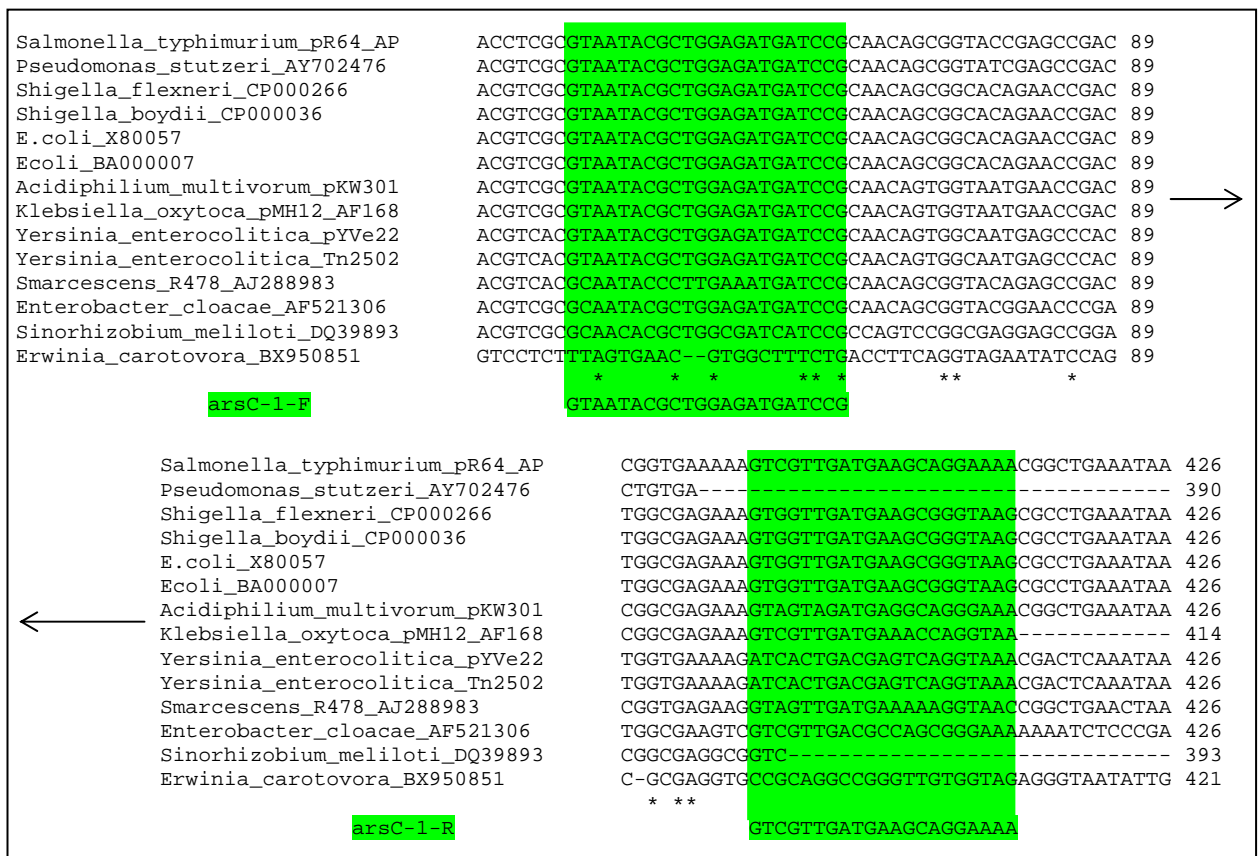
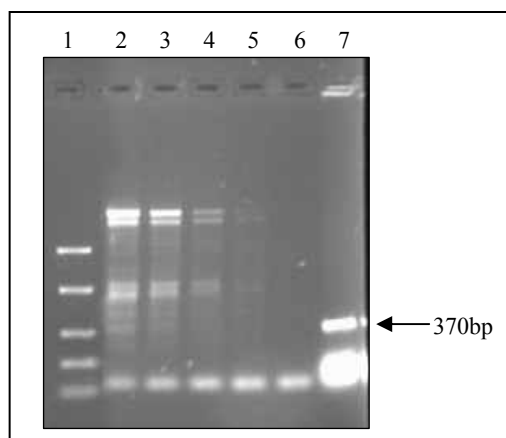


Figure 2.5 Alignments of *arsC* from Gram negative organisms with primer pair *arsC*-1-F / *arsC*-1-R indicated.

The PCR reaction contained 1.5mM MgCl<sub>2</sub> and primer annealing was performed from 46°C to 57°C<sup>65</sup>. A positive control *E. coli* W3110 was included in the experiment. PCR products of the expected size were only amplified in the control strain, and only non-specific amplification was obtained for *S. marcescens* SA Ant 16 (Figure 2.6).



**Figure 2.6** 1% TAE agarose gel with PCR products generated with primer pair *arsC*-1-F / *arsC*-1-R. Lane 1: FastRuler™ Low Range; Lane 2: *S. marcescens* SA Ant 16 genomic DNA with primer annealing at 46°C; Lane 3: 49°C; Lane 4: 52°C; Lane 5: 54°C; Lane 6: 57°C; Lane 7: *E. coli* W3110 positive control.

A second PCR with the same primer set was performed with increasing primer concentrations ranging from 100nM to 300nM and 2mM MgCl<sub>2</sub> with primer annealing at 51°C<sup>65</sup>. Amplification yielded products of approximately 2600bp for the test strain and of 370bp for the *E. coli* W3110 control strain (Figure 2.7).

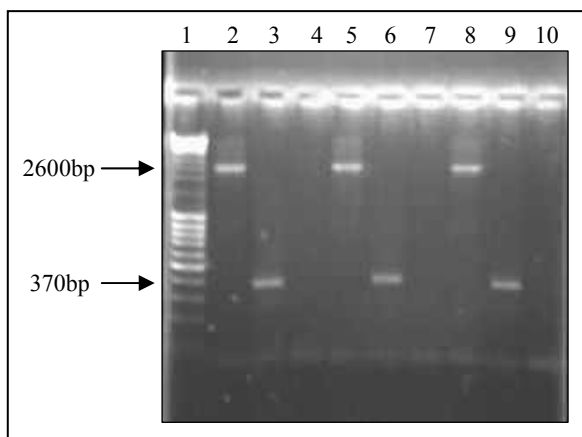


**Figure 2.7** PCR products from primer set *arsC*-1-F / *arsC*-1-R. Lane 1: Massuler™; Lane 2: *S. marcescens* SA Ant 16; Lane 3: *E. coli* W3110 each amplified with 100nM of each primer; Lane 4: negative control; Lane 5: *S. marcescens* SA Ant 16; Lane 6: *E. coli* W3110 each amplified with 200nM of each primer; Lane 7: negative control; Lane 8: *S. marcescens* SA Ant 16; Lane 9: *E. coli* W3110 each amplified with 300nM of each primer; Lane 10: negative control.

PCR amplified fragments of 370bp and 2600bp were sequenced and the product from the positive control (370bp) was confirmed to be *arsC* from *E. coli* (E-value: 3e-164). Sequencing results from the approximately 2600bp bands from *S. marcescens* SA Ant 16 varied from a preprotein translocase (92% identity, 33% query coverage and E-value 3e-22) to malate dehydrogenase (83% identity, 58% query coverage, E-value 3e-72), but showed no similarity to any known arsenate reductases.

It was therefore decided to design a set of degenerate primers based on alignments of *arsC* sequences from various Gram negative bacteria. This primer set had an expected amplicon size of approximately 430bp (Figure 2.8).

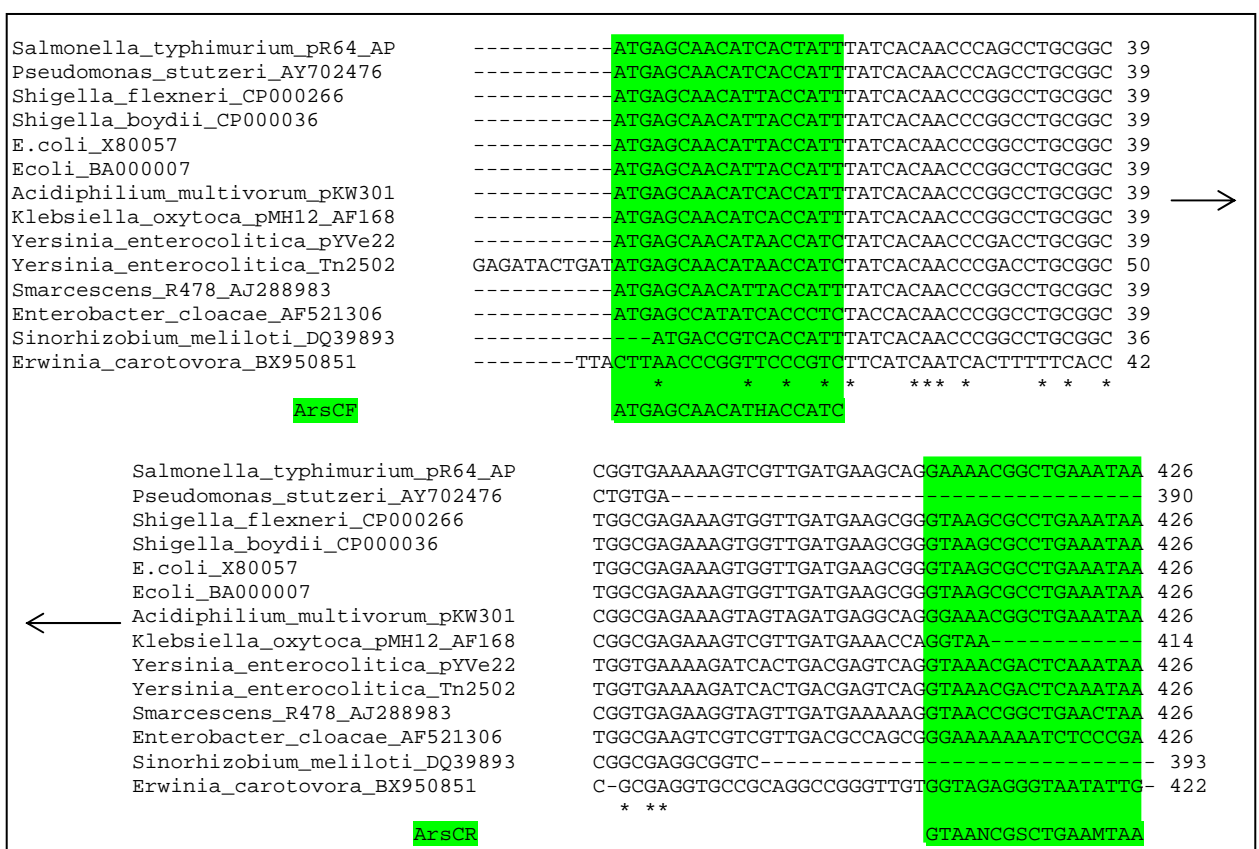


**Figure 2.8** Alignments of *arsC* from Gram negative organisms for design of degenerate primer pair ArsCF / ArsCR.

Reactions were performed as described in section 2.4.3.2, with the exception that MgCl<sub>2</sub> was added to a final concentration of 0.5mM, 0.75mM or 1mM to vary primer binding specificity. The approximately 430bp band (Figure 2.9a), generated in tubes containing 0.75mM and 1mM MgCl<sub>2</sub> respectively, was cleaned from the gel and re-amplified using the same reaction conditions to improve yield (Figure 2.9b). Cloned inserts were verified by

restriction analysis of the plasmids (Figure 2.9c).

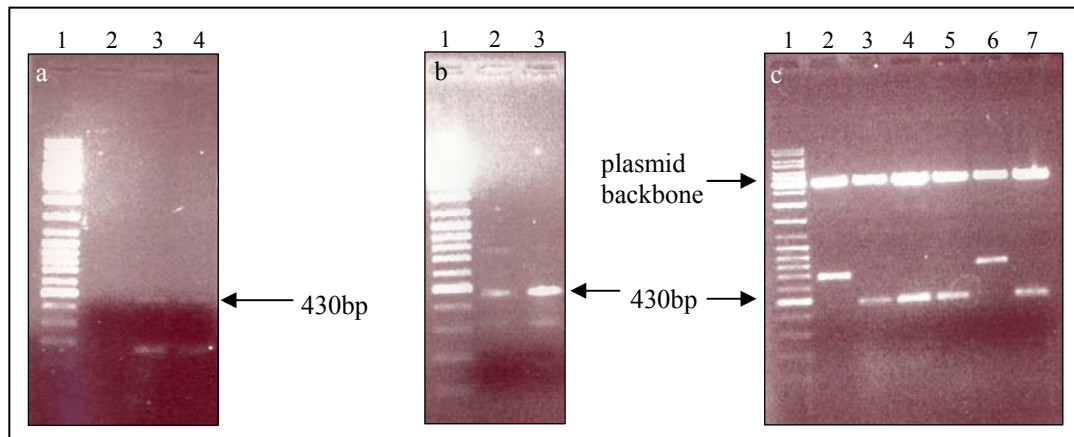


**Figure 2.9** PCR products generated with primer pair ArsCF / ArsCR.

(a) Lane 1: Massuler™; Lane 2: 0.5mM MgCl<sub>2</sub>; Lane 3: 0.75mM MgCl<sub>2</sub>; Lane4: 1mM MgCl<sub>2</sub>.

(b) Lane 1: Massuler™; Lane 2: 0.75mM MgCl<sub>2</sub>; Lane 3: 1mM MgCl<sub>2</sub>.

(c) Lane 1: Massuler™; Lane 2 - 7: Inserts cut from plasmid with *EcoRI*.

Sequencing of the PCR products revealed 96% identity (with an E-value of 0.0) with cytochrome oxidase subunit II (*cyoxB*) (Figure 2.10). This is a membrane bound, anaerobic oxidating enzyme, that clearly shares no functionality with arsenate reductases.

Query	8	ACATTACCATCCAGAACGGGATGACGGTCAGCACCACCGCCAGCACGAAGCCGATCAGGT	67
<i>cyoxB</i>	3192	ACATCACCATCCAGAACGGGATGACGGTCAGCACCACCGCCAGCACGAAGCCGATCAGGT	3133
Query	68	ACGACTTCACGCTGCCGTGGCTTTTCGCCGCCGGTGCCGTGGTTCGTGTCGTGGTTGTCAT	127
<i>cyoxB</i>	3132	ACGACTTCACGGTGCCATGGCTTTTCGCCGCCGGTGCCGTGGTTCGTGTCGTGGTTGTCAT	3073
Query	128	GTGCCATTACAGCGCTCCATTGAGGTAGACGACGGAGAACACGCCGATCCAGATCAGGTC	187
<i>cyoxB</i>	3072	GTGCCATTACAGGGCTCCATTGAGGTAGACGACGGAGAACACGCCGATCCAGATCAGGTC	3013
Query	188	CAGGAAGTGCCAGAACAGGCTCAGGCACGCCATGCGGGTCTTGTTGGTCGGGGTCAGGCC	247
<i>cyoxB</i>	3012	CAGGAAGTGCCAGAACAGGCTCAGGCACGCCATGCGGGTCTTGTTGGTCGGGGTCAGGCC	2953
Query	248	GTACTTCTTCAGCTGCACGAACATCACCAGCAGCCACAGCAGGCCGGCGCTGACGTGCAG	307
<i>cyoxB</i>	2952	GTACTTCTTCAGCTGCACGAACATCACCAGCAGCCACAGCAGGCCGGCGCTGACGTGCAA	2893
Query	308	GCCGTGGGTACCGACCAGGGCGAAGAACGCCGACAGGAAGGCACTTCGGTCCGGACCGTA	367
<i>cyoxB</i>	2892	GCCGTGGGTACCGACCAGGGCAAAGAACGCCGACAGGAAGGCACTTCGGTCCGGACCGTA	2833
Query	368	GCCCTGATGGATCAGGTGCTGGAAGTCCATAGACTTCCATGCACATGAAGCCGAAGCCCAG	427
<i>cyoxB</i>	2832	GCCCTGGTGGATCAGGTGCTGGAAGTCCCACACTTCCATGCACATGAAGCCGAAGCCCAG	2773
Query	428	CAGCCAGGTAAT	439
<i>cyoxB</i>	2772	CAGCCAGGTGAT	2761

**Figure 2.10** Alignment of DNA sequence of ArsCF / ArsCR PCR product with cytochrome oxidase subunit II (*cyoxB*).

Degenerate primer pairs ArsCF / ArsCR and the initial primer set arsC-1-F / arsC-1-R were used in combination to attempt amplification of the arsenate reductase from *S. marcescens* SA Ant 16. Primer set ArsCF / arsC-1-R was expected to amplify a 410bp fragment and primer set arsC-1-F / ArsCR a 380bp fragment from the positive control *E. coli* W3110. The reaction contained 1.5mM MgCl<sub>2</sub>, 100nM of each primer and annealing was performed at 45°C, 47°C and 50°C. Primer set ArsCF / arsC-1-R amplified an approximately 410bp product as well as non-specific bands estimated at 1500bp and 2000bp for *E. coli* and no amplification was obtained for *S. marcescens* SA Ant 16 (Figure 2.11a). Primer set arsC-1-F / ArsCR did not amplify products of the expected size, but yielded non-specific products of approximately 1500bp with *E. coli* W3110 and 2000bp with the test organism (Figure 2.11b).

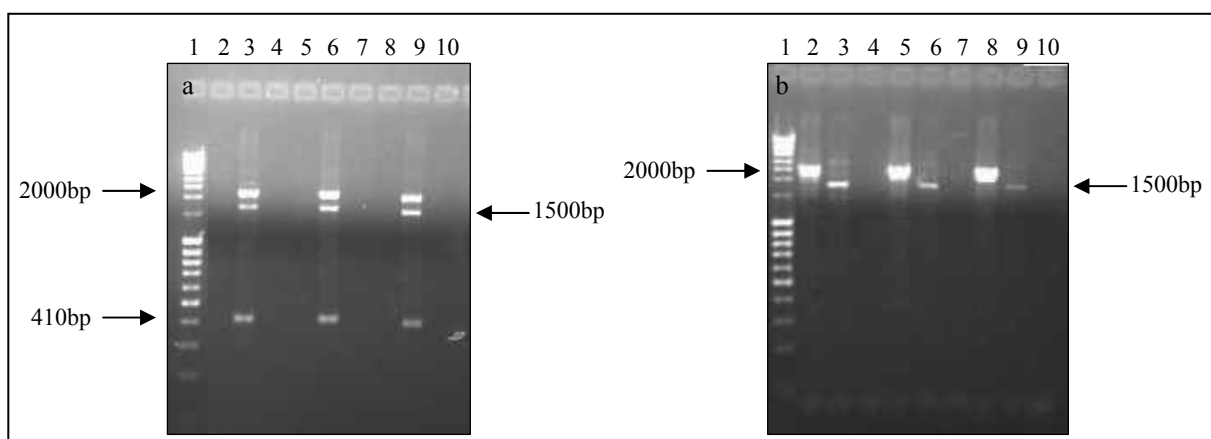


**Figure 2.11** PCR products from combinations of primer sets ArsCF / arsCR and arsC-1-F / arsC-1-R.

a) Lane 1: Massuler™; Lane 2: *S. marcescens* SA Ant 16; Lane 3: *E. coli* W3110 positive control with primer annealing at 45°C; Lane 4: negative control; Lane 5: *S. marcescens* SA Ant 16; Lane 6: *E. coli* W3110 positive control with primer annealing at 47°C; Lane 7: negative control; Lane 8: *S. marcescens* SA Ant 16; Lane 9: *E. coli* W3110 positive control with primer annealing at 50°C, amplified with primers ArsCF / arsC-1-R; Lane 10: negative control.

b) Lane 1: Massuler™; Lane 2: *S. marcescens* SA Ant 16; Lane 3: *E. coli* W3110 positive control with primer annealing at 45°C; Lane 4: negative control; Lane 5: *S. marcescens* SA Ant 16; Lane 6: *E. coli* W3110 positive control with primer annealing at 47°C; Lane 7: negative control; Lane 8: *S. marcescens* SA Ant 16; Lane 9: *E. coli* W3110 positive control with primer annealing at 50°C, amplified with primers arsC-1-F / ArsCR; Lane 10: negative control.

These PCR products were sequenced and the product amplified from the positive control *E. coli* W3110 confirmed to be arsenate reductase (E-value of 2e-65). Non-specific bands from *S. marcescens* SA Ant 16 did not match with any known arsenate reductases, but showed high similarity (82% identity, 99% query coverage, E-value 0.0) to a preprotein translocase.

Consequently, the organism *Serratia marcescens*, instead of Gram negative bacteria in general, became the focus of PCR primer design. The incompatibility group H plasmids (InchI2) encode multiple antibiotic and heavy metal resistances and have a common association with bacteria of the family *Enterobacteriaceae*<sup>73, 74</sup>. R478 is the prototype InchI2 plasmid and was first isolated in 1969 in the US from a clinical isolate of *Serratia marcescens*. It is a 272kb plasmid encoding a variety of antibiotic and heavy metal resistances including resistance to arsenate, arsenite, antimony, mercury, tellurite, tetracycline, chloramphenicol,

and kanamycin<sup>75</sup>. The arsenical resistance operon of plasmid R478 has been sequenced<sup>76</sup> and a new primer set, ArF / ArR, based on R478 was designed that was expected to amplify product of approximately 700bp (Figure 2.12)<sup>64</sup>.

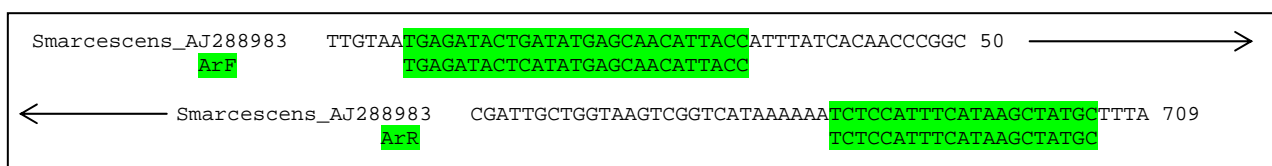


**Figure 2.12** Design of primer pair ArF / ArR based on the sequence of *S. marcescens* plasmid R478.

PCR amplification on a total DNA extract from *S. marcescens* SA Ant 16 with primer set ArF / ArR was performed at concentrations of 200 $\mu$ M or 500 $\mu$ M of each dNTP; 250nM or 500nM of each primer, 1X or 1.5X Reaction Buffer and 1.5mM MgCl<sub>2</sub>. None of these variations yielded any amplification products. Possible explanations could be that PCR conditions during the attempted amplification was unfavourable or that the arsenical resistance determinants of *S. marcescens* SA Ant 16 are different from that found on plasmid R478. If a PCR amplification is attempted within acceptable reaction conditions (1X Reaction Buffer, 0.1-1 $\mu$ g (usually 50ng) target DNA, 0.1-1 $\mu$ M of each primer, 1-5mM MgCl<sub>2</sub>, 50-500 $\mu$ M of each dNTP and 0.5-2.5U DNA Polymerase), usually inhibiting substances present in the target DNA extract are the most likely factor in this regard.

Therefore, in order to eliminate the former possibility, genomic DNA of *S. marcescens* SA Ant 16, both undiluted and a 100X dilution of genomic DNA was used as template for both primer sets (ArsCF / ArsCR and ArF / ArR) to attempt to minimise the effect of inhibitory substances, if any, present in the DNA extracts. To serve as a positive control, 16S rDNA fragments of approximately 1500bp were amplified by PCR on undiluted to 1000X serially diluted genomic DNA (Figure 2.13a). For *arsC* PCR, MgCl<sub>2</sub> concentrations were adjusted to 3mM to promote more specific binding of the primers to target DNA regions (Figure 2.13b).



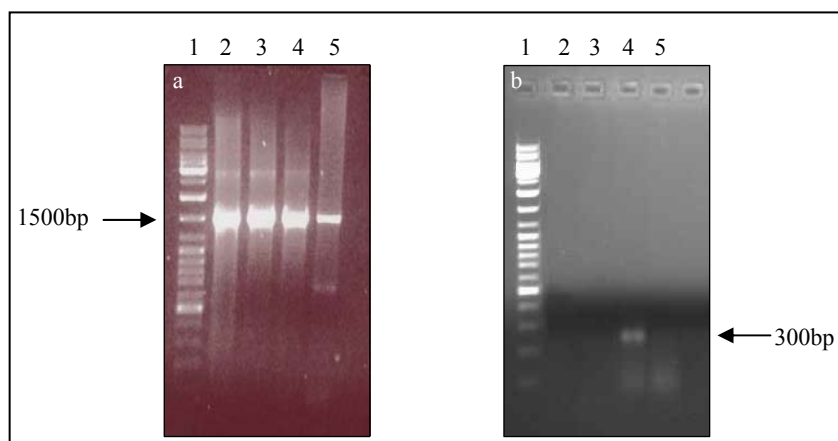


**Figure 2.13** Agarose gel with PCR fragments generated on serially diluted DNA of *S. marcescens* SA Ant 16.

**(a) 16S rDNA PCR:**

**Lane 1: MassRuler™; Lane 2: *S. marcescens* SA Ant 16 undiluted DNA; Lane 3: *S. marcescens* SA Ant 16 10X diluted DNA; Lane 4: *S. marcescens* SA Ant 16 100X diluted DNA; Lane 5: *S. marcescens* SA Ant 16 1000X diluted DNA;**

**(b) PCR amplification with primer sets ArsCF / ArsCR and ArF / ArR:**

**Lane 1: MassRuler™; Lane 2: *S. marcescens* SA Ant 16 undiluted DNA with primer set ArsC; Lane 3: *S. marcescens* SA Ant 16 100X diluted DNA with primer set ArsC; Lane 4: *S. marcescens* SA Ant 16 undiluted DNA with primer set Ar; Lane 5: *S. marcescens* SA Ant 16 100X diluted DNA with primer set Ar.**

Although amplicons of 430bp and 700bp were expected for primer sets ArsCF / ArsCR and ArF / ArR respectively, only non-specific amplification was observed. A band of 300bp was excised from the gel cloned and sequenced. Results were varied and the hit with highest percentage identity (100%), with 84% query coverage and an E-value of  $3e-88$ , was with a translocase. No similarity with any known arsenate reductases were found.

In most instances, bacterial arsenic resistance operons consist of either three<sup>2</sup> or five<sup>17</sup> genes that are in the order *arsR*, (*arsD*, *arsA*), *arsB* and *arsC*. Since it had become clear that targeting the *arsC* of *S. marcescens* SA Ant 16 alone, was an unsuccessful strategy, a degenerate forward primer, based on the sequence of the arsenate resistance operon regulatory protein, *arsR*, was designed based on sequence similarity between several *arsR* sequences. This primer was then used in combination with the previously published *arsC*-1-R<sup>65</sup> reverse primer based on the *arsC* sequence (Figure 2.14).

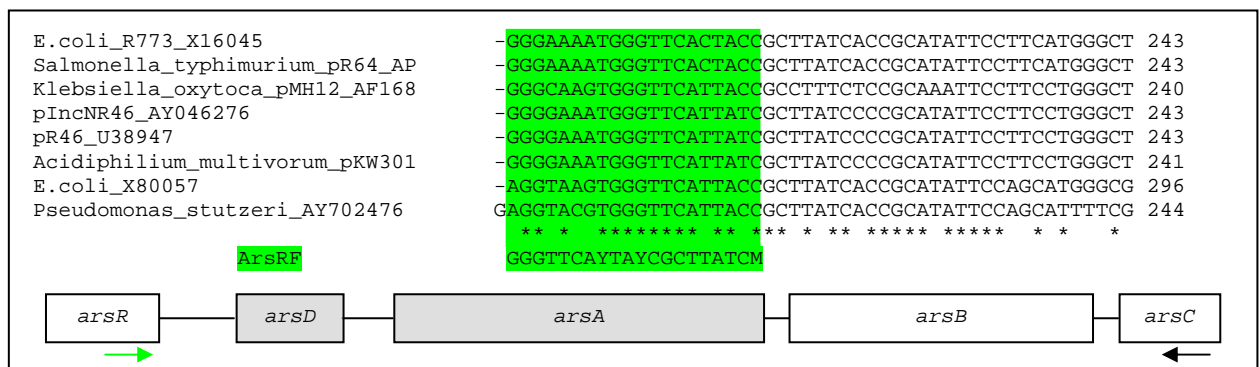


**Figure 2.14** Alignment of *arsR* sequences and schematic of arsenate resistance operon spanning genes *arsR* to *arsC*. (Shaded boxes indicate *arsD* and *arsA* genes, possibly absent.)

This primer set could either amplify an approximately 2050bp product if only *arsR*, *arsB* and *arsC* were present on the target DNA, or an approximately 4200bp product in the presence of all 5 genes. Reactions contained 100nM of each primer and annealing was performed at 49°C to 57°C with 2°C increments. PCR products of approximately 2050bp were amplified only for genomic DNA from the positive control *E. coli* W3110 strain except when annealing was performed at 57°C, indicating the presence of *arsRBC*, but no products were amplified in the test strain (Figure 2.15).

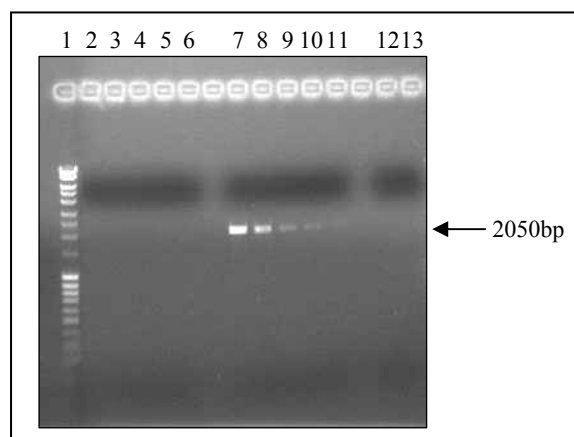


**Figure 2.15** PCR products amplified with forward primer ArsRF and reverse primer *arsC*-1-R. Lane 1: Massuler™; Lane 2-6: *S. marcescens* SA Ant 16 with primer annealing at 49°C, 51°C, 53°C, 55°C and 57°C; Lane 7-11: *E. coli* W3110 positive control annealed at 49°C, 51°C, 53°C, 55°C and 57°C; Lane 12-13: negative control with annealing at 49°C and 57°C.

Alignments from various *arsC* sequences were performed once more, and degenerate primers were designed based on homologous regions that had not been targeted by previous primer sets. Amplicons of approximately 150bp were expected (Figure 2.16).



**Figure 2.16** Alignments of *arsC* from selected Gram negative bacteria for design of degenerate primer set ArsC7F / ArsC7R.

The PCR reactions contained 1.15X PCR Buffer, 230µM of each dNTP, 230µM of each primer and 2.3mM MgCl<sub>2</sub>. Primer annealing was performed from 45°C to 53°C with 2°C increments. Specific PCR products of the expected size were amplified from positive control DNA, while for *S. marcescens* SA Ant 16 a band of approximately 150bp was observed along with non-specific amplification (Figure 2.17).

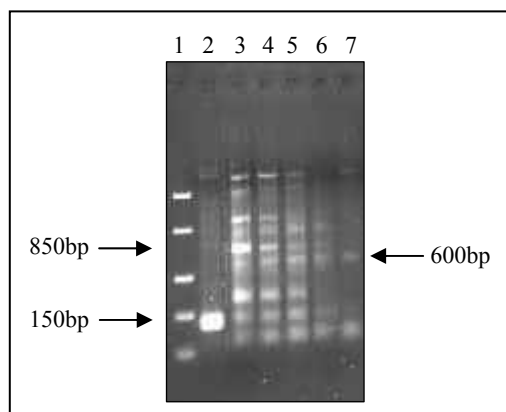


**Figure 2.17** PCR products amplified with primer set ArsC7F / ArsC7R on a 1.5% TAE agarose gel. Lane 1: FastRuler™ Low Range; Lane 2: *E. coli* W3110 positive control DNA; Lane 3: *S. marcescens* SA Ant 16 genomic DNA template with primer annealing at 45°C; Lane 4: 47°C; Lane 5: 49°C; Lane 6: 51°C; Lane 7: 53°C.

The amplified bands of 150bp were cloned, plasmids extracted and the inserts sequenced. The PCR product from the positive control was confirmed to be *arsC* (E-value  $2e-65$ ), but sequencing results from *S. marcescens* SA Ant 16 did not resemble any known arsenate reductases. The sequenced product showed high similarity (76% identity, 90% query coverage, E-value  $7e-74$ ) with a secretion protein of the IISP family and also to serine proteases (83% identity, 66% coverage, E-value  $1e-174$ ). The larger bands of 600bp and 850bp that were consistently amplified over the annealing temperature range were subsequently cloned and sequenced. Sequencing hits had the highest similarity to portions of  $\beta$ -lactamase (100% identity, 33% coverage, E-value  $4e-52$ ) and also to a hypothetical protein from *Yersinia enterocolitica* (91% identity, 25% coverage, E-value  $2e-08$ ) but did not match any known arsenate reductases.

Since arsenic resistance determinants are often found on plasmids, plasmid DNA was extracted from *S. marcescens* SA Ant 16 and used as template with degenerate primer set ArsC7F / ArsC7R. Products of the expected size (150bp) were amplified from plasmid extracts of *S. marcescens* SA Ant 16 (Figure 2.18).

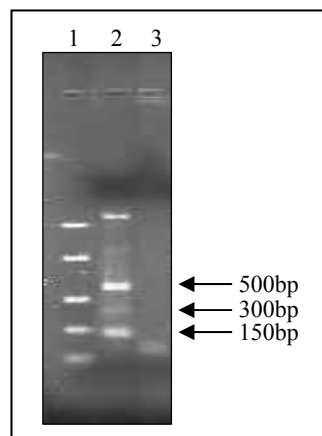


**Figure 2.18** 1.5% TAE agarose gel with PCR products generated with primer set ArsC7F / ArsC7R using plasmid extracts as template.

**Lane 1: FastRuler™ Low Range; Lane 2: *S. marcescens* SA Ant 16 template; Lane 3: Negative control.**

Bands of the expected size (150bp) amplified from *S. marcescens* SA Ant 16 were excised from the gel, cloned and sequenced and showed similarity to  $\beta$ -lactamase genes (98% identity, 90% coverage, E-value 0.0). Non-specific products of 300bp and 500bp were also

recovered and sequenced. Sequencing results showed similarity to intergenic regions (100% identity, 35% coverage, E-value  $2e-50$ ) and malate dehydrogenase (86% identity, 50% coverage, E-value  $4e-96$ ) but no similarity to any known arsenate reductases.

As more genome sequences have become available, it has become apparent that initial delineations into Gram negative (R773 *E. coli*) and Gram positive (pI258 *S. aureus*) *arsC* families are clearly not as straightforward as first thought. Gram positive-type arsenate reductases have been found in Gram negative organisms and *vice versa*. What does appear to be accurate is that Gram negative *arsC* sequences are much more conserved than their Gram positive counterparts.

Arsenate reductases from the few well characterised Gram positive type arsenate reductases were aligned, but as can be seen from Figure 2.19, very little homology exists between these sequences, making PCR primer design virtually impossible.

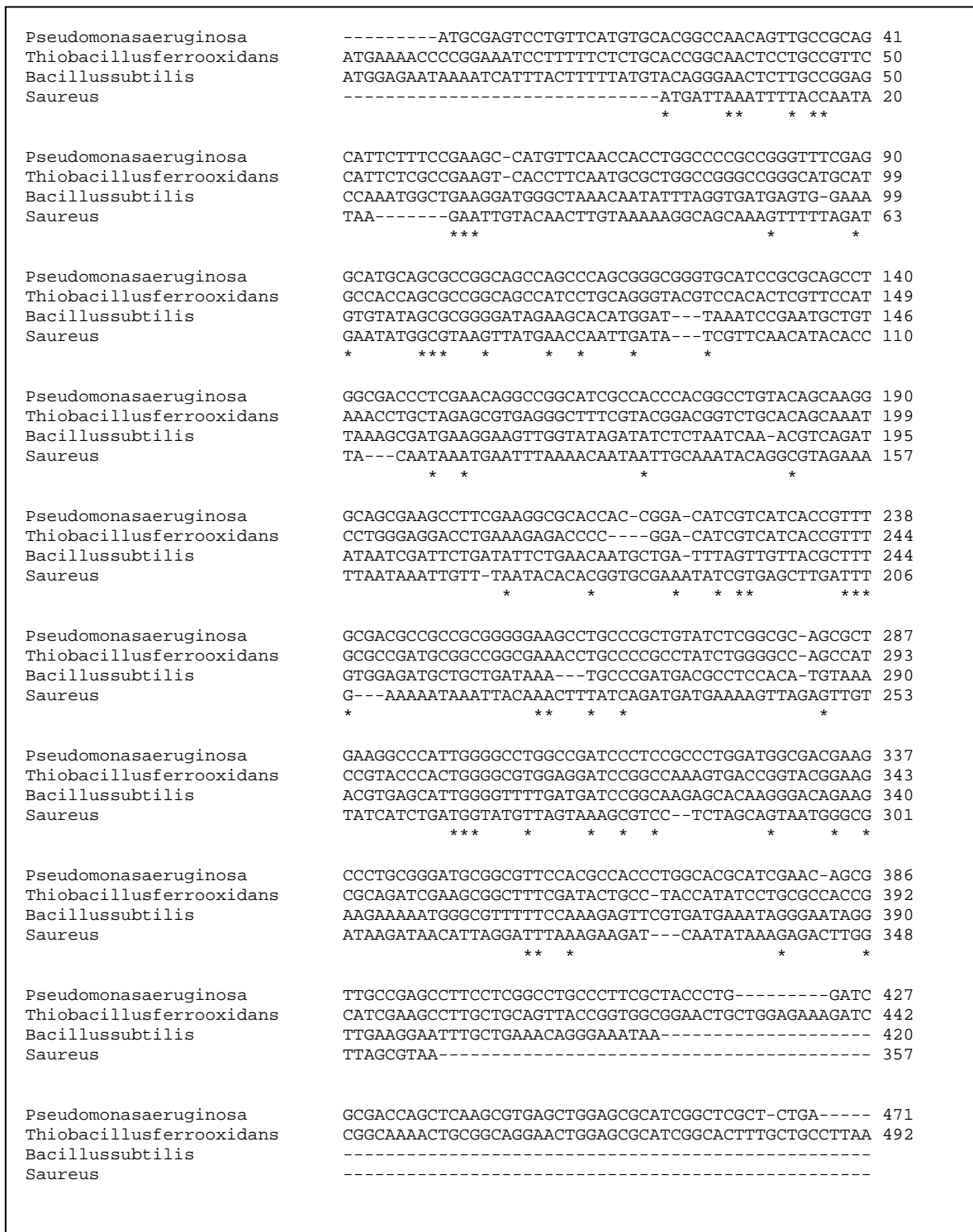


**Figure 2.19** Alignment of *arsC* from Gram positive type arsenate reductases.

The best alignment was found between *arsC* from *Pseudomonas aeruginosa* AF010234 and *Thiobacillus ferrooxidans* AF173880. Degenerate primers were designed based on regions of high homology and was expected to amplify an approximately 200bp product (Figure 2.20).

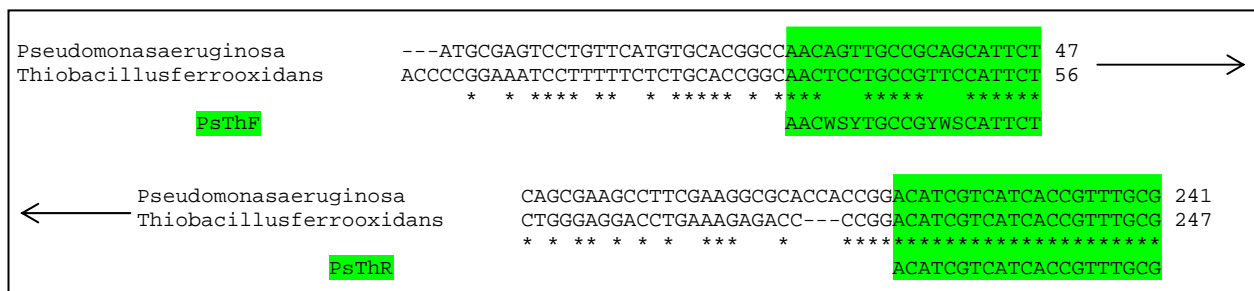


**Figure 2.20** Alignment of *arsC* from *P. aeruginosa* and *T. ferrooxidans* for design of degenerate primer set PsThF / PsThR.

PCR was performed with primer annealing from 41°C to 51°C with *S. marcescens* SA Ant 16 genomic DNA as template. Non-specific products of bigger that 1kb were consistently amplified over the temperature range tested, along with products of 300bp and 200bp (Figure 2.21).

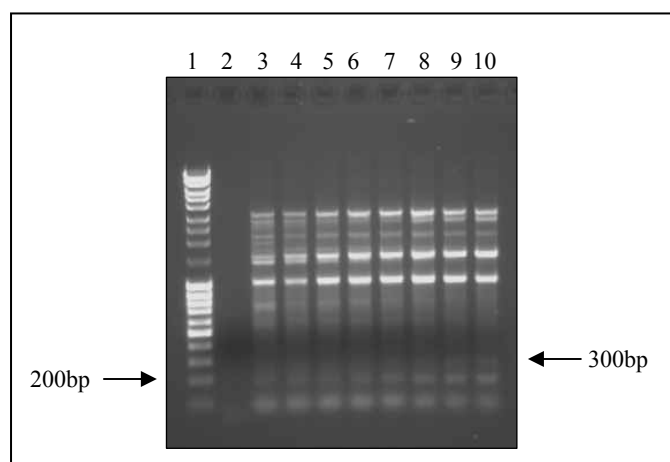


**Figure 2.21** PCR amplification of *S. marcescens* SA Ant 16 genomic DNA with Gram positive primer set PsThF / PsThR.

Lane 1: MassRuler™; Lane 2: Negative control lacking template. Lane 3: Annealing temperature of 41°C; Lane 4: 42.5°C; Lane 5: 44°C; Lane 6 46°C; Lane 7: 47.5°C; Lane 8 49°C; Lane 9: 50°C; Lane 10: 51°C.

Sequencing results showed similarity with tryptophanyl-tRNA synthetase (83% identity, 48% query coverage, E-value 8e-60) and phage replication proteins (72% identity, 80% coverage, E-value 7e-54). None of these hits share any sequence similarity or function with any arsenate reductases.

The inability to PCR amplify DNA fragments predicted by sequence similarity

alignment does not imply the absence of the targeted gene. *S. marcescens* SA Ant 16, this organism has clearly been shown to be able to actively reduce arsenate and therefore has to genetically encode a protein capable of this function. The lack of PCR amplicons using a variety of primers targeting a wide range of homologous regions as well as an atypical Gram positive type reductase in a Gram negative organism constitute enough evidence to imply that the gene of interest has a divergent sequence arrangement from hitherto described genes. An alternate possibility could be that the protein responsible for arsenate reduction may have a different biological function and that arsenate reductase activity is merely a fortuitous reaction.

### **2.5.2 Genomic libraries**

The PCR-based approach was abandoned in favour of a more function-based, sequence independent screening method. Genomic libraries were constructed from the DNA of *S. marcescens* SA Ant 16 and expressed in *E. coli* in an attempt to isolate the gene responsible for arsenate resistance in this hyper resistant bacterium.

*E. coli* knockout strain AW3110 (*arsRBC* replaced with a chloramphenicol resistance gene - refer back to Figure 2.14) were made chemically competent and transformed with empty pUC18 plasmid to determine sensitivity to arsenate and also to ascertain whether transformation and the presence of plasmid had any effect on resistance to arsenate. Transformed cells were plated on LB-plates supplemented with ampicillin and arsenate ranging from 0 $\mu$ M to 10mM.

Growth was completely inhibited at concentrations exceeding 500 $\mu$ M arsenate (Figure 2.22), signifying this as an adequate concentration for screening.



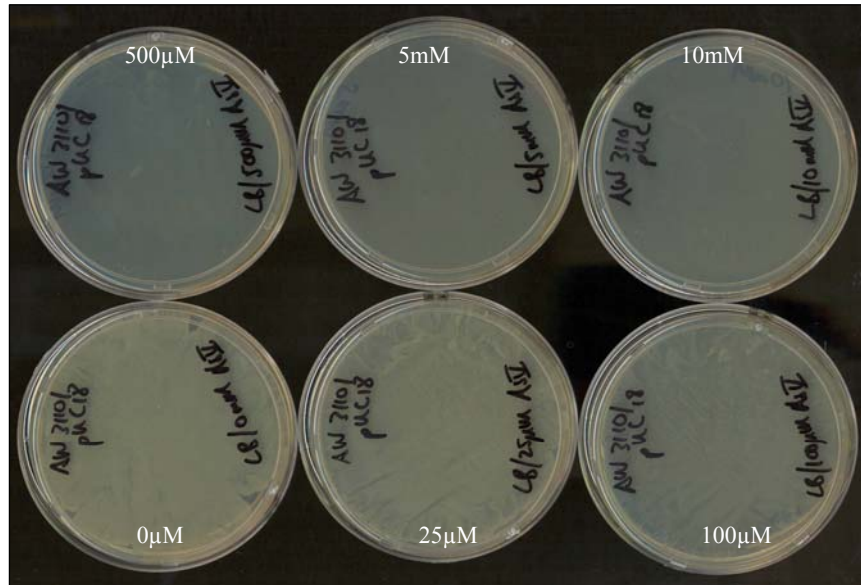


**Figure 2.22** Minimum inhibitory As(V) concentration for *E. coli arsC* knockout strain AW3110 transformed with pUC18 and plated on increasing concentrations of arsenate.

Supercoiled pUC18 plasmid DNA was digested with *Sau3AI* and complementary ends dephosphorylated. Genomic DNA from *S. marcescens* SA Ant 16 was partially digested with *Bam*HI (Figure 2.23) and fragments ranging from 1-10kb with an average size of 3kb ligated into pUC18. Ligation reactions were transformed into competent *E. coli* AW3110 cells and plated onto LB-plates containing ampicillin (plasmid selection marker), chloramphenicol (*arsRBC*: : Cam), IPTG, X-gal (induction and selection) and 500µM arsenate.

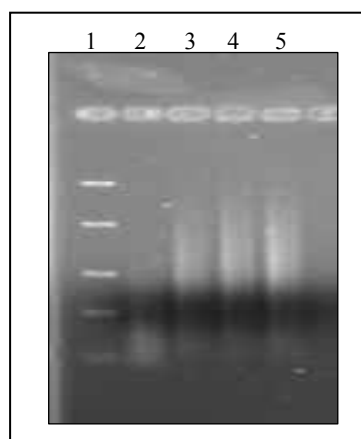


**Figure 2.23** Partial digest of genomic DNA from *S. marcescens* SA Ant 16.  
 Lane 1: FastRuler™ High Range; Lane 2: Undiluted *Bam*HI; Lane 3: 10X dilution; Lane 4: 100X dilution; Lane 5: 1000X dilution.

No colonies were obtained after selection. A number of possible explanations exist for this result; the most likely being that the antibiotic resistance level of the cells were exceeded by the presence of both antibiotics. LB-plates containing each of the antibiotics individually as well as a combination of both antibiotics were prepared. Competent AW3110 cells were transformed with empty pUC18 plasmid backbone and plated onto LB-plates containing chloramphenicol (to assess viability of the cells after transformation), ampicillin (to determine the transformation efficiency of the cells) and both antibiotics (to establish the effect, if any, of both combined) From Figure 2.24 it can be concluded that cells were viable after transformation, as an overgrown plate was obtained in the presence of only chloramphenicol. Competency of the cells were extremely low (see plate containing ampicillin), but no interaction was evident when the cells were exposed to both antibiotics simultaneously.

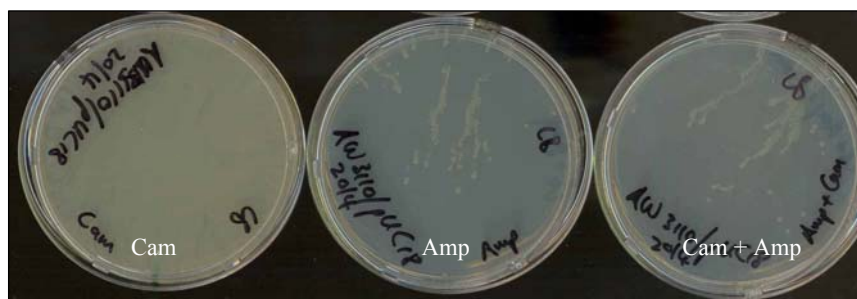


**Figure 2.24** Effect of interaction of ampicillin and chloramphenicol with *E. coli* strain AW3110.

Low transformation efficiency (in the order of  $10^5$  cfu/ $\mu$ g vector) of the knockout strain was not completely unexpected, since genetically manipulated strains often demonstrate inferior performance to native strains, and this is particularly relevant for strain AW3110 (Rawlings, personal communication). It was therefore decided to test routine laboratory strains *E. coli* JM109 and TOP10 as possible candidates for genomic library construction. Both strains were streaked out onto LB-plates containing increasing concentrations of arsenate as well as arsenite. Strain TOP10 was more resistant to arsenate than strain JM109 and growth was only inhibited at 20mM, whereas the latter was inhibited at 5mM (Figure 2.25). For arsenite, growth was severely inhibited for strain JM109 at 1mM and no growth was observed for TOP10 cells at 5mM arsenite (Figure 2.26).

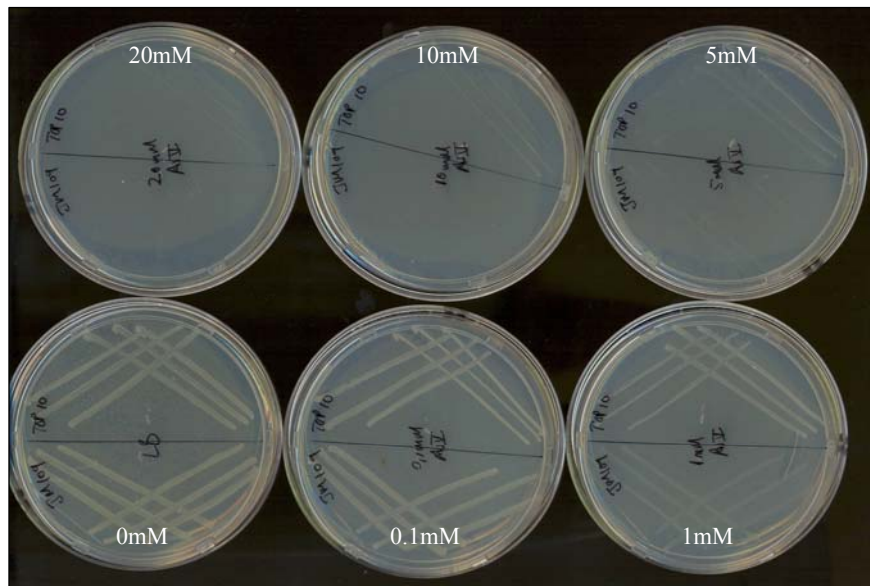


**Figure 2.25** Minimum inhibitory arsenate concentration for untransformed *E. coli* JM109 and TOP10.

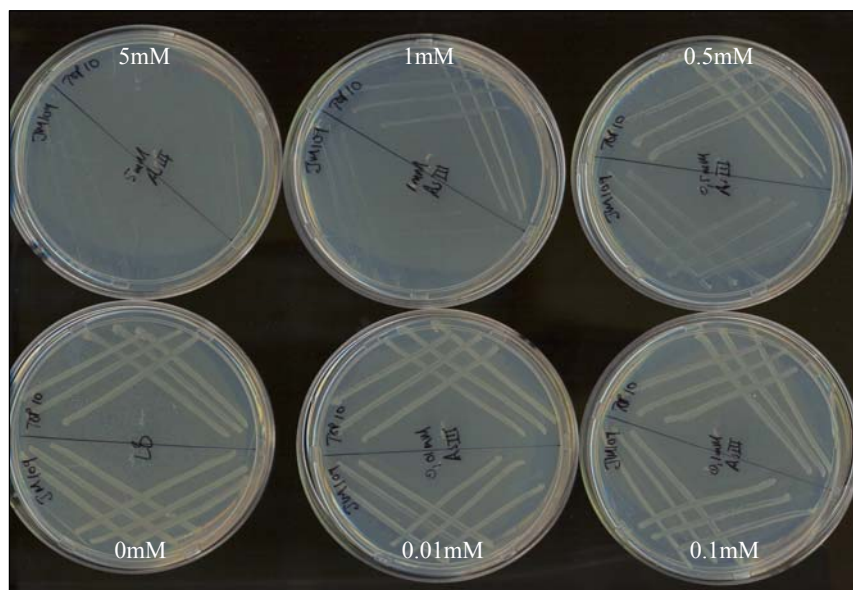


**Figure 2.26** Minimum inhibitory arsenite concentration for untransformed *E. coli* JM109 and TOP10.

Since strain JM109 was more sensitive to both arsenite and arsenate, it was decided to proceed with this strain. Competent JM109 cells were transformed with pUC18 and plated onto LB-plates containing arsenate. No growth was observed on plates containing arsenate at test concentrations as determined earlier (Figure 2.27).

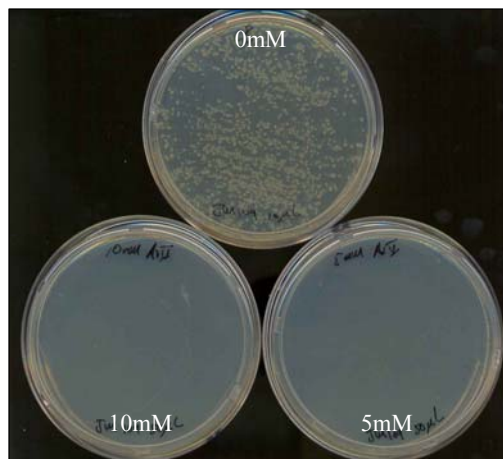


**Figure 2.27** Minimum inhibitory arsenate concentration for *E. coli* JM109 cells transformed with pUC18.

Partially digested genomic DNA (Figure 2.23) was ligated into linearised pUC18, transformed into competent JM109 cells and plated onto LB-plates containing 5mM arsenate and ampicillin. No positive transformants were obtained. Since JM109 cells were sufficiently competent ( $10^7$  cfu/ng vector) it then became necessary to resolve other issues surrounding library construction, such as the ligation efficiency. Phage  $\lambda$ DNA was digested with *EcoRI* and *BamHI* restriction enzymes respectively. These fragments were incubated with DNA ligase to re-ligate to visually verify ligation. Samples were withdrawn over a 1h period, snap-frozen to stop the reaction and analysed on a 1% TAE agarose gel. If fragments were re-ligated after restriction enzyme treatment it would be expected that the banding patterns would change during the course of the ligation, i.e. smaller bands would disappear and generate larger fragments. As can be seen from Figure 2.28, this was the case for *EcoRI* generated fragments, but not for fragments generated with *BamHI*. It was therefore decided to use *EcoRI* restriction enzyme for subsequent experiments.

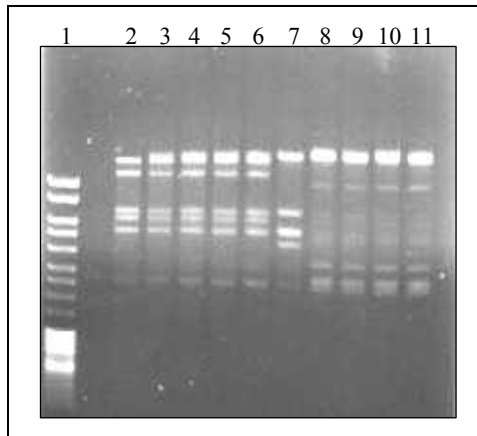


**Figure 2.28** Control ligation of *EcoRI* and *BamHI* digested  $\lambda$ DNA.

**Lane 1: MassRuler™; Lane 2: *BamHI* digested  $\lambda$ DNA before addition of ligase; Lane 3: ligation after 10 minutes; Lane 4: 20 minutes; Lane 5: 30 minutes; Lane 6: 1 hour.**

**Lane 7: *EcoRI* digested  $\lambda$ DNA before addition of ligase; Lane 8: 10 minute ligation; Lane 9: 20 minutes; Lane 10: 30 minutes; Lane 11: 1 hour.**

*EcoRI* digested phage  $\lambda$ DNA was ligated into compatible pUC18, and ligation efficiency visually verified by gel electrophoresis. If  $\lambda$ DNA fragments were ligated into the plasmid, it would be expected that banding patterns of the  $\lambda$ -fragments would change and that the plasmid backbone intensity would decrease as large DNA fragments would be generated through ligation. From Figure 2.29 it is clear that this is not the case and that the  $\lambda$ DNA fragments simply self-ligated. This result was confirmed by transforming a 30 minutes ligation reaction into competent JM109 cells and plated on LB-AIX plates. This transformation yielded only 2 colonies.

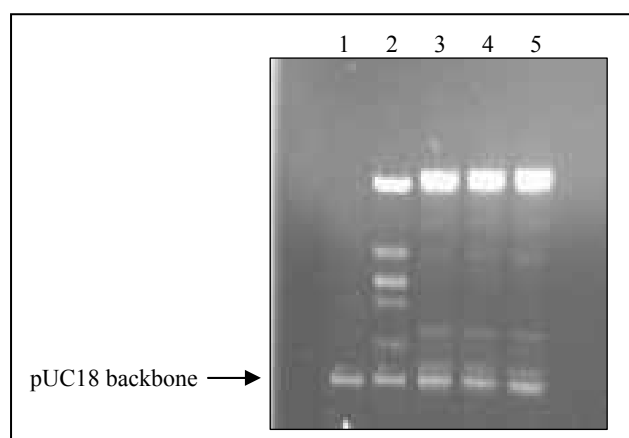


**Figure 2.29** Control ligation of *EcoRI* digested  $\lambda$ DNA into pUC18.

**Lane 1: Linearised pUC18 backbone; Lane 2: 10 minute ligation; Lane 3: 20 minute ligation; Lane 4: 30 minute ligation.**

When a ligation is performed, the desired product is a monomeric circular recombinant plasmid (i.e. a circular plasmid with only one copy of the insert DNA ligated). This, however, is only one of many ligation product possibilities and less desirable products include linear and circular homo- and heteropolymers<sup>70</sup>. The formation of preferred products can, to a certain extent, be controlled by the molar ratio of plasmid to insert and more importantly the total DNA concentration (i.e. vector + insert) in the ligation reaction<sup>77</sup>.

The effect of DNA concentration in the ligation as well as ligation time was investigated by ligating *EcoRI* digested  $\lambda$ DNA into pUC18. Two reactions were set up, both containing vector and insert in a 1 : 3 ratio, but for the first, a total DNA concentration of 2ng/ $\mu$ L, and the second, 10ng/ $\mu$ L was used. These reactions were incubated for 4 hours and half of the reaction volume transformed, while the rest of the reaction was incubated over night. It was found that 4X more transformants were obtained per ng total DNA at higher concentrations and that longer incubation times increased the number of transformants by up to 4X.

After control experiments had been performed with  $\lambda$ DNA, it was repeated for *S. marcescens* SA Ant 16. Genomic DNA was partially digested with *Sau3AI* (Figure 2.30a) and the generated fragments were incubated with ligase, to determine if sticky-ends were able to self-ligate.

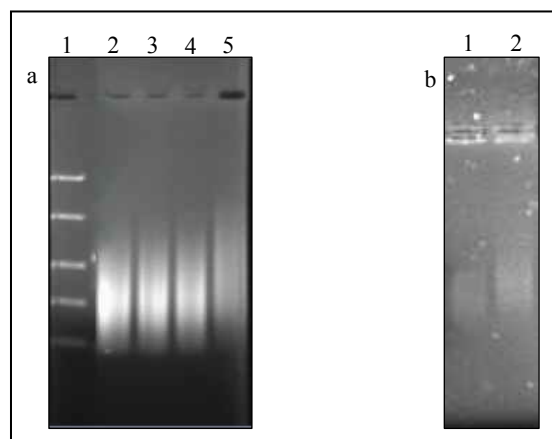


**Figure 2.30** (a): *S. marcescens* SA Ant 16 genomic DNA partially digested with *Sau3AI*.  
Lane 1: FastRuler™ High Range; Lane 2: Undiluted *Sau3AI*; Lane 3: 10X dilution; Lane 4: 100X dilution; Lane 5: 1000X dilution.  
(b): Self-ligation of *Sau3AI* generated fragments from genomic DNA of *S. marcescens* SA Ant 16. Lane 1: Partially digested DNA; Lane 2: self-ligated DNA fragments.

The ligation reaction was incubated for 3.5 hours and fragments compared to un-ligated DNA by agarose gel electrophoresis. In Figure 2.30b an upward shift from Lane 1 to Lane 2 was apparent, indicating self-ligation. However, if one refers back to Figure 2.28 and Figure 2.29, it is clear from the above mentioned figures that the ligation should be further advanced and that much larger fragments should be present after a 3.5 hour ligation (compare Figure 2.28 and Figure 2.29 10 minute ligation). From this, it might be inferred that ligation was prevented by an inhibiting substance present in the genomic DNA extract.

It was also necessary to ascertain if the sticky-ends of the vector were intact, as well as to verify if dephosphorylation was successful. Competent JM109 cells were transformed with uncut pUC18 (to determine transformation efficiency), pUC18 digested with *Bam*HI and re-ligated (to verify sticky-ends) and *Bam*HI digested pUC18, dephosphorylated and incubated with ligase (to confirm dephosphorylation). Transformation efficiency was high (in the order of  $10^7$  cfu/ng vector) and self-ligation of the vector sticky-ends yielded a high number of colonies, confirming that sticky ends were undamaged and that ligation was possible, and dephosphorylated self-ligated vector yielded no colonies, verifying successful dephosphorylation.

According to Bercovich *et al.* (1992)<sup>77</sup> optimum ligation efficiency can be obtained if a total DNA concentration of 10ng/ $\mu$ L is not exceeded, however, this was determined for blunt-end ligation and cannot necessarily be extrapolated to sticky-end ligations. Cranenburgh (personal communication)<sup>78</sup> stated that in a ligation reaction ‘if the vector ends have been dephosphorylated such that self-ligation is impossible there is theoretically no upper concentration limit provided that the insert is present at an equal or slightly greater concentration than the vector’.

With this in mind, ligation reactions with *S. marcescens* SA Ant 16 DNA were set up to determine the optimum total DNA concentration in a ligation reaction. Vector : insert ratios were 1 : 3 and total DNA concentration was 18.3ng/ $\mu$ L (high), 7.8ng/ $\mu$ L (intermediate) and 3.1ng/ $\mu$ L (low), respectively. The same amount of DNA from each reaction was transformed into competent JM109 cells. It was found that low total DNA concentrations yielded a lower number of transformants than intermediate DNA concentrations and that a very high concentration of total DNA inhibited ligation. In view of self-ligation results (see previous section) that suggested possible inhibiting substances present in the genomic DNA extract, the low number of transformants obtained from a high total DNA concentration was more likely

to be due to the bigger volume (i.e. higher concentration of inhibitor) of insert DNA added to the reaction than the final concentration of DNA. In previous experiments, partially digested DNA had been recovered from gel slices and it was suspected that the cleanup kits used were unable to remove sufficient amounts of inhibiting polysaccharides, constituting the agarose matrix, in the final eluate. Consequently, this DNA was discarded and in future, partially digested genomic DNA was not cut from gels, but directly purified after restriction digest.

The transformation efficiency of *E. coli* strains JM109 and TOP10 was compared by transforming both strains with equal amounts of pGem®-3Z (a pUC18 derivative). It was found that TOP10 cells were an order of magnitude more competent than JM109 cells. The minimum inhibitory growth concentration on both arsenate and arsenite of TOP10 cells transformed with empty pGem®-3Z were determined (Figure 2.31). (Also see Figure 2.25 and Figure 2.26.)

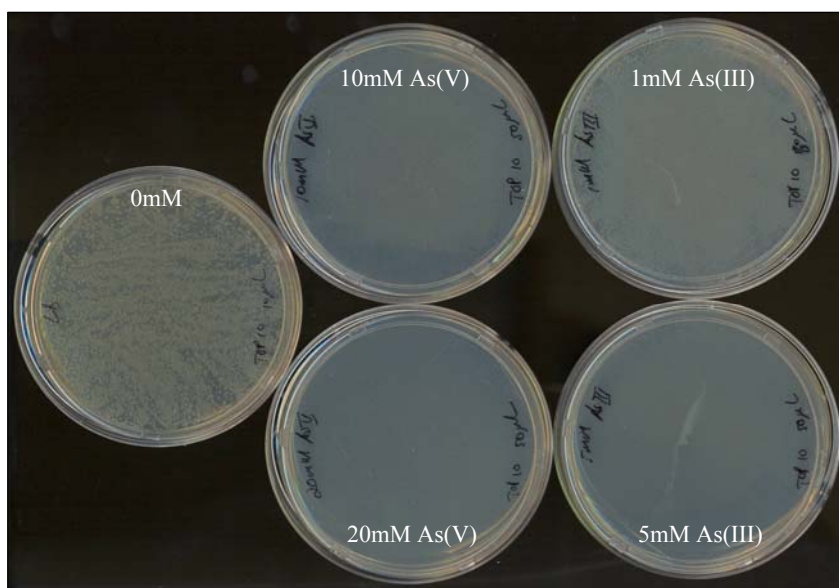


**Figure 2.31** Minimum inhibitory arsenate and arsenite concentration for *E. coli* TOP10 cells transformed with pGem®-3Z.

No growth on either arsenite or arsenate containing plates was observed at the test concentrations, and it was decided to use arsenate at 10mM for screening purposes.

Genomic DNA from *S. marcescens* SA Ant 16 was partially digested with *Sau3AI* and purified (Figure 2.32). DNA fragments ranging from 1kb to >10kb, with an average size of 3kb were ligated into the *Bam*HI site of pGem®-3Z and transformed into competent TOP10 cells.



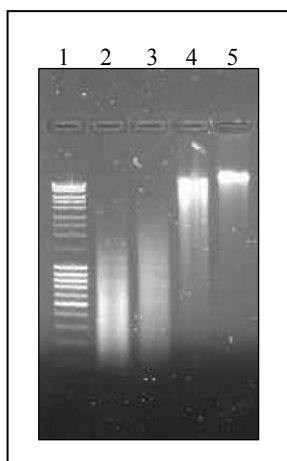


**Figure 2.32** Partial digest of genomic DNA from *S. marcescens* SA Ant 16.

**Lane 1: MassRuler™; Lane 2: Undiluted *Sau3AI*; Lane 3: 10X dilution; Lane 4: 100X dilution; Lane 5: 1000X dilution.**

Transformation reactions were plated onto master plates (LB + ampicillin, IPTG and X-gal) and incubated at 37°C over night. Ligation and transformation efficiency was determined to be  $3.24^5$  cfu/ng total DNA. Colonies from master plates were replica plated<sup>70</sup> onto LB-plates containing IPTG and 10mM arsenate and incubated at 37°C over night. All colonies transferred from the master plates to screening plates showed growth, and were subsequently transferred and streaked out onto fresh screening plates containing 10mM arsenate. Clones were transferred to screening plates containing 15mM arsenate (well above the minimum inhibitory concentration, see Figure 2.25 and Figure 2.31) by replica plating (Figure 2.33). Once again, most of the transferred colonies showed growth on these screening plates.

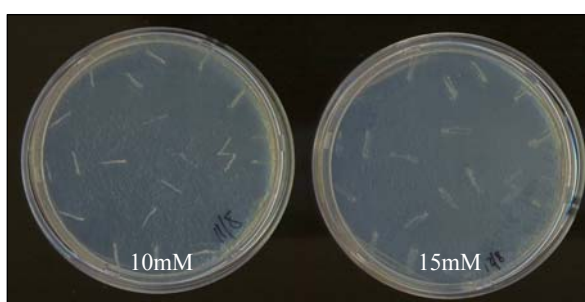


**Figure 2.33** Streaking out and replica plating of positive recombinants onto LB-plates containing 10mM and 15mM arsenate.

Colonies transferred from the 15mM arsenate screening plates into selective medium for plasmid proliferation. Inserts were verified by restriction digest with *EcoRI* and *HindIII* (Figure 2.34).

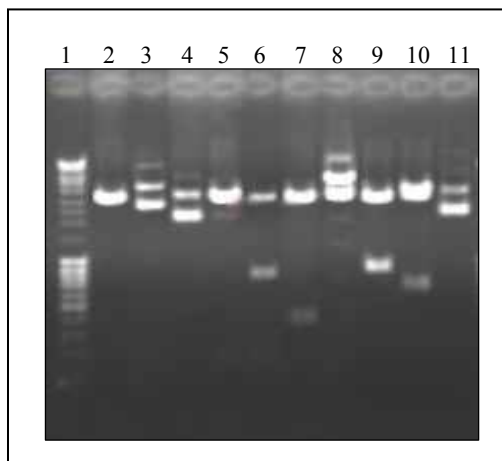


**Figure 2.34** Restriction analysis of plasmids containing inserts.

**Lane 1: MassRuler™; Lane 2: pGem®-3Z plasmid backbone; Lane 3-11: Inserts cut with *EcoRI* and *HindIII*.**

Inserts were subjected to sequencing and results varied from putative transferases to long chain fatty acid luciferin component ligases, but no arsenate reductases. The suspicion arose that the high number of cells localised in a single area during replica plating might have masked the toxic effects of arsenate in the screening plates, making growth possible and creating false positives.

To test this hypothesis, control reactions were performed by inserting any foreign DNA into digested plasmid, plating on master plates and replica plating to screening plates. Since arsenate functions as a substrate analog for phosphate ions, the reverse situation, in all likelihood, also takes place. Therefore, screening on complex medium (such as LB) may compound this situation and as a result, it was also decided to include arsenite at 5mM (as determined previously) for screening.

Plasmid backbone of pGem®-3Z (devoid of an arsenate reductase) was digested with *Sau3AI*, yielding 15 fragments ranging from 8bp to 985bp, and ligated into the *BamHI* site of pGem®-3Z. Ligation reactions were transformed into competent *E. coli* TOP10 cells and plated onto master plates where ligation and transformation efficiencies of up to  $10^5$ cfu/ng total DNA were achieved. Colonies were replica plated into screening plates containing up to 5mM arsenite and 20mM arsenate, respectively. Growth was observed on all screening plates indicating that replica plating onto screening plates was an ineffective method of screening.

It was then decided to use a well characterised model organism, *E. coli* W3110 to benchmark genomic library construction and isolation of *arsC*, using *E. coli* TOP10 cells for screening. *E. coli* W3110 was confirmed to possess a copy of *arsC* by PCR with primer set *arsC*-1-F / *arsC*-1-R<sup>65</sup> and subsequent sequencing of the amplified fragment (99% identity and an E-value of e-167) (Figure 2.35).

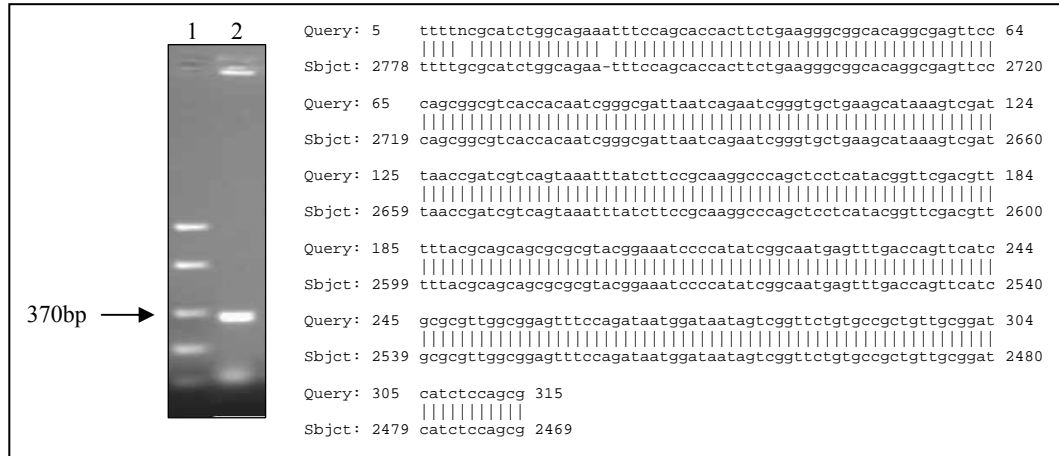


**Figure 2.35** 1.5% TAE agarose gel of the *arsC* of *E. coli* W3110 amplified with primer pair *arsC*-1-F / *arsC*-1-R and sequence alignment with *arsC* *E. coli* X80057.

Lane 1: FastRuler™ Low Range Marker; Lane 2: expected 370bp product.

W3110 genomic DNA was extracted and partially digested with *Sau3AI* (Figure 2.36). Fragments ranging between 1kb and >10kb with an average of 2.5kb were purified and ligated into *Bam*HI digested, dephosphorylated pGem®-3Z. This experiment was run in parallel with genomic DNA from *S. marcescens* SA Ant 16 (Figure 2.32).

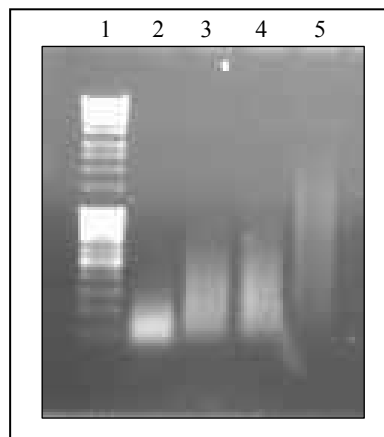


**Figure 2.36** Partial digest of genomic DNA from *E. coli* W3110.

Lane 1: MassRuler™; Lane 2: Undiluted *Sau3AI*; Lane 3: 10X dilution; Lane 4: 100X dilution; Lane 5: 1000X dilution.

A fraction of each transformation reaction was plated onto plates LB-plates containing ampicillin, IPTG and X-gal to determine the number of clones containing inserts. Ligation and transformation efficiencies of between 4 cfu/ng to 14 cfu/ng total DNA was achieved with white / blue ratio's of 64% - 72%. The number of clones needed to be screened to acquire a clone with the desired activity ( $N$ ) was estimated by calculating the fractional representation of the target genome in a single recombinant ( $f$ ) and the probability of a clone containing the target insert<sup>79</sup>.

$$N = \ln(1-P)/\ln(1-f)$$

If the highest probability ( $P = 99\%$ ), and average insert size of between 2.5kb and 3kb and an average genome size of 3000kb is substituted into the formula, approximately  $5.5 \times 10^3$  colonies need to be screened in order to obtain a positive transformant with the targeted activity. After ligation, transformation reactions were plated directly onto screening plates containing 1mM and 5mM arsenite and 10mM and 20mM arsenate respectively. In total, more than  $5.1 \times 10^4$  theoretical colonies from both the W3110 and *S. marcescens* SA Ant 16 libraries were screened, but none contained a DNA fragment that was able to confer increased resistance to arsenite or arsenate.

The lack of positive transformants could be due to the target gene not having been represented in the library, although this seems unlikely, since an order of magnitude additional colonies were screened than was anticipated. An alternate explanation may be that the host strain *E. coli* TOP10 was not able to be over-complemented by the addition of an exogenous arsenate reductase. Reasons for this can be numerous such as toxicity of the expressed gene, lack of recognition by the cellular machinery to actively express the cloned gene or the cloned gene may be so unusual in its mechanism of function, that the host may not be able to recognise and express the protein. This may very well be the case in the particular instance of *S. marcescens* SA Ant 16 where arsenate resistance is so extreme in this organism that it can easily be classified as hyper-resistant.

## **2.6 Literature Cited**

- 1 Novick RP & Roth C (1968). Plasmid-linked resistance to inorganic salts in *Staphylococcus aureus* .J Bacteriol 95: 1335-1342
- 2 Ji G & Silver S (1992). Regulation and expression of the arsenic resistance operon from *Staphylococcus aureus* plasmid pI258. J Bacteriol 174: 3684-3694
- 3 Rosenstein R, Peschel A, Wieland B & Gotz F (1992). Expression and regulation of the antimonite, arsenite, and arsenate resistance operon of *Staphylococcus xylosus* plasmid pSX267. J Bacteriol 174: 3676-3683
- 4 Silver S, Budd K, Leahy KM, Shaw WV, Hammond D, Novick, RP, Willsky GR, Malamy MH & Rosenberg H (1981). Inducible-plasmid determined resistance to arsenate, arsenite, and antimony(III) in *Escherichia coli* and *Staphylococcus aureus*. J Bacteriol 146: 983-996
- 5 Mobley HLT & Rosen BP (1982). Energetics of plasmid-mediated arsenate resistance in *Escherichia coli*. Proc Natl Acad Sci USA 79: 6119-6122
- 6 Silver S & Keach D (1982). Energy-dependent arsenate efflux: The mechanism of plasmid-mediated resistance. Proc Natl Acad Sci USA 79: 6114-6118
- 7 Cervantes C & Chavez J (1992). Plasmid-determined resistance to arsenic and antimony in *Pseudomonas aeruginosa*. Antonie van Leeuwenhoek 61: 333-337
- 8 Suzuki K, Wakao N, Kimura T, Sakka K & Ohmiya K (1998). Expression and regulation of the arsenic resistance operon of *Acidiphilum multivorum* AIU 301 plasmid pKW301 in *Escherichia coli*. Appl Environ Microbiol 64: 411-418
- 9 Sato T & Kobayashi Y (1998). The *ars* operon in the *skin* element of *Bacillus subtilis* confers resistance to arsenate and arsenite. J Bacteriol 180: 1655-1661
- 10 Cai J, Salmon K & DuBrow MS (1998). A chromosomal *ars* operon homologue of *Pseudomonas aeruginosa* confers increased resistance to arsenic and antimony in *Escherichia coli*. Microbiol 144: 2705-2713
- 11 Gotz F, Zabielski J, Philipson L & Lindberg M (1983). NA-homology between the arsenate resistance plasmid pSX267 from *Staphylococcus xylosus* and the penicillinase plasmid pI258 from *Staphylococcus aureus*. Plasmid 9: 126-137
- 12 Quan S & Dabbs ER (1993). Nocardioform arsenic resistance plasmid: characterization and improved *Rhodococcus* cloning vectors. Plasmid 29: 74-79
- 13 Hedges RW & Baumberg S (1973). Resistance to arsenic compounds conferred by a plasmid transmissible between strains of *Escherichia coli*. J Bacteriol 115, 459-460
- 14 Mobley HLT, Silver S, Porter FD & Rosen BP (1984). Homology among arsenate resistance determinants of R factors in *Escherichia coli*. Antimicrob Agents Chemother 25: 157-161
- 15 Smith HW (1978). Arsenic resistance in Enterobacteria: its transmission by conjugation and by phage. J Gen Microbiol 109: 49-56
- 16 San Francisco MJD, Hope CL, Owolabi JB, Tisa LS & Rosen BP (1990). Identification of the metalloregulatory element of the plasmid-encoded arsenical resistance operon. Nucleic Acids Res 18: 619-624
- 17 Kaur P & Rosen BP (1992). Plasmid-encoded resistance to arsenic and antimony. Plasmid 27: 29-40

- 18 Carlin A, Shi W, Dey S & Rosen BP (1995). The *ars* operon of *Escherichia coli* confers arsenical and antimonial resistance. *J Bacteriol* 177: 981-986
- 19 Jackson CR & Dugas SL (2003). Phylogenetic analysis of bacterial and archaeal *arsC* gene sequences suggests an ancient, common origin for arsenate reductase. *BMC Evol Biol* 3:18-28
- 20 Wu J & Rosen BP (1991). The ArsR protein is a trans-acting regulatory protein. *Mol Microbiol* 5: 1331-1336
- 21 Wu J & Rosen BP (1993). Metalloregulated expression of the *ars* operon. *J Biol Chem* 268: 52-58
- 22 Wu J & Rosen BP (1993). The *arsD* gene encodes a second trans-acting regulator protein of the plasmid-encoded arsenical resistance operon. *Mol Microbiol* 8: 615-623
- 23 Chen C, Misra TK, Silver S & Rosen BP (1986). Nucleotide sequence of the structural genes for an anion pump: the plasmid-encoded arsenical resistance operon. *J Biol Chem* 261: 15030-15038
- 24 Kaur P & Rosen BP (1992). Complementation between nucleotide binding domains in an anion-translocating ATPase. *J Bacteriol* 175: 351-357
- 25 Hsu CM, Kaur P, Steiner RF & Rosen BP (1991). Substrate-induced dimerization of the ArsA protein, the catalytic component of an anion-translocating ATPase. *J Biol Chem* 266: 2327-2332
- 26 Hsu CM & Rosen BP (1989). Characterization of the catalytic subunit of an anion pump. *J Biol Chem* 264: 17349-17354
- 27 Rosen BP, Weigel U, Karkaria C & Gangola P (1988). Molecular characterization of an anion pump. The ArsA gene product is an arsenite (antimonate)-stimulated ATPase. *J Biol Chem* 263: 31167-31170
- 28 Dey S, Dou D, Tisa LS & Rosen BP (1994). Interaction of the catalytic and the membrane subunits of an oxyanion-translocating ATPase. *Arch Biochem Biophys* 311: 418-424
- 29 Tisa LS & Rosen BP (1989). Molecular characterization of an anion pump: the ArsB protein is the membrane anchor for the ArsA protein. *J Biol Chem* 265: 190-194
- 30 Silver S, Ji G, Broer S, Dey S, Dou D & Rosen BP (1993). Orphan enzyme or patriarch of a new tribe: the arsenic resistance ATPase of bacterial plasmids. *Mol Microbiol* 8: 637-642
- 31 Rosen BP, Dey S, Dou D, Ji G, Kaur P, Ksenzenko MY, Silver S & Wu J (1992). Evolution of an ion-translocating ATPase. *Ann NY Acad Sci* 671: 257-272
- 32 Broer S, Ji G, Broer A & Silver S (1993). Arsenic efflux governed by the arsenic resistance determinant of *Staphylococcus aureus* plasmid pI258. *J Bacteriol* 175: 3840-3845
- 33 Rosen BP & Borbolla MG (1984). A plasmid-encoded arsenite pump produces arsenite resistance in *Escherichia coli*. *Biochem Biophys Res Commun* 124: 760-765
- 34 Gladysheva TB, Oden KL & Rosen BP (1994). Properties of the arsenate reductase of plasmid R773. *Biochem* 33:7288-7293
- 35 Ji G & Silver S (1992). Reduction of arsenate to arsenite by the ArsC protein of the arsenic resistance operon of *Staphylococcus aureus* plasmid pI258. *Proc Natl Acad Sci USA* 89: 7974-7978
- 36 Ji G, Garber EA, Armes LG, Chen C-M, Fuchs JA & Silver S (1994). Arsenate reductase of *Staphylococcus aureus* plasmid pI258. *Biochem* 33: 7294-7299
- 37 Holmgren A (1989). Thioredoxin and glutaredoxin systems. *J Biol Chem* 264: 13963-13966
- 38 Turner RJ, Hou Y, Weiner JH & Taylor DE (1992). The arsenical ATPase efflux pump mediates tellurite resistance. *J Bacteriol* 174: 3092-3094
- 39 Stevens SY, Hu W, Gladysheva TB, Rosen BP, Zuiderweg ERP & Lee L (1999). Secondary structure

- 
- and fold homology of the ArsC protein from the *Escherichia coli* arsenic resistance plasmid R773. *Biochem* 38:10178-10186
- 40 Mukhopadhyay R, Rosen BP, Phung LT & Silver S 2002. Microbial arsenic: from geocycles to genes. *FEMS Microbiol Rev* 26: 311-325
- 41 Liu J, Gladysheva TB, Lee L & Rosen BP (1995). Identification of an essential cysteinyl residue in the ArsC arsenate reductase of plasmid R773. *Biochem* 34: 13472-13476
- 42 Martin P, DeMel S, Shi J, Rosen BP & Edwards BFP (2001). Insights into the structure, solvation, and mechanism of ArsC arsenate reductase, a novel arsenic detoxification enzyme. *Structure* 9: 1071-1081
- 43 Oden KL, Gladysheva TB & Rosen BP (1994). Arsenate reduction mediated by the plasmid-encoded ArsC protein is coupled to glutathione. *Mol Microbiol* 12: 301-306
- 44 DeMel S, Shi J, Martin P, Rosen BP & Edwards BF (2004). Arginine 60 in the ArsC arsenate reductase of *E. coli* plasmid R773 determines the chemical nature of the bound As(III) product. *Protein Sci* 13: 2330-2340
- 45 Aslund F, Ehn B, Miranda-Vizuete A, Pueyo C & Holmgren A (1994). Two additional glutaredoxins exist in *Escherichia coli*: glutaredoxin 3 is a hydrogen donor for ribonucleotide reductase in a thioredoxin/glutaredoxin 1 double mutant. *Proc Natl Acad Sci USA* 91: 9813-9817
- 46 Bushweller JH, Aslund F, Wuthrich K & Holmgren A (1992). Structural and functional characterization of the mutant *Escherichia coli* glutaredoxin (C14\_S) and its mixed disulfide with glutathione. *Biochem* 31: 9288-9293
- 47 Shi J, Vlamis-Gardikas A, Aslund F, Holmgren A & Rosen BP (1999). Reactivity of glutaredoxins 1, 2, and 3 from *Escherichia coli* shows that glutaredoxin 2 is the primary hydrogen donor to ArsC-catalyzed arsenate reduction. *J Biol Chem* 274: 36039-36042
- 48 Mukhopadhyay R, Rosen BP, Phung LT & Silver S 2002. Microbial arsenic: from geocycles to genes. *FEMS Microbiol Rev* 26: 311-325
- 49 Messens J, Hayburn G, Desmyter A, Laus G & Wyns L (1999). The essential catalytic redox couple in arsenate reductase from *Staphylococcus aureus*. *Biochem* 38: 16857-16865
- 50 Messens J, Martins JC, Van Belle K, Brosens E, Desmyter A, De Gieter M, Wieruszkeski JM, Willem R, Wyns L & Zegers I (2002). All intermediates of the arsenate reductase mechanism, including an intramolecular dynamic disulfide cascade. *Proc Natl Acad Sci USA* 99: 8506-8511
- 51 Messens J, Van Molle I, Vanhaesebrouck P, Limbourg M, Van Belle K, Wahni K, Martins JC, Loris R & Wyns L (2004). How thioredoxin can reduce a buried disulphide bond. *J Mol Biol* 339: 527-537
- 52 Messens J, Van Molle I, Vanhaesebrouck P, Van Belle K, Wahni K, Martins JC, Wyns L & Loris R (2004). The structure of a triple mutant of pI258 arsenate reductase from *Staphylococcus aureus* and its 5-thio-2-nitrobenzoic acid adduct. *Acta Crystallogr Sect D Biol Crystallogr* 60: 1180-1184
- 53 Shi L, Potts M & Kennelly PJ (1998). The serine, threonine and/or tyrosine-specific protein kinases and protein phosphatases of prokaryotic organisms: a family portrait. *FEMS Microbiol Rev* 22: 229-253
- 54 Jacobs DM, Messens J, Wechselberger RW, Brosens E, Willem R, Wyns L & Martins JC (2001). <sup>1</sup>H, <sup>13</sup>C and <sup>15</sup>N backbone resonance assignment of arsenate reductase from *Staphylococcus aureus* in its reduced state. *J Biomol NMR* 20: 95-96
- 55 Messens J, Martins JC, Brosens E, Van Belle K, Jacobs DM, Willem R & Wyns L (2002). Kinetics and active site dynamics of *Staphylococcus aureus* arsenate reductase. *J Biol Inorg Chem* 7: 146-156

- 56 Zegers I, Martins JC, Willem R, Wyns L & Messens J (2001). Arsenate reductase from *S. aureus* pI258 is a phosphatase drafted for redox duty. *Nat Struct Biol* 8: 843-847
- 57 Li R, Haile JD & Kennelly PJ. (2003). An arsenate reductase from *Synechocystis* sp. strain PCC 6803 exhibits a novel combination of catalytic characteristics. *J Bacteriol* 185:6780-6789
- 58 Muller D, Medigue C, Koechler S, Barbe V, Barakat M, Talla E, Bonnefoy V, Krin E, Arsene-Ploetze F, Carapito C, Chandler M, Cournoyer B, Cruveiller S, Dossat C, Duval S, Heymann M, Leize E, Lieutaud A, Lievremont D, Makita Y, Mangenot S, Nitschke W, Ortet P, Perdrial N, Schoepp B, Siguier P, Simeonova DD, Rouy Z, Segurens B, Turlin E, Vallenet D, Van Dorsselaer A, Weiss S, Weissenbach J, Lett M-C, Danchin A, Bertin PN (2007). A Tale of Two Oxidation States: Bacterial colonization of arsenic-rich environments. *PLoS Genetics* 3: 518-530
- 59 Fauman EB, Cogswell JP, Lovejoy B, Rocque WJ, Holmes W, Montana VG (1998). Crystal structure of the catalytic domain of the human cell cycle control phosphatase, Cdc25A. *Cell* 93: 617-625
- 60 Bobrowicz P, Wysocki R, Owsianik G, Goffeau A & Ulaszewski S (1997). Isolation of three contiguous genes, *ACR1*, *ACR2* and *ACR3*, involved in resistance to arsenic compounds in the yeast *Saccharomyces cerevisiae*. *Yeast* 13: 819-828
- 61 Hofmann K, Bucher P & Kajava AV (1998). A model of Cdc25 phosphatase catalytic domain and Cdk-interaction surface based on the presence of a rhodanese homology domain. *J Mol Biol* 282: 195-208
- 62 Fauman EB & Saper MA (1996). Structure and function of the protein tyrosine phosphatases. *Trends Biochem Sci* 21: 413-417
- 63 Mukhopadhyay R & Rosen BP (2002). Arsenate reductases in Prokaryotes and Eukaryotes. *Environm Health Persp* 110: 745-748
- 64 Gilmour MW, Thomson NR, Sanders M, Parkhill J & Taylor DE (2004). The complete nucleotide sequence of the resistance plasmid R478: defining the backbone components of incompatibility group H conjugative plasmids through comparative genomics. *Plasmid* 52: 182-202
- 65 Saltikov CW & Olson BH (2002). Homology of *Escherichia coli* R773 *arsA*, *arsB*, and *arsC* genes in arsenic-resistant bacteria isolated from raw sewage and arsenic-enriched creek waters. *Appl Environ Microbiol* 68: 280-288
- 66 Saiki RK, Gelfand DH, Stoffel S, Scharf SJ, Higuchi R, Horn GT, Mullis KB & Erlich HA (1988). Primer-directed enzymatic amplification of DNA with a thermostable DNA polymerase. *Science* 239:487-491
- 67 Cobb BD & Clarkson JM (1994). A simple procedure for optimizing the polymerase chain reaction (PCR) using modified Taguchi methods. *Nucleic Acids Res* 22: 3801-3805
- 68 Bachmann BJ (1987). In: *Escherichia coli* and *Salmonella typhimurium*: Cellular and molecular biology. (Neidhardt FC, Ingraham JL, Low KB, Magasanik B, Schaechter M & Umberger HE, Eds.) pp. 1190-1219. American Society for Microbiology, Washington D.C.
- 69 Butcher BG & Rawlings DE (2002). The divergent chromosomal operon of *Acidithiobacillus ferrooxidans* is regulated by an atypical ArsR protein. *Microbiol* 148: 3983-3992
- 70 Sambrook J, Fritsch EF & Maniatis T (1989). *Molecular cloning: A laboratory manual*. Cold Spring Harbor Laboratory, Cold Spring Harbor, N.Y.
- 71 Hanahan DJ (1983). Studies on transformation of *Escherichia coli* with plasmids. *J Mol Biol* 166: 557-580



- 
- <sup>72</sup> Bercovich JA, Frinsein S & Zorzopulos J (1992). Effect of DNA concentration of recombinant plasmid recovery after blunt-end ligation. *BioTechn* 12: 190-193
- <sup>73</sup> Summers AO & Jacoby GA (1977). Plasmid determined resistance to tellurium compounds. *J Bacteriol* 129: 276-281
- <sup>74</sup> Taylor DE & Summers AO (1979). Association of tellurium resistance and bacteriophage inhibition conferred by R plasmids. *J Bacteriol* 137: 1430-1433
- <sup>75</sup> Whelan KF, Colleran E & Taylor DE (1995). Phage inhibition, colicin resistance, and tellurite resistance are encoded by a single cluster of genes on the IncHI2 plasmid R478. *J Bacteriol* 177: 5016-5027
- <sup>76</sup> Ryan D & Colleran E (2002). Arsenical resistance in the IncHI2 plasmids. *Plasmid* 47: 234-240
- <sup>77</sup> Bercovich JA, Frinsein S & Zorzopulos J (1992). Effect of DNA concentration on recombinant plasmid recovery after blunt-end ligation. *BioTechn* 12: 190-193
- <sup>78</sup> Cranenburgh RM (2004). An equation for calculating the volumetric ratios required in a ligation reaction. *Appl Microbiol Biotechnol* 65:200-202
- <sup>79</sup> Clarke I & Carbon J (1976). A colony bank containing a synthetic ColEI representative of the entire *Escherichia coli* genome. *Cell* 9: 91-99

## **Chapter 3**

### **Cellular Characterisation for Adhesion**

## **3.1 Literature review: Bacterial adhesion to inert surfaces**

The process of bacterial attachment to an available surface is dictated by a number of variables, including the species of bacteria, adsorbent surface composition, environmental factors, and essential gene products. Bacterial adhesion can be divided into a primary and secondary phase<sup>1</sup>, although some authors include an additional step of surface conditioning<sup>2</sup> to describe the interaction of the substratum with its environment.

### **3.1.1 Primary adhesion**

Primary adhesion constitutes the serendipitous meeting between a planktonic or free-living microorganism and a surface. Generally, bacteria prefer to grow on available surfaces rather than in the surrounding aqueous phase. Bacteria move to or are moved to a material surface through and by at least three mechanisms:

- (i) diffusive transport due to Brownian motion, van der Waals attraction forces, gravitational forces, the effect of surface electrostatic charge and hydrophobic interactions<sup>3</sup>, while chemotaxis (concentration gradients of diffusible chemical factors) and haptotaxis (surface bound chemoattractants such as amino acids, sugars or oligopeptides) also contribute to this process<sup>4</sup>,
- (ii) convective transport due to the liquid flow, and
- (iii) active movement of motile bacteria near the interface by flagella and pili.

Physical interactions are further classified as long- (more than 50nm) and short-range (less than 5nm) interactions<sup>3</sup>. Long-range interactions between cells and surfaces are described by mutual forces, which are a function of the distance and free energy. Short-range interactions become effective when the cell and surface come into close contact, these can be separated into chemical bonds (such as hydrogen bonding), ionic and dipole interactions and hydrophobic interactions<sup>5</sup>. Bacteria are transported to the surface by the so-called long-range interactions and upon closer contact, short-range interactions become more important<sup>6</sup>.

Primary adhesion is dictated by a number of physicochemical variables that define the interaction between the bacterial cell surface and the surface of interest<sup>7</sup>. First, the organism must be brought into close approximation with the surface, propelled either randomly (for example, by a stream of fluid flowing over a surface) or in a directed fashion via chemotaxis and motility. Once the organism reaches critical proximity to a surface (usually less than 1nm), it must overcome the secondary repulsive forces between itself and the surface and adsorb to the surface. The final determination of adhesion depends on the net sum of attractive or repulsive forces generated between the two surfaces<sup>8</sup>. These forces include electrostatic and hydrophobic interactions, steric hindrance, van der Waals forces, temperature and hydrodynamic forces. Primary adhesion is instantaneous but reversible and the microorganisms still exhibit Brownian motion during this phase<sup>9</sup>.

### **3.1.1.1 Theory of adhesion**

Under controlled conditions, the initial adhesion of bacteria onto solid surfaces is generally thought to be explained in terms of classic Derjaguin-Landau-Verwey-Overbeek (DLVO) theory which states that the total interaction energy of two particles is calculated by the sum of the van der Waals attractive and the electrostatic-like-charge repulsive energy<sup>10</sup>. It could be argued that classic DLVO theory describes one of several components of the attachment process - the probability of an organism overcoming any electrostatic barrier. However, it does not describe the various molecular interactions that would come into play when polymers at the bacterial surface enter into contact with molecular groups on the substratum as well as any conditioning film. Moreover, it does not account for physical factors such as structures and molecules on bacterial surfaces that affect cell-surface distance and the exact type of interaction or for the physical state of the substratum.

Thermodynamic theories take into account the various types of attractive and repulsive forces, such as van der Waals, electrostatic or dipole, but express them collectively in terms of free energy<sup>11</sup>. The approach requires estimation of numerical values of thermodynamic parameters, such as surface free energy of the bacterial and substratum surfaces and surface free energy of the suspending solution, in order to calculate the Gibbs adhesion energy for bacterial adhesion<sup>12</sup>. Adhesion is favored if the free energy per unit surface area is negative as a result of

adhesion, which means that spontaneous attachment is accompanied by a decrease in free energy of the system, as predicted by the second law of thermodynamics<sup>13</sup>. The most advanced thermodynamic theory demonstrates that acid-base, and in particular hydrogen bonding, is responsible for interactions leading to bacterial adhesion. Generally, it is almost impossible to obtain accurate values for bacterial surface free energies because these surfaces possess complex chemistry and hydration characteristics *in vivo*. Furthermore, the thermodynamic theory applies to closed systems where no energy is added to the system from outside. Bacteria, however, are living organisms that convert substrates to energy, and adhesion may be driven by energy consuming physiological mechanisms<sup>6</sup>.

Current thinking favours the “extended” DLVO theory (XDLVO) that takes into account the contribution of classical van der Waals and double layer interactions, but also the acid / base interactions which describe attractive hydrophobic interactions and repulsive hydration effects<sup>14</sup>.

### **3.1.2 Secondary adhesion**

The second stage of adhesion is the anchoring or locking phase and employs irreversible molecular and cellular mechanisms<sup>15</sup>. This is a time-dependent process and occurs when the bacterium synthesises extracellular adhesive materials that complex with surface materials<sup>16, 8</sup>. At the conclusion of the second stage, the bacterium is attached firmly to the surface, adhesion becomes irreversible in the absence of physical or chemical intervention, and the organism is described as being sessile.

### **3.1.3 Factors influencing bacterial adhesion**

#### **3.1.3.1 Surface of adhesion**

The matrix, or surface of adhesion, plays an important role in the determination of bacterial adhesion. The key factor influencing bacteria adherence to a biomaterial surface is the chemical composition of the material<sup>17</sup>, since materials with different functional groups change bacterial adhesion in a manner depending primarily on material hydrophobicity<sup>18</sup>, and charge<sup>19</sup>.

The physical surface also plays an important role and it has been found that the irregularities of polymeric surfaces promote bacterial adhesion whereas ultrasmooth surfaces tend to discourage adhesion<sup>20</sup>. Also, bacteria adhere and colonize porous surfaces preferentially over dense materials<sup>21</sup> and higher adhesion rates are observed on grooved and braided materials compared to flat materials<sup>22</sup>. This may happen since these surfaces have a greater surface area and provide more favourable sites for colonization. Bacteria preferentially adhere to irregularities that conform to their size since this maximizes bacteria-surface area<sup>6</sup>. Grooves or scratches that are on order of bacterial size increase the contact area and hence the binding potential, whereas grooves that are much larger / wider than the bacterial size approach the binding potential of a flat surface. Grooves or scratches too small, for the bacterium to fit them, reduce the contact area of the bacterium and provide steric hindrances and consequently, adhesion is negatively affected<sup>23</sup>.

### **3.1.3.2 Bacterial surface features**

Lipopolysaccharides (LPS) are one of the more complex molecules that are synthesised by bacteria. It typically has three structural regions: a lipid known as the lipid A, an oligosaccharide, known as the core, which is attached to the lipid A via 2-keto-3-deoxyoctonic acid (Kdo), and a polysaccharide known as the O-chain that is attached to the core oligosaccharide. Furthermore, the O-chain polysaccharide consists of a repeating oligosaccharide with varying degrees of polymerization. When long, charged side chains are attached to the LPS molecule, electrostatic interactions are the principal factors influencing surface physicochemistry and therefore adhesion<sup>24</sup>. Lipopolysaccharides devoid of highly charged, long side chains are dominated by their inner phosphoryl groups of the core and lipid A regions<sup>25</sup>, <sup>26</sup> and can therefore mediate in hydrophobic / hydrophilic interactions<sup>27</sup>.

Flagella could potentially perform three, non-mutually exclusive roles in adhesion:

- (i) flagellar-mediated chemotaxis could function to enable planktonic cells to swim towards nutrients associated with a surface;
- (ii) flagellar-mediated motility could enable bacteria to initially reach a surface, perhaps by overcoming repulsive forces at a surface; and
- (iii) flagella could function in a direct fashion by physically adhering to an abiotic surface.

In *E. coli* the crucial role played by flagella is providing motility to overcome repulsive forces at the surface-medium interface<sup>28</sup>, whereas in *Pseudomonas aeruginosa* the mechanism of primary adhesion is mediated by flagella<sup>29</sup>. In *E. coli*, primary adhesion is accomplished by type I pili (better described as fimbriae, since the sole function of this appendage is adhesion and not motility<sup>30</sup>) that contain the mannose-specific adhesin, FimH which is critical for attachment to abiotic surfaces via non-specific binding interactions<sup>28</sup>.

An important role is played by proteins localized in the bacterial surface that may directly mediate the interaction between bacterial cells and the solid substratum<sup>31, 32</sup>. Bacteria devote large stretches of genomic space (in the extreme case of *Chlorobium chlorochromatii*, 4.3%<sup>33</sup>) to encode large proteins with a repetitive structure termed adhesins. These adhesins have been shown to play a key role in biofilm formation on abiotic surfaces<sup>34</sup>. Proteins present on the cell surface can also serve as polyelectrolytes with various functional groups such as carboxyl, amino and phosphate that can mediate non-specific electrostatic adhesion<sup>35, 14</sup>.

### **3.1.3.3 Cell size and shape**

Some reports suggest that cell attachment to solid surfaces may be greater for elongated cells than for spherical cells. Fontes *et al.* (1991)<sup>36</sup> found that small coccoid cells showed much higher adhesion than larger, rod-shaped cells. Similarly, when comparing the transport characteristics of 19 bacterial isolates through soil columns, Gannon *et al.* (1991)<sup>37</sup> found that bacterial retention was statistically related to cell size only and not to other cell properties such as electrostatic charge, cell surface hydrophobicity and flagella. Bacteria shorter than 1µm usually had low adhesion. On the other hand, Camper *et al.* (1993)<sup>38</sup> were not able to statistically correlate cell size with adhesion. Weiss *et al.* (1995)<sup>39</sup> showed that cell shape, quantified as the ratio of cell width to cell length, and not simply cell size affects the transport of bacterial cells through porous media.

### **3.1.3.4 Bacterial hydrophobicity**

Hydrophobicity of a certain component indicates its tendency to interact with water. More specifically, hydrophobicity originates from the fact that water-water contacts are

thermodynamically more favorable than contacts between two non-polar groups or between a non-polar group and water<sup>40</sup>. Generally, the excess Gibbs energy of a surface decreases with increasing hydrophobicity, and therefore, with increasing hydrophobicity of a surface, higher adhesion strength will be observed<sup>41</sup>. Hydrophobic interactions are generally regarded as the key mediator of adhesion onto hydrophobic surfaces<sup>40</sup>, whereas hydrophilic interactions seem to favour attachment of hydrophilic bacteria to hydrophilic surfaces<sup>42</sup>.

### **3.1.3.5 Bacterial surface charge**

The surface charge of bacteria varies according to bacterial species and is influenced by the growth medium, the pH and the ionic strength of the suspending buffer, bacterial age<sup>43</sup>, and bacterial surface structures<sup>44</sup>. Most bacteria in aqueous suspension are negatively charged due to ionization of surface groups and this is dependent on the suspending environment in terms of pH and ionic strength. The bacterial charge is attributed to exposed ionogenic cell wall constituents like phosphate but predominantly carboxyl groups<sup>45</sup>, however, microdomains created by amine groups produce localized positive charges in cell walls<sup>46</sup>. Surface charge characteristics therefore, reflect the net charge resulting from the combined charges of the molecules comprising the cell surface and their counter ions under set conditions<sup>47</sup>.

### **3.1.4 Conditioning**

Conditioning of the adhesion surface can play an integral role during bacterial adhesion. Conditioning occurs when the native surface is modified by the adsorption of water, inorganic salts, proteins, lipids and extracellular matrix molecules. Once a surface has been conditioned, its properties are permanently altered, so that the affinity of an organism for a native or a conditioned surface can be quite different. Reports on the influence of conditioning of the surface and the subsequent role in bacterial adhesion are varied and at times contradictory. Poleunis *et al.* (2002)<sup>48</sup> monitored an increase in adsorbed material on a stainless steel surface immediately after immersion in natural seawater. They reported successive adsorption of firstly nitrogen-containing species (assumed to be proteins) followed by carbohydrates. It was concluded that even in the presence of adsorbed potential nutrients, the substratum influences, such as hydrophobicity and physical features like roughness, are more important to bacterial adhesion than the conditioning



film. Busscher *et al.* (1997)<sup>49</sup> showed weaker adhesion to materials coated with a conditioning film compared with the same surfaces without the conditioning film. Bradshaw *et al.* (1997)<sup>50</sup> evaluated the influence of conditioning films on biofilm development and concluded that conditioning films have a role in the degree and pattern of biofilm development. On the other hand, Ostuni *et al.* (2001)<sup>51</sup> demonstrated that there is little or no correlation between adsorption of protein on surfaces and adhesion of bacteria. These conflicting results are most likely a function of the variedness of surfaces, the bacteria and the dominant interactions that influence adhesion in each specific instance.

### **3.1.5 Concluding remarks**

Correlations between cell surface hydrophobicity, surface potential and adsorption capacity of various supports have given an assortment of both predictable as well as unexpected results. Van Loosdrecht *et al.* (1987)<sup>40</sup> have shown that the adsorption of hydrophobic microorganisms on negatively charged sulfated polystyrene was directly correlated to the hydrophobicity of the bacterial cell wall. On the other hand, adsorption of hydrophilic microorganisms in certain instances, have been shown to be inversely correlated with total electrophoretic charge. In this case, it was suggested that the surface free energy of the microorganisms was the dominant factor for cell adsorption, whereby the repulsive forces between the like charges on the surfaces of cells and support had been overcome. By studying the influence of the surface free energy of the support it has been shown that hydrophobic microorganisms are preferentially adsorbed on hydrophobic supports<sup>52, 53</sup>. There have also been investigations which indicate the importance of the surface potential for adsorption<sup>54</sup>. Krekeler *et al.* (1989)<sup>9</sup> concluded that: ‘...the adsorption of microorganisms to solid surfaces is influenced by both the surface potential and the surface free energy of the cells. To check whether the adsorption of microorganisms to materials with different surface characteristics is favored or not, the theoretical principles of the DLVO theory and the concept of the change in the interfacial free energy of adhesion might be useful. But one has to take into account that bacterial adhesion is not only due to physical interactions but also to surface polymers which may favor attachment under conditions where physical measurements alone suggest it would not be possible’.

Reports regarding adhesion of bacteria onto inert surfaces are highly contradictory, probably due to a combination of the complexity of the bacterial cell wall, local surface heterogeneities and shortcomings in investigative methods. Therefore, regardless of the most careful observations and elegant calculations, adhesion is an exceedingly complex interplay of a myriad of factors to such an extent that it is virtually impossible to predict bacterial adhesion based solely on physicochemical models, and in most instances, adhesion has to be determined empirically for each bacterium and support surface.

## **3.2    Aims**

1.    Optimum aerobic growth conditions for *S. marcescens* SA Ant 16 with regards to:
  - pH
  - temperature
  
2.    Electron donor / - acceptor ratios for anaerobic growth conditions
  
3.    Cell morphology and cell surface properties of
  - aerobically
  - anaerobically grown cells

### **3.3 Materials and methods**

#### **3.3.1 Growth parameters (pH and temperature)**

Cells of *S. marcescens* SA Ant 16 were inoculated from a cryopreserved culture into 100mL TYG medium, pH 5.8, grown to mid-exponential phase at 37°C at 200rpm and inoculated into fresh TYG medium and incubated in duplicate at 25°C, 30°C, 37°C, 40°C and 45°C. Duplicate flasks of media at pH 4.5, 5.8, 7.0 and 8.0 were also inoculated and incubated at 37°C with shaking. Growth was determined by measuring optical density spectrophotometrically at 560nm<sup>55</sup>.

#### **3.3.2 Motility**

Motility was observed microscopically under 1000X magnification by performing a hanging drop wet mount and also by stab-inoculating tubes of motility test medium<sup>56</sup>, incubating tubes at 37°C and observing growth compared to a positive *E. coli* control.

#### **3.3.3 Anaerobic growth**

A pre-inoculum was prepared as previously described (section 3.3.1) and cells were transferred into serum vials containing anaerobic TYG medium amended with 0.01g/L, 0.1g/L and 0.1g/L KNO<sub>3</sub> respectively, to an optical density of approximately 0.1. Both glucose (1g/L and 3g/L) and lactate (1g/L) were considered as electron donors. Samples were collected hourly, optical density measured, centrifuged and the supernatant stored at -20°C until analysis. Glucose was quantified by high performance liquid chromatography using a Waters SUGARPACK1 300 x 7.8mm column at 84°C with deionised water, flowrate 0.5mL/min, as mobile phase. Detection was performed using a Waters Breeze with Differential Refractive Index Detector 1200 Series. Lactate was acidified by adding phosphoric acid to a final concentration of 12.5% and quantified by HPLC with a Phenomenex Synergi 4µm Hydro-RP82A 250mm x 62mm column with KH<sub>2</sub>PO<sub>4</sub>, pH 3.5 as mobile phase at 50°C and a Shimadzu UV detector (SPD-20AV) at 215nm.

### **3.3.4 Cell size and morphology**

Cells were investigated microscopically in terms of cell size and cell morphology to observe differences when grown under aerobic and anaerobic conditions. Cells were heat fixed, Gram stained with crystal violet and iodine, counterstained with safranin<sup>57</sup> and visualised with a Zeiss Axioplan microscope. Images were imported into an image processing program, analySIS Image Processing, and analysed using built-in routines.

### **3.3.5 Pigmentation**

Cells were streaked onto peptone-glycerol plates (5g/L peptone, 10mL/L glycerol) and incubated at 30°C and 37°C respectively. The production of the pigment prodigiosin was assessed visually after 16h of growth<sup>58</sup>.

### **3.3.6 Cell surface properties**

The surface characteristics of aerobically and anaerobically grown cells of *S. marcescens* SA Ant 16 were studied to infer adhesion properties, and more importantly to determine if adhesion observed with aerobically grown cells could be extrapolated to cells grown under oxygen limitation.

#### **3.3.6.1 Hydrophobicity**

Bacteria were inoculated into 50mL of TYG medium, pH 7.0 and grown at 37°C (as determined previously) as a pre-inoculum. From this, a second flask of TYG medium was inoculated with exponential growth phase cells to an optical density of approximately 0.1 at 560nm and grown to mid-exponential phase under aerobic and anaerobic conditions (1g/L glucose and 0.1g/L nitrate). Cells were harvested by centrifugation in a Beckman J2-MC centrifuge at 11000 x g for 10 minutes at 4°C and washed twice in Artificial Ground Water (AGW)<sup>59</sup> (0.3mM Ca(NO<sub>3</sub>)<sub>2</sub>, 0.25mM MgSO<sub>4</sub>, 0.7mM NaHCO<sub>3</sub>, 20µM CaCl<sub>2</sub>, 0.145mM CaSO<sub>4</sub>, 0.1mM KNO<sub>3</sub>, 3µM NaH<sub>2</sub>PO<sub>4</sub>, pH 6.5). Cells were resuspended in AGW to 10<sup>8</sup> cells/mL and 2mL suspension added to an equal volume of hexdecane, toluene and xylene<sup>60</sup> respectively to determine the

bacterial adhesion to hydrocarbons (BATH)<sup>61</sup>. This was vortexed vigorously for 1 minute, the phases allowed to separate for 15 minutes and the optical density of the aqueous phase determined at 560nm. The hydrophobicity was expressed as  $(a - b)/a * 100$ , where  $a$  = initial optical density of cells, and  $b$  = optical density of cells in aqueous phase after mixing. Experiments were performed in triplicate.

Hydrophobicity of the cells were also determined by packing small columns with 1mL hydrated Phenyl-Toyopearl (hydrophobic, particle size: 65 $\mu$ m) and HW50F-Toyopearl resin (slightly hydrophilic, 45 $\mu$ m particle size) respectively and equilibrated with AGW. (Both these resins have similar particle sizes and the HW50F resin therefore served as a control for interactions between the cells and resin). Columns were loaded with 1mL cell suspension and washed with 10mL AGW to remove unbound cells<sup>62</sup>. Fractions of 1mL were collected and the optical density at 560nm determined. The percentage retention was expressed as  $(a - b)/a * 100$ , where  $a$  = optical density of cells added to column, and  $b$  = optical density of cells in the eluate. Experiments were performed in duplicate.

### **3.3.6.2 Electrostatic and acid / base properties**

Cells grown both aerobically and anaerobically to mid-exponential growth phase were harvested, washed and resuspended in AGW to 10<sup>8</sup> cells/mL. Duplicate small columns were packed as before with 1mL hydrated DEAE-Toyopearl and CM-Toyopearl (particle size of 65 $\mu$ m). Columns were loaded with 1mL cell suspension, washed with 10mL AGW to remove unbound cells and the percentage retention calculated as previously.

The electron donor / electron acceptor characteristics of the cells were determined by adding washed cells to an equal volume of ethyl acetate and chloroform<sup>63</sup>. This was vortexed, the phases allowed to separate and the percentage partitioning calculated as previously. Experiments were performed in triplicate.

### **3.3.6.3 Lipopolysaccharides (LPS)**

Bacterial capsules were visualised by staining cells with crystal violet and then decolorising and counterstaining with 20% copper sulfate. LPS were extracted with an adapted method of

Hitchcock and Brown (1983)<sup>64</sup>. Cells were suspended to  $10^8$  cells/mL and 1mL of this suspension pelleted by centrifugation. The pellet was resuspended in 100 $\mu$ L lysis buffer (2% SDS, 4%  $\beta$ -mercaptoethanol, 10% glycerol, 1M Tris pH 6.8) and boiled for 10 minutes. The lysate was cooled to room temperature, 0.025% (w/v) proteinase-K added and incubated at 60°C for 1h. This was loaded onto a 10% SDS-PAGE<sup>65</sup> gel, run at a constant current of 25mA and visualized by silver staining<sup>66</sup>.

#### **3.3.6.4 Carbohydrate and protein content**

Aerobically and anaerobically grown cells in mid-exponential growth phase were harvested and washed in AGW as previously described (Section 2.6.1). Cells were resuspended in AGW to  $10^8$  cells/mL and total protein content was determined with the BCA (Bicinchoninic Acid) Protein Kit, Standard Test Tube Procedure (Pierce)<sup>67</sup>. Protein concentration was determined by combining 100 $\mu$ L sample with 2mL Working Reagent, incubating at 37°C for 30 minutes and reading absorbance at 562nm. Carbohydrate content was determined using the Phenol Sulphuric Acid Carbohydrate Assay<sup>68</sup> by mixing 200 $\mu$ L sample with 200 $\mu$ L 5% phenol (w/v), adding 1mL concentrated H<sub>2</sub>SO<sub>4</sub>, incubating at room temperature for 1 hour and reading absorbance at 490nm.

## **3.4 Results and discussion**

### **3.4.1 Growth parameters (pH and temperature)**

*S. marcescens* SA Ant 16 was able to grow at temperatures between 25°C to 45°C. Biomass yield was severely decreased at higher temperatures, while the growth rate was much lower at lower temperatures. The highest biomass production was observed when the bacterium was cultured at 30°C, while the highest growth rate was found at 37°C. The amount of biomass produced at 37°C was only 4% less than at 30°C, while approximately 17% lower growth rate was calculated at 30°C. It was therefore decided to culture this strain at 37°C (Figure 3.1).

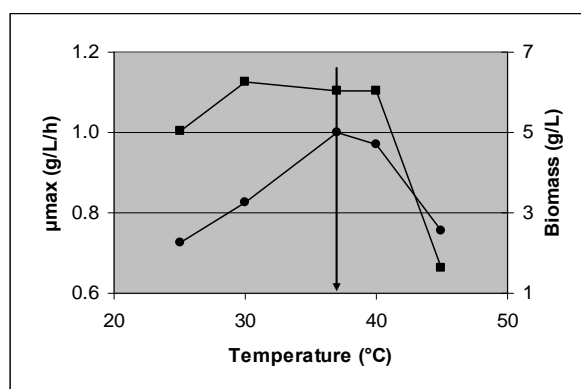


**Figure 3.1** Optimum growth temperature for *S. marcescens* SA Ant 16. (● growth rate; ■ biomass production.)

When the organism was cultured in TYG medium ranging from pH 4.5 – 8.0, it was able to grow comparably over the entire pH range tested. Biomass production was maximal at pH 4.5, but growth was severely inhibited. Optimum pH for growth was determined to be at pH 7.0 (Figure 3.2).



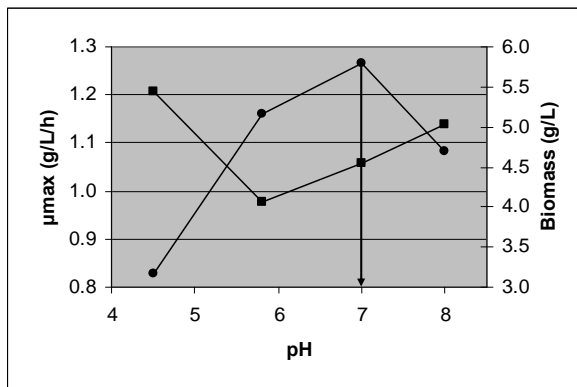


Figure 3.2 Optimum growth pH for *S. marcescens* SA Ant 16. (● growth rate; ■ biomass production.)

### 3.4.2 Motility

Cells of *S. marcescens* SA Ant 16 were determined to be motile by microscopic examination. Cells were also inoculated into semi-solid agar (Figure 3.3 a) and growth compared to an *E. coli* positive control (b).

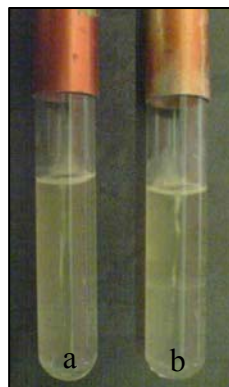


Figure 3.3 Motility of *S. marcescens* SA Ant 16 and *E. coli*.

The presence of flagella has a positive contribution towards adhesion not only by physically bringing cells into close contact with the surface of adhesion but also through specific or non-specific interactions with the matrix.

### 3.4.3 Anaerobic growth

*S. marcescens* is a facultative anaerobe, and could therefore potentially derive energy from utilizing nitrate as a terminal electron acceptor. Under anaerobic growth conditions both glucose

and lactate were considered as electron donors with  $\text{NO}_3^-$  as terminal electron acceptor at concentrations ranging from 0.01g/L to 1g/L (Figure 3.4). (Results are summarised in Table 3.1).

In general, compared to growth conditions with oxygen as the terminal electron acceptor, anaerobic growth conditions yielded markedly less biomass and growth rates were much slower. With lactate as electron donor, low biomass yield and low growth rates were obtained, especially at low electron acceptor concentrations (0.01g/L). Lactate was utilised very rapidly at low electron acceptor concentrations, but inefficiently, as only 20% of the total lactate available was utilized during growth. At higher nitrate concentrations, lactate was utilised at a slower rate, but even less efficiently. The electron acceptor was completely depleted after only 2 hours of growth, in the case of 0.01g/L  $\text{KNO}_3$ , indicating that this might be the limiting factor during growth. In the case of 0.1g/L  $\text{KNO}_3$ , nitrate was utilised at high rates and only 15% was residual after the experiment had been completed.

When glucose was tested at 3g/L as electron donor, it was found that higher growth rates and biomass were obtained than with lactate. Glucose at these high concentrations was utilized rapidly but incompletely as approximately 85% glucose was still present in the medium after the total duration of the experiment. The electron acceptor was utilised almost completely after 2 hours of growth in the case of 0.01g/L  $\text{KNO}_3$ , again indicating that this low concentration of electron acceptor was limiting. More than 90% of the 1g/L  $\text{KNO}_3$  was left in the medium after 3 hours, suggesting that 1g/L was the upper limit for electron acceptor. After the onset of stationary phase,  $\text{KNO}_3$  was depleted to less than 10%. Since this consumption was not connected to growth, it was not considered in calculations regarding volumetric rates of utilisation. Interestingly, at the highest  $\text{KNO}_3$  concentration (1g/L), it was found that both biomass and growth rate was inhibited, further confirming that this concentration was suboptimal.

With glucose added to 1g/L in the medium, the highest overall growth rates and biomass yields were obtained with the exception of 1g/L  $\text{KNO}_3$ , correlating with data obtained from 3g/L glucose as electron donor. Rates of glucose utilisation showed a decreasing trend with higher nitrate concentration, and with the exception of  $\text{KNO}_3$  at 1g/L, less than 20% of the glucose added initially was still present in the medium at the end of the growth experiment. Electron acceptor utilisation rates, on the other hand, showed an increase with increasing concentrations of  $\text{KNO}_3$ . In line with earlier data, when nitrate was added to 0.01g/L, it was completely depleted after 4

hours of growth, confirming this concentration to be too low for growth. Higher initial electron acceptor concentrations were utilised efficiently to between 5% and 15% residual  $\text{KNO}_3$ .

The highest growth rate (0.13g/L/h), total biomass (1.15g/L), most efficient electron donor (98%) and electron acceptor utilization (96%) was obtained with glucose as electron donor at 1g/L and  $\text{KNO}_3$  as electron acceptor at 0.1g/L. These glucose and  $\text{NO}_3^-$  concentrations were therefore used when cells were grown under oxygen limited conditions.

**Table 3.1 Summary of growth parameters during anaerobic growth of *S. marcescens* SA Ant 16.**

Electron Donor Electron acceptor (g/L $\text{KNO}_3$ )	1g/L Lactate		3g/L Glucose		1g/L Glucose		
	0.01	0.1	0.01	1.0	0.01	0.1	1.0
$\mu_{\text{max}}$ (/h)	0.06	0.10	0.11	0.14	0.11	0.13	0.11
Total biomass yield (g/L)	0.72	0.85	1.11	0.93	1.13	1.15	0.89
Volumetric rate of e-donor utilisation (mM/h)	0.84	0.41	0.77	1.01	1.11	0.72	0.44
Volumetric rate of e-acceptor utilisation (mM/h)	NC	1.25	0.21	0.12	0.03	0.22	0.98
e-donor utilisation (%)	20.43	10.26	14.20	15.96	83.09	97.77	49.70
e-acceptor utilisation (%)	100.00	84.99	96.26	7.23	100.00	96.45	84.95

NC: not calculated  
 $\mu_{\text{max}}$ : maximum growth rate during exponential growth phase  
 Total biomass: biomass produced at end of experiment  
 Volumetric rates: regression of linear portion of utilisation  
 e-donor & e-acceptor utilisation: ratio of substrate consumed during linear portion of utilisation

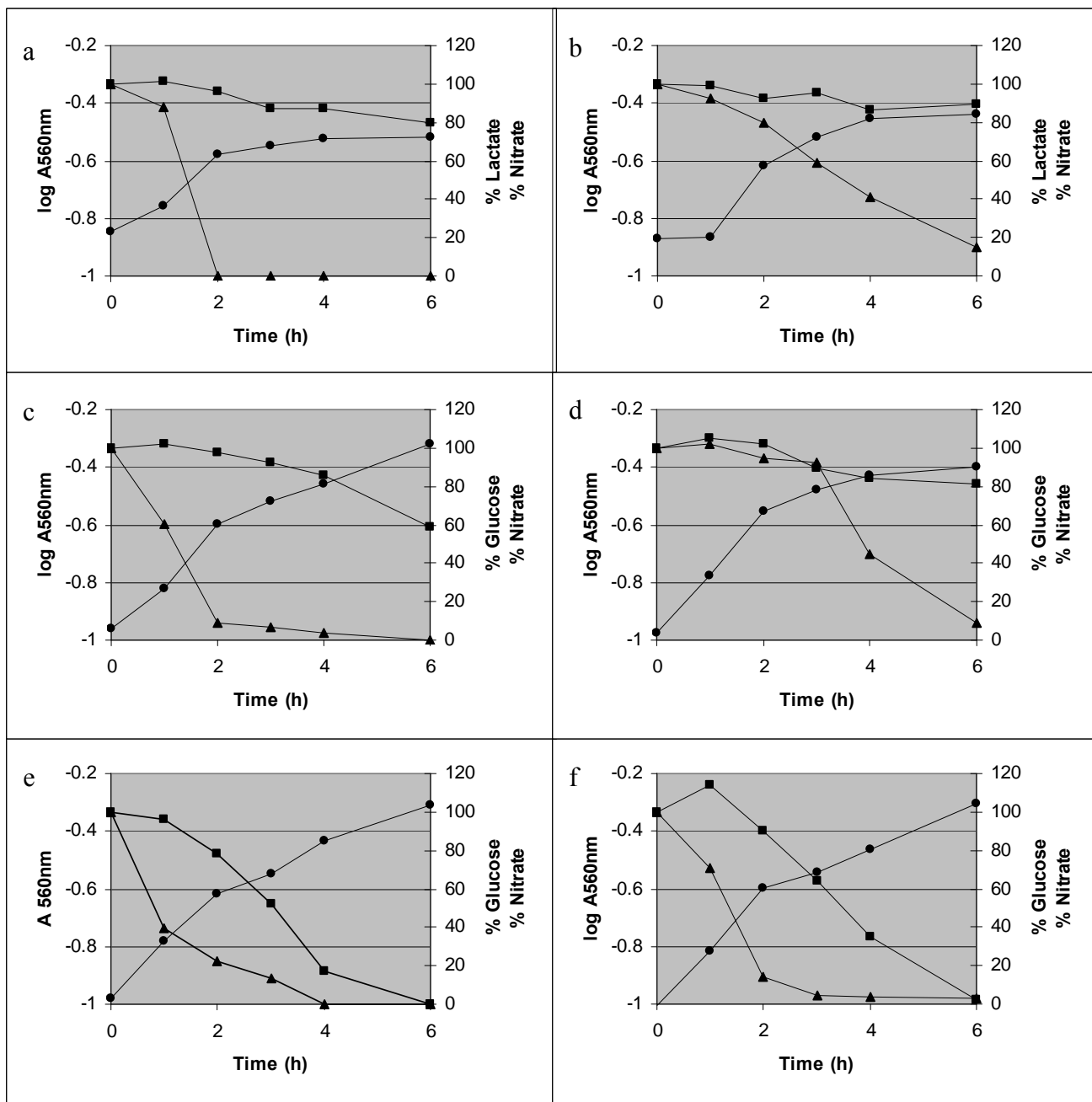


**Figure 3.4** Anaerobic growth of *S. marcescens* SA Ant 16 with nitrate as electron acceptor (● growth; ■ glucose / lactate; ▲ nitrate).

(a) 1g/L lactate, 0.01g/L KNO<sub>3</sub>

(b) 1g/L lactate, 0.1g/L KNO<sub>3</sub>

(c) 3g/L Glc, 0.01g/L KNO<sub>3</sub>

(d) 3g/L Glc, 1g/L KNO<sub>3</sub>

(e) 1g/L Glc, 0.01g/L KNO<sub>3</sub>

(f) 1g/L Glc, 0.1g/L KNO<sub>3</sub>

(g) 1g/L Glc, 1g/L KNO<sub>3</sub>.

### **3.4.4 Morphological and surface properties**

Van Schie and Fletcher<sup>69</sup> found that exposure of *Syntrophomonas wolfei* and *Desulfovibrio* sp. strain G11 to aerobic conditions greatly influenced adhesion to a solid surface compared to cells that had not been exposed to oxygen. It was therefore necessary to characterise both aerobically and anaerobically grown cells of *S. marcescens* SA Ant 16 with regards to cell surface properties in order to infer adhesion to a solid matrix.

#### **3.4.4.1 Cell size and morphology**

Aerobically and anaerobically grown *S. marcescens* SA Ant 16 cells were Gram stained (Figure 3.5) and measured. Cells grown in the presence of oxygen were  $2.155\mu\text{m} \pm 0.240\mu\text{m}$  in length and  $0.705\mu\text{m} \pm 0.107\mu\text{m}$  in breadth. Anaerobically grown cells were marginally longer ( $2.278\mu\text{m} \pm 0.299\mu\text{m}$ ) and thinner ( $0.655\mu\text{m} \pm 0.075\mu\text{m}$ ) than aerobically grown cells.

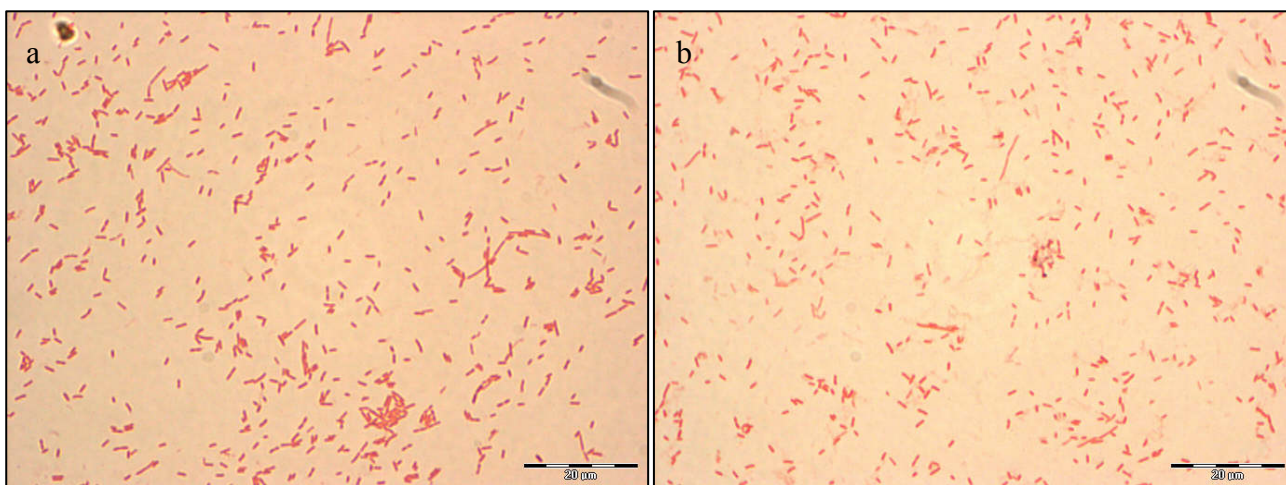


**Figure 3.5** Gram stained cells of *S. marcescens* SA Ant 16 grown under aerobic (a) and anaerobic (b) growth conditions.

Morphological differences observed between aerobically and anaerobically grown cells were less than the standard deviations calculated from 20 measurements, and the cells can therefore be considered to be in effect identical.

### 3.4.4.2 Pigmentation

Strains of *S. marcescens* that are able to produce the pigment prodigiosin only do so when grown at 30°C<sup>70</sup>. When *S. marcescens* SA Ant 16 was evaluated for prodigiosin production at both 30°C and 37°C (the growth optimum) it was found that the pigment was not produced at either 30°C or 37°C (Figure 3.6) after incubation over night.

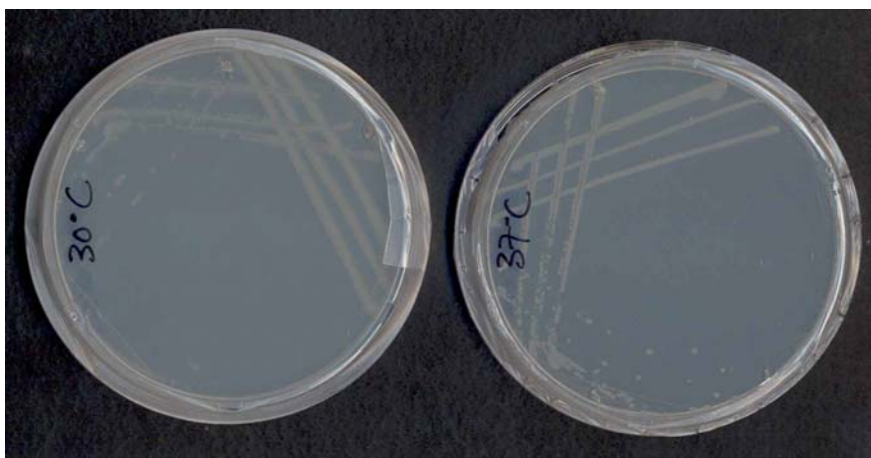


**Figure 3.6** *S. marcescens* SA Ant 16 grown at 30°C and 37°C on peptone-glycerol agar to observe pigment production.

It has been shown that prodigiosin production significantly increases the hydrophobicity of *S. marcescens*<sup>70, 71</sup>, but clearly, in the case of SA Ant 16, pigment production is not a contributing factor to the overall surface hydrophobicity.

### 3.4.4.3 Hydrophobicity

Cell surface hydrophobicity was examined by using a classical bacterial adhesion to hydrocarbons (BATH) test. By this method the percentage of cells which are excluded from the aqueous phase in a water / hydrocarbon two-phase system is measured and gives a reflection of the overall surface hydrophobicity<sup>60</sup>. From the high percentage partitioning of cells out of the aqueous phase with hexadecane (dielectric constant of 2.0), toluene (2.4) and xylene (2.4), respectively, it was found that the cell surface was moderately to highly<sup>63</sup> hydrophilic (Figure 3.7). Although, if data obtained from partitioning into xylene (with a standard deviation of

approximately 20%) is disregarded, results from hexadecane and toluene confirm the cell surface to be highly hydrophilic.

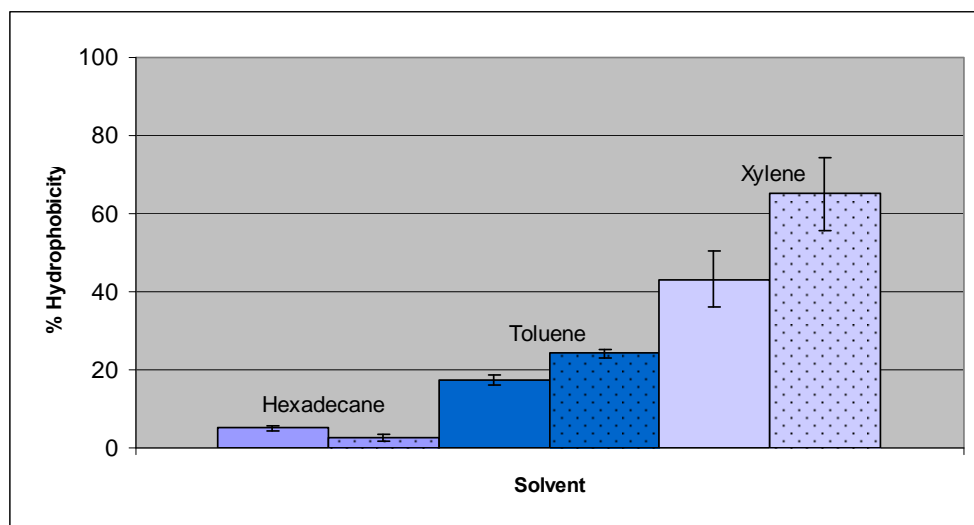


**Figure 3.7** Percentage hydrophobicity of aerobically (solid bars) and anaerobically (dotted bars) grown cells of *S. marcescens* SA Ant 16 as determined with BATH. (Values are expressed as a percentage of cells partitioning relative to the total initial cell load.)

Cell surface hydrophobicity was further investigated by hydrophobic interaction chromatography (HIC). This is generally regarded as a measure of localized hydrophobicity, whereas BATH gives an indication of overall hydrophobicity<sup>60</sup>. Less interaction between cells and the hydrophobic resin was observed than with a slightly hydrophilic resin, confirming the hydrophilic nature of both types of cells (Figure 3.8).

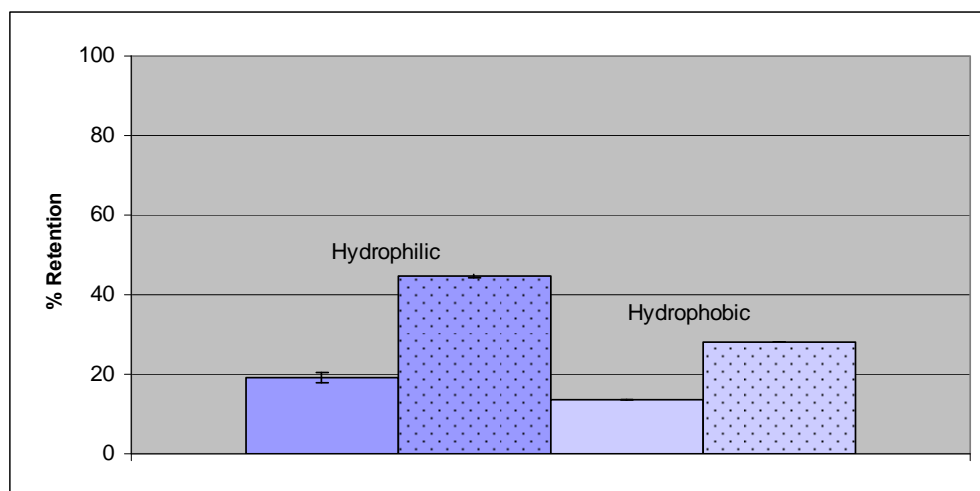


**Figure 3.8** Percentage hydrophobicity of aerobically (solid bars) and anaerobically (dotted bars) grown cells of *S. marcescens* SA Ant 16 as determined with HIC. (Values are expressed as a percentage of cells retained relative to the total initial cell load. For interaction with the HIC resin, standard deviations were too small to be indicated.)

It was suggested by Sorongdon *et al.*, 1991<sup>72</sup> that some of the organic solvents used in BATH might extract certain cell wall components, and this could explain the differences in results obtained from hexadecane, toluene and xylene as well as notable standard deviations for xylene. The absence of the pigment prodigiosin is also indicative of the highly hydrophilic surface of *S. marcescens* SA Ant 16<sup>71</sup>.

#### 3.4.4.4 Electrostatic and acid / base properties

The acid / base properties of the cell surface were assessed by the percentage partitioning of aerobically and anaerobically grown cells out of an aqueous phase when in the presence of the Lewis acid, chloroform and the Lewis base, ethyl acetate. Partitioning of cells between ethyl acetate (dielectric constant of 6.0) and an aqueous phase revealed the cell surface to have a low affinity for this basic solvent and electron acceptor. This highly acidic/electron donor character of the cell surface was confirmed by partitioning of cells between chloroform (4.8) and an aqueous phase (Figure 3.9).



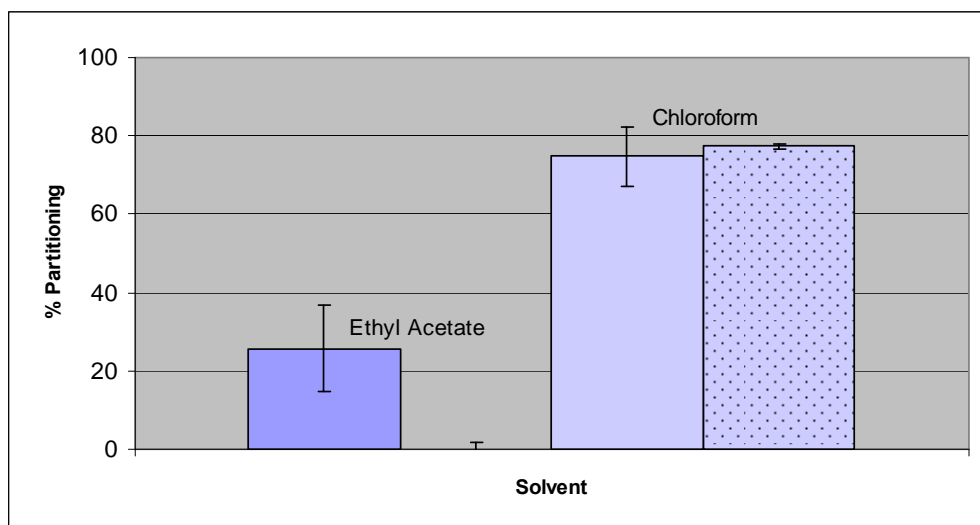


**Figure 3.9** Acid / base properties of aerobically (solid bars) and anaerobically (dotted bars) grown cells of *S. marcescens* SA Ant 16. (Values are expressed as a percentage of cells partitioning relative to the total initial cell load.)

Cell surface properties were further investigated by applying cells to anionic and cationic chromatographic resins. Both aerobically and anaerobically grown cells were shown to be negatively charged by the interaction with the anion exchange resin (diethylaminoethyl) and the lack of interaction with the negatively charged carboxymethyl (CM) resin (Figure 3.10).

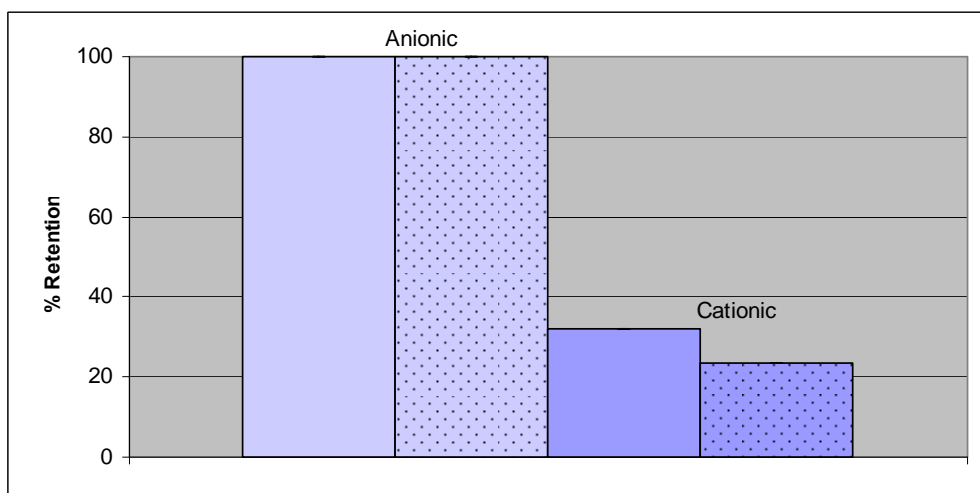


**Figure 3.10** Percentage retention of aerobically (solid bars) and anaerobically (dotted bars) grown cells of *S. marcescens* SA Ant 16 with various chromatographic resins. (Values are expressed as a percentage of cells retained relative to the total initial cell load. Standard deviations were too small to be indicated.)

The notable difference of partitioning of cells in ethyl acetate and chloroform respectively, solvents having identical van der Waals forces<sup>73</sup>, and an aqueous phase, demonstrates the capacity of the cells to establish some interactions with a support other than those of van der Waals<sup>10</sup>. These interactions are likely to be electrostatic as indicated by the high affinity for the anion exchange resin, and the concomitant low affinity for the cation exchange resin.

#### 3.4.4.5 Lipopolysaccharides (LPS)

The presence of lipopolysaccharides was confirmed microscopically as a colourless capsule surrounding the bacteria against the purple background (Figure 3.11 a and b).

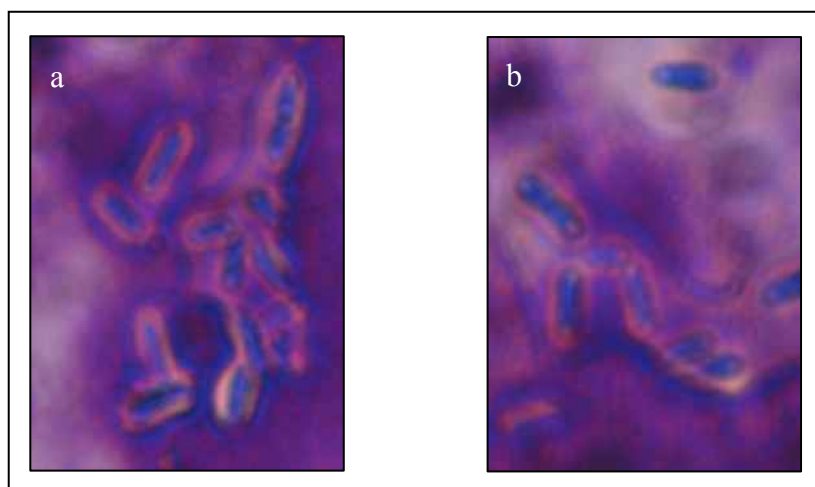


**Figure 3.11** Lipopolysaccharides visualised with crystal violet and copper sulfate of (a) aerobically grown cells and (b) anaerobically grown cells of *S. marcescens* SA Ant 16.

LPS were extracted from cells grown in the presence and absence of oxygen. When the LPS were separated on SDS-PAGE, it was possible to discern the O-antigen, core polysaccharides and the lipid A regions (Figure 3.12).

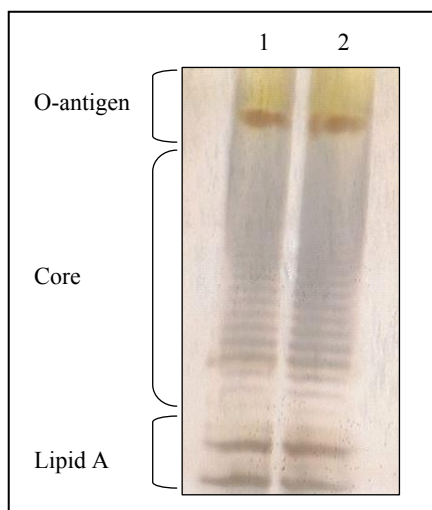


**Figure 3.12** Lipopolysaccharides from aerobically and anaerobically grown cells of *S. marcescens* SA Ant 16 separated on SDS-PAGE. (Lane 1: aerobic LPS extract; Lane 2: anaerobic LPS extract.)

The LPS profiles for both aerobic and anaerobically grown cells were identical. It has been demonstrated that LPS are involved in hydrophilic adhesion and that hydrophilicity is the result of the presence of the uncharged O-side chains and core oligosaccharides<sup>27</sup> as is the case with *S. marcescens* SA Ant 16. The LPS present on aerobically and anaerobically grown cells are likely to contribute to the highly hydrophilic character of the cell surfaces as observed with BATH and HIC.

#### **3.4.4.6 Carbohydrate and protein content**

The carbohydrate to protein content of cells grown in the presence and absence of oxygen were determined. It was found that the carbohydrate : protein ratio for aerobically grown cells was 1:3.7 and was slightly higher, 1:4.5, for anaerobically grown cells (Table 3.2) although the percentage difference is comparable to the standard deviation observed for total protein in anaerobically grown cells and is therefore not significant.

**Table 3.2** Total protein and carbohydrate content of cells of *S. marcescens* SA Ant 16 grown aerobically and anaerobically. (N = Number of replicates; AVG: Average; SD: Standard Deviation expressed as a percentage of total protein or carbohydrate content).

		AVG	N	% SD	Ratio
Aerobic	Carbohydrate ( $\mu\text{g}/\text{cell}$ )	$7.01 \times 10^{-8}$	2	3.01	1:3.73
	Protein ( $\mu\text{g}/\text{cell}$ )	$2.62 \times 10^{-7}$	2	5.54	
Anaerobic	Carbohydrate ( $\mu\text{g}/\text{cell}$ )	$7.05 \times 10^{-8}$	4	6.54	1:4.43
	Protein ( $\mu\text{g}/\text{cell}$ )	$3.54 \times 10^{-7}$	4	21.26	

Bacteria express a range of proteins and carbon polymers on their outer surfaces that considerably influence adhesion by not only contributing to localised charges but also to overall hydrophobicity of the cells. In *S. marcescens* outer surface proteins<sup>74</sup>, serratamolide (an amphipathic aminolipid)<sup>75</sup> and mannose sensitive adhesins<sup>76</sup> have been shown to play a significant role in adhesion to biological surfaces.

### **3.5 Conclusions**

Growth parameters with regards to pH and temperature were investigated for *S. marcescens* SA Ant 16 under aerobic growth conditions where optima of pH 7.0 and 37°C were established. When cells were grown under anaerobic conditions (which would mimic conditions in an oxygen limited column reactor), it was found that glucose (1g/L) was the preferential electron donor rather than lactate, and that KNO<sub>3</sub> at 0.1g/L produced high growth rates, the highest biomass and the most complete electron donor and electron acceptor utilisation during the growth period without being limiting during growth.

Aerobically and anaerobically grown cells of *S. marcescens* SA Ant 16 were investigated with regards to various cell surface properties and features in order to infer adhesion to sand particles for application in a bioreactor. Cells grown in the presence and absence of oxygen were highly similar with respect to all parameters investigated. Slight differences could be attributed to the stress conditions represented by utilizing nitrate as terminal electron acceptor instead of oxygen. (The redox potential for the redox pair NO<sub>3</sub><sup>-</sup> ↔ N<sub>2</sub> is 0.747kcal/mol/e<sup>-</sup> with a potential

energy yield of 649kcal/mol as compared to  $O_2 \leftrightarrow H_2O$  with a redox potential of 0.812kcal/mol/ $e^-$  and energy yield of 686kcal/mol<sup>77</sup>.) But in general, these differences were smaller or comparable to standard deviations between experiments. Both types of cells exhibited highly hydrophilic surface characteristics and the overall net charge of the cells were negative. It would therefore not be unreasonable to assume that both types of cells would interact similarly with any matrix of adhesion.

### **3.6 Literature cited**

- 
- <sup>1</sup> Piette JPG & Idzak ES (1992). A model study of factors involved in adhesion of *Pseudomonas fluorescens*. Appl Environ Microbiol 58: 2783-2791
- <sup>2</sup> Gristina AG (1987). Biomaterial-centered infection, microbial vs tissue integration. Science 237: 1588-1597
- <sup>3</sup> Gottenbos B, Busscher HJ, Van Der Mei HC & Nieuwenhuis P (2002). Pathogenesis and prevention of biomaterial centered infections. J Mat Sci 13: 717-722
- <sup>4</sup> Kirov SM (2003). Bacteria that express lateral flagella enable dissection of the multifunctional roles of flagella in pathogenesis. FEMS Microbiol Lett 224: 151-159
- <sup>5</sup> Mayer C, Moritz R, Kirschner C, Borchard W, Maibaum R, Wingender J & Flemming H-C (1999). The role of intermolecular interactions: studies on model systems for bacterial biofilms. Intern J Biol Macromol 26: 3-16
- <sup>6</sup> Katsikogianni M & Missirlis YF (2004). Concise review of mechanisms of bacterial adhesion to biomaterials and of techniques used in estimating bacteria-material interactions. Eur Cells Mat 8: 37-57
- <sup>7</sup> Marshall KC, Stout R & Mitchell R (1971). Mechanism of initial events in the sorption of marine bacteria to surfaces. J Gen Microbiol 68: 337-348
- <sup>8</sup> Marshall KC (1992). Biofilms: an overview of bacterial adhesion, activity, and control at surfaces. ASM News 58: 202-207
- <sup>9</sup> Krekeler C, Ziehr H & Klein J (1989). Physical methods for characterisation of microbial cell surfaces. Experientia 45: 1047-1055
- <sup>10</sup> Nir S (1976). Van der Waals interactions between surfaces of biological interest. Progr Surf Sci 8: 1-58
- <sup>11</sup> Morra M & Cassilini C (1997). Bacterial adhesion to polymer surfaces: A critical review of surface thermodynamic approaches. J Biomater Sci Polymer Edn 9: 55-74
- <sup>12</sup> Busscher HJ, Weerkamp AH, van der Mei HC, van Pelt AWJ, de Jong HP & Arends J (1984). Measurement of the surface free energy of bacterial cell surfaces and its relevance for adhesion. Appl Environ Microbiol 48: 980-983
- <sup>13</sup> Mozes N, Marchal K, Hermesse MP, van Haecht JL, Reuliaux L, Leonard AJ & Rouxhet PG (1987). Immobilization of microorganisms by adhesion: interplay of electrostatic and non-electrostatic interactions. Biotech Bioeng 29: 439-450
- <sup>14</sup> Jucker BA, Zehnder AJB & Harms H (1998). Quantification of polymer interactions in bacterial adhesion. Environ Sci Technol 32: 2909-2915
- <sup>15</sup> An YH & Friedman RJ (1998). Concise review of mechanisms of bacterial adhesion to biomaterial surfaces. J Biomed Mater Res 43: 338-348
- <sup>16</sup> Fletcher M & Floodgate GD (1973). An electron-microscopic demonstration of an acidic polysaccharide involved in the adhesion of a marine bacterium to solid surfaces. J Gen Microbiol 74: 325-334
- <sup>17</sup> Speranza G, Gottardi G, Pederzoli C, Lunelli L, Canteri R, Pasquardini I, Carli E, Lui A, Mngiglio D, Brugnara M & Anderle M (2004). Role of chemical interactions in bacterial adhesion to polymer surfaces.

- 18 Balazs DJ, Triandafillu K, Chevolut Y, Aronsson B-O, Harms H, Descouts P & Mathieu HJ (2003). Surface modification of PVC endotracheal tubes by oxygen glow discharge to reduce bacterial adhesion. *Surf Interf Anal* 35: 301-309
- 19 Gottenbos B, van der Mei HC & Busscher HJ (2000). Initial adhesion and surface growth of *Staphylococcus epidermidis* and *Pseudomonas aeruginosa* on biomedical polymers. *J Biomed Mater Res* 50: 208-214
- 20 Scheuerman TR, Camper AK & Hamilton MA (1998). Effects of substratum topography on bacterial adhesion. *J Col Interf Sci* 208: 23-33
- 21 Bos R, van der Mei HC, Gold J & Busscher HJ (2000). Retention of bacteria on a substratum surface with micropatterned hydrophobicity. *FEMS Microbiol Lett* 189: 311-315
- 22 Medilanski E, Kaufmann K, Wick L, Wanner O & Harms H (2002). Influence of surface topography of stainless steel on bacterial adhesion. *Biofoul* 18: 193-203
- 23 Edwards KJ & Rutenberg AD (2001). Microbial response to surface microtopography: the role of metabolism in localized mineral dissolution. *Chem Geol* 180: 19-32
- 24 Mullen MD, Wolf DC, Ferris FG, Beveridge TJ, Flemming CA & Bailey GW (1989). Bacterial sorption of heavy metals. *Appl Environ Microbiol* 55: 3143-3149
- 25 Ferris FG & Beveridge TJ (1984). Binding of a paramagnetic metal cation to *Escherichia coli* K12 outer membrane vesicles. *FEMS Microbiol Lett* 24: 43-46
- 26 Ferris FG & Beveridge TJ (1986). Site specificity of metallic ion binding in *Escherichia coli* K12 lipopolysaccharide. *Can J Microbiol* 32: 52-55
- 27 Williams V & Fletcher M (1996). *Pseudomonas fluorescens* adhesion and transport through porous media are affected by lipopolysaccharide composition. *Appl Environ Microbiol* 62: 100-104
- 28 Pratt LA & Kolter R (1998). Genetic analysis of *Escherichia coli* biofilm formation: roles of flagella, motility, chemotaxis and type I pili. *Mol Microbiol* 30: 285-293
- 29 O'Toole GA & Kolter R (1998). Flagellar and twitching motility are necessary for *Pseudomonas aeruginosa* biofilm development. *Mol Microbiol* 30: 295-304
- 30 Pizarro-Cerda J & Cossart P (2006). Bacterial adhesion and entry into host cells. *Cell* 124: 715-727.
- 31 Hinsna SM, Espinosa-Urgel M, Ramos JL & O'Toole GA (2003). Transition from reversible to irreversible attachment during biofilm formation by *Pseudomonas fluorescens* requires an ABC transporter and a large secreted protein. *Mol Microbiol* 49: 905-918
- 32 Lasa I (2006). Towards the identification of the common features of bacterial biofilm development. *Int Microbiol* 9: 21-28
- 33 Yousef F & Espinosa-Urgel M (2007). *In silico* analysis of large microbial surface proteins. *Res Microbiol* 158: 545-550
- 34 Lasa I & Penades JR (2006). Bap: a family of surface proteins involved in biofilm formation. *Res Microbiol* 157: 99-107
- 35 Tsuneda S, Aikawa H, Hayashi H, Yuasa A & Hirata A (2003). Extracellular polymeric substances responsible for bacterial adhesion onto solid surface. *FEMS Microbiol Lett* 223: 287-292

- 
- 36 Fontes DE, Mills AL, Hornberger GM & Herman JS (1991). Physical and chemical factors influencing transport of microorganisms through porous media. *Appl Environ Microbiol* 57: 2473-2481
- 37 Gannon JT, Manilal VB & Alexander M (1991). Relationship between cell surface properties and transport of bacteria through soil. *Appl Environ Microbiol* 57: 190-193
- 38 Camper AK, Hayes JT, Sturman PJ, Jones WL & Cunningham AB (1993). Effects of motility and adsorption rate coefficient on transport of bacteria through saturated porous media. *Appl Environ Microbiol* 59: 3455-3462
- 39 Weiss TH, Mills AL, Hornberger GM & Herman JS (1995). Effect of bacterial cell shape on transport of bacteria in porous media. *Environ Sci Technol* 29: 1737-1740
- 40 Van Loosdrecht MC, Lyklema J, Norde W, Schraa G & Zehnder AJ (1987). Electrophoretic mobility and hydrophobicity as a measure to predict the initial steps of bacterial adhesion. *Appl Environ Microbiol* 53: 1898-1901
- 41 Schafer A, Harms H & Zehnder AJ (1998). Bacterial accumulation at the air-water interface. *Environ Sci Technol* 32: 3704-3712
- 42 Makin SA & Beveridge TJ (1996). The influence of A-band and B-band lipopolysaccharide on the surface characteristics and adhesion of *Pseudomonas aeruginosa* to surfaces. *Microbiol* 142: 299-307
- 43 Vigeant MAS, Ford RM, Wagner M & Tamm LK (2002). Reversible and irreversible adhesion of motile *Escherichia coli* cells analyzed by total internal reflection aqueous fluorescence microscopy. *Appl Environ Microbiol* 68: 2794-2801
- 44 Comesano TA & Logan BE (1998). Influence of fluid velocity and cell concentration on the transport of motile and nonmotile bacteria in porous media. *Environ Sci Technol* 32: 1699-1708
- 45 Hancock IC (1991). Microbial cell surface architecture. In: *Microbial Cell Surface Analysis: Structural and Physicochemical methods*. (Mozes N, Handley PS, Busscher HJ & Rouxhet PG Eds.). VCH Publishers. Inc., New York N.Y. pp 21-59
- 46 Urrutia MM & Beveridge TJ (1993). Mechanism of silicate binding to the bacterial cell wall in *Bacillus subtilis*. *J Bacteriol* 175: 1936-1945
- 47 Bayer ME & Sloyer JL (1990). The electrophoretic mobility of Gram negative and Gram positive bacteria: an electrokinetic analysis. *J Gen Microbiol* 136: 867-874
- 48 Poleunis C, Compere C & Bertrand P (2002). Time-of-flight secondary ion mass spectrometry: characterisation of stainless steel surfaces immersed in natural seawater. *J Microbiol Meth* 48: 195-205
- 49 Busscher HJ, Geertsema-Doornbusch GI & van der Mei HC (1997). Adhesion of silicone rubber of yeasts and bacteria isolated from voice prostheses: influence of salivary conditioning films. *J Biomed Mater Res* 34: 201-209
- 50 Bradshaw DJ, Marsh PD, Watson GK & Allison C (1997). Oral anaerobes cannot survive oxygen stress without interacting with facultative / aerobic species as a microbial community. *Lett Appl Microbiol* 25: 385-387



- 
- 51 Ostuni E, Chapman RG, Liang MN, Meluleni G, Pier G, Ingber DE & Whitesides GM (2001). Self-assembled monolayers that resist the adsorption of proteins and the adhesion of bacterial and mammalian cells. *Langmuir* 17: 6336-6343
- 52 Minagi S, Miyake Y, Inagaki K, Tsuru H & Suginaka H (1985). Hydrophobic interaction in *Candida albicans* and *Candida tropicalis* adherence to various denture base resin materials. *Infect Immun* 47: 11-14
- 53 Miyake Y, Fujita Y, Minagi S & Suginaka H (1986). Surface hydrophobicity and adherence of *Candida* to acrylic surfaces. *Microbios* 46: 7-14
- 54 Abbott A, Rutter PR & Berkeley RCW (1983). The influence of ionic strength, pH and a protein layer on the interaction between *Streptococcus mutans* and glass surfaces. *J Gen Microbiol* 129: 439-445
- 55 Bermudez J & Wagensberg J (1985). Microcolimetric and thermodynamic studies of the effect of temperature on the anaerobic growth of *Serratia marcescens* in a minimal glucose-limited medium. *J Therm Anal* 30: 1397-1402
- 56 Tittsler RP & Sandholzer LA (1936). The use of semi-solid agar for the detection of bacterial motility. *J Bacteriol* 31: 575-580
- 57 Bartholomew JW & Mittwer T (1952). The Gram stain. *Bacteriol Rev* 16: 1-29
- 58 Williams RP & Hearn WR (1967). Prodigiosin. In: *Antibiotics* (Gottlieb D & Shaw PD Eds.), vol. 2. p. 410-449 Springer-Verlag, Berlin
- 59 Fuller ME, Dong H, Mailloux BJ, Onstott TC & DeFlaun MF (2000). Examining bacterial transport in intact cores from Oyster, Virginia: Effect of sedimentary facies type on bacterial breakthrough and retention. *Water Resour Res* 36: 2417-2431
- 60 Zita A & Hermansson M (1997). Determination of bacterial cell surface hydrophobicity of single cells in cultures and in wastewater *in situ*. *FEMS Microbiol Lett* 152: 299-306
- 61 Rosenberg M, Gutnick D & Rosenberg E (1980). Adherence of bacteria to hydrocarbons: A simple method for measuring cell-surface hydrophobicity. *FEMS Microbiol Lett* 9: 29-33
- 62 Hermansson M, Kjelleger S, Korhonen TK & Stenstrom TA (1982). Hydrophobic and electrostatic characterization of surface structures of bacteria and its relationship to adhesion to an air-water interface. *Arch Microbiol* 131: 308-312
- 63 Ocana VS, Bru E, De Ruiz Holgado AAP & Nader-Macias ME (1999). Surface characteristics on lactobacilli isolated from human vagina. *J Gen Appl Microbiol* 45: 203-212
- 64 Hitchcock PJ & Brown TM (1983). Morphological heterogeneity among *Salmonella* lipopolysaccharide chemotypes in silver-stained polyacrylamide gels. *J Bacteriol* 154: 269-277
- 65 Laemmli UK (1970). Most commonly used discontinuous buffer systems for SDS electrophoresis. *Nature* 227: 680-688
- 66 Rabilloud T (1990). Mechanisms of protein silver staining in polyacrylamide gels: A 10-year synthesis. *Electrophoresis* 11: 785-794
- 67 Smith PK, Krohn RI, Hermanson GT, Mallia AK, Gartner FH, Provenzano MD, Fujimoto EK, Goetze NM, Olson BJ & Klenk DC (1985). Measurement of protein using bicinchoninic acid. *Anal Biochem* 150: 76-85
- 68 DuBois M, Gilles KA, Hamilton JK, Rebers PA & Smith F (1956). Colorimetric method for determination

- 
- of sugars and related substances. Anal Chem 28: 350-356
- 69 Van Schie PM & Fletcher M (1999). Adhesion of biodegradative anaerobic bacteria to solid surfaces. Appl Environ Microbiol 65: 5082-5088
- 70 Bar-Ness R, Avrahamy N, Matsuyama T & Rosenberg M (1988). Increased cell surface hydrophobicity of a *Serratia marcescens* NS 38 mutant lacking wetting activity. J Bact 70: 4361-4364
- 71 Hermansson M, Kjelleberg S & Norkrans B (1979). Interaction of pigmented wild type and pigmentless mutant of *Serratia marcescens* with lipid surface film. FEMS Microbiol Lett 6: 129-133
- 72 Sorongdon ML, Bloodgood RA & Burchard RP (1991). Hydrophobicity, adhesion and surface-exposed proteins of gliding bacteria. Appl Environ Microbiol 57: 3193-3199
- 73 Bellon-Fontaine MN, Rault J & Van Oss CJ (1996). Microbial adhesion to solvents: a novel method to determine the electron-donor / electron-acceptor of Lewis acid-base properties of microbial-cells. Colloids Surf 7: 47-53
- 74 Bar-Ness R & Rosenberg M (1989). Putative role of a 70kDa outer-surface protein in promoting cell-surface hydrophobicity of *Serratia marcescens* RZ. J Gen Microbiol 135: 2277-2281
- 75 Matsuyama T, Fujita M & Yano I (1985). Wetting agent produced by *Serratia marcescens*. FEMS Microbiol Lett 28: 25-129
- 76 Rumelt S, Metzger Z, Kariv N & Rosenberg M (1988). Clearance of *Serratia marcescens* from blood in mice: role of hydrophobic *versus* mannose-sensitive interactions. Inf & Imm 56: 1167-1170
- 77 Thauer RK, Jungermann K & Decker K (1977). Energy conservation in chemotrophic anaerobic bacteria. Bacteriol Rev 41: 100-180

## **Chapter 4**

### ***In situ* reduction of arsenate by *S. marcescens* SA Ant 16**

## **4.1 Literature review: Arsenic remediation technologies**

Considering the lethal impact of arsenic on human health, environmental authorities have taken a more stringent attitude towards the presence of arsenic in water and in 1993 the World Health Organisation adopted a provisional guideline of 10ppb (0.01mg/L)<sup>1</sup>. Arsenic remediation technologies have historically focused heavily on a variety of chemical processes, but more recently biological methods have been gaining momentum because of their potential in providing an alternate cost-effective technology for heavy metal remediation. The main advantage of biological treatment is that these processes do not require the use of harsh chemicals, but as the name implies, uses biological agents such as plants or microorganisms to remove or transform groundwater contaminants. These technologies can either be the sole treatment technique, or can easily be combined with other conventional physicochemical processes.

### **4.1.1 Chemical techniques for arsenic remediation**

Conventional as well as advanced techniques have been applied for the removal of arsenic from contaminated water that may be divided into four broad categories: precipitative processes, adsorption processes, ion exchange processes, and separation (membrane) processes.

#### **4.1.1.1 Precipitative processes**

Coagulation / filtration is a treatment process by which the physical or chemical properties of dissolved colloidal or suspended matter are altered such that agglomeration is enhanced to an extent that the resulting particles will settle out of solution by gravity or will be removed by filtration<sup>2</sup>. Coagulants change surface charge properties of solids to allow agglomeration and / or enmeshment of particles into a flocculated precipitate<sup>3</sup>. In either case, the final products are larger particles, or flocs, which more readily filter or settle under the influence of gravity. The coagulation / filtration process has traditionally been used to remove solids from drinking water supplies<sup>4</sup>. However, the process is not restricted to the removal of particles. Coagulants render some dissolved species (such as natural organic matter, inorganics and hydrophobic synthetic organic compounds) insoluble and the metal hydroxide particles produced by the addition of metal salt coagulants (typically aluminum sulfate<sup>5</sup>, ferric salts<sup>6</sup>, or copper sulfate<sup>7</sup>) can adsorb

other dissolved species. As(III) removal during coagulation with alum, ferric chloride, and ferric sulfate has been shown to be less efficient than As(V) under comparable conditions<sup>8</sup>. Coagulation is a successful technology for achieving As(V) removals greater than 90%<sup>9</sup>. In general, enhanced arsenic removal efficiencies are achieved with increased coagulant dosages<sup>10</sup>.

Iron / manganese oxidation is dominant in facilities treating groundwater. Oxidation to remove iron and manganese leads to formation of hydroxides that remove soluble arsenic by precipitation or adsorption reactions<sup>11</sup>. Removal of 2mg/L of iron (by oxidation) achieved a 92.5% removal by adsorption of As(V) from a 10µg/L (0.13µM) As(V) solution. With removal of 1mg/L of iron, 83% absorption of As(V) in a 22µg/L (290µM) influent concentration was achieved. However, removal of arsenic during manganese precipitation is relatively ineffective when compared to iron even when removal by both adsorption and coprecipitation are considered. For instance, precipitation of 3mg/L manganese removed only 69% of a 12.5µg/L (160µM) As(V) influent concentration<sup>12</sup>.

Microfiltration can be used in tandem with the coagulation process to remove smaller particles and arsenic is effectively removed. Thus, total plant capacity is increased by reducing the amounts of coagulants required<sup>13</sup>.

Lime softening removes hardness (predominantly caused by calcium and magnesium compounds in solution) by creating a shift in the carbonate equilibrium and thereby raising the pH. Bicarbonate is converted to carbonate as the pH increases, and as a result, calcium is precipitated as calcium carbonate. For magnesium removal, excess lime is added beyond the point of calcium carbonate precipitation. Arsenic in the pentavalent state is more readily removed than arsenite<sup>14</sup>. Softening is a successful technology for achieving greater than 90% As(V) removals. The optimum pH for As(V) removal by softening is approximately 10.5 and the optimum pH of As(III) is approximately 11.0. Recent studies have shown that As(V) removal is independent of initial concentration whereas this seems to be the predominant factor in As(III) removal. Facilities precipitating only calcium carbonate observed lower As(V) removals when compared to facilities precipitating calcium carbonate, and magnesium and ferric hydroxide. Addition of iron improves As(V) removal. An important consideration in a lime softening system is the large quantities of sludge are produced and the associated disposal costs<sup>15</sup>.

#### **4.1.1.2 Adsorptive processes**

Activated alumina is used in packed beds to remove arsenic and other contaminants from continuously passed feed water. This is considered an adsorption process, although the chemical reactions involved are actually an exchange of ions<sup>16</sup>. This is a physical / chemical process by which ions in the feed water are adsorbed to the oxidized activated alumina surface. The contaminant ions are exchanged with surface hydroxides on the alumina until adsorption sites on the surface are saturated. At this point the bed is regenerated through a sequence of rinsing with regenerant (typically a strong base such as sodium hydroxide), flushing with water, and neutralizing with acid (usually sulfuric acid)<sup>17</sup>. Factors such as pH, arsenic oxidation state, competing ions, empty bed contact time, and regeneration have significant effects on arsenic removal efficiency<sup>18</sup>.

Another method uses iron oxide coated sand treatment that consists of sand grains coated with ferric hydroxide. These sands are used in fixed bed reactors to remove various dissolved metal species<sup>19</sup>. The metal ions are exchanged with the surface hydroxides on the treated sand surface. When the bed is exhausted it must be regenerated by a sequence of operations similar to activated alumina. Like activated alumina treatment, factors such as pH, arsenic oxidation state, competing ions, empty bed contact time and regeneration have significant effects on the removals achieved with iron oxide coated sand<sup>20</sup>.

#### **4.1.1.3 Ion exchange**

Ion exchange is a physical / chemical process by which an ion on the solid phase is exchanged for an ion in the feed water. This solid phase is typically a synthetic resin which has been chosen to preferentially adsorb the particular contaminant of concern<sup>21</sup>. To accomplish this exchange of ions, feed water is continuously passed through a bed of ion exchange resin beads until all sites on the resin beads have been filled by contaminant ions. At this point, the bed is regenerated by rinsing the ion exchange column with a regenerant. Important considerations in the applicability of the ion exchange process for removal of a contaminant include water quality parameters such as pH, competing ions, resin type, alkalinity, and influent arsenic concentration<sup>22</sup>.

#### **4.1.1.4 Membrane processes**

Membranes are a selective barrier, allowing some constituents to pass and blocking the passage of others. The movement of constituents across a membrane requires a potential difference between sides of the membrane and therefore membrane processes are often classified by the type of driving force, such as pressure or electrical potential<sup>23</sup>. Pressure-driven membrane processes are often classified by pore size into four categories: microfiltration ( $>0.01\mu\text{m}$ ), ultrafiltration ( $>0.001\mu\text{m}$ ), nanofiltration ( $0.001\mu\text{m} - 0.01\mu\text{m}$ ), and reverse osmosis ( $< 0.01\mu\text{m}$ )<sup>24</sup>. Membrane processes can remove arsenic through filtration, electric repulsion, and adsorption of arsenic-bearing compounds<sup>25</sup>. If particulate arsenic compounds are larger than a given membrane pore size, they will be rejected due to size exclusion. Size, however, is only one factor which influences rejection. Studies have shown that some membranes can filter arsenic compounds which are one to two orders of magnitude smaller than the membrane pore size, indicating removal mechanisms other than just physical straining. Shape and chemical characteristics of arsenic compounds play important roles in arsenic rejection. Membranes may also remove arsenic compounds through repulsion by or adsorption on the membrane surface. The filtration mechanisms also depend on the chemical characteristics, particularly charge and hydrophobicity, of both the membrane material and the feed water constituents.

#### **4.1.1.5 Alternative technologies**

Combinations of some of the principles discussed above have been used to effectively remove arsenic from contaminated water such as coagulation followed by microfiltration. These processes include greensand, a zeolite-type glauconite mineral which is produced by treating glauconite sand with  $\text{KMnO}_4$  until the granular material (sand) is coated with a layer of manganese oxides, particularly manganese dioxide<sup>26</sup>. The principle behind this arsenic removal treatment is multi-faceted and includes oxidation, ion exchange, and adsorption. Another technique, granular ferric hydroxide<sup>27</sup>, combines the advantages of the coagulation-filtration process, efficiency and small residual mass, with the fixed bed adsorption on activated alumina, and simple processing<sup>28</sup>. Iron filings combined with sand is essentially a filter technology, much like greensand filtration, wherein the source water is filtered through a bed of sand and iron

filings. What distinguishes this from other similar technologies discussed above, is sulfate that is introduced in this process to encourage arsenopyrite precipitation.

#### **4.1.2 Biological methods**

Several biological strategies exist for the treatment of contaminated groundwater, which can be divided in two main categories: *ex situ* technologies, such as pump-and-treat systems, and *in situ* technologies, where there is no need for the removal of contaminated water, but treatment is applied at the contaminated site. In conventional pump-and-treat systems the contaminated groundwater is extracted from the polluted aquifer by pumping, treated above ground and, finally, discharged or reinjected into the source aquifer. On the contrary, innovative *in situ* technologies permit physical, chemical, or biological treatment of contaminated groundwaters by means of injection of reactive materials into contaminated aquifers<sup>29</sup>.

Biological treatment strategies may also be divided into passive processes, such as biosorption, or active remediation through enhanced uptake, sequestration or redox transformations. Bioremediating agents can either be plant-based (phytoremediation) or microbial, both of which may have superior native properties or can be genetically modified for application in arsenic remediation.

##### **4.1.2.1 Passive biosorbents**

The removal mechanism of biosorbents is similar to that of adsorption techniques and the biomass / biosorbent is susceptible to chemical and engineering improvements and regeneration. It has recently been observed that the capability of fungal biomass for treating metal contaminated effluents is better than activated carbon (F-400) or the industrial resin Dowex-50<sup>30</sup>.

Shaban and coworkers<sup>31</sup> demonstrated that powdered air dried roots of the water hyacinth (*Eichornia crassipes*) rapidly reduce arsenic concentrations in water. More than 93% of arsenite and 95% of arsenate was removed from a solution containing 200µg/L (2.6µM) arsenic within 1 hour of exposure to the powder. The residual arsenic concentration was less than the World Health Organisation drinking water guideline value of 10µg/L.



In another study, the fungus, *Penicillium purpurogenum*, was examined for cadmium, lead, mercury, and arsenic ion removal from water. Heavy metal loading capacity increased with increasing pH under acidic conditions, presumably as a function of heavy metal speciation versus the H<sup>+</sup> competition at the same binding sites. The adsorption of heavy metal ions reached a plateau at pH 5.0. The fungus adsorption capacity for As(III) was 35.6mg/g and the metal ions were eluted with 0.5M HCl to rejuvenate the fungal biosorbent. This process was successfully repeated through 10 adsorption cycles. The pretreatment of biomass of *P. chrysogenum* with common surfactants (such as hexadecyl-tri-methyl ammonium bromide and do-decyl amine) and a cationic-polyelectrolyte was found to improve the biosorption efficiency to between 33% and 56% for various treatments. Moreover, this biosorptive process was shown to reduce capital cost by 20%, operational cost by 36% and total treatment cost by 28% when compared with conventional processes<sup>32</sup>. Another example of pretreatment was the use of autoclaved tea fungus, a waste produced during black tea fermentation. The tea fungus was evaluated with and without FeCl<sub>3</sub> pretreatment for arsenic sequestration. The FeCl<sub>3</sub>-pretreated fungal mats removed 100% of As(III) after a 30 minute contact time and 77% of As(V) was removed after 90 minutes contact time. Fungal mat biomass without FeCl<sub>3</sub> was not effective for arsenic removal<sup>33</sup>.

For metal uptake *Chlorella* sp. and *Scenedesmus* sp<sup>34</sup>. are the two most commonly used algal species. It has been demonstrated that *Chlorella* sp. retained approximately 50% of arsenite from a solution<sup>35</sup>, while *Scenedesmus abudans* can retain up to 70% arsenite from a 0.1mg/L (1.3μM) solution. Algae respond to heavy metals by the synthesis of low molecular weight compounds such as carotenoids and glutathione, and the initiation of several antioxidants, as well as enzymes including superoxide dismutase, catalase, glutathione peroxidase and ascorbate peroxidase<sup>36</sup>. *Lessonia nigrescens*, another algae, was utilized for arsenate removal with maximum adsorption capacities of 45.2mg/g (pH 2.5); 33.3mg/g (pH 4.5); and 28.2mg/g (pH 6.5) from an As(V) solution ranging of 50mg/L (0.65mM) - 600mg/L (7.8mM)<sup>37</sup>.

Bacteria have been genetically modified to express metal binding peptides such as synthetic phytochelatin<sup>38, 39</sup>. Expression of phytochelatin synthase in *Escherichia coli* resulted in production of phytochelatin and concurrent enhanced arsenate accumulation, but this strategy lacked selectivity, as the engineered cells also demonstrated enhanced binding to Cd(II), Zn(II), Pb(II) and Cu(II)<sup>40</sup>. Kostal *et al.* (2004)<sup>41</sup> exploited the physiological role of ArsR as an arsenite

inducible derepressor of the *ars*-operon by overexpressing this protein in *E. coli*. They demonstrated specific, targeted accumulation and removal efficiencies of arsenite of 98%.

#### 4.1.2.2 Phytoremediation

Phytoremediation utilises the potential of certain plant species to accumulate high concentrations of arsenic in their above-ground tissues. Phytoremediation is an emerging technology generally applicable only to shallow soil contamination that can be reached by plant roots and selection of the phytoremediating species, therefore, depends upon the species ability to treat the contaminants and the depth of contamination<sup>42</sup>. Plants that are currently used as phytoremediating agents to remove arsenic include poplar, cottonwood<sup>43</sup>, sunflower, Indian mustard, maize<sup>44</sup>, grasses such as ryegrass and prairie grasses<sup>45</sup> and hyper-accumulating ferns<sup>46, 47</sup>. Plants with shallow roots (such as grasses and corn) are appropriate only for contamination near the surface, typically in shallow soil. Plants with deeper roots, (for example, trees) may be capable of remediating deeper contaminants in soil or groundwater plumes. Phytoremediation is conducted *in situ* and therefore does not require soil excavation. In addition, revegetation for the purpose of phytoremediation also can enhance restoration of an ecosystem<sup>48</sup>. The mechanisms of phytoremediation include enhanced rhizosphere biodegradation, phytodegradation, phytostabilisation and phytoextraction / phytoaccumulation<sup>49</sup>. Of these technologies, extraction coupled with accumulation has been applied in the field of arsenic remediation. Phytoextraction comprises the uptake and translocation of contaminants by plant roots which can then be accumulated in plant shoots and / or leaves<sup>50</sup>. A major concern of this technology is that plant uptake and translocation of metals to the aboveground portions of the plant may introduce these contaminants into the food chain and bioaccumulate in animals if the plants are ingested<sup>51</sup>.

The potential of using recently identified arsenic hyperaccumulating ferns to remove arsenic from drinking water have been investigated<sup>52</sup>. Hydroponically cultivated arsenic-hyperaccumulating fern species (*Pteris vittata* and *Pteris cretica* cv. Mayii) were suspended in water containing <sup>73</sup>As arsenic with initial arsenic concentrations ranging from 20µg/L (0.26µM) to 500µg/L (6.5µM)<sup>53</sup> and arsenic phytofiltration efficiency was determined by monitoring the depletion of <sup>73</sup>As arsenic. *P. vittata* reduced the 20µg/L (0.26µM) arsenic solution to 7.2µg/L (0.09µM) in 6 hours and to 0.4 µg/L (0.005µM) in 24 hours, while in 24 hours the 200µg/L

(2.6 $\mu$ M) arsenic solution was reduced by 98.6% to 2.8 $\mu$ g/L. The high efficiency of arsenic phytofiltration by arsenic-hyperaccumulating fern species is associated with their ability to rapidly translocate absorbed arsenic from roots to shoots. Webb *et al.* (2003)<sup>54</sup> showed that *P. vittata* accumulated As(III) predominantly in the leaves to high arsenic concentrations (1% w/w dry biomass). Concentrations of contaminants in hyperaccumulating plants are limited to a maximum of approximately 3% of the plant weight on a dry weight basis: Based on this limitation, for fast-growing plants, the maximum annual contaminant removal is approximately 400kg/hectare/year. However, many hyperaccumulating species do not achieve contaminant concentrations of 3%, and are slow growing<sup>55</sup>.

Genetically modified *Arabidopsis* plants expressing the bacterial *arsC* gene encoding arsenic reductase and  $\gamma$ -glutamylcysteine synthetase have been constructed<sup>56</sup>. Arsenate is taken up by the root system and translocated to the aboveground tissues of the plants. The cloned bacterial genes are under a light-induced promoter and can therefore convert arsenate to arsenite in the leaves, while  $\gamma$ -glutamylcysteine acts as a thiol sink for arsenite. Due to this genetic alteration, these plants can transport and trap three times more arsenic in their leaves and are resistant to several times more arsenic in the medium than wild-type plants.

#### 4.1.2.3 Bioremediation with microorganisms

Although biological treatments have usually been applied to the degradation of organic contaminants, some innovative techniques have applied biological remediation to the treatment of arsenic contamination. Currently, two processes for arsenic remediation with bacteria have been developed, but neither of these explicitly requires the biological transformation of arsenic directly:

The first water treatment process depends upon oxidation of Fe(II) and Mn(II) with the precipitation of the iron oxides (FeO<sub>2</sub>H)<sup>57</sup> and MnO<sub>2</sub><sup>58</sup> by the bacteria *Gallionella ferrunginea* and *Leptothrix ochracea*. The precipitates are deposited within a filter matrix, which provides a large surface area over which arsenic containing water can contact the oxides. The aqueous solution is passed through the filter, where arsenic is removed from solution through coprecipitation or adsorption<sup>59</sup>. Arsenic removal rates were enhanced from 65% to 95% by bacterial oxidation which reduced a 200 $\mu$ g/L (2.6 $\mu$ M) solution to below 10 $\mu$ g/L (0.13 $\mu$ M)<sup>60</sup>. One

advantage of this technology is that it removes three important water contaminants simultaneously – iron, manganese and arsenic. An equivalent chemical method of arsenic treatment involves coating zeolite with Fe and Mn where arsenic is adsorbed or coprecipitated. This method has been registered under patent number 6790363 as “Method of treating arsenic-contaminated waters”.

The second technology utilises sulfate reducing bacteria to biogenically generate  $H_2S$  by reducing organic compounds such as lactate and utilising sulfate as the terminal electron acceptor. This biogenically produced sulfide can react with dissolved metals and metalloids to form metal sulfide precipitates since the solubilities of most toxic metal sulfides are generally very low ( $\log K_{sp}$  for  $As_2S_3$  is  $-11.9$ <sup>61</sup>). One application of this technology uses anaerobic sulfate-reducing bacteria to produce hydrogen sulfide, as well as arsenic-reducing bacteria (to convert arsenate to arsenite) to precipitate arsenic from solution as insoluble arsenic-sulfide complexes<sup>62</sup> such as orpiment ( $As_2S_3$ ), realgar ( $AsS$ ) or other sulfide minerals containing coprecipitated arsenic species<sup>63</sup>. A major advantage of this precipitation method is that the volume of metal sulfide produced is generally lower than compared to hydroxide sludge produced by traditional chemical methods<sup>64</sup>. A few studies, and upscaled field tests have been conducted with exceptional success. As early as 1993, Belin *et al.*<sup>65</sup> demonstrated 97% removal of arsenic ( $910\mu M$  starting concentration) by sulfidogenically active bacteria. After 6 days of incubation, 96% of the initial  $10\text{mg/L}$  (approximately  $130\mu M$ ) arsenic was removed from solution in serum bottles containing sulfate reducing biomass<sup>66</sup>. These results lead to a study using short-term bench scale upflow anaerobic packed bed reactors where 77% removal from a  $50\text{mg/L}$  ( $666\mu M$ ) solution arsenic was achieved due to precipitation as  $As_2S_3$  as well as the concomitant coprecipitation with iron oxides<sup>67</sup>. The most resounding success applying biogenically generated sulfide precipitation of arsenic has undoubtedly been the Wood Cadillac mine site in northwestern Quebec. An ingenious biofilter,  $50\text{m} \times 57\text{m}$  by  $1\text{m}$  thick, was constructed from decomposing yellow birch bark chips which provide the reducing conditions necessary for sulfate reducing bacterial activity<sup>68</sup>. Over a three year period, even during winter, up to 93% arsenite removal from  $585\mu\text{g/L}$  ( $7.6\mu M$ ) to less than  $40\mu\text{g/L}$  ( $0.52\mu M$ ) was achieved<sup>69</sup>. Again, a chemical analog for precipitating arsenic with sulfides has been registered as Patent number 51509.

Due to the nature of biological processes, the performance of the above technologies is dependent on pH, available nutrients and temperature. Its efficiency is also sensitive to arsenic concentrations. These requirements, however, are not limited to biological systems, most

chemical processes are highly dependent on pH, co-contaminants, influent arsenic concentrations and the valence state of arsenic. Popular literature suggests that if bacteria isolated from a contaminated site are applied to the same site for bioremediation, much higher contaminant concentrations can be tolerated and that more efficient conversion is achieved. What distinguishes biological processes from chemical, besides being environmentally friendly, is that if a suitable remediating microorganism is identified bioremediation has the potential for application at much higher contaminant concentrations than chemical remediation strategies.

Despite the wide variety of arsenic tolerant and resistant bacteria that have been isolated and described, application of these microorganisms under field conditions for bioremediation is lacking. In a US EPA report of 2002<sup>44</sup>, only one full scale, three pilot scale and one bench scale wastewater treatment processes were identified. If this is compared to the 45 full scale projects utilising chemical precipitation / co-precipitation, it becomes very apparent that bioremediation of arsenic is indeed a novel and exciting prospect.

Bioremediation has the potential to be incorporated into a variety of existing chemical processes, where a simple bacterial oxidation or reduction step may easily be incorporated as a pretreatment for a variety of existing chemical processes such as adsorption or filtration. It also has the possibility of being developed as an integrated stand-alone technology where no harsh chemicals are used, resulting in low sludge volumes and providing a cost effective, environmentally friendly alternative to existing technologies.

## **4.2 Aims**

1. Determining arsenate and glucose concentrations for arsenate reduction
  - aerobically and anaerobically
  
2. Adhesion of *S. marcescens* SA Ant 16 to sand grains
  - establishing contact time between cells and sand for maximal adhesion
  - monitoring bacterial movement through a sand column
  - determining bacterial loading of a sand reactor
  
3. Demonstrating *in situ* reduction of arsenate by *S. marcescens* SA Ant 16

## **4.3 Materials and methods**

### **4.3.1 Optimisation of arsenate reducing conditions**

*S. marcescens* SA Ant 16 was grown, washed as previously described (section 2.6.1) and resuspended in Artificial Ground Water (AGW)<sup>70</sup> to  $10^8$  cells/mL. Glucose was added to 100mL cell suspension in 500mL shake flasks at concentrations of 0.1mM, 1mM and 10mM. Arsenate was added to 1mM, 5mM or 10mM as shown in Figure 4.1. Flasks were incubated at room temperature (approximately 20°C, since this temperature more likely represents a bioremediation scenario) with shaking at 200rpm on a rotary shaker. From results obtained, a second experiment, with the same parameters but under anaerobic conditions, was performed in serum vials with 5mM As(V) and glucose concentrations at 0.1mM, 1mM and 10mM respectively (represented by shaded areas in Figure 4.1).

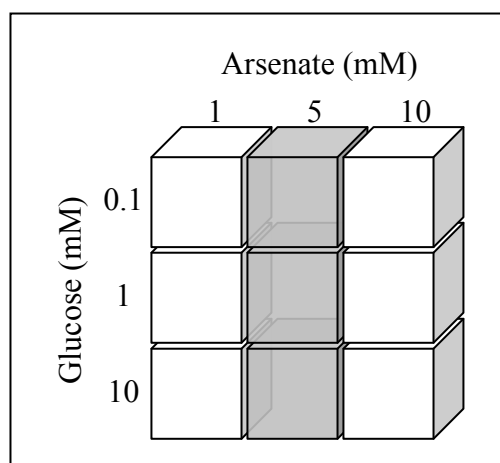


**Figure 4.1** Factorial design layout.

In both experiments samples were withdrawn periodically over a 100h period, clarified through a 0.2µm filter and stored at -20°C until analysis. Arsenite was quantified using an ICP-MS (Shimadzu ICPM-8500) after separation of the arsenic species by HPLC on a Hamilton PRP X-100 anion exchange column with isocratic elution using 20mM ammonium carbonate, 3% methanol (v/v) at pH 10. Glucose was quantified using the QuantiChrom™ Glucose Assay Kit (BioAssay Systems) and throughout the experiment both optical density at 560nm and pH (as indicators of growth) were monitored. Lactic acid was detected by HPLC by comparing retention

times with that of standards using a Phenomenex Synergi 4 $\mu$ m Hydro-RP82A 250mm x 62mm column with KH<sub>2</sub>PO<sub>4</sub>, pH 3.5 as mobile phase at 50°C and a Shimadzu UV detector (SPD-20AV) at 215nm. Arsenate conversion was calculated as

$$\% \text{ Conversion} = [As(V)_{\text{initial}} - As(III)_{\text{supernatant}}] / As(V)_{\text{initial}} * 100$$

to negate the effect of alternate mechanisms such as biosorption which could lead to a possible over-estimation of arsenate reduction rates.

### **4.3.2 Adhesion of cells to sand matrix**

Adhesion of the cells was determined according to the method of Bolster *et al.* 1998<sup>71</sup>. Six sets of 20mL plastic syringes were packed up to the 20mL mark with sterile quartz sand obtained from BHP Billiton (hydrophilic, negatively charged, grain size between 1180 $\mu$ m and 1700 $\mu$ m, confirmed at the Department of Geology, UFS) and saturated with Artificial Ground Water (AGW)<sup>70</sup>. *S. marcescens* SA Ant 16 was grown aerobically in TYG medium, harvested, washed and resuspended to 10<sup>6</sup> cells/mL, 10<sup>7</sup> cells/mL and 10<sup>8</sup> cells/mL in AGW. The columns were loaded with 6mL of the cell suspension and incubated at room temperature. Duplicate columns were sacrificed after 6 hours of incubation at room temperature by draining non-adhering cells from the column. To ensure optimal adhesion, contact time between the cells and sand grains was determined in a similar fashion, except that columns were incubated and sacrificed over a 24 hour period.

### **4.3.3 Real-Time PCR for quantification**

*S. marcescens* SA Ant 16 cells were enumerated by Real-Time PCR on a Rotor-Gene RG-3000A Cycler (Cobett Research. Primers set SerRT-F (5'-GGAGGAAGGTGGTGAGCTTAA TACG-3') and SerRT-R (5'-CGATTGCACAACCTCCCAAATCG-3') were designed to exclusively amplify a fragment of the 16S rDNA gene of *Serratia marcescens* and correspond to positions 439-463 and 818-835 of the 16S rDNA sequence deposited for *S. marcescens* SA Ant 16 AY551938. Cycling was performed after an initial denaturing step at 95°C for 10 minutes and thereafter cycling with primer annealing at 56°C for 5 seconds, strand elongation at 72°C for 20



seconds and denaturing at 95°C for 1 second. Reactions consisted of 1X Sensimix (Quantace), 200nM of each primer, 1X SYBR®Green I Solution and 4.4µL template DNA in a total volume of 10µL. Specificity of this primer set was verified by performing BLAST<sup>72</sup> searches as well as including template DNA from *E. coli* and *Bacillus pumilus*, as control organisms representing both Gram negative and Gram positive bacteria.

#### **4.3.4 Setup, conservative tracer and bacterial breakthrough**

Perspex columns (250mm height x 70mm inner diameter) (Figure 4.2a) were packed with sterile sand. Each column had 4 inlet ports at the bottom (Figure 4.2b), 2 outlet ports at the top (c) and side ports at 5cm intervals for sampling liquid along the length of the column (d 1&2). A fine mesh consisting of material net was placed at the bottom to prevent sand flowing into or blocking the inlet tubes. A 1cm layer of glass beads (2mm diameter) was placed on the bottom of each column to ensure equal dispersion of influent (Figure 4.2e). The columns were packed to approximately 2cm from the top with sand and another layer of glass beads added before the addition of fine mesh. Columns were washed with artificial ground water for 24 hours at 1mL/min<sup>73</sup> to saturate, stabilise and condition the sand bed before the commencement of an experiment. A conservative tracer breakthrough curve was constructed by pumping 40mL 5mM NaCl in AGW into each column and measuring conductivity at the outlet ports. A bacterial breakthrough curve was constructed in the same way, with cell breakthrough determined by optical density at 560nm<sup>70</sup>.

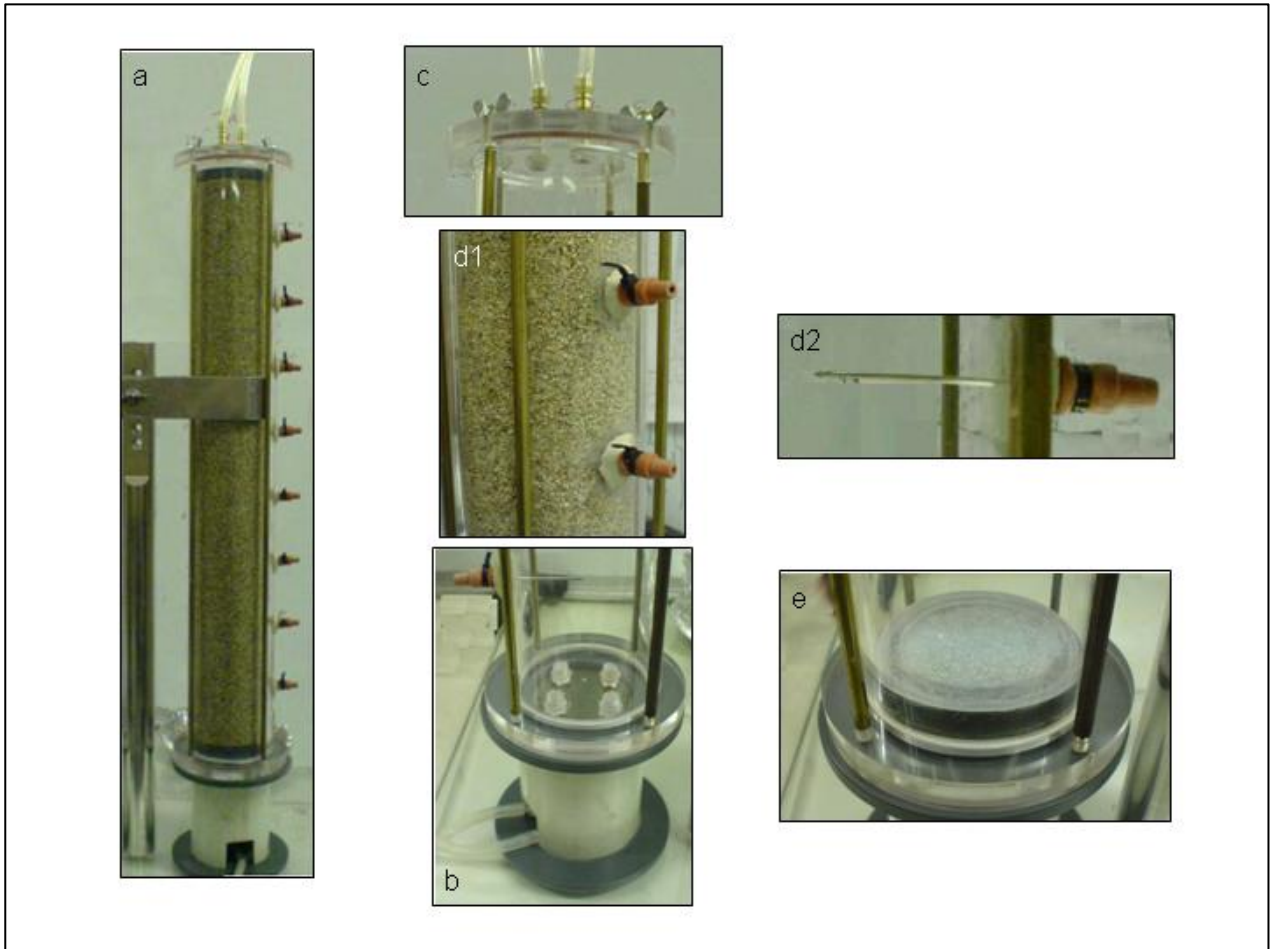


**Figure 4.2** Setup of column reactors. (a) 500mm reactor, (b) bottom inlet ports, (c) top outlet ports, (d) side ports for sampling, (e) glass beads for equal dispersion of influent.

### **4.3.5 Column loading**

The volume of cells to load binding sites on sand grains was determined by replacing AGW in the columns with *S. marcescens* SA Ant 16 cells ( $10^8$  cells/mL) by continuous flow. Cell numbers were tracked through the column by sampling at the side ports over a period of 44 hours (representing 8 pore volumes) and quantified by Real-Time PCR. Viability of the cells was assessed by plating aliquots onto TYG plates and incubating at 37°C overnight.

### **4.3.6 In situ As(V) reduction**

Upscaled bioreactor columns (overall height of 500mm, internal diameter of 70mm) were used for *in situ* arsenate reduction. Setup, tracer and bacterial breakthrough was performed as described in section 4.3.5.

Reactors were flushed with AGW overnight and one pore volume (PV) of washed *S. marcescens* SA Ant 16 cells ( $10^8$  cells/mL) were pumped into the reactor followed by 1PV of TYG medium amended with 0.1g/L KNO<sub>3</sub> (as determined in Chapter 3) to foster cell growth at approximately 0.7mL/min which represents approximately 1 pore volume per day (determined from earlier results). After multiplication of the cells inside the column the influent was switched to 5mM arsenate and either 3mM or 6mM glucose, and introduced into the reactor at room temperature by means of a precalibrated variable speed dialysis pump. Samples were withdrawn for each pore volume at the inlet, outlet and side ports. Arsenic speciation, glucose, lactic acid and cell viability determined as previously. Dissolved oxygen was measured with an O<sub>2</sub> Amplifier Type 170 % air and the influent was used as the 100% calibration point. Arsenate conversion was calculated as described in section 4.3.1.

### **4.3.7 Scanning electron microscopy**

Sand grains from dismantled columns were fixed in 3% gluteraldehyde and 1% osmium tetroxide, gradually dehydrated in an ethanol series ranging from 50% to 100% and dried in a critical point drier. Dried samples were sputter coated with gold and imaged with a Shimadzu SSX-550 Scanning electron microscope at the Centre for Confocal- & Electron Microscopy, UFS.

## **4.4 Results and discussion**

### **4.4.1 Factorial design for arsenate reduction optimisation**

Arsenate reduction was optimised in a factorial design layout incorporating increasing concentrations of arsenate and glucose under both aerobic and anaerobic conditions. Under aerobic conditions it was found that when glucose was added at high concentrations (10mM), this carbon source was used to generate cell biomass. With increasing concentrations of arsenate, more glucose was utilised. It is also interesting to observe that under these conditions no arsenate was reduced (no arsenite present), but that it appeared that the generated biomass could adsorb the added arsenate, since barely detectable amounts of arsenate was present in the suspending liquid during growth. Also, during growth a concomitant drop in pH was observed (Figure 4.4 g, h, i). When cells were incubated with 1mM glucose, but without arsenic, glucose was utilised to produce cell biomass, with a related decrease in pH (Figure 4.3 a, b). A similar decrease in pH over the growth period of *S. marcescens* was also observed by Eaves & Jefferies (1962)<sup>74</sup>. In the case of *S. marcescens* SA Ant 16, this decline in pH was correlated to lactic acid production (Figure 4.3 b inset). Glucose utilisation increased from 40%, to 60%, to 100% within the first 24 hours with increasing arsenate concentrations, yet no arsenate was reduced (Figure 4.5 g, h, i).

Arsenate was reduced by resting cells of *S. marcescens* SA Ant 16 under aerobic conditions at glucose concentrations lower than 10mM and at arsenate concentrations ranging from 1mM to 10mM. During arsenate reduction, no increase in biomass was observed and pH was constant after an initial small decrease (Figure 4.4 a - f). This slight decrease in pH over the first 2 hours was also observed in the negative control flask lacking any cells (Figure 4.3 c), and could be ascribed to an equilibration period of the weakly buffered AGW due to oxygenation as a result of agitation. During arsenate reduction glucose was utilised, and was generally depleted within the first 4 hours at a concentration of 0.1mM (Figure 4.5 a - c) and within the first 12 hours at 1mM glucose (Figure 4.5 d - f). From these results it could be concluded that neither 0.1mM nor 1mM glucose would not be sufficient for arsenate reduction over an extended period of time. The highest reduction rate (approximately 1 $\mu$ M/h) and highest total conversion (0.56%) was observed with 10mM arsenate and 1mM glucose (Figure 4.5 f).

Since it was expected that oxygen may be less available in a sand column bioreactor, it was necessary to determine the arsenate reduction capabilities of *S. marcescens* SA Ant 16 under the most extreme possibility of anaerobic conditions. The experiment was therefore duplicated in anaerobic serum vials at 5mM arsenate and varying concentrations of glucose.

No significant growth took place (Figure 4.6 a - c) except in the case of the 10mM glucose amendment where an approximate 5% increase in absorbance was observed after a 24 hour lag period (c). During the duration of the experiment and a very gradual drop in pH was observed, but this was comparable to that seen in the negative control containing only cells (d).

Glucose was utilised to depletion in the case of 0.1mM and 1mM glucose, but in the latter case over a 24 hour period as compared to within the first hour at the lowest concentration (Figure 4.7 a, b). This is in agreement with observations made during arsenate reduction under aerobic conditions, where it was speculated that these glucose concentrations might be too low to sustain extended arsenate reduction. With glucose amended to a final concentration of 10mM, approximately 80% of this glucose was not utilised after 100 hours (c), leading to the conclusion that this concentration would be excessive, and ultimately wasteful.

Arsenate was reduced under all anaerobic conditions (Figure 4.7 a - c), but differently from reduction under aerobic conditions, reduction was most efficient at high concentrations of glucose. The highest arsenate reduction rate of 2.1 $\mu$ M/h and a total conversion of 4% were obtained with 10mM glucose (c).

To obtain an overview of the parameters monitored during arsenate reduction by *S. marcescens* SA Ant 16 under both aerobic and anaerobic conditions, rates of arsenate reduction, glucose consumption, changes in pH and absorbance at 560nm are presented in 3 dimensions in Figure 4.8 .This data would thus enable an effective selection of parameters for application in scaling up bioreactors.

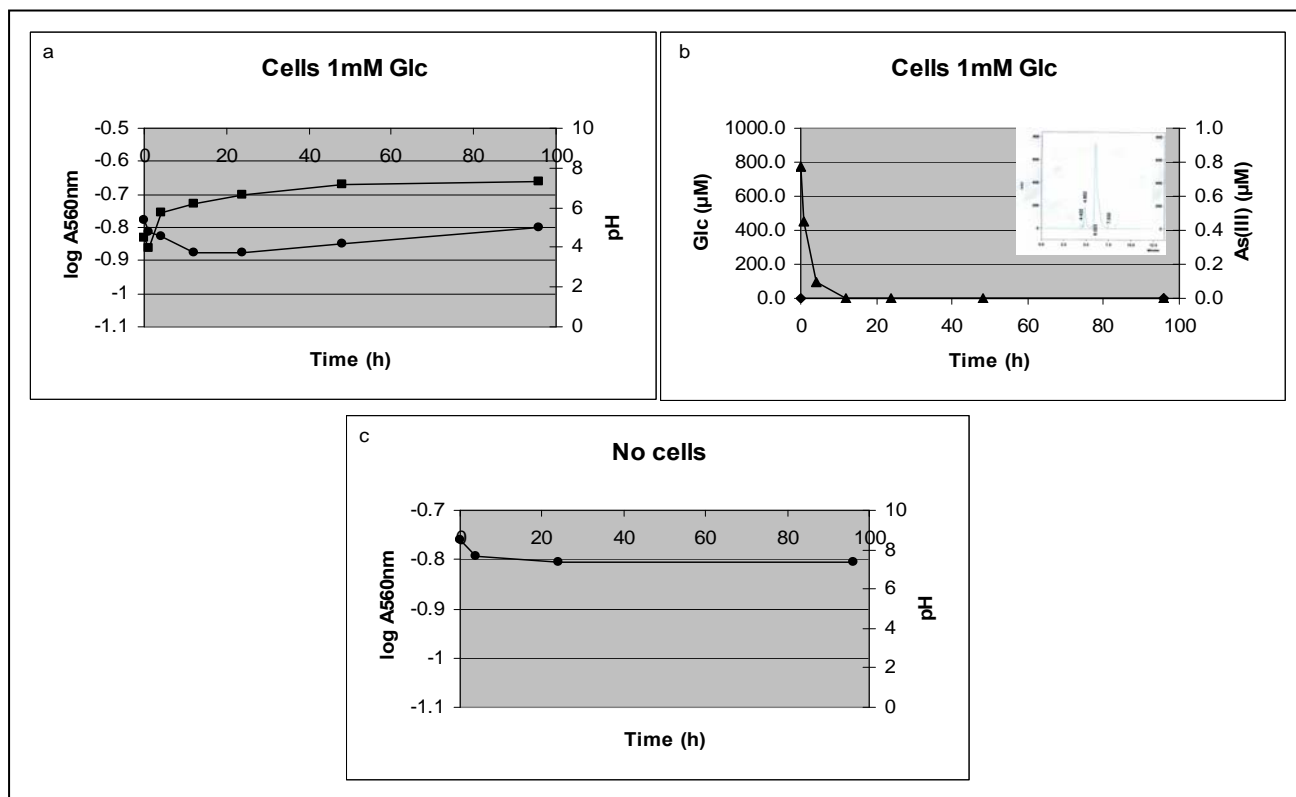


**Figure 4.3** Negative controls (with no arsenate addition) for changes in pH (●), growth (■) and glucose consumption (▲) under aerobic conditions. (Inset: HPLC profile of lactic acid formed at high glucose concentrations.)

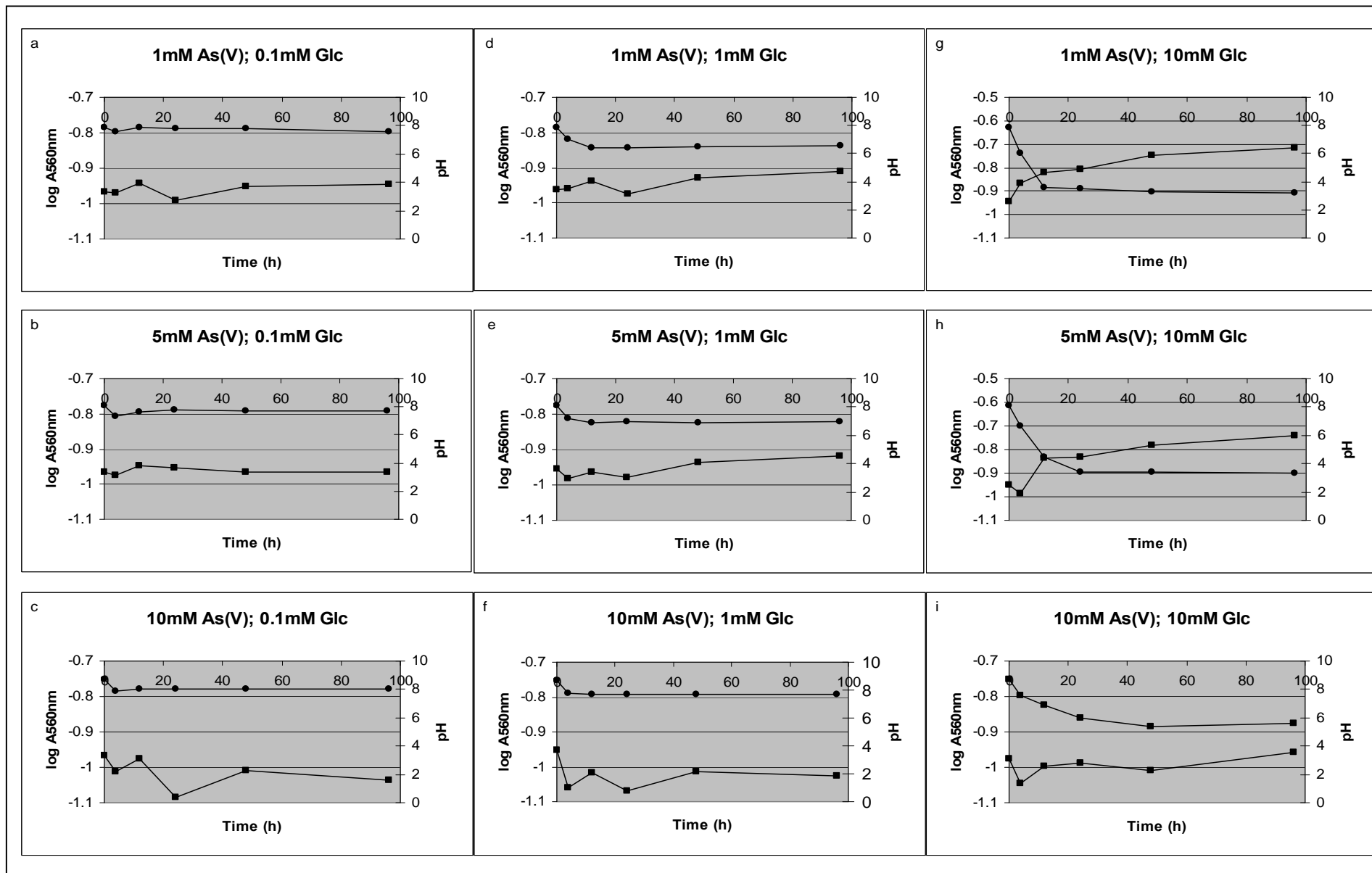


Figure 4.4 Growth (■) and changes in pH (●) during arsenate reduction under aerobic conditions.

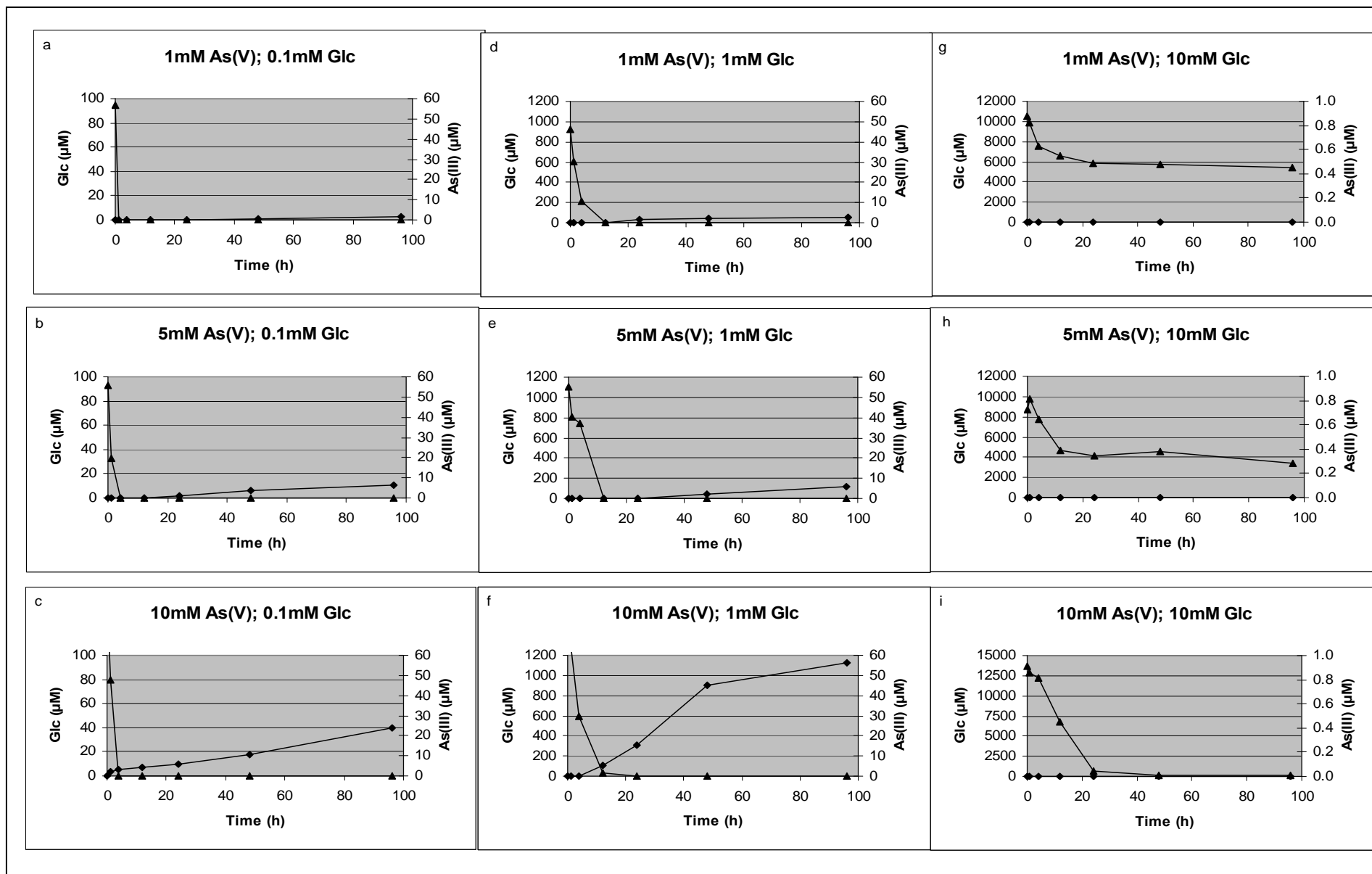


Figure 4.5 Arsenate reduction (◆) and glucose consumption (▲) under aerobic conditions.



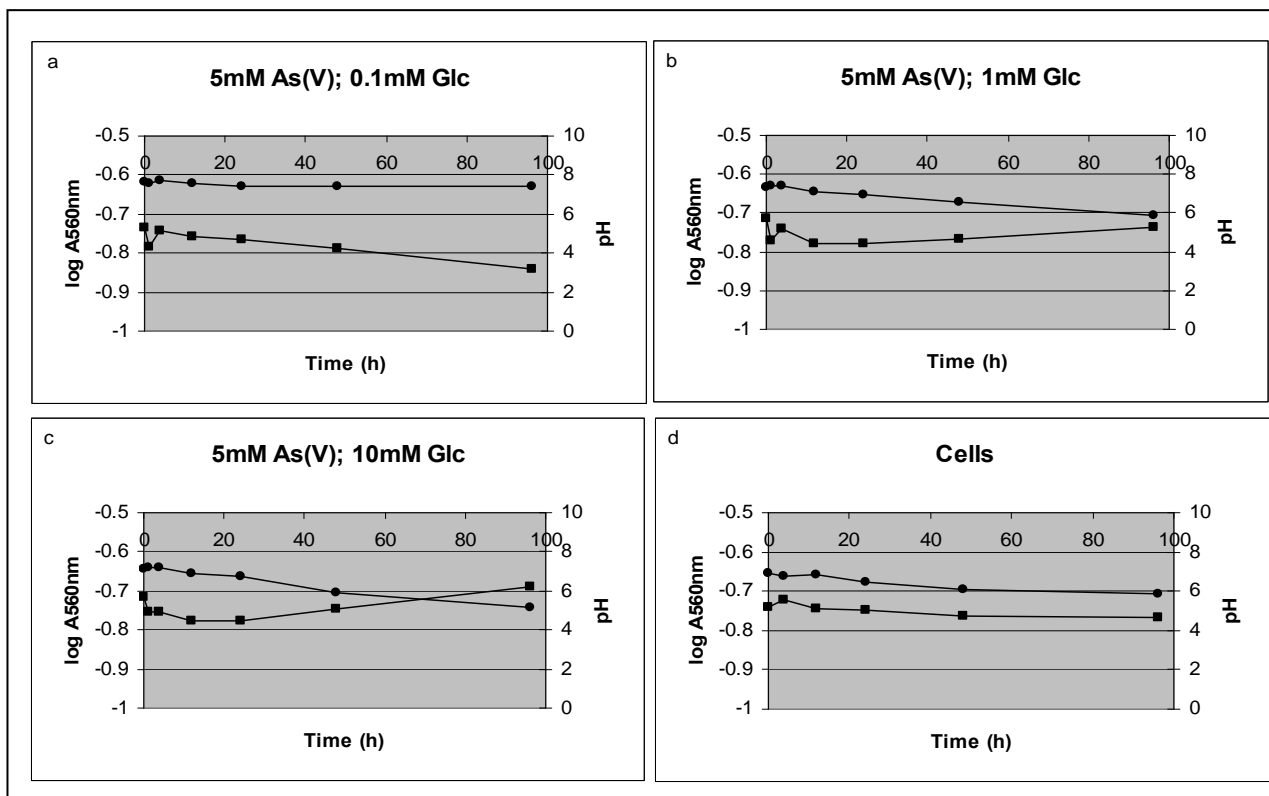


Figure 4.6 Growth (■) and pH changes (●) during arsenate reduction under anaerobic conditions.

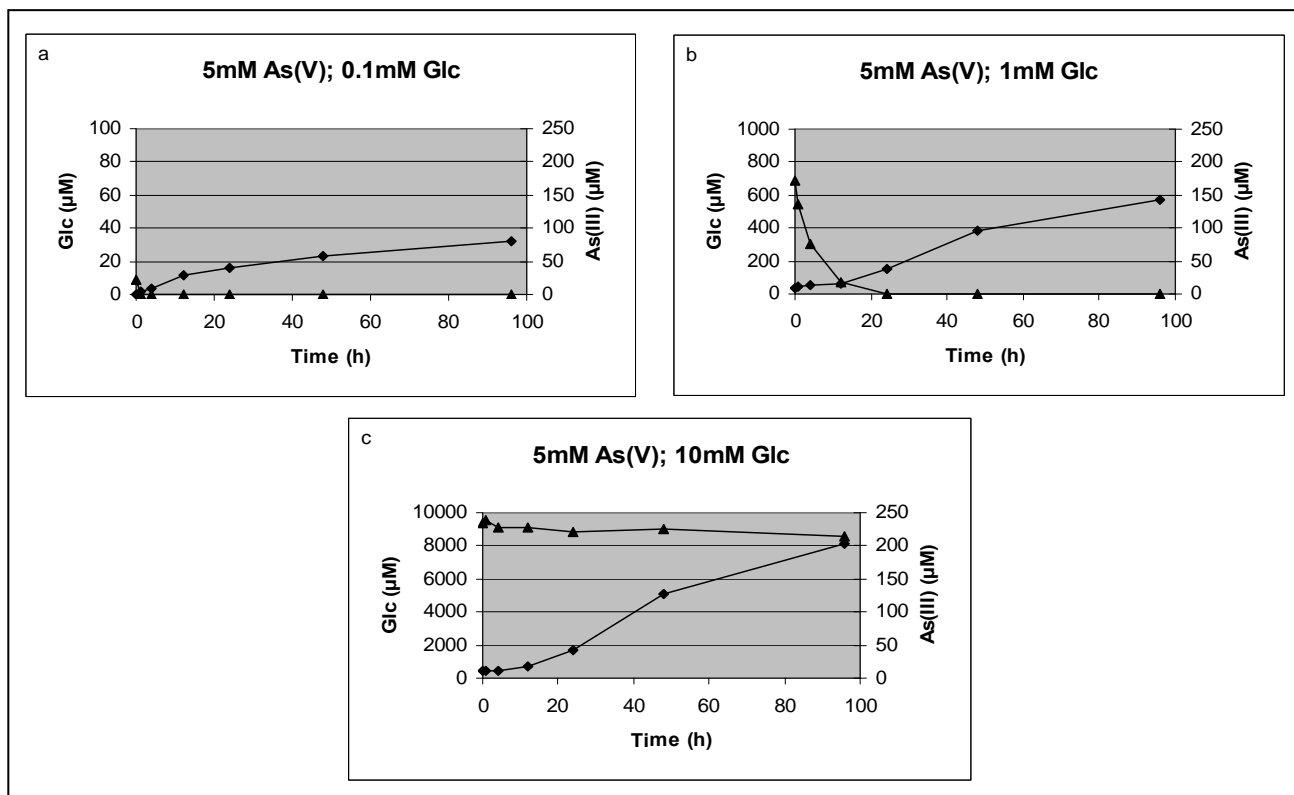
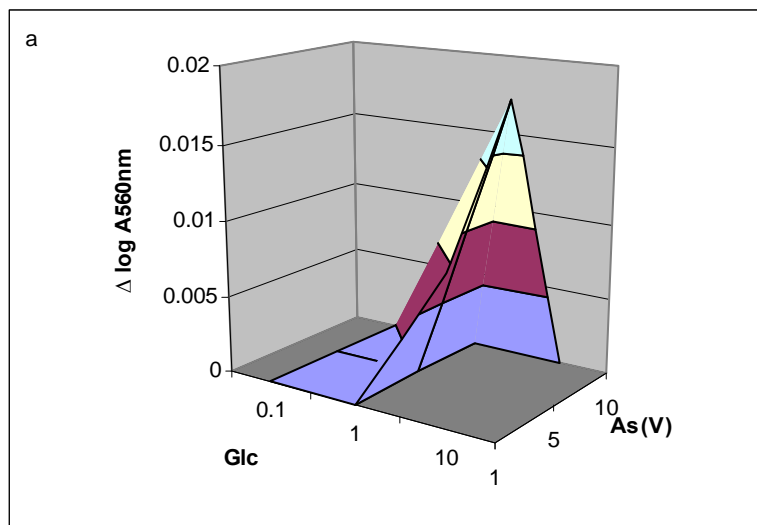


Figure 4.7 Arsenate reduction (◆) and glucose consumption (▲) under anaerobic conditions.

### Aerobic



### Anaerobic

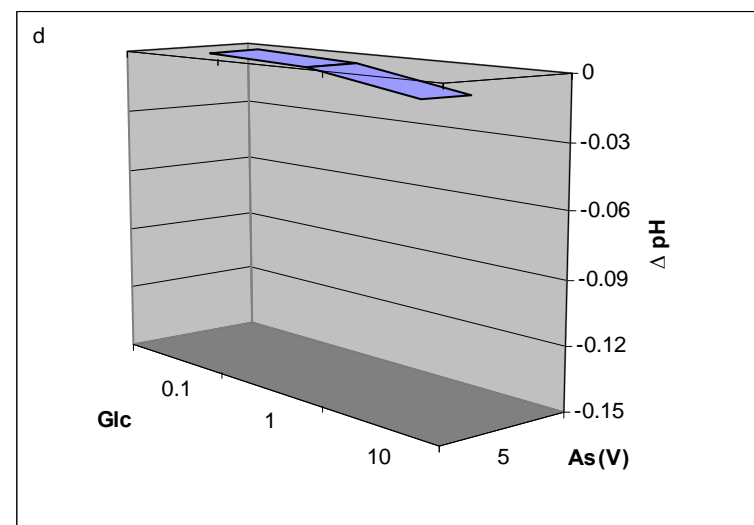
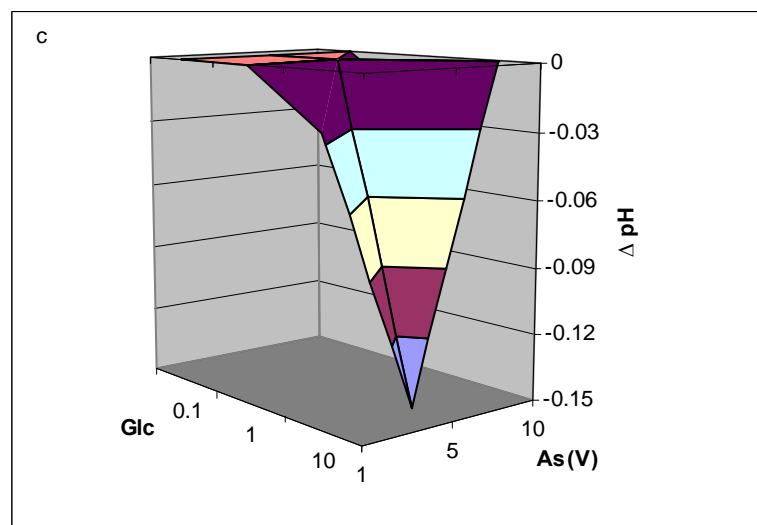
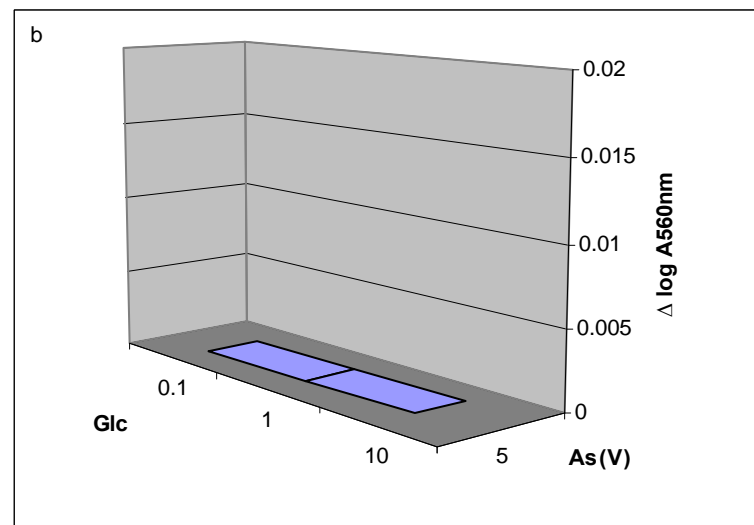
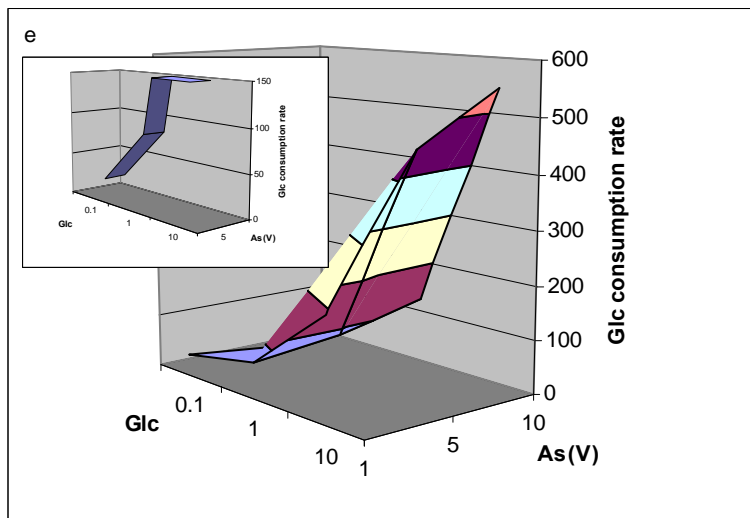


Figure 4.8 3D representation of growth (a & b) and changes in pH (c & d) during arsenate reduction.

### Aerobic



### Anaerobic

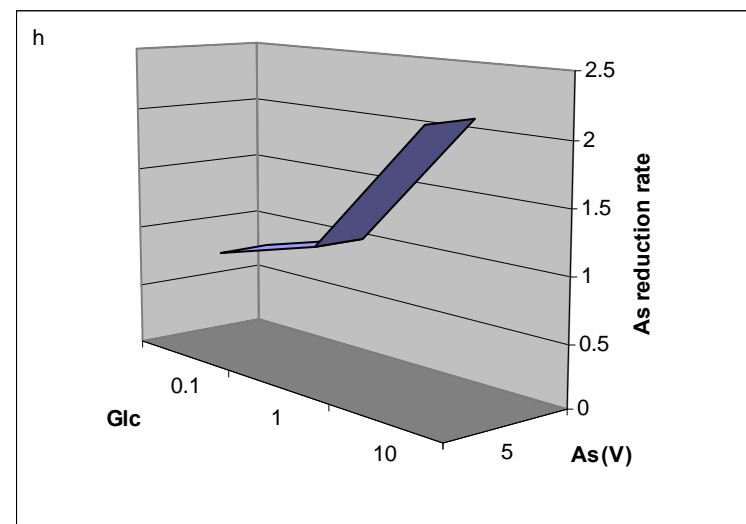
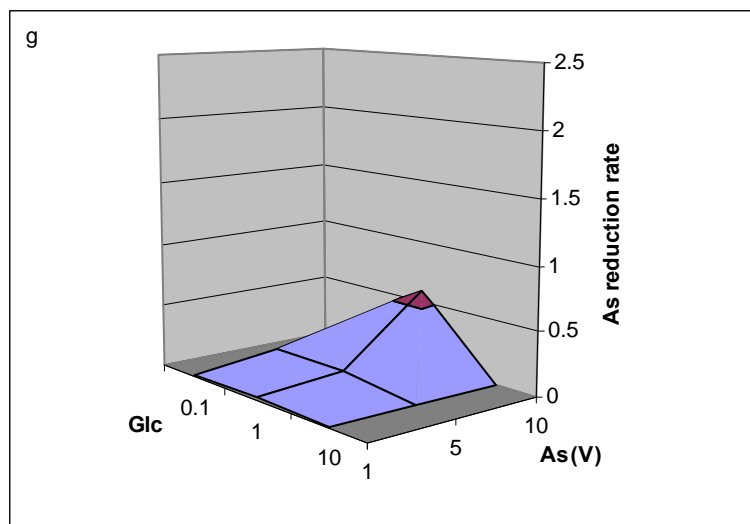
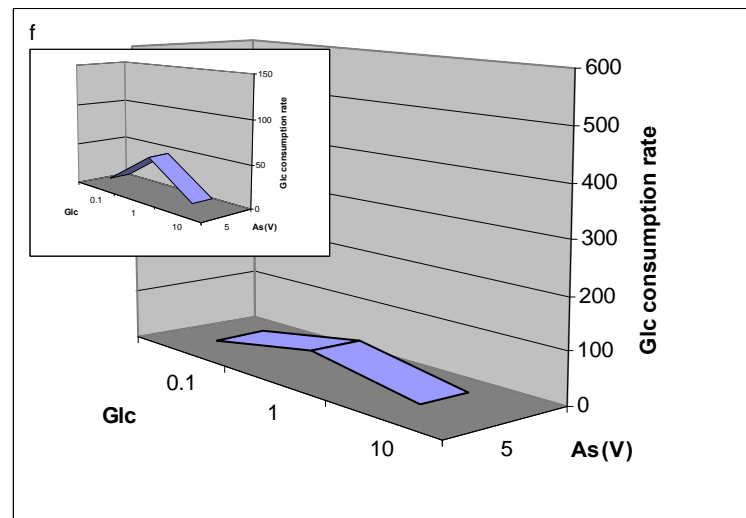
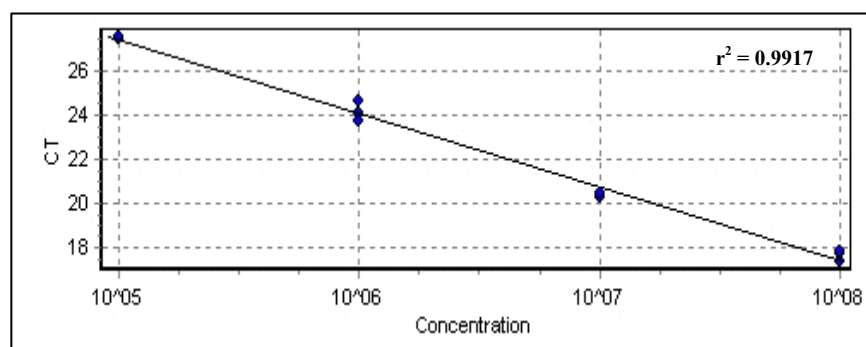


Figure 4.9 (continued) 3D representation of glucose consumption (e & f) and arsenate reduction (g & h) rates. (Insets: rescaled comparison between aerobic and anaerobic data.)

If results concerning growth and resulting changes in pH are compared (Figure 4.8 a - d), it is very clear that these two parameters are only important with regards to reduction under aerobic conditions, and should not be a concern in a bioreactor system where oxygen is limited. Glucose consumption rates were much higher under aerobic conditions (Figure 4.8 e, f), and even though at 10mM glucose, this could be attributed to utilisation for growth, at lower glucose concentrations (0.1mM and 1mM), consumption rates were consistently twice as high under aerobic conditions as compared to the anaerobic counterpart (figure insets). Arsenate reduction was much more successful under anaerobic conditions (Figure 4.8 g, h), and at glucose concentrations of 0.1mM and 1mM reduction rates were an order of magnitude higher than under aerobic conditions.

#### **4.4.2 Real-Time enumeration and primer specificity**

A standard curve for enumeration of cells was constructed by plotting cell concentration against threshold cycle ( $C_T$ ) values where product formation was detected and performing linear regression analysis (Figure 4.9).



**Figure 4.9** Standard curve of cell concentration (cells/mL) vs. cycle number ( $C_T$ ).

BLAST searches revealed high homology towards *Serratia marcescens* and specificity was confirmed by including template DNA from a Gram positive and Gram negative organism in a Real-Time PCR reaction (Figure 4.10).

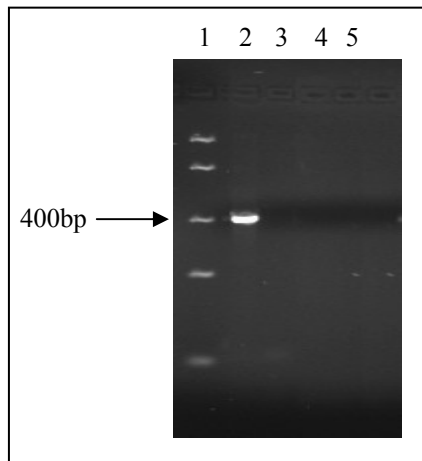


**Figure 4.10** Specificity of *S. marcescens* specific primers. Lane 1: Low Range FastRuler molecular weight marker (Fermentas), Lane 2: *S. marcescens* SA Ant 16, Lane 3: *B. pumilus*, Lane 4: *E. coli*, Lane 5: non-template control (NTC).

The primers amplified a band of the correct size (approximately 400bp) only from template DNA of *S. marcescens* and did not yield amplicons with other test organisms, indicating that this primer set could be used for enumeration of *S. marcescens* SA Ant 16.

#### **4.4.3 Adhesion**

In Chapter 3 it was determined that the cell surface of *S. marcescens* SA Ant 16 was negatively charged, acidic and had both localised and overall hydrophilic characteristics. In addition, the cells were motile, possessed an LPS layer as well as carbohydrates and proteins on the outer cellular surface which could all potentially mediate in cellular adhesion. Since bacterial adhesion depends primarily on hydrophobicity<sup>75</sup> and hydrophilic interactions seem to favour attachment of hydrophilic bacteria to hydrophilic surfaces<sup>76</sup>, it would not be unreasonable to expect that *S. marcescens* SA Ant 16 should be able to adhere to the hydrophilic quartz sand used in this study.

Aerobically grown cells suspended in AGW ( $10^6$  cells/mL to  $10^8$  cells/mL)<sup>77</sup> were applied to a sand matrix packed into 20mL syringe barrels. This was incubated for 6 hours and non-adhering cells drained from the column and quantified. The percentage of adhering cells did not increase with increasing cell concentrations and it was evident that cellular adhesion was

dependent on the initial concentration of cells loaded and that the sand grains had an adhesion capacity of at least  $10^8$  cells/mL (Figure 4.11). Subsequent experiments were therefore performed at the maximum cell concentration ( $10^8$  cells/mL) to ensure higher turnover rates.

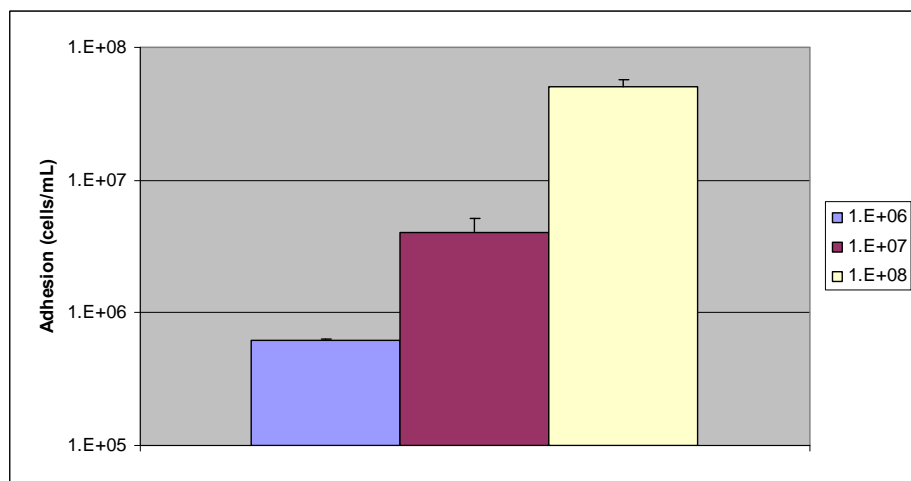


**Figure 4.11** Adhesion of concentration ranges of *S. marcescens* SA Ant 16 cells to sand grains.

When adhesion was monitored over a period of 24 hours, it was found that the number of cells adhering to the matrix increased from  $4 \times 10^7$  cells/mL after 2 hours of incubation to approximately  $1 \times 10^8$  cells/mL after 24 hours (Figure 4.12).

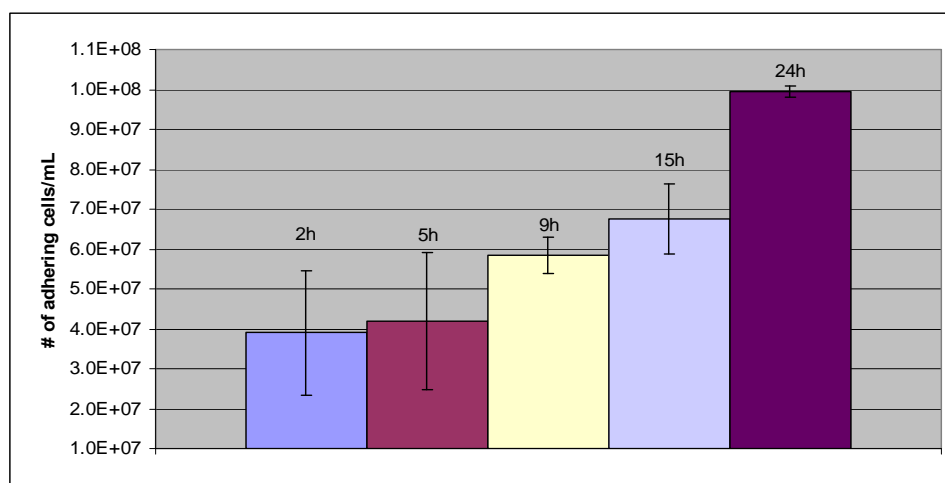


**Figure 4.12** Adhesion of *S. marcescens* SA Ant 16 to sand in syringe columns over a period of 24 hours.

If these results were to be extrapolated to a column reactor, the implication would be that  $10^8$  cells/mL would not exceed the loading capacity of the matrix and even a short contact time

between the cells and the sand would ensure adhesion of a large number of cells. Longer contact times, however, would result in higher numbers of adhering cells.

#### **4.4.4 Tracer and breakthrough curves**

Breakthrough curves for bacteria and chloride were very similar in shape in all cases indicating a homogenous sand matrix which would imply that limitations in specific areas of the reactor due to preferential flow paths should not occur. A representative example of a 500mm reactor is shown in Figure 4.13. Typically, both curves were symmetrical and from the tracer peak, the pore volume of the reactors was determined to be approximately 800mL. The breakthrough peak of the bacteria was earlier than that for the tracer, and this may be clarified in terms of differential advection<sup>78</sup>.

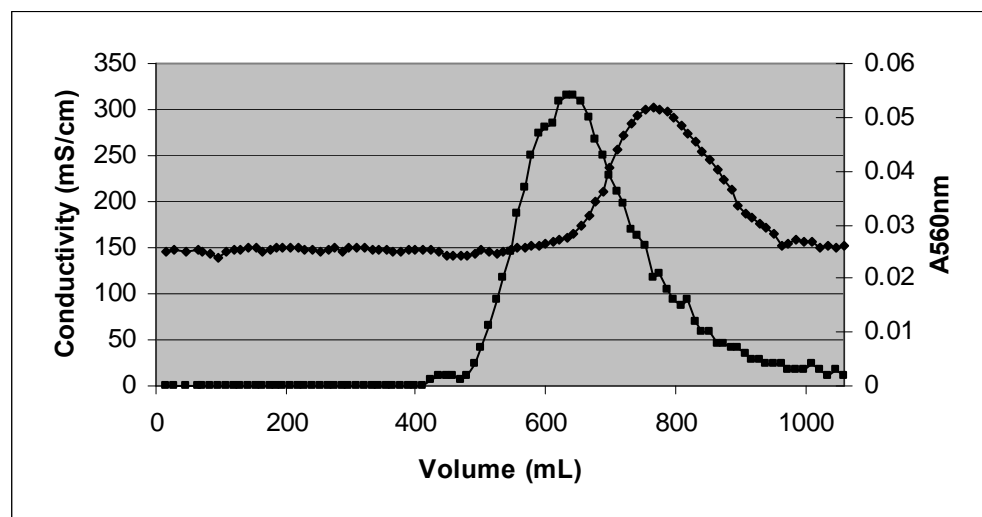


**Figure 4.13** Typical profile of NaCl tracer (◆) and bacterial breakthrough (■) in a 500mm column.

The primary mechanisms influencing differential advection include prohibition of the cells from the smaller matrix pores due to size exclusion<sup>79</sup>, preferential flow paths through high conductivity regions<sup>80</sup> or hydrodynamic retardation<sup>81</sup>. In the case of *S. marcescens* SA Ant 16 the generally symmetrical shape of both the tracer and breakthrough curves suggest that there was no preferred flow along the edges of the columns<sup>82</sup>, and it can therefore be concluded that differential advection can be attributed to hydrodynamic retardation and / or size exclusion due to heterogeneities in the bacterial solution such as varying cell surface characteristics and cell sizes.

#### **4.4.5 Loading of column with cells**

Cells ( $10^8$  cells/mL) were continually pumped into a packed column over a period representing 8 pore volumes. Adhesion of the bacterial cells did not increase beyond one pore volume, and in fact, a slight decline in cell numbers was observed (Figure 4.14). Even though enumeration by RT-PCR showed approximately  $10^7$  cells/mL throughout the column after 8 pore volumes, plate counts revealed viability of only  $10^6$  cells/mL.

RT-PCR is based on the presence of target DNA (in this case, a 400bp fragment from the small ribosomal subunit of *Serratia marcescens*) and will therefore also enumerate dead and unculturable cells. Plate counts, on the other hand, may give an under-estimation of cell numbers, since only culturable cells are counted.

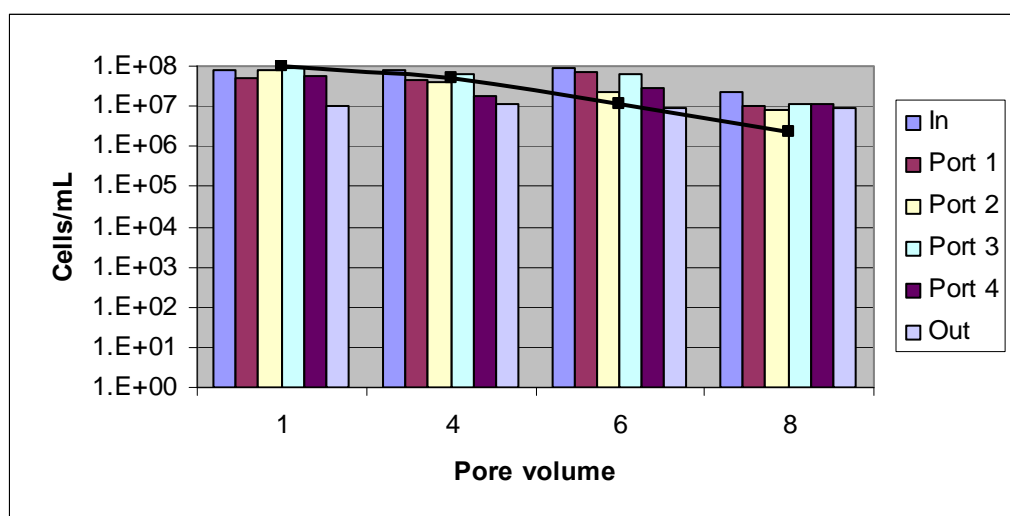


**Figure 4.14** Cell numbers in small column reactor for maximum saturation (Bars: Real-Time enumeration; plate counts ■).

#### **4.4.6 Arsenate reduction in column reactors**

Perspex columns were packed with sand media to enhance arsenate reduction activity by providing a solid support (surface) to which bacteria could adhere. The factorial optimisation study indicated that the concentration of glucose added should be higher than 1mM to avoid glucose depletion, but lower than 10mM so as not to stimulate cell growth. Glucose depletion may



inhibit sustainable arsenate reduction, whereas it was shown that when cells were actively growing, no arsenate reduction was observed (Figure 4.8 a & b and g & h). From initial adhesion (Figure 4.12) and loading experiments (Figure 4.14), it was clear that 24 hours of contact time between the cells and sand and one pore volume of cells would be sufficient for the maximum number of cells to adhere to the matrix. Conservative breakthrough curves determined pore volumes of approximately 800mL and to ensure complete displacement, a working pore volume of 1L was assumed. To obtain retention times of 24 hours, a flowrate of 0.7mL/min was calculated.

The first reactor was amended with 3mM glucose. Figure 4.15 illustrates a decrease in glucose utilisation from the influent to outflow of the reactor decreased to a minimum at pore volume 3 whereafter utilisation increased to 100%. A drop in pH between the influent and outflow was observed to increase over the first 5 pore volumes. These two parameters seen together may suggest an initial adaptation phase of the cells to new conditions represented by firstly exposure to arsenate, and secondly, being immobilised in a bioreactor. Arsenate reduction was observed from the first pore volume onwards, and reached a maximum after 5 pore volumes. The apparent limit of arsenate conversion was approximately 30% (calculated as percentage As(III) formed relative to As(V) initially added). It has been found that bacteria tend to aggregate in areas which offer some physical protection and are then able to condition the immediate environment through their metabolism to form microcosms that are conducive to their survival<sup>83</sup>, and enhanced arsenate conversion efficiencies by sessile cells are therefore not unexpected.

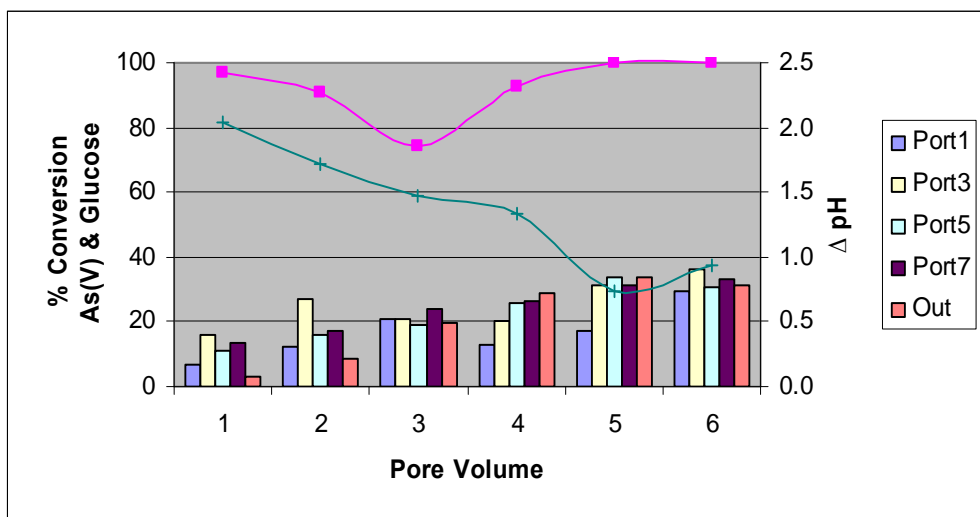


**Figure 4.15** Arsenate reduction (bars), glucose utilisation (■) and changes in pH (+) in column reactor containing 3mM glucose.

At the end of the experiment, the reactor was sacrificed and the sand grains examined by scanning electron microscopy.

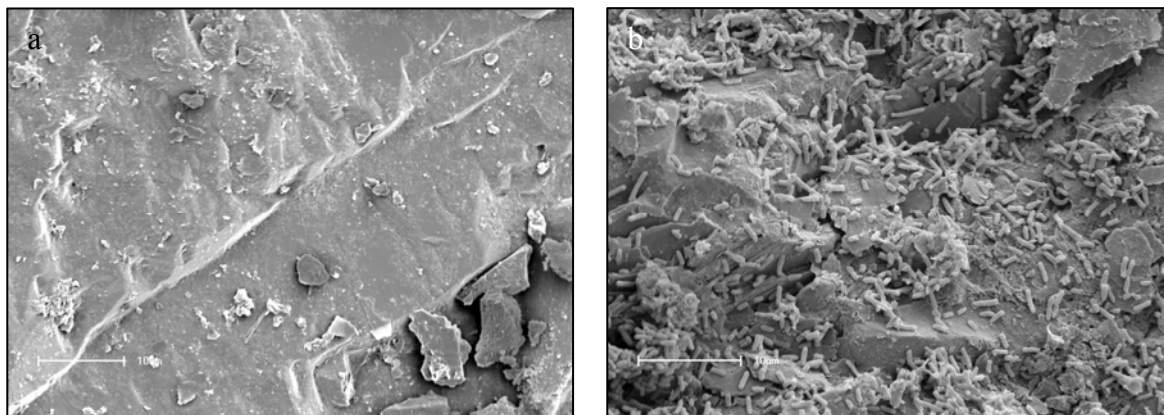


**Figure 4.16** SEM imaging of (a) a clean sand grain not exposed to cells, and (b) a sand grain covered with cells (Bar represents 10µm).

From Figure 4.16 it is evident that a large number of cells are still present on the sand grains which would suggest that it may be possible to simply stimulate cell growth inside the reactor instead of replenishing with fresh cells.

Since earlier results (see section 4.4.1 and Figure 4.13 e & f) suggested that arsenate reduction may be dependent on the glucose concentration, a second reactor was amended with 6mM glucose. This reactor was also monitored for arsenate reduction, glucose consumption and changes in pH and additionally for oxygen consumption and cell viability.

Viable cells, assessed by plate counts, increased after the initial addition of growth medium to approximately  $10^8$  cells/mL, and over the following 10 pore volumes a decrease to  $10^7$  cells/mL was seen. Addition of another pore volume of growth medium restored the cell counts to almost  $10^8$  cells/mL (Figure 4.17). This would suggest that if arsenate reduction efficiency diminished due to cell depletion in the reactor, that it may possibly be restored by stimulating cell growth.

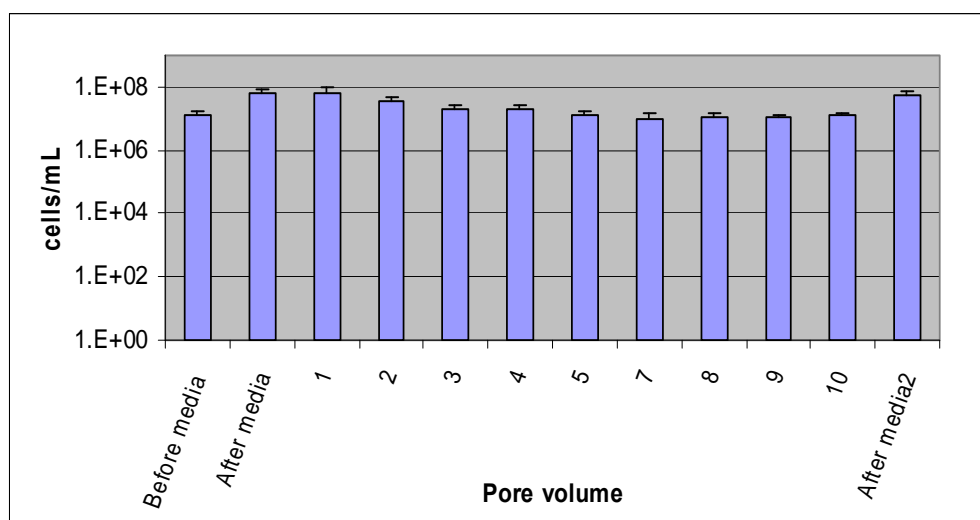
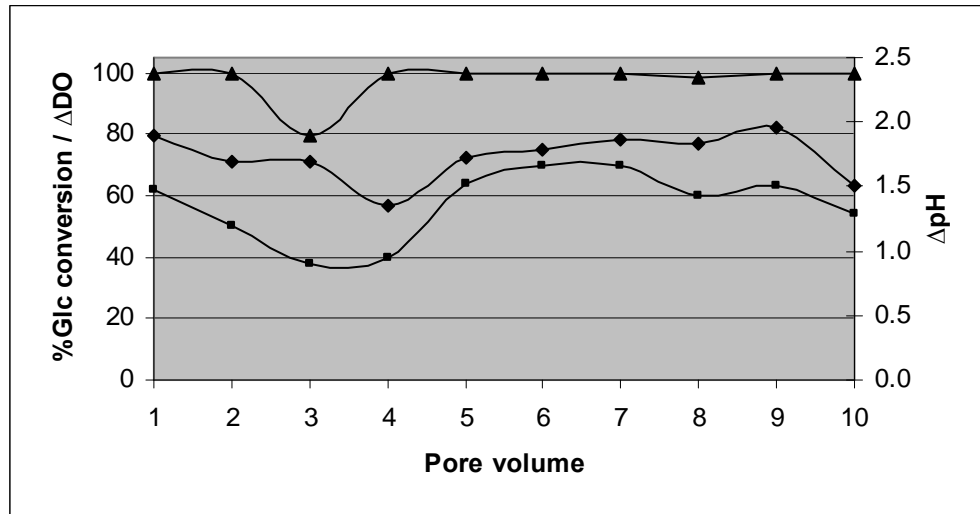


Figure 4.17 Viable cells in the reactor (5mM As(V), 6mM glucose) during run.

Glucose consumption decreased at PV3 to approximately 80%, but stabilised at approximately 100% during the rest of the run. Changes in pH and dissolved oxygen percentage from the inlet to the outlet showed a similar trend (Figure 4.18), where the first three pore volumes may represent an adaptation phase of the cells to their new environment. At pore volume 10, larger changes in dissolved oxygen percentage and pH could suggest a change in the physiological state of the cells.



**Figure 4.18** Changes in pH (◆), dissolved oxygen percentage (■) and glucose conversion (▲) in the reactor amended with 5mM arsenate and 6mM glucose.

Similar to the previous reactor, arsenate was reduced from the addition of the first pore volume of arsenate and glucose. Again, arsenate conversion increased up to 5 pore volumes where, arsenate conversion stabilised between 40% - 50% up to pore volume 9 (Figure 4.19). Onset of a possible decline in arsenate was seen at pore volume 10, confirming a possible change in cell physiology and arsenate reducing capabilities. At PV8, glucose consumption was approximately 98% (Figure 4.18), while other parameters such as changes in pH and arsenate conversion (Figure 4.19) remained constant, which could possibly be seen as an indication that glucose utilisation is maximal without being limiting.

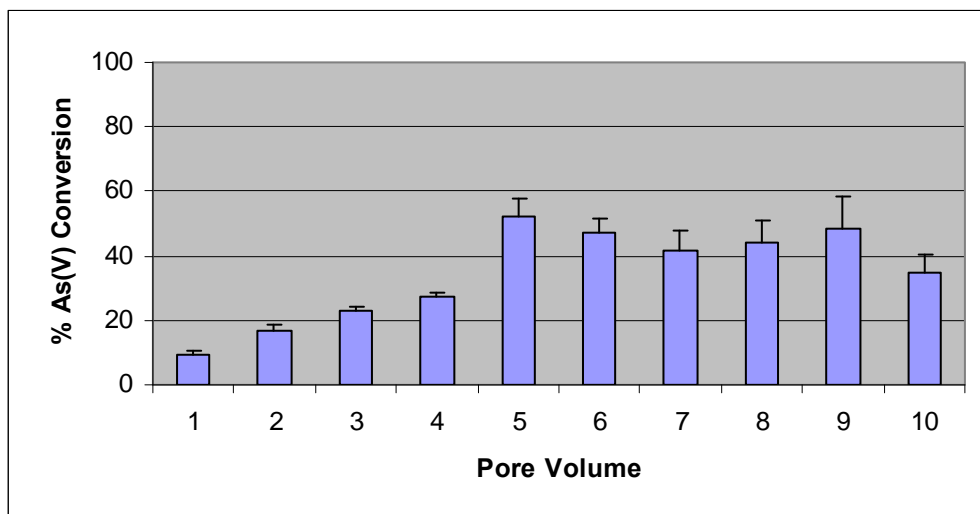


**Figure 4.19** Percentage arsenate conversion over 10 pore volumes for bioreactor amended with 5mM arsenate and 6mM glucose.

It is difficult to contextualise the results presented here, since only one analogous technology exists where arsenic removal from contaminated groundwater is accomplished by arsenate reducing bacteria. For this particular case study, the arsenic concentration was reduced to less than 0.5mg/L, without any additional information such as the initial arsenic concentration. Full scale operation of chemical remediation processes report efficiencies ranging from 40% to 99% depending on the specific technology, and initial arsenic concentrations are generally in the  $\mu\text{M}$  range. The data presented in this report suggest that the potential exists for the development of a feasible bioremediation alternative to chemical treatments by *S. marcescens* SA Ant 16.

## **4.5 Conclusions**

*S. marcescens* SA Ant 16 could have major implications in the search for innovative methods for arsenic waste management: even without bioreactor optimisation, arsenate conversion exceeded 50%. Moreover, a unique characteristic of *Serratia marcescens* SA Ant 16 that sets it apart from other technologies, is that this organism achieved these efficiencies from initial arsenate concentrations of 5mM (approximately 380mg/L). Considering that arsenic concentrations at the original sampling site is approximately 1mM, application of this bacterium to this arsenic contamination is indeed a possibility.

The short term nature of the reactor experiments implies that sustainability concerns such as clogging, contamination and competition are not addressed. Longer term studies, focusing on cell viability, stimulation of growth and replenishment of the reactor with cells would be important areas of investigation. Preliminary Denaturing Gradient Gel Electrophoresis (not presented here) indicated shifts in the bacterial population over the duration of reactor experiments and assessment of microbial diversity in the reactors would therefore also be essential.

If general trends with regards to the factorial analysis are followed, results obtained from reduction under aerobic conditions suggest a correlation between initial arsenate concentration and arsenate reduction rates, while experiments under anaerobic conditions revealed a similar trend with regards to the glucose concentration. These two parameters can be varied singly and in combination to possibly enhance arsenate conversion efficiency in bioreactors.

Lower flow rates would increase contact times between the cells, arsenate and glucose and this may have a positive effect on arsenate conversion efficiency. Increased contact times could also be accomplished by lengthening the reactors, but glucose limitation may prove a critical factor in this regard. Bacterial adhesion to the sand grains indicated that the loading capacity was not exceeded by  $10^8$  cells/mL and higher conversion efficiencies could, therefore, also be achieved by increasing the initial cell loading concentrations.

Initial arsenate reduction experiments suggested that in addition to reduction, adsorption or sequestration of arsenic (as either arsenate or arsenite) could be an alternative resistance mechanism. This area will need elucidation to fully grasp the bioremediative potential of this organism.

The mechanism of arsenate reduction may be clarified by genome sequencing, although if the gene is completely different from previously described genes, mutagenesis and characterisation of arsenate sensitive mutants may prove a more successful strategy.

If the possibility of coupling an arsenate reducing bioreactor to a biogenic H<sub>2</sub>S reactor is considered, this could provide a strategy that has the potential for widespread use in contaminated water systems. Metal removal by sulfide precipitation is a well-known process that is characterised by compact residues, selective and very high metal removal efficiencies<sup>64</sup>. With regards to arsenic remediation, sulfide precipitation has been shown to achieve removal efficiencies ranging between 77%<sup>69</sup> and 97%<sup>65</sup>. Our results suggest the use of this hyper-resistant bacterium as a bioremediation agent in areas where arsenic contamination levels has hitherto been considered prohibitively high.

## **4.6 Literature cited**

- 
- <sup>1</sup> WHO, Guidelines for drinking water quality. World Health Organisation, Geneva, P-41, 1993.
  - <sup>2</sup> Cheng RC, Wang CC & Beuhler MD (1994). Enhanced coagulation for arsenic removal. *J Am Water Works Assoc* 86: 79-90
  - <sup>3</sup> Hansen HK, Nunez P & Grandon R (2006). Electrocoagulation as a remediation tool for wastewaters containing arsenic. *Minerals Engineer* 19 521-524
  - <sup>4</sup> Scott KN, Green JF, Do HD & Mclean SJ (1995). Arsenic removal by coagulation. *J Am Water Works Assoc* 86: 79
  - <sup>5</sup> Pinon-Miramontes M, Bautista-Margulis RG & Perez-Hernandez A (2003). Removal of arsenic and fluoride from drinking water with cake alum and a polymeric anionic flocculent. *Fluoride* 36: 122-128
  - <sup>6</sup> Krishna MVB, Chandrasekaran K, Karunasagar D & Arunachalam J (2001). Combined treatment approach using Fenton's reagent and zero valent iron for the removal of arsenic from drinking water. *J Hazardous Mat* 84: 229-240
  - <sup>7</sup> Dowson WM (1959). Studies in qualitative inorganic analysis. XIII - Reduction of arsenic(V) with ammonium iodide and subsequent precipitation of arsenic sulphide. *Mikrochim Acta* 47: 841-846
  - <sup>8</sup> Hering JG, Chen P, Wilkie JA, Elimelech M & Liang S (1996). Arsenic removal by ferric chloride. *J Am Water Works Assoc* 88: 155-167
  - <sup>9</sup> Benjamin MM, Sletten RS, Bailey RP & Bennett T (1996). Sorption and filtration of metals using iron-oxide coated sand. *Water Research* 30: 2609
  - <sup>10</sup> Fox KR & Sorg TJ (1987). Controlling arsenic, fluoride, and uranium by point-of-use treatment. *J Am Water Works Assoc* 10: 81-84
  - <sup>11</sup> Bissen M & Frimmel FH (2003). Arsenic – A Review. Part II: Oxidation of arsenic and its removal in water treatment. *Acta Hydroch Hydrob* 31: 97-107
  - <sup>12</sup> Edwards MA (1994). Chemistry of arsenic removal during coagulation and Fe-Mn oxidation. *J Am Water Works Assoc* 86: 64-77
  - <sup>13</sup> Muilenberg T (1997). Microfiltration basics: Theory and practice. Proceedings Membrane Technology Conference, New Orleans, L.A.
  - <sup>14</sup> Edwards M, Patel S, McNeill L, Chen H, Frey M, Eaton AD, Antweiler CR & Taylor E (1998). Considerations in arsenic analysis and speciation. *J Am Water Works Assoc* 90: 103
  - <sup>15</sup> US Environmental Protection Agency (1999). Technologies and costs for removal of arsenic from drinking water. EPA 815-P-01-001
  - <sup>16</sup> Clifford D & Lin CC (1995). Ion exchange, activated alumina, and membrane processes for arsenic removal from groundwater. Proceedings of the 45<sup>th</sup> Annual Environmental Engineering Conference, University of Kansas.



- 
- 17 Daus B, Wennrich R & Weiss H (2004). Sorption materials for arsenic removal from water: a comparative study. *Water Res* 38: 2948-2954
- 18 Dambies L (2004). Existing and prospective sorption technologies for the removal of arsenic in water. *Separ Sci Technol* 39: 603-627
- 19 De Vitre R, Belzile N & Tessier A (1991). Speciation and adsorption of arsenic on diagenetic iron oxyhydroxides. *Limnol Oceanogr* 36: 1480-1485
- 20 Elizalde-Gonzales MP, Mattusch J, Einicke WD & Wennrich R (2001). Sorption on natural solids for arsenic removal. *Chem Eng J* 81: 187-195
- 21 Korngold E, Belayev N & Aronov L (2001). Removal of arsenic from drinking water by anion exchangers. *Desalination* 141: 81-84
- 22 Mondal P, Majumder CB & Mohanty B (2006). Laboratory based approaches for arsenic remediation from contaminated water: Recent developments. *J Hazard Mat* 137: 464-479
- 23 Yi SH, Ahmed S, Watanabe Y & Watari K (2003). Arsenic removal by MF membrane with chemical sludge adsorption and NF membrane equipped with vibratory shear enhanced process. *Water Sci Technol* 3: 303-310
- 24 Lin TF, Hsiao HC, Wu JK & Jeh JH (2002). Removal of arsenic from groundwater using point-of-use reverse osmosis and distilling devices. *Environ Technol* 23: 781-790
- 25 Floch J & Hideg M (2004). Application of ZW-1000 membranes for arsenic removal from water sources. *Desalination* 162: 75-83
- 26 Subramanian KS, Viraraghavan T, Phommavong T & Tanjore S (1997). Manganese greensand for removal of arsenic in drinking water. *Water Qual Res J Canada* 32: 551-561
- 27 Garcia-Sanchez A, Alvarez-Ayuso E & Rodriguez-Martin F (2002). Sorption of As(V) by some oxyhydroxides and clay minerals. Application to its immobilization in two polluted mining soils. *Clay Miner* 37: 187-194
- 28 Bajpai S & Chaudhuri M (1999). Removal of arsenic from groundwater by manganese dioxide coated sand. *J Environ Eng-Asce* 10: 782-784
- 29 Chwirka JD, Thomson BM & Stomp JM (2000). Removing arsenic from groundwater. *J Am Water Works Assoc* 92: 79-88
- 30 Loukidou MX, Matis KA, Zouboulis AI & Kyriakidou ML (2003). Removal of As(V) from waste water by chemically modified fungal biomass. *Water Res* 37: 4544-4552
- 31 Shaban W, Rmalli A, Harrington CF, Ayub M & Haris PI (2005). A biomaterial based approach for arsenic removal from water. *J Environ Monit* 7: 279-282
- 32 Ridvan S, Nalan Y & Adil D (2003). Biosorption of cadmium, lead, mercury, and arsenic ions by the fungus *Penicillium purpurogenum*. *Sep Sci Technol* 38: 2039-2053
- 33 Murugesan GS, Sathishkumar M & Swaminathan K (2006). Arsenic removal from groundwater by pretreated waste tea fungal biomass. *Bioresour Technol* 97: 483-487
- 34 Harris PO & Ramelow GJ (1990). Binding of metal ions by particulate biomass derived from *Chlorella vulgaris* and *Scenedesmus Quadricauda*. *Environ Sci Technol* 24: 220-228

- 35 Beceiro-Gonzalez E, Taboada-de la Calzada A, Alonso-Rodriguez E, Lopez-Mahia P, Muniategui-Lorenzo S & Prada-Rodriguez D (2000). Interaction between metallic species and biological substrates: approximation to possible interaction mechanisms between the alga *Chlorella vulgaris* and arsenic(III). *Trends Anal Chem* 19: 475-480
- 36 Suhendrayatna A, Ohki TK & Maeda S (1999). Arsenic compounds in the freshwater green microalga *Chlorella vulgaris* after exposure to arsenite. *Appl Organomet Chem* 13: 127-133
- 37 Hansen HK, Ribeiro A & Mateus E (2006). Biosorption of arsenic(V) with *Lessonia nigrescens*, *Miner Eng* 19: 486-490
- 38 Bae W, Mehra R, Mulchandani A & Chen W (2001). Genetic engineering of *Escherichia coli* for enhanced bioaccumulation of mercury. *Appl Environ Microbiol* 67: 5335-5338
- 39 Bae W, Chen W, Mulchandani A & Mehra R (2000). Enhanced bioaccumulation of heavy metals by bacterial cells displaying synthetic phytochelatin. *Biotechnol Bioeng* 70: 518-523
- 40 Sauge-Merke S, Cuine S, Carrier P, Lecomte-Pradines C, Luu DT & Peltier G (2003). Enhanced toxic metal accumulation in engineered bacterial cells expressing *Arabidopsis thaliana* phytochelatin synthase. *Appl Environ Microbiol* 69: 490-494
- 41 Kostal J, Yang R, Wu CH, Mulchandani A & Chen W (2004). Enhanced arsenic accumulation in engineered bacterial cells expressing ArsR. *Appl Environ Microbiol* 70: 4582-4587
- 42 Cunningham SD, Berti WR & Huang JW (1995). Phytoremediation of contaminated soils. *Trends Biotechnol* 13: 393-397
- 43 Visoottiviset P, Francesconi K & Sridokchan W (2002). The potential of Thai indigenous plant species for the phytoremediation of arsenic contaminated land. *Environ Pollut* 118: 453-461
- 44 US Environmental Protection Agency (2002). Arsenic treatment technologies for soil, waste and water. EPA 542-R-02-004
- 45 Alkorta I, Hernandez-Allica J & Garbisu C (2004). Plants against the global epidemic of arsenic poisoning. *Environ Int* 30: 949-951
- 46 Ma QL, Komar KM, Tu C, Zhang W, Cai Y & Kennelley ED (2001). A fern that hyperaccumulates arsenic. *Nature* 409: 579
- 47 Tu S, Ma LQ, Fayiga AO & Zillioux EJ (2004). Phytoremediation of arsenic- contaminated groundwater by the arsenic hyperaccumulating fern *Pteris vittata*. *Int J Phytoremediat* 6: 35-47
- 48 Clifford D, Subramonian S & Sorg T (1998). Removing dissolved inorganic contaminants from water. *Environ Sci Technol* 20: 1072-1080
- 49 Kerkeb L & Kramer U (2003). The role of free histidine in xylem loading of nickel in *Alyssum lesbiacum* and *Brassica juncea*. *Plant Physiol* 131: 716-724
- 50 Cunningham SD & Ow DW (1996). Promises and prospects of phytoremediation. *Plant Physiol* 110: 715-719
- 51 Vassilev A, Schwitzguebel JP, Thewys T, Van Der Lelie D & Vangronsveld J (2004). The use of plants for remediation of metal-contaminated soils. *Sci World J* 4: 9-34

- 
- 52 Srivastava M, Ma LQ & Santos JAG (2006). Three new arsenic hyperaccumulating ferns. *Sci Total Environ* 364: 24-31
- 53 Huang JW, Poynton CY, Kochian LV & Elless MP (2004). Phytofiltration of arsenic from drinking water using arsenic-hyperaccumulating ferns. *Environ Sci Technol* 38: 3412-3417
- 54 Webb SM, Gaillard JF, Ma LQ & Tu C. (2003). XAS speciation of arsenic in a hyper-accumulating fern, *Environ Sci Technol* 37: 754-760
- 55 Lasat M (2002). Phytoextraction of toxic metals: A review of biological mechanisms. *J of Environ Qual* 31: 109-120
- 56 Dhankher OP, Li Y, Rosen BP, Shi J, Salt D, Senecoff JF, Sashti NA & Meagher RB (2002). Engineering tolerance and hyperaccumulation of arsenic in plants by combining arsenate reductase and gamma-glutamylcysteine synthetase expression. *Nat Biotechnol* 20: 1140-1145
- 57 Mouchet P (1992). From conventional to biological removal of iron and manganese in France. *J Am Water Works Assoc* 84: 158-166
- 58 Knocke WR, Hannon JR & Thompson CP (1988). Soluble manganese removal on oxide-coated filter. *J Am Water Works Assoc* 80: 65-70
- 59 Katsoyiannis I, Zouboulis A, Althoff H & Bartel H (2002). As(III) removal from groundwaters using fixed-bed upflow bioreactors. *Chemosphere* 47: 325-332
- 60 Katsoyiannis I & Zouboulis A (2004). Application of biological processes for the removal of arsenic from groundwaters. *Water Res* 38: 17-26
- 61 Eary, LE (1992). The solubility of amorphous  $As_2S_3$  from 25 to 90°C. *Geochim Cosmochim Acta* 56: 2267-2280
- 62 Kim SD, Kilbane JJ & Cha DK (1999). Prevention of acid mine drainage by sulfate reducing bacteria: organic substrate addition to mine waste piles. *Environ Eng Sci* 16: 139-145
- 63 Rittle KA, Drever JI & Colberg PJS (1995). Precipitation of arsenic during bacterial sulfate reduction. *Geomicrobiol* 13: 1-11
- 64 Jong T & Parry DL (2005). Evaluation of the stability of arsenic immobilized by microbial sulfate reduction using TCLP extractions and long-term leaching techniques. *Chemosphere* 60: 254-265
- 65 Belin DD, Dinsdale BE & Altringer PB (1993). Arsenic removal from mining waste using sulfate-reducing bacteria in a 2-stage bioreactor. In: *Biohydrometallurgical Technologies - Bioleaching Processes Vol1*. (Torma AE, Wey JE, Lakshmann VI Eds.) The minerals, metals and materials society. Warrendale, P.A. pp. 613-620
- 66 Uhrie JL, Drever JI, Colberg PJS & Nesbitt CC (1996). *In situ* immobilization of heavy metals associated with uranium leach mines by bacterial sulfate reduction. *Hydrometallurgy* 43: 231-239
- 67 Jong T & Parry DL (2003). Removal of sulfate and heavy metals by sulfate reducing bacteria in short-term bench scale upflow anaerobic packed bed reactor runs. *Water Res* 37: 3379-3389
- 68 Tassé N, Isabel D & Fontaine R (2003). Wood Cadillac Mine Tailings : Design of a biofilter for arsenic control. Conference Proceedings: Sudbury 2003 - Mining and the Environment. Ontario, Canada. Available online at <http://www.ott.wrcc.osmre.gov/library/proceed/sudbury2003/sudbury03/prof148.html>

- 
- 69 Germain D & Cyr J (2003). Evaluation of biofilter performance to remove dissolved arsenic: Wood Cadillac. Conference Proceedings: Sudbury 2003 - Mining and the Environment. Ontario, Canada. Available online at <http://www.ott.wrcc.osmre.gov/library/proceed/sudbury2003/sudbury03/prof55.html>
- 70 Fuller ME, Dong H, Mailloux BJ, Onstott TC & DeFlaun MF (2000). Examining bacterial transport in intact cores from Oyster, Virginia: Effect of sedimentary facies type on bacterial breakthrough and retention. *Water Res Research* 36: 2417-2431
- 71 Bolster CH, Hornberger GM, Mills AL & Wilson JL (1998). A method for calculating bacterial deposition coefficients using the fraction of bacteria recovered from laboratory columns. *Environ Sci Technol* 32: 1329-1332
- 72 Altschul SF, Gish W, Miller W, Myers EW & Lipman DJ (1990). Basic local alignment search tool. *J Mol Biol* 215: 403-410
- 73 Van Wyk A, Usher BH & Van Heerden E-R (2006). Biobarrier formation for hydraulic control in groundwater remediation in South Africa. Ph.D Thesis.
- 74 Eaves GN & Jefferies CD (1962). Effect of pH on the formation of extracellular nuclease in aging broth cultures of *Serratia marcescens*. *J Bacteriol* 85: 1194-1196
- 75 Balazs DJ, Triandafillu K, Chevolut Y, Aronsson B-O, Harms H, Descouts P & Mathieu HJ (2003). Surface modification of PVC endotracheal tubes by oxygen glow discharge to reduce bacterial adhesion. *Surf Interf Anal* 35: 301-309
- 76 Makin SA & Beveridge TJ (1996). The influence of A-band and B-band lipopolysaccharide on the surface characteristics and adhesion of *Pseudomonas aeruginosa* to surfaces. *Microbiol* 142: 299-307
- 77 Huysman F & Verstraete W (1992). Effect of cell surface characteristics on the adhesion of bacteria to soil particles. *Biol Fertil Soils* 16: 21-26
- 78 Dong H, Rothmel R, Onstott TC, Fuller ME, DeFlaun MF, Streger SH, Dunlap R & Fletcher M (2002). Simultaneous transport of two bacterial strains in intact cores from Oyster, Virginia: biological effects and numerical modeling. *Appl Environ Microbiol* 68: 2120-2132
- 79 Powelson DK, Gerba CP & Yahya MT (1993). Virus transport and removal in wastewater during aquifer recharge. *Water Res* 27: 583-590
- 80 Toran L & Palumbo AV (1992). Colloid transport through fractured and unfractured laboratory sand columns. *J Contam. Hydrol* 9: 289-303
- 81 Bales RC, Gerba CP, Grondin GH & Jensen SL (1989). Bacteriophage transport in sandy soil and fractured tuff. *Appl Environ Microbiol* 55: 2061-2067
- 82 Fontes DE, Mills AL, Hornberger GM & Herman JS (1991). Physical and chemical factors influencing transport of microorganisms through porous media. *Appl Environ Microbiol* 57: 2473-2481
- 83 Meyer-Reil LA (1994) Microbial life in sedimentary biofilms - the challenge to microbial ecologists. *Mar Ecol Prog Ser* 112: 303-311

## 5      Summary

Soil and water sites were sampled at a South African antimony mine with elevated levels of arsenic due to the refining process. Enriched media yielded six pure bacterial cultures able to grow in both arsenite and arsenate. These bacteria were identified as two strains of *Bacillus* sp. (SA Ant 10(1) and SA Ant 14) with close relatedness to *B. maltophilia* and *B. thuringiensis*, another as *Stenotrophomonas maltophilia* SA Ant 15 and two isolates as *Serratia marcescens* (SA Ant 10(2) and SA Ant 16). *Bacillus* sp. SA Ant 14, *S. maltophilia* SA Ant 15 and *S. marcescens* SA Ant 16 were used for further investigation. All three isolates were able to grow in arsenite and arsenate respectively and *S. marcescens* SA Ant 16 grew in up to 500mM arsenate, making it the most arsenic resistant organism described to date. During growth, addition of arsenate or arsenite anions adversely affected biomass production and maximum specific growth rate and, in some instances, longer lag phases were induced. Reduction of arsenate to arsenite partly accounted for the high tolerance of the bacteria to arsenate.

It was attempted to isolate the arsenate reductase from *S. marcescens* SA Ant 16 by making use of a PCR based approach using a both documented as well as degenerate primers based on sequence similarities of related Gram negative bacteria as well as Gram positive bacteria. After many unsuccessful attempts, this line of investigation was abandoned in favour of constructing genomic libraries. An *Escherichia coli* arsenate reductase knockout strain as well as a variety of laboratory strains was used for screening purposes. After screening of more than  $5 \times 10^4$  colonies, no positive transformants were obtained. It may be possible that since *S. marcescens* SA Ant 16 exhibited hyper-tolerance to arsenate, the screening hosts used may not have been able to recognise and express the arsenate reductase from this organism successfully.

The growth optima with regards to pH and temperature were established for *S. marcescens* SA Ant 16 grown under aerobic conditions as well as a suitable electron donor and electron acceptor concentration when grown under anaerobic conditions. The surface characteristics of *S. marcescens* SA Ant 16 cells, grown both in the presence and absence of oxygen, was investigated to infer adhesion capacity. It was found that both types of cells exhibited a negatively charged, highly hydrophilic and acidic character which would imply successful and similar adhesion of both aerobically and anaerobically grown cells to sand grains.

Arsenate reduction was optimised in a factorial design layout with regards to electron donor (glucose) and substrate (arsenate) concentration under both aerobic and anaerobic conditions. Optimum contact time between cells and sand and loading capacity of the sand were determined. Cells were tracked through the sand columns and parameters for *in situ* arsenate reduction established. Successful conversion of up to 50% arsenate to arsenite was demonstrated from an initial 5mM starting concentration. This hyper-resistant bacterium could be the solution to water contaminated with extremely high arsenate concentrations.

## **6 Opsomming**

Grond en water monsters is versamel by 'n Suid-Afrikaanse antimoon myn met hoë konsentrasies van arseen as gevolg van die herwinningsproses. Verrykte media het ses suiwer bakteriële kulture opgelewer wat in staat was om in beide arseniet en arsenaat te groei. Die bakterieë is identifiseer as twee stamme van *Bacillus* sp. (SA Ant 10(1) en SA Ant 14) met noue verwantskap tot *B. maltophilia* en *B. thuringiensis*, 'n ander as *Stenotrophomonas maltophilia* SA Ant 15 en twee isolate as *Serratia marcescens* (SA Ant 10(2) en SA Ant 16). *Bacillus* sp. SA Ant 14, *S. maltophilia* SA Ant 15 en *S. marcescens* SA Ant 16 is gebruik vir verdere ondersoeke. Al drie isolate was in staat tot groei in beide arseniet en arsenaat en *S. marcescens* SA Ant 16 in tot 500mM arsenaat, wat dit die mees arsenaat weerstandbiedende organisme beskryf tot op hede maak. Gedurende groei het byvoeging van arsenaat of arseniet ione biomassa produksie en die maksimum spesifieke groeisnelheid negatief beïnvloed, en in sekere gevalle is langer sloerfases geïnduseer. Reduksie van arsenaat na arseniet kon gedeeltelik verantwoord vir die hoë weerstand van die bakterium tot arsenaat.

Daar was gepoog om die arsenaat reductase van *S. marcescens* SA Ant 16 te isoleer deur gebruik te maak van 'n PKR-gebaseerde benadering met beide gedokumenteerde asook degenererende priemstukke gebaseer op basispaar ooreenstemmings van verwante Gram negatiewe en Gram positiewe bakterieë. Na vele onsuksesvolle pogings, is hierdie trant van ondersoek laat vaar ter wille van genomiese biblioteek konstruksie. 'n *Escherichia coli* arsenaat reductase delesiemutant asook 'n verskeidenheid van laboratorium stamme is gebruik vir siftingsprosedures. Na sifting van meer as  $5 \times 10^4$  kolonies is geen positiewe transformante verkry nie. Dit is moontlik dat as gevolg van die hiper-weerstandbiedendheid van *S. marcescens* SA Ant 16, die siftings gasheer nie die arsenaat reductase van hierdie organisme kon herken en suksesvol uitdruk nie.

Groei-optima met betrekking tot pH en temperatuur is vasgestel vir *S. marcescens* SA Ant 16 onder aerobiese toestande sowel as gepaste elektron-donor en elektron-akseptor konsentrasies vir groei onder anaerobiese toestande. Die oppervlak-eienskappe van *S. marcescens* SA Ant 16 selle, gegroei beide in die teenwoordigheid en afwesigheid van suurstof, is ondersoek om adhesie-kapasiteit af te lei. Daar is gevind dat beide tipes selle 'n negatiewe lading, hoogs hidrofiliese en suur eienskappe het wat suksesvolle en eenderse adhesie van beide aerobies- sowel as anaerobies-gegroeide selle aan sandkorrels sou impliseer.

Arsenaat reduksie is geoptimiseer in 'n faktoriale ontwerp met betrekking tot elektron-donor (glukose) en substraat (arsenaat) konsentrasie onder beide aerobiese en anaerobiese toestande. Optimale kontaktyd tussen selle en sandkorrels sowel as ladingskapasiteit van die sand is bepaal. Selle is gevolg deur die sandkolomme en parameters vir *in situ* arsenaat reduksie vasgestel. Suksesvolle omskakeling van tot 50% arsenaat na arseniet is gedemonstreer vanaf 'n aanvanklike beginkonsentrasie van 5mM. Hierdie hiperweerstandbiedende bakterium kan die oplossing wees vir water wat met uitermatig hoë konsentrasies van arsenaat besoedel is.